Unsupervised Multi-Scale Analysis for the Identification of Placental Subtypes of Human Preeclampsia and Fetal Growth Restriction

by

Katherine Michelle Leavey

A thesis submitted in conformity with the requirements
for the degree of Doctor of Philosophy

Department of Physiology
University of Toronto

Unsupervised Multi-Scale Analysis for the Identification of Placental Subtypes of Human Preeclampsia and Fetal Growth Restriction

Katherine Michelle Leavey

Doctor of Philosophy

Department of Physiology
University of Toronto

2018

Abstract

Preeclampsia (PE) and fetal growth restriction (FGR) are two of the most common pathologies of pregnancy, both thought to be primarily driven by placental dysfunction. Despite decades of research into the underlying etiologies of these disorders, as well as potential biomarkers and treatments, no single discovery has been found to be applicable to the entire clinical spectrum of PE or FGR patients, likely due to the existence of multiple disease subtypes. Therefore, the main goal of this thesis was to investigate if the application of unsupervised clustering techniques to placental gene expression data could elucidate transcriptional subtypes of PE and FGR with increased clinical and histopathological homogeneity. Clustering of three overlapping large microarray datasets revealed 3-5 molecular clusters, depending on the study. However, three subtypes of PE placentas were consistently identified within clusters 1-3, and, eventually, each co-clustered with a group of placentas from normotensive suspected FGR pregnancies. Within cluster 1, PE and suspected FGR samples demonstrated less severe clinical outcomes, molecular similarity to healthy term controls, and either no placental lesions or mild histopathology, suggesting a dominant non-placental source of the disease. Cluster 2 PE and FGR placentas

revealed overwhelming evidence of “canonical” maternal vascular malperfusion features and increased placental expression of hypoxia and hormone activity genes. Cluster 3 PE and FGR samples displayed signs of an “immunological” pathology, with a transcriptional signature of immune response, apoptosis, and cytokine activity, and histological lesions affiliated with allograft rejection, such as massive perivillous fibrin deposition. In the largest microarray dataset (N=330), two additional clusters were discovered. Cluster 4 samples were preterm controls with histological chorioamnionitis, while cluster 5 was associated with confined placental mosaicism, but no clinical or histological cohesion. Furthermore, specific differences in the expression of three genes by qPCR were found to be sufficient for separating placentas into transcriptional clusters 1-4, which will allow future studies to focus on the identification of subtype-specific biomarkers and therapeutics for PE/FGR without having to first cluster microarray data. Matched maternal samples will also be necessary to comprehend the development of hypertension in some patients but not others with similar placental profiles.

Acknowledgments

First and foremost, I would like to express my sincere gratitude to my supervisor, Dr. Brian Cox for all of his support, patience, encouragement, and, perhaps most importantly, kindness. Your brilliant mind (and extensive knowledge of almost every topic!) is inspiring. Thank you for always listening to my rants, scientific or otherwise, and for all of your excellent advice. It was a privilege to have worked for and with you for the past five years.

I would also like to acknowledge my supervisory committee members Dr. Gary Bader, Dr. John Kingdom, and Dr. Anna Goldenberg for their invaluable feedback and guidance. Thank you to our collaborators in Ottawa, Dr. Shannon Bainbridge, Dr. David Grynspan, and Dr. Samantha Benton, without whom these projects would not have been possible. To past and current members of the Cox, Brubaker, and Wheeler labs, thank you for your helpful suggestions and technical assistance. A special thanks to Isaac Gibbs for all of his hard work on the FGR study.

Thank you to the funding agencies that provided support for these projects (Canadian Institutes of Health Research, the Ontario Graduate Scholarship program, and the UofT Open Fellowship fund) and the donors and RCWIH BioBank for the human placentas used in these studies.

Last but not least, I would like to thank my parents and my (almost!) husband Dani for their unwavering encouragement and patience. I am very grateful for your efforts trying to understand what I've been working on all of these years and for always knowing when to pull out the emergency chocolate stash. And finally, to Daisy, thank you for your unconditional love and for having such lovely soft puppy ears.

Publications

1. **Leavey K**, Wilson SL, Bainbridge SA, Robinson WP, Cox BJ. (2018). Epigenetic Regulation of Placental Gene Expression in Transcriptional Subtypes of Preeclampsia. *Clinical Epigenetics*. 10:28.

2. Wilson SL, **Leavey K**, Cox BJ, Robinson WP. (2018). Mining DNA Methylation Alterations Towards a Classification of Placental Pathologies. *Human Molecular Genetics*. 27(1):135-146.

3. Christians JK, **Leavey K**, Cox BJ. (2017). Associations Between Imprinted Gene Expression in the Placenta, Human Fetal Growth and Preeclampsia. *Biology Letters*. 13(11):20170643.

4. **Leavey K**, Benton SJ, Grynspan D, Bainbridge SA, Morgen EK, Cox BJ. (2017). Gene Markers of Normal Villous Maturation and Their Expression in Placentas with Maturational Pathology. *Placenta*. 58:52-59.

5. **Leavey K**, Benton SJ, Grynspan D, Kingdom JC, Bainbridge SA, Cox BJ. (2016). Unsupervised Placental Gene Expression Profiling Identifies Clinically Relevant Subclasses of Human Preeclampsia. *Hypertension*. 68 (1):137-147.

6. Liu Y, Prentice KJ, Eversley JA, Hu C, Batchuluun B, **Leavey K**, Hansen JB, Wei DW, Cox B, Dai FF, Jia W, Wheeler MB. (2016). Rapid Elevation in CMPF May Act as a Tipping Point in Diabetes Development. *Cell Reports*. 14(12):2889–2900.

7. Cox B, **Leavey K**, Nosi U, Wong F, and Kingdom J. (2015). Placental Transcriptome in Development and Pathology: Expression, Function, and Methods of Analysis. *American Journal of Obstetrics and Gynecology*. 213(4):S138-S151.

8. **Leavey K**, Bainbridge SA, Cox BJ. (2015). Large Scale Aggregate Microarray Analysis Reveals Three Distinct Molecular Subclasses of Human Preeclampsia. *PloS one*. 10(2):e0116508.

Table of Contents

List of Tables

List of Figures

List of Abbreviations

8-OHdG: 8-hydroxy-2'-deoxy-guanosine
AAV-2: adeno-associated virus-2
AC: abdominal circumference
aCGH: array-based comparative genomic hybridisation
AEDF: absent end-diastolic flow
AFP: alpha-fetoprotein
AGA: average-for-gestational-age
ALT: alanine aminotransferase
ART: assisted reproductive technologies
AST: aspartate transaminase
AVM: advanced villous maturity
BIC: Bayesian Information Criterion
BMI: body mass index
BP: blood pressure
BPA: bisphenol A
BPD: biparietal diameter
BPS: biophysical profile score
cDNA: complementary deoxyribonucleic acid
CH-SGA: chronic hypertensive and small-for-gestational-age
CH: chronic hypertension
CMV: cytomegalovirus
CO: cardiac output
CPM: confined placental mosaicism
CRH: corticotropin-releasing hormone
CT: cytotrophoblast
DTT: dithiothreitol
DVH: distal villous hypoplasia
EB: Empirical Bayes
EDTA: ethylenediaminetetraacetic acid
EFW: estimated fetal weight
ENG: endoglin
eNOS: endothelial nitric oxide synthase
EOPE: early-onset preeclampsia
EVT: extravillous trophoblast
FDR: false discovery rate
FFPE: formalin-fixed paraffin-embedded
FGR: fetal growth restriction
FL: femur length
FLT1: fms-related tyrosine kinase 1
FPR: false positive rate
FSTL3: follistatin-like 3

GA: gestational age
GCM1: glial cells missing 1
GEO: Gene Expression Omnibus
GO: Gene Ontology
GSEA: Gene-Set Enrichment Analysis
GVHD: graft-versus-host disease
GWAS: genome-wide association study
H-SGA: hypertensive and small-for-gestational-age
HC: head circumference
hCG: human chorionic gonadotropin
HELLP: hemolysis, elevated liver enzymes, and low platelets
HIF-1: hypoxia-inducible factor-1
HIF-2: hypoxia-inducible factor-2
HIV: human immunodeficiency virus
HLA: human leukocyte antigen
HPV: human papilloma virus
HR: heart rate
HTRA1: HtrA serine peptidase 1
IDO: indoleamine dioxygenase 2,3-dioxygenase
IGFBP-1: insulin-like growth factor-binding protein 1
IgG: immunoglobulin G
IL-8: interleukin-8
IL1RAP: interleukin-1 receptor accessory protein
INHA: inhibin A
INHBA: inhibin B
IP-10: interferon-inducible protein-10
IVF: in vitro fertilization
IVIG: intravenous immunoglobulin
KDR: kinase insert domain receptor
KEGG: Kyoto Encyclopedia of Genes and Genomes
KIR: killer-cell immunoglobulin-like receptor
LEP: leptin
LGA: large-for-gestational-age
LIMCH1: LIM and calponin homology domains 1
LMWH: low-molecular-weight heparin
LOPE: late-onset preeclampsia
MAP: mean arterial pressure
MFI: maternal floor infarction
MHC: major histocompatibility complex
MnSOD: mitochondrial superoxide dismutase
MPFD: massive perivillous fibrin deposition
MRI: magnetic resonance imaging
MsigDB: Molecular Signatures Database
MVM: maternal vascular malperfusion
N-AGA: normotensive and average-for-gestational-age

N-SGA: normotensive and small-for-gestational-age
NICU: neonatal intensive care unit
NO: nitric oxide
PAPP-A: pregnancy associated plasma protein A
PAPP2: pappalysin 2
PC: principal component
PCA: principal component analysis
PE-SGA: preeclamptic and small-for-gestational-age
PE: preeclampsia
PI: pulsatility index
PlGF: placental growth factor
PP13: placental protein 13
PRL: prolactin
PVCA: principal variance component analysis
qPCR: quantitative polymerase chain reaction
RCWIH: Research Centre for Women's and Infants' Health
REDF: reversed end-diastolic flow
ROC: receiver operator characteristic
ROS: reactive oxygen species
RT: reverse transcriptase
sENG: soluble endoglin
sFLT1: soluble fms-related tyrosine kinase 1
SGA: small-for-gestational-age
SNP: single nucleotide polymorphism
SV: stroke volume
SynT: syncytiotrophoblast
t-SNE: t-distributed stochastic neighbor embedding
TAP1: transporter 1, adenosine 5'-triphosphate-binding cassette, subfamily B
TGF-β: transforming growth factor-beta
TNFα: tumor necrosis factor α
TORCH: toxoplasmosis, other (syphilis, varicella-zoster, parvovirus B19), rubella, cytomegalovirus, and herpes
TPR: true positive rate
uE3: unconjugated estriol
uNK: uterine natural killer
VEGF: vascular endothelial growth factor
VUE: villitis of unknown etiology
WBC: white blood cell
WHO: World Health Organization

List of Appendices

1 Chapter 1 – Introduction

1.1 Overview of Preeclampsia (PE)

Preeclampsia (PE) is a complex hypertensive disorder of pregnancy. Diagnosed by the onset of maternal hypertension in the second half of gestation (i.e., after 20 weeks), with signs of liver, kidney and/or neurological involvement [1], this disorder affects 3-8% of all pregnancies [2]. A significant concern for women with preeclampsia is the progression to an eclamptic state, involving life-threatening seizures, as well as an increased risk of stroke, liver/kidney failure, and pulmonary edema [3]. In developing countries, the rates of maternal morbidities and mortalities remain high [3], with PE/eclampsia associated with more than 60,000 maternal deaths worldwide each year [2]. To date, the only cure and definitive treatment for preventing acute maternal complications in preeclamptic women is the delivery of the placenta, which is thought to be the causative organ [2, 4-6]. Unfortunately, this also requires the delivery of the fetus, which, when deemed necessary before 34 weeks (iatrogenic preterm birth), is robustly linked to poor fetal outcomes [7, 8]. It is, therefore, not surprising that PE is also affiliated with a perinatal and neonatal mortality rate of 10% worldwide [2, 9].

1.1.1 Risk factors for PE development

The incidence of preeclampsia has been increasing relentlessly [10, 11], predominately due to the increasing prevalence of several of the leading risk factors for PE development (**Figure 1**) [12, 13]. A number of these factors involve an underlying maternal cardiovascular and/or metabolic pathology, such as obesity, diabetes, and chronic hypertension [11, 12, 14, 15]. Obesity has been shown to demonstrate a dose-dependent relationship with PE, with class III obese women (body mass index (BMI) > 40) exhibiting the greatest likelihood of a hypertension diagnosis [16]. This relationship is not surprising as the obese maternal state is associated with elevated levels of inflammatory factors, oxidative stress, and fatty acid accumulation, which can also have a direct effect on the placenta [17-19]. Even higher frequencies of PE development have been observed in pregnancies complicated by maternal chronic hypertension (CH), with the rate of PE increasing from 3-8% in the general population to 17-28% in CH women [20-23]. While chronic hypertension is multifactorial in nature [24], it has been linked to vascular

endothelial dysfunction [25], which is strongly implicated in the pathogenesis of PE [26]. Additionally, PE is more common in women of African ancestry, a group of patients with higher rates of chronic hypertension [27, 28]. Therefore, the overall underlying maternal pathology associated with these risk factors likely contributes significantly to the development of preeclampsia in a given pregnancy, as well as the increased likelihood of recurrent PE across multiple pregnancies [14, 29, 30].

Another susceptibility factor for a PE pregnancy is advanced maternal age (**Figure 1**) [11, 22, 31]. This is of particular concern as the average age of a woman's first pregnancy is rising in many countries, including Canada [32]. Advanced maternal age is also tightly linked to the increased use of assisted reproductive technologies (ART) for conception [33], which is its own predisposing factor for PE occurrence [14]. Furthermore, in vitro fertilization (IVF) with a donor oocyte instead of an autologous oocyte shows an even more robust association with PE [34-36], suggesting an important immunological component to this disorder. This immune system involvement is further supported by the observation of reduced PE rates in women with significant sperm exposure prior to pregnancy [37, 38], as well as increased frequencies of PE in nulliparous women (with no prior pregnancies reaching a viable gestational age) [30, 39] and women with anti-phospholipid antibody syndrome [14], an autoimmune pathology of hypercoagulability. Additionally, preeclampsia is affiliated with cytomegalovirus (CMV) [40, 41], adeno-associated virus-2 (AAV-2) [42], human papilloma virus (HPV) [43, 44], Epstein-Barr virus [45], and human immunodeficiency virus (HIV) [46], indicating the potential importance of viral infection status for pregnancy outcome [47].

Preeclampsia also has a significant genetic component (**Figure 1**). The estimated heritability of PE is somewhere between 0.22 and 0.54 [48-50], and pregnancies complicated by a fetal trisomy can have a higher risk of PE development [51]. Understandably, a wide range of genes have been implicated in this disorder [52], either through a candidate approach for single nucleotide polymorphisms (SNPs) in genes with expected PE involvement or using genome-wide association studies (GWAS) [53, 54]. The majority of these studies have focused on the maternal genotype, and have identified genes with significant PE associations involved in angiogenesis [55-57], solute transport [58], and immune and inflammatory [59-61] pathways, as well as thrombophilia [22, 62]. In a few cases, fetal inheritance of the maternal genotype further increased the risk of preeclampsia [60, 63], although most of these targeted studies exhibited low

reproducibility [62]. Recently, the first GWAS study of offspring from PE pregnancies was performed using >310,000 patients and revealed one highly significant susceptibility SNP (rs4769613) near the fms related tyrosine kinase 1 (FLT1) gene, which was then replicated in an independent cohort [64]. This has considerable biological significance, as this gene and its corresponding protein are known to be aberrantly expressed in the PE placenta and to have substantial involvement in the maternal pathology [65]. These results suggest that further GWAS studies, with sufficient statistical power, may be able to identify additional robust genetic maternal and fetal relationships to PE, with the goal of fully comprehending the heritability of this disorder.

Additionally, several environmental influences have demonstrated a strong relationship with PE development (**Figure 1**). Risk factors include increased exposure to bisphenol A (BPA) [66], a common chemical in plastics, and elevated air pollution exposure [67]. Interestingly, maternal smoking is considered protective against the development of this hypertensive disorder, with smokers showing up to a 50% reduction in PE diagnoses [30, 68, 69]. Although not fully understood, carbon monoxide is thought to be essential for these lower rates of PE pathology, due to both its direct effects on the placenta and its role as a vascular protective agent [69]. Lastly, male fetuses have also been linked to increased rates of maternal preeclampsia development, although this finding is not consistent across cohorts [70].

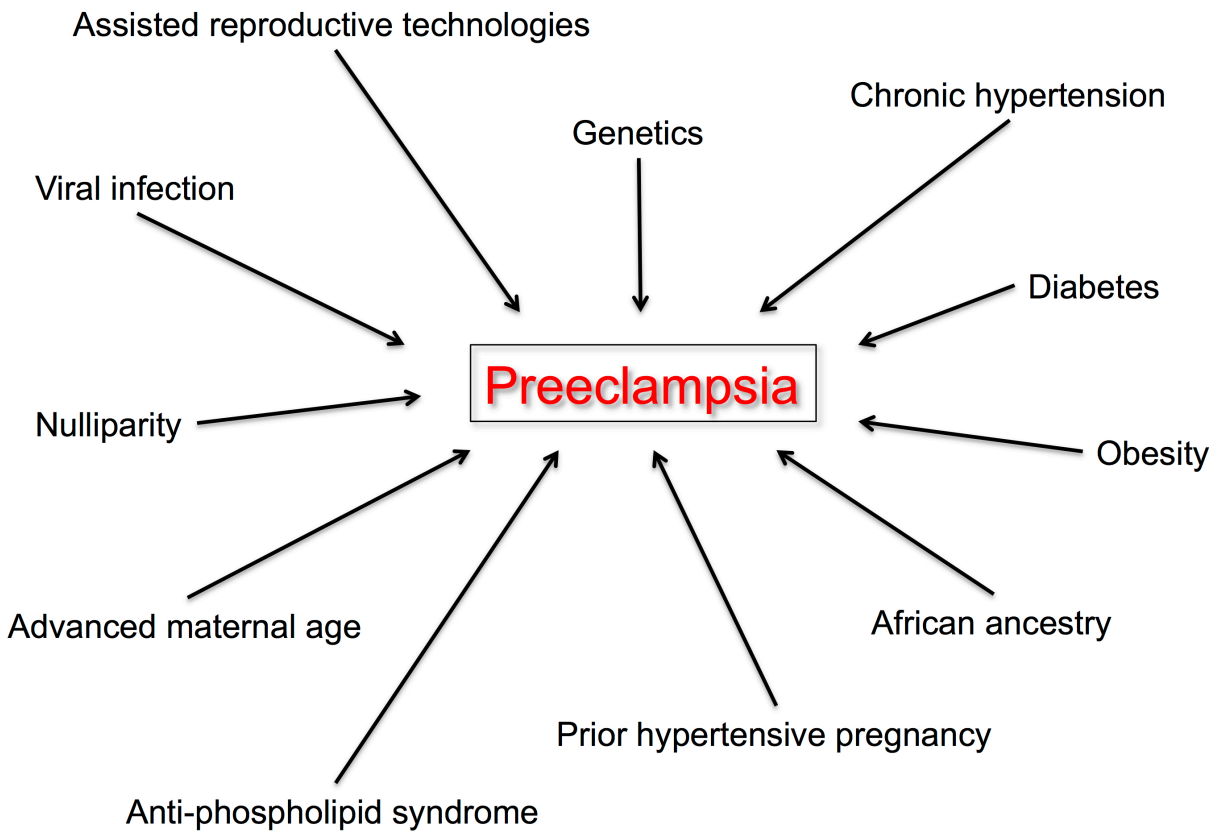

Figure 1 – Pre-pregnancy risk factors for the development of preeclampsia during pregnancy.

1.1.2 Diagnosis of PE

When the current project was initiated in 2013, preeclampsia was defined in Canada as the onset of maternal systolic blood pressure (BP) ≥140 mmHg and/or diastolic BP ≥90 mmHg after the 20th week of gestation, accompanied by maternal proteinuria (>300 mg protein/day, or at least 2+ by dipstick) [71]. These blood pressure values are consistent with the guidelines established in other countries; however, the proteinuria requirement and quantity has been debated worldwide [72-74]. The frequent observation of proteinuria in preeclampsia is associated with kidney endothelial dysfunction and podocyte injury [75, 76]. However, a number of other maternal organs also demonstrate considerable (often vascular) damage during a PE pregnancy. As such, in 2014, the diagnosis of PE in Canada was updated to include other signs of maternal

end-organ dysfunction in place of, or in addition to, the proteinuria requirement [1]. These include maternal neurological symptoms (headache and/or vision disruption), cardiorespiratory indications (chest pain, dyspnea, and/or low oxygen saturation), haematological abnormalities (elevated white blood count and/or low platelet count), hepatic changes (abdominal pain, severe nausea or vomiting and/or elevated liver enzymes), and signs of fetal morbidity (poor fetal growth, abnormal blood flow to the fetus, and/or non-reassuring fetal heart rate) [1]. While encompassing more women into a PE diagnosis, this expanded criteria further increases the clinical heterogeneity observed in an already complex and heterogeneous disorder.

To try and reduce this heterogeneity, PE diagnoses are often divided into clinical subgroups. Early-onset preeclampsia (EOPE) is the diagnosis of PE before 34 weeks gestation, while late-onset preeclampsia (LOPE) involves a diagnosis after 34 weeks of pregnancy [77]. Severe PE is noted when maternal blood pressures over 160/110 mmHg are measured, while mild PE is associated with blood pressures remaining between 140/90 mmHg and 160/110 mmHg [77]. Early-onset PE is more likely to be of the severe kind, and frequently co-occurs with other pathologies of pregnancy, such as fetal growth restriction (FGR) and hemolysis, elevated liver enzymes, and low platelets (HELLP) syndrome [11]. In contrast, gestational hypertension is defined as hypertension (>140/90 mmHg) that develops for the first time after 20 weeks gestation, but without any additional adverse complications [1]. Also relevant to this thesis is the diagnosis of chronic hypertension in pregnancy, which is established when a woman's BP is $\geq$140/90 mmHg before 20 weeks of gestation [1].

1.1.3 Management of PE pregnancies

Once a diagnosis of preeclampsia has been confirmed, the main goal is to avoid maternal complications, such as stroke and eclampsia, while simultaneously prolonging pregnancy as much as possible to reduce the risk of poor neonatal outcomes [3, 4, 7, 22]. Fortunately, with appropriate surveillance and antenatal care [39], rates of poor maternal outcomes and death are low in high-income/developed countries [3, 5]. The prediction of adverse maternal complications in women with PE (particularly within the first 48 hours after diagnosis) can be fairly accurately anticipated using oxygen saturation, gestational age, and blood work values (fullPIERS model) [22, 78]. To avoid pulmonary edema, fluid restriction is recommended [22], while in severe PE, anti-hypertensive medications, such as methyldopa, nifedipine, and labetalol, are employed to

reduce maternal blood pressure [1]. Very tight control of maternal BP (target diastolic pressure of 85 mmHg) has not been associated with definitive improvements in maternal or fetal outcomes [79], and there is some evidence to suggest that substantial decreases in maternal blood pressure due to treatment can have a negative impact on fetal growth [80]. As such, the Canadian guideline suggests a target blood pressure below 160/110 mmHg [1].

If the maternal and/or fetal status deteriorates, and the risk of eclampsia and/or delivery becomes high, administration of magnesium sulfate, an anti-convulsive medication, is recommended to prevent seizures [9], while corticosteroid therapy is utilized to accelerate fetal lung maturity and reduce the risk of neonatal respiratory distress syndrome in preterm infants [1, 81]. Magnesium sulfate may also have neuroprotective effects in the fetus [22]. Both of these drugs are considered beneficial for maternal and infant outcomes with correct treatment timing; however, both have also been affiliated with potentially harmful effects if employed long-term [1, 82, 83]. The majority of severe PE cases require a cesarean section delivery, which can also improve clinical outcomes [84].

1.1.4 Long-term maternal consequences of PE

Pregnancy is considered a "stress test" for later life [1, 85], with diagnosed pathologies during gestation indicative of future maternal health. Preeclampsia has been linked to subsequent development of renal disease, type 2 diabetes, ophthalmic complications, hypothyroidism, and impaired cognitive functioning [86-90]. However, the dominant long-term association is the development of cardiovascular disease in these women [91-96]. In a study from Denmark involving more than 700,000 subjects [97], the risk of subsequent hypertension development was 3.6-fold higher after mild preeclampsia and 6.1-fold higher after severe preeclampsia, while the risk of thromboembolism was elevated 1.5-fold and 1.9-fold after mild and severe PE, respectively. A massive meta-analysis of almost 3.5 million women confirmed that preeclampsia was affiliated with an increased risk of hypertension, ischaemic heart disease, stroke, and venous thromboembolism (relative risks: 3.7, 2.2, 1.8, and 1.8, respectively) in later life [93]. Alarmingly, women who have experienced an early-onset PE pregnancy are at a 9.5-fold increased risk of dying from these cardiovascular diseases [91]. However, interestingly, abnormal cardiovascular and metabolic profiles can be observed as early as 6-12 months postpartum [98, 99], suggesting the potential to identify those women at greatest risk relatively

quickly after pregnancy. Overall, the relationship between preeclampsia and future cardiovascular dysfunction is not fully understood, but may be due to common risk factors in these women, persistent endothelial damage from the hypertensive pregnancy, or a combination of both of these underlying mechanisms [22, 100, 101].

1.2 Overview of Small-for-Gestational-Age (SGA) and Fetal Growth Restriction (FGR)

Fetal growth restriction (FGR) is another common pathology of pregnancy that is highly related to preeclampsia. FGR is diagnosed based on a fetus's failure to reach its full growth potential *in utero* due to a pathological process [102, 103]. This is distinct from a small-for-gestational-age (SGA) infant that is born at a lower than expected birth weight compared to other neonates of the same gestational age and sex, usually in the bottom 10^{th} percentile. While SGA infants may fulfill the criteria for an FGR diagnosis, they can also be constitutionally small (i.e., normally grown for maternal size and ethnicity) with little or no signs of pathology [104]. As such, when newborns worldwide are assessed against the same growth standard (based on a United States population), infants in low- and middle-income countries exhibit an exceptionally high prevalence of SGA (27% of live births), especially those born in South Asia [105]. However, it is critical to accurately identify fetuses with a true pathological FGR, as they are at a substantially increased risk of stillbirth and neonatal mortality [106, 107], as well as a wide range of long-term sequelae [108-110]. Since it is well established that the risk of stillbirth increases with gestational age in FGR fetuses, while the risk of neonatal mortality decreases [7, 111], a significant concern when faced with a fetus with suspected FGR, not unlike when managing a PE pregnancy, is the timing of delivery [111, 112].

1.2.1 Risk factors for pathological FGR development

There are two clinical types of FGR based on fetal growth: symmetrical FGR, where the fetus is proportionally small, and asymmetrical FGR (or "brain sparing" FGR), where the fetal weight is low, but the head circumference is relatively normal [113]. These two types of FGR are often associated with different risk factors (**Figure 2**). Symmetrical FGR, accounting for 20-30% of FGR cases, is thought to originate early in pregnancy, thereby affecting the fetal body equally [114, 115]. Several congenital malformations have been linked to symmetrical FGR [116], in

addition to a number of inborn errors in metabolism, such as pancreatic agenesis [115, 117]. FGR development, especially symmetrical, is more likely to occur in pregnancies involving congenital infections, including TORCH (toxoplasmosis, other (syphilis, varicella-zoster, parvovirus B19), rubella, CMV, and herpes), malaria, HPV, and HIV infections [43, 115, 118-120]. An elevated risk of symmetrical FGR has also been observed after increased exposure to a number of other teratogens, such as heavy metals [121], alcohol [122], cocaine [123], caffeine [124], polychlorinated biphenyls [125], BPA [126], and angiotensin receptor antagonists [127].

Asymmetrical FGR, accounting for the remaining 70-80% of FGR cases, occurs when there is a reduction in the blood flow and nutrients to the fetus, and what is available is preferentially redistributed in favor of the fetal brain [114, 115]. Asymmetrical FGR is suspected to originate later in gestation when fetal growth and nutritional requirements are higher and is thought to be predominately caused by placental insufficiency [114, 115]. As such, one of the greatest risk factors for asymmetrical FGR is pre-existing or co-occurring maternal hypertension (preeclampsia or chronic hypertension), as this is robustly affiliated with changes in maternal blood flow to the placenta, and therefore to the fetus [115, 128]. Understandably then, PE and FGR share several maternal predispositions, such as extreme age (older or younger) [129], use of ART [130], diabetes [131], and anti-phospholipid antibody syndrome [132] (**Figure 2**). Additionally, a number of environmental factors can also contribute to asymmetrical fetal growth. For example, pregnancy at a high altitude (>2700 m) is known to be associated with FGR, predominately as a consequence of reduced blood flow to the fetus [133, 134], while, unlike with PE, maternal smoking is a significant risk factor for asymmetrical FGR [135, 136] due to direct effects on the placenta [137]. Furthermore, maternal nutritional status contributes substantially to fetal growth [138]. Maternal anemia [135], zinc deficiency [139], reduced dairy consumption [140], and salt restriction [141], have all been linked to an increased risk of FGR, although whether the impact is symmetrical or asymmetrical depends on the type, timing, and mechanism of the nutritional deficiency (**Figure 2**).

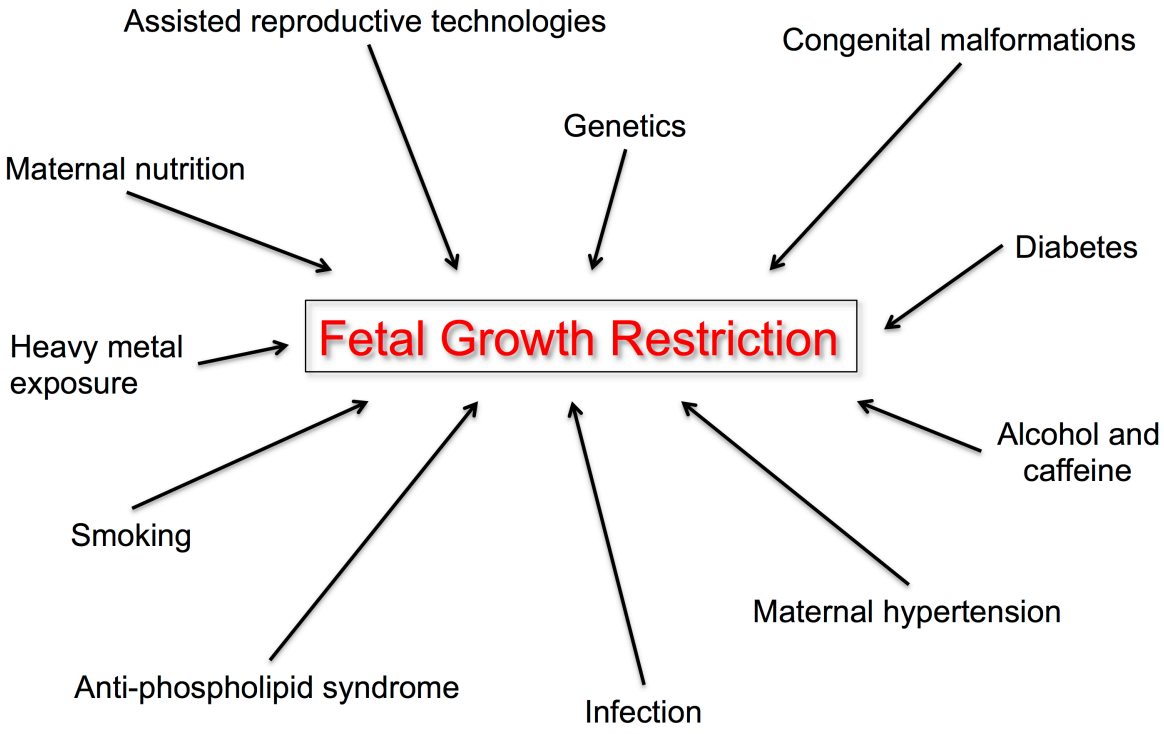

Figure 2 – Pre-pregnancy/early pregnancy risk factors for symmetrical or asymmetrical fetal growth restriction.

1.2.2 Identification and management of SGA/FGR pregnancies

To accurately assess fetal growth, it is important that the pregnancy is correctly dated. Gestational age (GA) assignment is performed by ultrasound in the first trimester using the crown-rump length, which is the length from the top of the head to the bottom of the buttocks [142-144]. Between 16 and 18 weeks, fetal biparietal diameter (BPD) would be employed to assess GA, while later in pregnancy, GA dating has been accurately established based on the fetal transcerebellar diameter (the maximum diameter between the cerebellar hemispheres on an axial scan), even in SGA and large-for-gestational-age (LGA) fetuses [145]. Additionally, estimated fetal weight (EFW) can be obtained using a wide range of different formulas, usually based on BPD, head circumference (HC), abdominal circumference (AC), and/or femur length

(FL) measurements, some of which perform better than others for SGA fetuses [146]. In cases of asymmetrical FGR, it is important to avoid methods that incorporate femur length, as this has, understandably, been shown to highly underestimate weight in these fetuses [147]. Once the gestational age and EFW has been determined, they can then be compared to a growth chart. A commonly employed growth standard is the one established by Hadlock et al. [148]. If multiple measurements are taken over gestation, this can establish the growth trajectory of the fetus; thereby revealing if the fetus remains small throughout pregnancy (more likely a constitutional SGA fetus or a symmetrical FGR fetus) or the growth trajectory drops off later in pregnancy, indicating a pathological (probably asymmetrical) FGR fetus [149, 150]. It is essential that FGR is identified during pregnancy, as those that are not antenatally detected are five times more likely to result in a stillbirth [151]. However, separating constitutionally small SGA fetuses from pathological FGR fetuses is exceptionally difficult [152, 153], especially in cases where multiple serial ultrasound measurements throughout pregnancy are not available.

To try and improve the *in utero* separation of SGA and FGR fetuses, customized growth charts were first proposed by Gardosi et al. in 1992 [154]. Based on EFW and fetal sex, a significant portion of infants are falsely categorized as growth restricted, simply due to constitutional differences in maternal ethnicity, parity, height, and weight [155-159]. Customized growth charts incorporate these fundamental maternal differences, establishing the "growth potential" of the fetus, and consequently, determining if this growth potential is not being achieved [154, 160, 161]. Additionally, as fetuses do not necessarily have to be SGA to be growth restricted [162], these customized charts provide the opportunity to discover fetuses with a reduced growth trajectory, but that remain above the 10^{th} percentile for gestational age and sex (average-for-gestational-age (AGA)), a group that is also at an elevated risk of stillbirth [162]. Recently, a direct comparison of the ability of a customized growth chart and a population growth chart [163] to identify small infants at risk of adverse outcomes was performed in the multi-ethnic city of Auckland, New Zealand [164]. The customized method was found to be superior for discerning the SGA infants at the greatest risk of mortality and morbidity [164]. Furthermore, customized growth charts have also been established in Australian [165], Spanish [166], American [167], and Irish [168] populations. In Toronto, fetal growth is often assessed using the fetal AC, and birth weight percentiles are only sex-specific [169], although a customized method has been suggested [170].

Management of an FGR pregnancy depends on the timing of reduced fetal growth onset. In early-onset FGR cases (before 34 weeks), co-occurring maternal hypertension is common, and, to avoid stillbirth, the risk of iatrogenic preterm birth is high [171]. Therefore, management is similar to a PE pregnancy, with attempts to reduce maternal blood pressure and administration of corticosteroids to accelerate fetal lung maturity. However, the increased fetal stress of an FGR state and the elevated risk of lactic acidosis makes the safety of corticosteroids for early-onset FGR fetuses questionable [150, 172-175]. In general, it is still recommended to provide a single dose of glucocorticoids in cases of preterm FGR, although increased fetal surveillance is also required [175]. In late-onset FGR (after 34 weeks), the primary concern is the risk of stillbirth [171], as the rates of stillbirth have been shown to increase considerably after 37 weeks of gestation [111]. Therefore, delivery of fetuses with suspected FGR is advised at 37-38 weeks [111, 112]. A cesarean section is often required for early-onset FGR, while the induction of labor is standard for late-onset FGR [176, 177].

1.2.3 Neonatal and long-term consequences of FGR

The consequences for infants who survive an FGR pregnancy are extensive (**Figure 3**). FGR newborns are associated with low Apgar scores, high rates of neonatal intensive care unit (NICU) admissions, and a wide range of short-term complications, including respiratory distress syndrome, necrotizing enterocolitis, neonatal sepsis, persistent pulmonary hypertension, jaundice, pulmonary hemorrhage, temperature instability, and neonatal death [106, 114, 115, 178]. Neonates also demonstrate an increased likelihood of renal disease and immune dysfunction [179, 180]. Additionally, these infants already exhibit altered metabolic profiles and cardiovascular structure and function [181, 182], adaptive changes that may be indicative of their future elevated prevalence of cardiovascular and metabolic disease [183]. For example, the hearts of preterm FGR neonates show greater free wall thickening, decreased ejection fractions, and abnormal diastolic function compared to their normally grown counterparts [182]. The length of required respiratory support after delivery is also significantly longer in FGR patients [182].

In childhood, these immune and cardiovascular changes persist, with reduced T lymphocyte proliferative capacity, abnormal cardiac shape, reduced stroke volume, and higher blood pressure in 1-5 year olds [180, 184]. In school-aged children, FGR is associated with lower cognitive

scores and academic performances, as well as reduced lung function [110, 185]. These cognitive impairments are significantly more severe in symmetrical FGR children [108, 113], although asymmetrical ("brain sparing") FGR children have also been reported to exhibit social issues and problems with attention [186].

As adults, differences in total brain volume, as well as muscle mass and strength, have been noted in those born FGR [187, 188]. However, most commonly, FGR adults demonstrate a strong link to cardiovascular and metabolic disease [189, 190]. First proposed in 1990 by the British epidemiologist David Barker, the "Barker hypothesis" suggests that reduced fetal growth promotes a "thrifty" phenotype, programming fetuses for future hypertension, coronary heart disease, and diabetes development [189, 191]. Since then, this has been observed in many cohorts, with birth weights exhibiting robust inverse relationships with cardiovascular pathology [192, 193], as well as strong associations between the rate of catch-up growth after delivery and future obesity [194-196]. Fetal programming is now a rapidly expanding area of international research [197], with considerable effort focused on understanding how the *in utero* environment, and the placenta [198], contributes to the later development of adult diseases, and the transmission of these diseases across multiple generations [199].

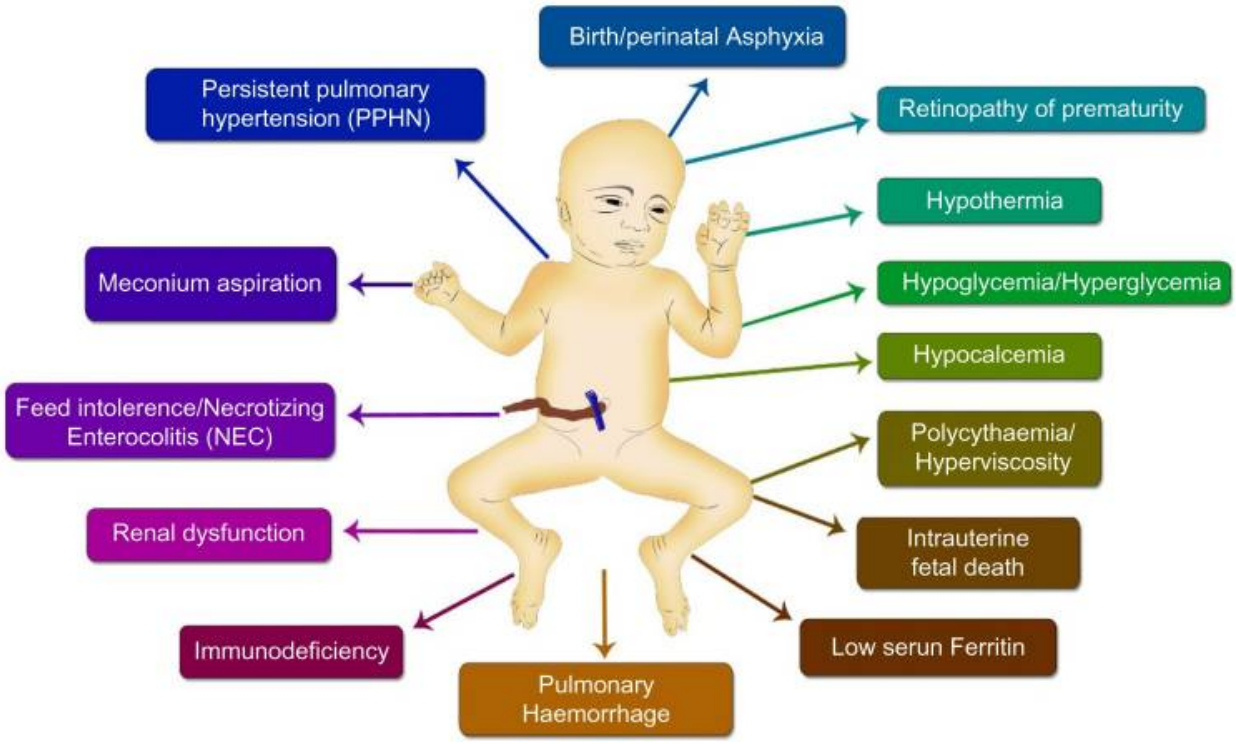

Figure 3 – Short-term possible consequences of fetal growth restriction. This figure is published in [115]. © The authors. Reused under the terms of the Creative Commons Attribution License (https://creativecommons.org/licenses/by/3.0/legalcode).

1.3 Overview of the Placenta and Healthy Pregnancy

The placenta is the unique organ of pregnancy and is widely considered to be the central component of the PE and FGR disease processes. The most incriminating evidence for this is the appearance of early-onset PE in hydatidiform molar pregnancies in which the placenta is highly proliferative, but no fetal tissue is present [200, 201]. Furthermore, twin pregnancies, accompanied by an increased placental mass, report an incidence of PE 2-3 times higher than singleton pregnancies and often exhibit a more severe form of PE with very high maternal blood pressure (>160/110 mmHg) and a greater likelihood of eclampsia development [202, 203]. Additionally, the majority of FGR pregnancies exhibit clear signs of placental insufficiency, resulting in reduced blood flow and oxygen/nutrient transport to the fetus [204].

1.3.1 Early placental development

Post-ovulation, when progesterone levels are high in the mid-secretory phase of the menstrual cycle, an initial remodeling of the female endometrium is triggered, a process termed "decidualization" [205, 206]. In humans, unlike most other mammals, this process commences in anticipation of a possible pregnancy and does not require the presence of an embryo [207]. Decidualization, which continues throughout pregnancy if one were to occur, involves considerable extracellular matrix, vascular, and uterine gland alterations [205, 206, 208]. Additionally, the decidua is transformed into an immune-tolerant environment [209]. After successful fertilization and rapid cell division, the conceptus takes the form of a blastocyst. The blastocyst is composed of an inner cell mass that will develop into the fetal and extraembryonic tissues (yolk sac, chorion, amnion, and allantois) and an outer trophectoderm layer that will differentiate into the placenta [210]. Implantation of the blastocyst into the decidua begins 6-7 days after fertilization, and involves a number of cytokines, growth factors, and inflammatory factors [206], in a multi-day and multi-step process.

Almost immediately after blastocyst attachment to the decidua, the trophectoderm begins to divide and differentiate into the cell types required for placentation [211], including the mononuclear, highly proliferative cytotrophoblast (CT) cells that contribute to both the villous and the extravillous compartments of the functional human placenta. In the villous compartment, the cytotrophoblasts are found within highly branched structures called villous trees, which are the sites of maternal-fetal nutrient and gas exchange. The CTs fuse to produce multi-nucleated syncytiotrophoblasts (SynT), which cover the outer layer of the trees, forming a syncytium. These syncytiotrophoblasts are critical for pregnancy as they secrete several of the required hormones for fetal and placental development, such as progesterone and human chorionic gonadotropin (hCG) [206]. Under the highly proliferative villous CT cells is the villous mesenchymal core encasing the fetal capillaries [212]. Included within this mesenchyme are the Hofbauer cells, placental macrophages that may play a role in the development and maturation of the villous tree [213]. To form the extravillous compartment, populations of CT cells break through the syncytium and develop into proliferative columns, which then generate the extravillous trophoblast (EVT) cells that invade the maternal decidua (and the proximal third of the myometrium) [214]. These "anchoring villi" are responsible for the physical link between the placental and maternal tissue (**Figure 4**). Within the decidua, two types of EVTs are visible and

participate in transforming the maternal spiral arteries, downstream branches of the two uterine arteries, into low-resistance blood vessels capable of adequate perfusion of the placenta [215]: interstitial EVTs are observed within the uterine stroma (and will become the terminally differentiated placental bed giant cells), and endovascular EVTs transition from an epithelial to an endothelial phenotype and are located within the lining of the vessels [216, 217]. The remaining villous trees that are not attached to the uterine wall are termed "floating villi" (**Figure 4**).

1.3.2 Immune cell involvement

Several maternal immune cell types play an important role in early pregnancy and placental development. The majority of the immune cells found at the maternal-fetal interface (i.e., in the decidua) are uterine-specific natural killers (uNK) cells and macrophages, although some T-cells and dendritic cells are present [209]. Uterine NK cells are CD56+ immune cells that, unlike their peripheral counterparts, are highly granulated and demonstrate low cytotoxicity [209]. Decidual macrophages are mostly of the immune-regulatory (M2) phenotype, although perhaps not exclusively [209]. Despite the fact that trophoblasts are required for complete spiral artery remodeling [218], uNK and decidual macrophages can be observed in the early stages of the process before trophoblast invasion, disrupting vascular smooth muscle cells by apoptosis [219, 220]. Uterine NK cells have also been thought to regulate trophoblast behavior itself during invasion and remodeling, perhaps through the production of interleukin-8 (IL-8) and interferon-inducible protein-10 (IP-10) chemokines [216, 221].

Additionally, important trophoblast-decidual immune cell interactions are required to establish immune tolerance of the semi-allograft placenta and fetus [222]. Except for human leukocyte antigen (HLA)-C, the invading extravillous trophoblast lacks classical, highly polymorphic, major histocompatibility complex (MHC) class I proteins, and instead expresses non-classical HLA-E, HLA-F, and HLA-G, to avoid attack from the maternal immune system [223]. These non-classical MHC I proteins are thought to protect trophoblast cells by binding to killer-cell immunoglobulin-like receptors (KIRs) on the uterine NK cells, as NK cells are known to rapidly target entities with no MHC class I [223]. HLA-G, binding to KIR2DL4, is involved in the inhibition of cell lysis, the modulation of the maternal immune system, and the promotion of tolerance at the maternal-fetal interface [224-226]. HLA-E has been shown to interact with

CD94/NKG2 receptors on uterine NK cells, reducing NK cytotoxicity [227]. HLA-C retention also plays an important role, as interactions between trophoblast HLA-C and uNK KIRs are associated with appropriate trophoblast invasion of the decidua and optimal blood supply to the placenta, regulating neonatal birth weight [228]. Furthermore, trophoblast cells do not express MHC class II molecules, such as HLA-DP, HLA-DM, HLA-DOA, HLA-DOB, HLA-DQ, and HLA-DR, which may also contribute to immune protection during pregnancy [229].

1.3.3 Blood flow and oxygen levels

In early placental development, the endovascular EVTs invade into the maternal spiral arteries, accumulate, and form trophoblast plugs, blocking maternal blood flow to the villi [230]. As such, the first-trimester placenta and embryo develop in a low oxygen environment. This serves several purposes. First, oxygen, and its inevitable downstream free radicals and reactive oxygen species (ROS), can considerably damage the developing embryo during organogenesis and increase the likelihood of congenital malformations if in excess [231, 232]. The early first-trimester syncytiotrophoblast is also highly susceptible to oxidative damage, as, unlike the cytotrophoblast, the syncytium does not express mitochondrial superoxide dismutase (MnSOD), an important antioxidant, until later in pregnancy [233]. Additionally, oxygen levels have been shown to significantly impact the behavior of cytotrophoblasts, and hypoxic conditions are required for their necessary rapid proliferation and poor differentiation during this time frame [234]. These effects are thought to be at least partially mediated by elevated hypoxia-inducible factor-1 (HIF-1) and transforming growth factor-beta (TGF-β), an inhibitor of trophoblast differentiation, in the early placenta [235]. During this critical first phase of pregnancy, the majority of embryonic and placental nutrients are obtained from the uterine gland secretions and the yolk sac [236-238].

Around the 8th week of pregnancy, organogenesis is complete, and the trophoblast plugs loosen, beginning the establishment of the hemochorial placenta in direct contact with the maternal blood. Between 8 and 14 weeks of gestation, the partial pressure of oxygen in the placenta dramatically increases [239], and the SynT demonstrates signs of MnSOD activity [233] to protect itself against the sudden increase in oxidative stress [231]. These normoxic conditions also promote an invasive EVT phenotype in the cytotrophoblasts, resulting in increased remodeling of the maternal spiral arteries and increased perfusion into the intervillous space

[234, 235]. The complete remodeling of the arteries, including the loss of smooth muscle from the vessel walls, is critical to reduce the rate of blood flow into the placenta from 2-3m/s to 10cm/s and avoid villous damage [240]. The syncytiotrophoblasts are then able to perform their primary role as the site of maternal-fetal nutrient and gas exchange [241].

1.3.4 Placental villous maturation and function

Before five weeks of gestation, the placental villi consist only of cytotrophoblasts and syncytiotrophoblasts, and are, therefore, termed "primary villi" [217, 242]. Around five weeks, the fetal mesenchyme invades, producing the "secondary villi," and, within days, fetal capillaries form, turning these into "tertiary villi" [217, 242]. The formation of these new fetal blood vessels, including the umbilical cord, initially occurs via vasculogenesis, followed by a period of branching angiogenesis (development of new branches from existing vessels) that considerably increases the density of the fetal capillary network [217, 242], and may be stimulated by early placental hypoxia [243]. Around the same time as the fetus becomes viable (24-26 weeks), branching angiogenesis switches to non-branching angiogenesis (elongation of the current capillaries), which further expands the surface area of terminal villi available for maternal-fetal exchange [217, 242]. Several growth factors, including vascular endothelial growth factor (VEGF) and placental growth factor (PlGF), are produced by the placenta and function to promote angiogenesis [242].

Additionally, throughout this process, the trophoblast network also expands, with villous CT cells continually proliferating and replenishing the overlying syncytium, under the control of the transcription factor glial cells missing 1 (GCM1) and its downstream target syncytin-1 [244, 245]. However, eventually, the cytotrophoblasts become more dispersed, and the distance between the syncytiotrophoblasts and the fetal capillary endothelial cells thins [217, 242, 246, 247], thereby increasing the quantity of vasculo-syncytial membranes, regions where the maternal and fetal circulations are separated by 1-2 microns [248]. These changes improve the capacity for maternal exchange with the fetus, which becomes particularly important in the latter part of pregnancy when the rate of fetal growth is high. Using several methods of diffusion and active transport, as well as potential nutrient sensing mechanisms [241], oxygen, carbohydrates (especially glucose), water, lipids, fatty acids, vitamins, and additional nutrients are transferred to the fetus through the placenta, while carbon dioxide and waste products are preferentially

removed from the fetal circulation [217]. The functional placenta is also involved in metabolism, hormone production, and protection of the fetus against some foreign xenobiotics in the maternal blood [217, 249].

Given the considerable functions of the placental syncytiotrophoblasts, consistent turnover, apoptosis, and shedding of the syncytium is part of the healthy growth and maintenance of the villi [250, 251]. SynT release of extracellular vesicles, exosomes, and microvesicles into the maternal circulation is also thought to play an essential role in maintaining immune tolerance and conferring resistance to viral infection [252-254]. Furthermore, normal placental maturation leads to small placental infarctions and the accumulation of syncytial knots (aggregates of syncytial nuclei) on the surface of the terminal villi [255]. At 20 weeks, the portion of villi with syncytial knots is less than 10%; however, by term (37-40 weeks), knots are visible in ~28% of villi [255]. By the 36th week of gestation, placental growth has slowed, unless there is a pathological requirement for it to continue [246], fitting with the decreased expression of cell cycle genes in term placentas [256].

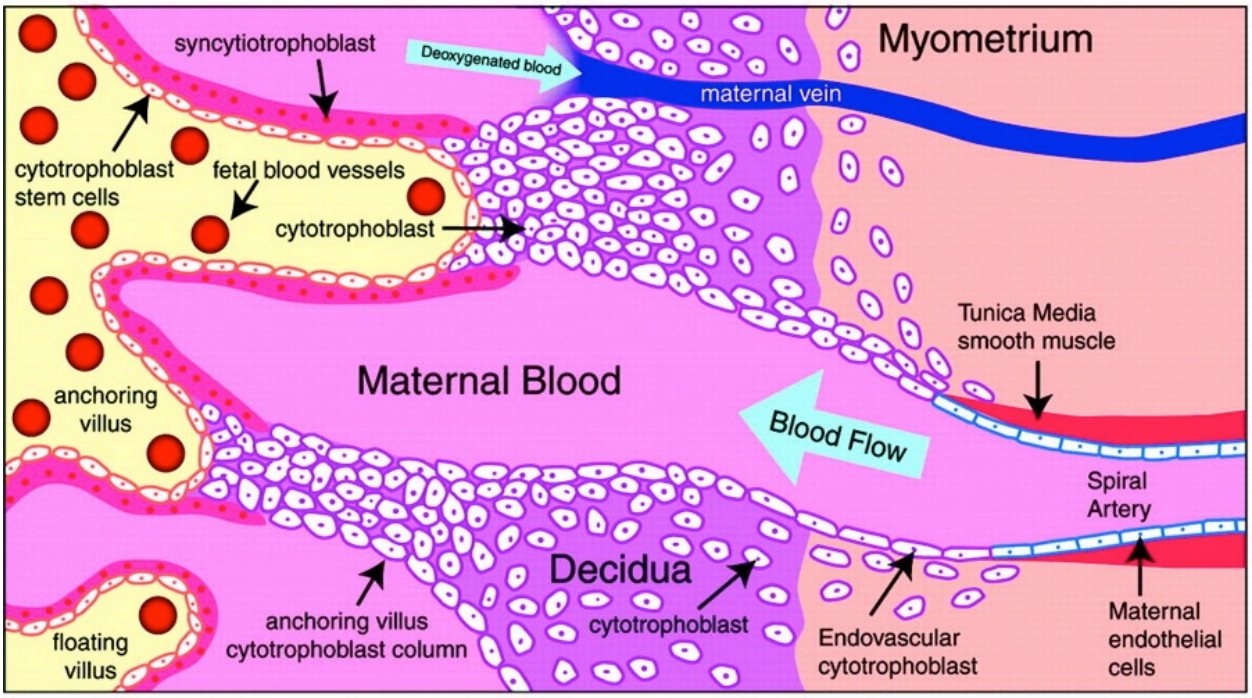

Figure 4 – Normal placental development. In healthy placentation, extravillous cytotrophoblasts invade the decidua and proximal third of the myometrium, anchor the placenta

to the uterus, and participate in transforming the maternal uterine spiral arteries into low-resistance blood vessels, allowing sufficient perfusion of maternal blood into the intervillous space. One type of extravillous cytotrophoblasts is the endovascular cytotrophoblast, which takes on an endothelial phenotype. Within the villous compartment, a continuous layer of fetal syncytiotrophoblasts, which constitute the site of maternal-fetal exchange, covers the floating villous trees. Under this syncytium are the highly proliferative villous cytotrophoblast cells, followed by the villous mesenchymal core encasing the fetal blood vessels. This figure is published in [257] and is reused here with permission from the publisher (**Appendix D**).

1.3.5 Sources of heterogeneity in the healthy placenta

By term, the healthy placenta is round/oval in shape, weighs 500-600 grams, and contains hundreds of terminal villi [258]. However, its multiple layers, different cell types, and large surface area make the normal human placenta a highly heterogeneous organ. EVTs in the center of the placenta have been suggested to demonstrate greater invasive activity and increased plugging of the maternal arteries than peripheral EVTs [259]. Maternal blood flow, therefore, commences in the peripheral regions of the placenta and is more forceful, leading to increased oxidative stress in this outer area [260]. Understandably, considerable evidence of transcriptional variability has been observed across the placenta [261], with differences in gene expression patterns based on both sampling depth and location [262, 263]. In one particular study, expression of FLT1 was found to be quite diverse across 12 sites in the normal placenta, and it was suggested that at least ten sites needed to be sampled to obtain a representative level of expression [264].

Furthermore, several fundamental differences between healthy placentas can significantly affect the observed gene expression. A considerable number of genes have demonstrated differential expression between male and female placentas, including many located on autosomes [262, 265, 266]. Interestingly, several of the genes upregulated in the female placenta are involved in immune tolerance [266], which may fit with the noted increased risk of placental pathology in male fetuses [267]. The occurrence of labor has also exhibited considerable impact on healthy placental gene expression. Uterine contractions have been linked to an interruption or reduction in uterine blood flow to the placenta, although umbilical blood flow to the fetus is not affected [268, 269]. Placentas associated with labor, therefore, demonstrate enriched expression of genes related to oxidative stress, apoptosis, and inflammation [270]. As such, fetal sex and occurrence

of labor are important considerations in the assessment of inter-patient transcriptional variation in normal term placentas.

1.3.6 Maternal adaptations to pregnancy

In order to handle the various demands of pregnancy, the maternal system undergoes a wide range of physiological adaptations, a number of which are cardiovascular in origin. Pregnant women demonstrate a 30-50% increase in total plasma volume, which is associated with an increase in water content and retention and is critical for the necessary increased blood flow to the placental/fetus, skin, and kidneys [241, 271, 272]. To accomplish this, the maternal heart rate (HR) and the cardiac stroke volume (SV; the amount of blood pumped out of the heart per beat) are significantly augmented during pregnancy, resulting in a dramatic rise in cardiac output (CO = HR x SV) [241, 271, 273]. In early pregnancy, systemic vascular resistance decreases considerably, due to the effects of progesterone, estrogen, and nitric oxide on the relaxation of the vascular smooth muscle [271, 273, 274]. As such, despite the elevated cardiac output, the maternal blood pressure decreases somewhat in early pregnancy, before rising again closer to term [271, 273]. The maternal heart also undergoes several structural modifications, with a physical rotation and shift upward, as well as an increase in muscle mass [271]. Notably, even in healthy women, vascular endothelial function progressively deteriorates throughout pregnancy [275].

Several other maternal systems are also subject to significant alterations during pregnancy. Despite a greater required oxygen consumption, maternal lung capacity is reduced, at least in part due to the physical elevation of the diaphragm [271]. As such, pregnant women naturally have a higher risk of hypoxia, and a large portion experience respiratory issues in the third trimester [271, 273]. Pregnancy is also linked to an expansion of the maternal pituitary gland, in addition to increased secretion of a number of pituitary hormones. Hemoglobin levels decrease throughout pregnancy, while white blood cell (WBC) counts are expected to climb [271]. Although pancreatic insulin secretion rises and glucose is rapidly consumed by the fetus, pregnancy is considered a state of insulin resistance, improving glucose availability for the fetus but sometimes resulting in gestational diabetes [271]. Additionally, the kidneys are displaced due to the expanding uterus, and the renal vessels dilate, producing a 40-50% increase in the glomerular filtration rate [271, 273]. As such, normal pregnancy is associated with some

anticipated proteinuria [271], making the diagnosis of abnormal protein levels and renal function somewhat more difficult in pregnant women.

1.4 Placental Pathology in PE and FGR

1.4.1 "Canonical" placental pathology

Numerous placental defects have been linked to the clinical development of preeclampsia and fetal growth restriction. The most commonly described, classic paradigm of placental pathology associated with these two disorders involves abnormal placentation. In this "canonical" model, EVT invasion of the uterine wall is shallow, resulting in limited remodeling of the uterine spiral arteries [276] (**Figure 5**). Perfusion of the placenta then demonstrates reduced quantity and/or quality, causing (hypoxia or hypoxia-reperfusion) injury and impaired nutrient/oxygen transfer to the fetus, leading to FGR. The damaged placenta also sheds higher than normal levels of fetal/syncytial material and debris into the maternal circulation, damaging the maternal endothelium and triggering PE development. This is the extremely well-characterized "two-stage" model of PE [277, 278].

Over 40 years ago, Brosens et al. described reduced trophoblast invasion and spiral artery remodeling in both PE- and FGR-associated deciduas [279, 280]. Since then, several mechanisms have been suggested to explain this poor invasion. It has been shown that in PE, the invading endovascular EVTs may fail to correctly mimic a vascular phenotype, demonstrating inadequate expression of the required adhesion molecules [281], although this was debated in later studies [282, 283]. Endothelial nitric oxide synthase (eNOS) expression by EVTs may affect dilation of the arteries and, by consequence, invasion [284]. This possibility is supported by findings in placenta accreta research where the trophoblast is overly invasive [285], but less evidence is available in the PE and FGR fields [286]. Insufficient timing or quantity of oxygen delivery may result in poor differentiation of cytotrophoblasts into an invasive phenotype [287], while abnormal secretion of various growth factors by the syncytium likely also has an important role [288]. Furthermore, it is feasible that in some PE pregnancies, defective maternal decidualization is involved in the development of the pathology [289], while there is substantial evidence that trophoblasts within the uterine wall may be subject to increased apoptosis in PE

and FGR [290]. Although maternal macrophages are common in the decidua, they usually are in low abundance in the maternal arteries [291]. However, in PE/FGR, they appear to be recruited in significant numbers to the spiral arteries, and, through the actions of tumor necrosis factor α (TNFα), have been shown to induce endovascular EVT apoptosis [291-294], thereby dramatically affecting remodeling efforts.

If this poor invasion occurs, it is strongly associated with chronic hypoxia within the placenta, which in turn promotes a non-invasive cytotrophoblast phenotype, further exasperating the problem [6]. The timing and pattern of maternal perfusion are also important. If invasion and trophoblast plugging of the spiral arteries is poor, this can result in the premature and widespread onset of maternal blood flow, as opposed to the controlled peripheral to central pattern of exposure observed in a healthy placenta [260, 295], in addition to turbulent blood flow, causing damage [240]. In its most severe form, this is significantly linked to miscarriage [260, 295]. Furthermore, if artery remodeling is incomplete and smooth muscle still exists in the vessel walls, this can result in spontaneous vasoconstriction, leading to intermittent blood flow and hypoxia-reperfusion injury (**Figure 5**) [240, 296].

This abnormal placental perfusion and hypoxia/hypoxia-reperfusion state induces a number of stress-related changes in the villous trees [297]. Hypoxia leads to elevated expression of FLT1, possibly through the actions of HIF, and decreased expression of PlGF by the trophoblast [298, 299], which has been shown to inhibit angiogenesis in the placenta [300]. Additionally, fetal endothelial cells are shifted towards a vasoconstricted phenotype [301], and smooth muscle cells around the fetal arteries are dedifferentiated [302], resulting in increased placental resistance [303]. Blood flow through the two umbilical arteries, carrying deoxygenated blood and waste, should be in the forward direction from the fetus to the placenta. However, if the placental vascular resistance becomes too high, this blood flow will decrease, then become absent (absent end-diastolic flow (AEDF)), and then reverse towards the fetus (reversed end-diastolic flow (REDF)) as increasing resistance is observed [302]. Both AEDF and REDF are significantly associated with FGR and fetal hypoxia [242, 302, 304]. Moreover, placental hypoxia induces degradation of the transcription factor GCM1 in the trophoblast, along with its target syncytin-1 (an endogenous retroviral gene) [298]. This results in reduced cell-cell fusion of the cytotrophoblasts and, therefore, decreased syncytialization [244, 305], affecting nutrient transport across the syncytium and contributing to FGR development [6, 306]. In both PE and

FGR, oxidative stress and this impaired cell-cell fusion are also linked to increased trophoblast senescence and apoptosis/necrosis [307-309].

In the healthy placenta, some syncytial apoptosis and shedding into the maternal circulation is expected for normal trophoblast turnover. However, in abnormal placentas, substantially increased rates of shedding, as well as changes in shed content, are observed, leading to an exacerbated maternal response, and the second stage of the "two-stage" PE model. Released syncytial debris includes soluble factors, cell-free DNA, and extracellular vesicles, such as macrovesicles/apoptotic bodies, microvesicles, and exosomes [250, 252, 310, 311]. The type of secretions depends on the type of placental injury. For example, it has been shown that hypoxia favors necrotic shedding, as the proteins required for apoptosis can't reach the syncytiotrophoblast due to the lack of cell fusion, while intermittent placental perfusion/hypoxia-reperfusion damage stimulates apoptosis [296, 309]. PE extracellular vesicles also exhibit changes in cargo compared to normal vesicles [312].

The increased rate and volume of shed syncytial factors into the maternal blood are thought to act either directly or indirectly on the widespread maternal endothelium, causing damage and vasoconstriction [313, 314], and the multi-organ clinical signs of preeclampsia. In several studies, vesicles from PE placentas were revealed to be capable of activating the maternal endothelium [315, 316], with necrotic debris demonstrating preferential activation over apoptotic debris [317]. However, it was recently shown that the maternal endothelial dysfunction in PE is predominately mediated by soluble factors, not extracellular vesicles [311, 318]. Pathogenesis surrounding these soluble factors generally focuses on the anti-angiogenic molecule soluble FLT1 (sFLT1), an antagonist of VEGF, expressed in the trophoblast and found highly elevated in women with PE. In a healthy pregnancy, VEGF signals through its surface receptors FLT1 and kinase insert domain receptor (KDR) on the maternal vasculature [319], mediating endothelial health and angiogenesis [75]. In PE, excess soluble FLT1 sequesters VEGF in the maternal blood, limiting its ability to bind to receptors on the vasculature and function normally [319]. In particular, reduced VEGF activity has a significant impact on the glomerular endothelium and podocyte of the kidney, leading to proteinuria [320]. In animal models, sFLT1 administration induces a hypertensive preeclampsia-like phenotype, possibly also involving the increased production of endothelin-1, a potent vasoconstrictor [321, 322]. Also important for endothelial health is TGF-β signaling, which acts through a receptor complex that includes endoglin (ENG)

[319]. In PE, elevated soluble endoglin (sENG) is also secreted from the trophoblast, antagonizing TGF-β, and contributing to maternal endothelial dysfunction [311, 319, 323]. Compellingly, co-administration of sFLT1 and sENG in pregnant rats leads to simultaneous signs of severe PE, HELLP syndrome, and FGR [323]. In humans, the impact of PE on the maternal endothelium can be observed even after pregnancy, as these women demonstrate both decreased dilation and increased vasoconstrictor sensitivity [100, 324]. Interestingly, the development of maternal hypertension has also been suggested to be an adaptive response to placental insufficiency, attempting to maintain adequate blood flow to the placenta and fetus [242]. This is supported by evidence that a significant reduction in maternal blood pressure due to anti-hypertensive medications can affect fetal growth [80].

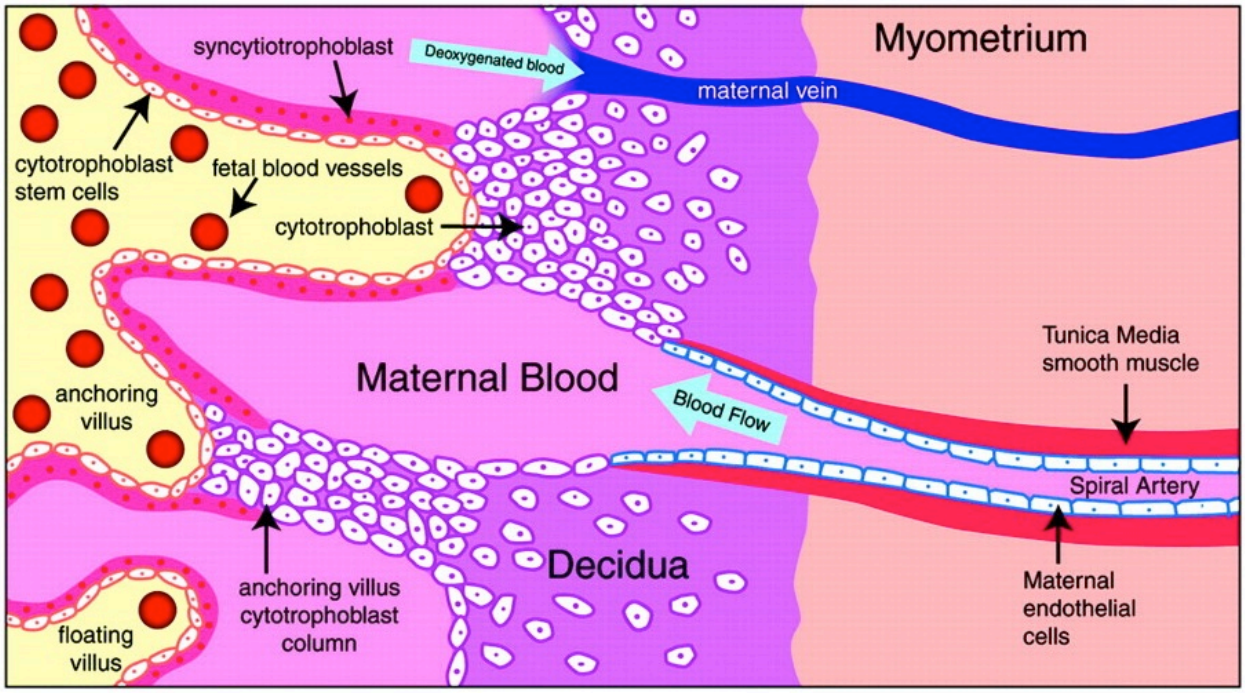

Figure 5 – Placental insufficiency in the two-stage model of preeclampsia. Shallow invasion of the uterine wall leads to limited remodeling of the uterine spiral arteries. Perfusion of the placenta then demonstrates reduced quantity and/or quality, causing hypoxia or hypoxia-reperfusion injury and reduced nutrient transfer to the fetus. The damaged placenta also sheds higher than normal levels of fetal/syncytial material and debris into the maternal circulation, damaging the maternal endothelium and triggering the maternal symptoms of preeclampsia. This figure is published in [257] and is reused here with permission from the publisher (**Appendix D**).

1.4.2 Additional or alternative evidence of placental pathology

A number of additional placental abnormalities have also been described in PE and FGR that are not directly related to poor invasion and spiral artery remodeling. Placental shape and viscoelasticity have been observed to be important for fetal growth, with non-oval/round shapes indicating problems with the underlying vasculature and villous tree structure of the organ [325], while reduced placental stiffness and viscosity may have consequences for functionality in FGR [326]. Abnormal vasculature is also linked to a non-central location of the umbilical cord insertion into the placenta, which has additional implications for transport efficiency, further affecting fetal growth [327]. In FGR, dysfunctional transport mechanisms across the placenta have been noted for several nutrients, including calcium and amino acids [328-330].

Confined placental mosaicism (CPM), a chromosomal abnormality only observed in the placenta, not the fetus, has also been associated with both PE and FGR [331-333]. CPM can occur through either a later mutational event specifically in the cell type(s) forming the placenta ("mitotic" CPM), or can occur if the original conception is chromosomally abnormal, but the cells destined to become the embryo are "rescued" ("meiotic" CPM) [334]. Furthermore, CPM can be classified into three types: type I (aneuploidy only in the trophoblast), type II (aneuploidy only in the villous stroma), and type III (aneuploidy observed in both the trophoblast and villous stroma (likely meiotic)) [334]. Meiotic/type III CPM, in particular, has been linked to abnormal pregnancy outcome, especially FGR [334, 335]. Moreover, considerable variability has been observed regarding the pattern of CPM across the placental tissue, with some sites demonstrating 100% trisomy, while others nearby are chromosomally normal [336]. This has important implications for the sampling and assessment of placental tissue.

Interestingly, manifestations of PE have been observed that do not have a significant placental component [337, 338]. In this "one-stage" model of PE, women enter pregnancy with pre-existing endothelial dysfunction, either due to a clinically evident predisposition, such as chronic hypertension or obesity, or an unknown sub-clinical pathology. In these cases, PE may develop in women who are simply unable to adequately adapt to the normal physiological demands of pregnancy [212, 338, 339]. This model of PE would not be expected to co-occur with FGR [338].

Additionally, a "three-stage" model of PE has also been proposed, adding a step prior to poor placental perfusion, early in pregnancy, where tolerization of the maternal system to the semi-allogeneic fetus is incomplete [340, 341]. In this new first stage, the highly polymorphic HLA-C, with more than 100 alleles, is likely involved, as the combination of a fetal HLA-C belonging to the HLA-C2 group and a maternal KIR receptor AA genotype is significantly affiliated with the development of preeclampsia and low neonatal birth weights [228, 342]. This combination of KIR and HLA-C genotypes has been further observed in recurrent miscarriage cases [343]. The abherrent expression of indoleamine dioxygenase 2,3-dioxygenase (IDO), an immune-regulating enzyme, early in pregnancy by the decidua and the trophoblast may be an additional contributor, as its presence has been shown to promote a regulatory phenotype in T cells [344-346]. A mouse model treated with an IDO inhibitor supports this claim, as this induces the specific rejection of allogeneic fetuses [340, 347]. Additional evidence of abnormal immune activity in PE is also obtained from a study revealing the activation of leukocytes in the maternal blood as they enter the uterus in PE, but not healthy, pregnancies [348]. Furthermore, an early source of pathology associated with the maternal-fetal interface and the trophoblast has been proposed in cases of maternal antiphospholipid syndrome where autoantibodies are involved and the likelihood of miscarriage and immune rejection is high [349, 350].

1.4.3 Transcriptional observations

In recent years, researchers have begun to employ genome-wide microarray analysis of placenta samples to better understand the differences in placental gene expression between PE/FGR and healthy control pregnancies. In FGR, this analysis has been somewhat successful with a few genes showing differential expression across multiple studies (ex. leptin (LEP), interleukin-1 receptor accessory protein (IL1RAP), and follistatin-like 3 (FSTL3)), and involved in pathways such as angiogenesis, hypoxia, inflammation, endocrine signaling, and metabolism [351-356]. Upregulation of several other genes related to growth and metabolism, such as insulin-like growth factor-binding protein 1 (IGFBP-1), prolactin (PRL), and corticotropin-releasing hormone (CRH), have also been discovered in FGR placentas [351, 355, 357]. Of these, the expression of LEP, IGFBP-1, and CRH genes were all shown to negatively correlate with infant birth weight [351]. CRH has been linked to glucose transport in the placenta, which is likely its main line of impact on fetal growth; however, interestingly, CRH expression increases with gestation, resulting in its actions as a "placental clock," involved in the timing of delivery [358,

359]. Leptin, an adipocyte-derived hormone with considerable known functions in nutrient balance, has been recently shown to be highly upregulated in activated endothelial cells, potentially contributing to "canonical" placental pathology [360], but may also be involved in promoting immune tolerance and reducing apoptosis [361]. Additionally, in one study, IDO was reported as differentially expressed in FGR placentas [354], indicating an immune modulation pathology, while in another, FLT1 levels were elevated [355], implying aberrant angiogenesis. The increased expression of FLT1 in FGR placentas has been further confirmed by targeted analysis [362].

Preeclamptic placentas have been even more extensively examined by genome-wide microarray analysis. These studies fairly consistently identify upregulated FLT1 and ENG compared to the controls, as well as elevated LEP, FSTL3, pappalysin 2 (PAPP2), HtrA serine peptidase 1 (HTRA1), inhibin A (INHA), and inhibin B (INHBA), which are involved in cell signaling, lipid response, apoptosis, hypoxia, immune, inflammation, and oxidative stress pathways [353, 363-371]. Additionally, HTRA1 has been specifically implicated in trophoblast migration and invasion [372], while the inhibin A level in maternal blood is regularly employed as part of second-trimester screening for fetal Down syndrome (trisomy 21) [373]. Furthermore, a single study investigating gene expression in HELLP syndrome-affected placentas found a similar transcriptional pattern to early-onset PE samples [374], indicating a common placental pathology in these two pregnancy states.

While the number of samples in each individual PE microarray study has been fairly small, several groups have chosen to combine the power of multiple cohorts by performing meta-analyses [375-379]. One of the first PE meta-analyses was performed by Kleinrouweler et al. in 2013 using 14 individual microarray datasets with a total of 159 PE patients [376]. Based on the original author-defined lists of significantly differentially expressed genes, only 40 genes were independently discovered in at least three out of the 14 studies [376]. These included LEP, FLT1, INHBA, ENG, INHA, CRH, HTRA1, PAPPA2, and FSTL3 [376]. Almost concurrently, a meta-analysis was published by Vaiman et al. assessing six studies with 79 PE cases and 96 controls [375], while another one was completed by Moslehi et al. with four of these six studies for a total of 50 PE placentas and 53 control placentas [377]. Despite utilizing similar sample sets, Vaiman et al. observed only 98 significant genes, involved in signaling, blood vessel size, and oxidative stress, while Moslehi et al. noted 419 significant genes, associated with growth factor signaling,

hypoxia, immune response, and carbohydrate metabolism [375, 377]. Although the globally altered pathways were similar, and all known to be involved in PE, the discrepancy in the number of identified genes of interest was likely due to fundamental differences in the two study designs: Moslehi et al. were stricter and more biased with their dataset selection, only including those where the PE and control patients already appeared sufficiently different by principal component analysis (PCA), and calculations of significance were performed in an integrative manner by averaging p-values and fold-changes, whereas Vaiman et al. employed a vote counting method [375, 377].

Since then, a couple of other PE microarray meta-analyses have been conducted using improved statistical methods, where raw data was downloaded, pre-processed, and sometimes aggregated [378, 379]. In 2015, van Uitert et al. performed a meta-analysis of 11 PE-focused microarray experiments, involving 116 preeclamptic placentas and 139 controls, including two of their own cohorts and two additional datasets where the original authors had not previously made their data available to external researchers [378]. This assessment revealed a 388-gene PE meta-signature, including the majority of the 40 genes discovered by Kleinrouweler et al. [376]. These 388 genes demonstrated a 77% overlap with those identified by Vaiman et al. and a 44% overlap with Moslehi et al., and were highly involved in hypoxia pathways [378]. In 2016, Brew et al. published a meta-analysis of 167 samples (68 PE and 99 control placentas) [379]. Using a ranking system, 9540 genes were deemed significant in PE patients and were linked to a wide range of pathways including TGF-β signaling, metabolism, allograft rejection, VEGF signaling, and apoptosis [379].

However, despite the discovery of many known PE and FGR genes and pathways in these individual and meta-analysis cohorts, these were all generally performed using whole placenta tissue biopsies without consideration for cell composition. In fact, even more surprisingly, all of these PE meta-analyses, except for Brew et al., included a dataset [380] where tissue was clearly obtained from the maternal-fetal interface despite stating that their investigations were focused on the placental villi. As it is well established that the various placental cell types and compartments are involved in different functions, these are significant limitations. In order to attempt to rectify this, a 2012 study focused on placental endothelial cells in FGR, isolated using a magnetic bead method [381]. However, this approach was not particularly successful as it discovered few significant genes [381]. More recently, a separate group employed laser

microdissection to specifically enrich for syncytiotrophoblast, interstitial EVT, and endovascular EVT sub-populations within PE and control placentas (N=4 for each) [382]. The PE syncytiotrophoblast data revealed dysregulation of immune functions, transport, and responses to VEGF and progesterone; the interstitial EVTs demonstrated abnormal cell movement, and immune, lipid, oxygen, and TGF-β responses, while the PE endovascular EVTs exhibited changes in metabolism, signaling, and vascular development compared to controls [382]. Therefore, while small, this study, and another recent one involving single-cell placental transcriptomic analysis [383], are important first steps towards the investigation of cell type-specific transcriptional modifications in PE (and FGR) placentas.

1.4.4 Histological observations

PE and FGR placentas have also been extensively examined microscopically by histopathology. Although perhaps more biased than transcriptional analysis, and associated with inter-observer reliability issues [384], only histology, from its higher scale perspective, is truly capable of assessing the final effect of all the molecular changes on the structure of the placenta, the relationships between cell types, and the overall functionality of the tissue, which are essential for understanding the underlying pathological etiologies. Histological examination of placentas can identify a wide range of lesions, and methods for diagnosing and classifying these features have been highly debated in the field. Fortunately, a recent consensus statement was published defining these lesions and their mechanistic affiliations [385, 386]. The pathological features most frequently observed in PE and FGR samples, and most relevant to the current thesis, are generally those involved in maternal vascular malperfusion [150, 387-389], fetal vascular malperfusion [150, 387], maternal-fetal interface disturbance [150, 390-392], or chronic inflammation [150, 222, 393].

Maternal vascular malperfusion (MVM) consists of lesions associated with reduced perfusion of the placenta/hypoxia, high-velocity malperfusion, and/or hypoxia-reperfusion injuries [385, 394], fitting with the “canonical” placental etiology of inadequate or incorrect trophoblast invasion and spiral artery remodeling. Histological features of this MVM pathology include placental infarctions, syncytial knots, distal villous hypoplasia, advanced villous maturity, and focal perivillous fibrin. Placental infarction is often appreciated on a gross pathology exam, and is seen on the fixed placenta as a tan region (old infarct) or a red region (new infarct). It is observed

when blood flow to the placenta is interrupted, causing cell death/necrosis [385]. These, along with syncytial knots, are progressively more common with increasing gestational age [255], but are observed with excessive size and frequency in the pathological PE/FGR placenta and can impact the transport of nutrients [242]. By histology, true syncytial knots can be difficult to separate from false knots, which are artifacts of sectioning, and syncytial sprouts, an indication of trophoblast proliferation [395]. However, understandably, true knots uniquely demonstrate markers of nuclear senescence and oxidative damage [395]. Distal villous hypoplasia (DVH) is characterized by poorly developed villous trees, appearing both sparse and thin by histopathology, with a widening of the intervillous space and increased syncytial knots [385, 396]. DVH has been linked to the appearance of a "wobbly" placenta on ultrasound during pregnancy [150]. This lesion fits with the knowledge that hypoxia/hypoxia-reperfusion damage can have a substantial impact on the developing villous tree, in terms of both the vasculature and the trophoblast [298, 300]. Advanced villous maturity (AVM) can be a difficult lesion to diagnose, especially near term, as it is defined by placental villi that appear more mature than would be expected in a healthy placenta at the same gestational age [359, 385]. Gene markers of normal villous maturity have also been shown to be prematurely elevated in AVM samples [359]. In general, AVM is considered to be an adaptive response of the placenta to insufficient perfusion and hypoxia, involving an expansion of the fetoplacental capillary network and an increasing of vasculo-syncytial membranes to improve gas exchange [242, 385]. Finally, focal perivillous fibrin presents with an increased coating of fibrin, a protein involved in the clotting of blood, on some of the villi [397]. This lesion is thought to be caused by damage/trauma to the syncytium, resulting in exposure of the underlying cytotrophoblasts, which induces their secretion of fibrin, covering the damaged syncytiotrophoblasts and forming a new barrier [397-399]. Currently, as a focal (non-diffuse) lesion, it has consistently been classified as a consequence of maternal vascular malperfusion [385]. Overall, severe MVM pathology has been associated with a number of clinical attributes, such as early deliveries, severe PE clinical presentations, low birth weights, and reduced placental weights [359, 400-403].

Lesions categorized under the term fetal vascular malperfusion are linked to an obstruction of the fetal blood flow, often due to a mechanical disruption of the umbilical cord [150, 385, 404]. Most relevant to the current project is the avascular fibrotic villi lesion. This is diagnosed by the observation of three or more regions of villi that show a loss of fetal capillaries and increased

density of the stromal connective tissue ("bland hyaline fibrosis") [385]. The severity of this feature depends on how many villi are involved in each region: 2-4 terminal villi is classified as small, 5-10 is intermediate, and more than ten villi is considered large [385].

Less frequently described, and much more rare, are lesions affiliated with a maternal-fetal interface disturbance, such as massive perivillous fibrin deposition (MPFD), maternal floor infarction (MFI), and intervillous thrombi. MPFD and MFI are related pathologies characterized by the excessive deposition of fibrin (the use of the word "infarction" in MFI is a recognized misnomer) [405]. The distinction is based on the location of the fibrin: in MFI, it is observed along the maternal floor/basal plate of the placenta, the site of maternal-placental contact, while MPFD is diagnosed by excessive fibrin in the intervillous space, taking up at least 30% of the intervillous volume, if not more [405] (**Figure 6**). This exaggerated quantity of fibrin is thought to physically impede the placental capacity for maternal-fetal exchange, resulting in reduced fetal growth [406]. As such, the severe forms of these lesions are usually lethal and strongly associated with miscarriage and stillbirth, with exceptionally high recurrence rates (>70%) [150, 390, 391, 405, 407-409]. While the general mechanism of fibrin deposition in the placenta has been thoroughly investigated (and briefly described above), the etiology of MPFD and MFI is still not fully elucidated. However, the most commonly proposed explanation is an immune rejection of the fetoplacental unit by the mother. This is supported by the increased risk of these lesions in women with autoimmune disease [391, 409, 410], as well as evidence of antibodies against fetal MHC class I and class II molecules and increased concentrations of CXCL-10, a T-cell chemokine associated with rejection, in the maternal plasma in pregnancies diagnosed with placental MPFD/MFI [406]. In these cases, maternal immune cell attack might be expected to be involved in the trophoblast damage leading to fibrin deposition. Additionally, MPFD/MFI has been linked to a different abnormal pattern of sFLT1, sENG, and PlGF levels in the maternal blood than usually observed in cases of PE and FGR [411], suggesting an angiogenic contribution. Intervillous thrombi, the remaining lesion in this category, are blood clots in the intervillous space, recognized based on lamina of fibrin within a mix of red and white blood cells, possibly of both maternal and fetal origins [412]. These have also been suggested to occur in the proximity of damaged trophoblasts [412]. Unlike most histopathological features, intervillous thrombi are reasonably identifiable during pregnancy by ultrasound, often noted as "echogenic cysts" [150].

An additional group of histological lesions sometimes observed in PE and FGR placentas are those affiliated with chronic inflammation, identified based on the discovery of increased maternal immune cells within the placenta, causing destruction [222]. Of particular interest within this category are lesions that involve inflammation of the villi ("villitis"), such as infectious villitis and villitis of unknown etiology (VUE), as well as chronic intervillositis. Infectious villitis is noted when the specific pattern of placental villous inflammation suggests an infectious agent, such as CMV or toxoplasmosis [413]. VUE is diagnosed when the villous inflammation has no clear source and involves the infiltration of maternal T cells into the villi and the activation of the fetal (placental) Hofbauer cells [222, 393]. Interestingly, however, VUE has been suggested to have a maternal anti-fetal rejection etiology in many cases, similar to MPFD/MFI [222, 414, 415], and has been observed at higher frequencies in oocyte donor pregnancies [416]. The villous inflammation in VUE can be low grade or high grade, with low grade (inflammation affecting less than ten villi in any given region) commonly observed and with limited clinical relevance [150, 385]. On the other hand, high-grade VUE (more than ten inflamed villi across multiple regions) demonstrates greater clinical significance and high recurrence rates (~37%) [150, 385, 417]. Finally, chronic intervillositis presents with infiltrating histiocytes (tissue macrophages) into the intervillous space, and is associated with increased fibrin material and very high recurrence risk (67-80%) (**Figure 6**) [418-420]. This lesion has been suggested to have mechanistic similarities to villitis [421], and, therefore, may also be involved in the maternal rejection of the placenta/fetus [422].

A few additional lesions are frequently observed in placental pathology, although they do not demonstrate the same significant relationships with PE and FGR development. Delayed villous maturity is characterized by villi that appear less mature than expected for their gestational age, demonstrating more stroma, more centralized fetal capillaries, and decreased vasculo-syncytial membranes [359, 385]. This lesion is easier to diagnose near term and is affiliated with aberrant expression of normal villous maturity gene markers [359]. The presence of meconium histiocytes in the placenta is linked to fetal distress and prolonged labor [423]. Lastly, acute (histological) chorioamnionitis is a group of histological observations involving inflammation of the fetal membranes (chorion and amnion) that is strongly associated with ascending intrauterine infection (also called clinical chorioamnionitis) and preterm birth [424, 425].

1.5 Potential biomarkers and interventions for PE and SGA/FGR

Given the importance of avoiding fetal stillbirth and maternal complications, considerable effort has been applied towards predicting women and fetuses at high risk of PE and/or FGR development early enough in pregnancy such that treatment to prevent or reduce poor clinical outcomes can be administered. In this case, accurate identification of all SGA fetuses, not necessarily just those with FGR, would still be a good step towards the primary goal of averting stillbirth [111]. Furthermore, once pathology has been predicted, it is also essential that the appropriate prophylactic treatment is provided [426].

1.5.1 Molecular biomarkers

Some of the first molecular biomarkers in maternal serum investigated for the prediction of PE and FGR were those that are often involved in fetal aneuploidy screening during pregnancy: hCG and pregnancy associated plasma protein (PAPP-A) in the first trimester and hCG, alpha-fetoprotein (AFP), unconjugated estriol (uE3), and/or inhibin A in the second trimester [427]. In the absence of fetal aneuploidy or neural-tube defects, abnormal levels of these molecules have been linked to several adverse obstetrical outcomes [428-430]. Women with combinations of low uE3, low PAPP-A, high AFP, and/or high hCG demonstrated an increased risk of fetal loss and/or preterm birth in a large Canadian population [431]. Additionally, in a systematic review, elevated AFP and hCG exhibited high likelihood ratios for predicting PE (5.7) and SGA (6.2) [432], which may be associated with accelerated differentiation of the villous cytotrophoblasts (i.e., AVM) [433]. However, in a separate study, decreased PAPP-A, not high hCG, revealed significant predictive value for FGR (odds ratio 2.9) and PE (odds ratio 2.3) [434]. Ultimately, none of these molecules perform particularly well for the prediction of PE and SGA/FGR [432, 435], although these are still the molecular markers most commonly utilized in the clinic due to their dual function and widespread availability.

In the past decade, the most frequently studied potential serum biomarkers for PE and FGR have been the anti-angiogenic factors sFLT1 and sENG, as well as the pro-angiogenic factor PlGF, all of which are produced and secreted by the placental trophoblast. In a healthy pregnancy, sFLT1 and sENG levels are expected to increase with gestational age, while PlGF has been shown to decrease (after peaking between 25-30 weeks), suggesting normal levels of elevated oxidative stress in the latter part of pregnancy [65, 436, 437], and fitting with the previously mentioned

normal progressive deterioration of maternal vascular endothelial function [275]. In two seminal papers in 2004 and 2006, Levine et al. demonstrated that in women destined to develop PE, circulating levels of sFLT1 and sENG were significantly elevated as early as 20 weeks of gestation, 1-3 months before the onset of clinical symptoms, compared to healthy women, while serum PlGF levels were significantly decreased by 16 weeks [65, 438]. Furthermore, the measured values were most severe in patients who went on to deliver preterm and/or with an SGA infant [65, 438]. However, considerable overlap still exists when the expression patterns of these biomarkers are examined in controls and PE women [65, 438, 439]. As such, in 2012, by which time more than 30 studies had been performed investigating these markers, a meta-analysis revealed that these proteins provide only modest predictive value for PE, with an accuracy of 0.72, 0.67, and 0.75 for sFLT1, sENG, and PlGF, respectively, corresponding to a sensitivity of only 0.26, 0.18, 0.32, respectively, at a 5% false-positive rate [440]. These values can be somewhat improved by using the ratio of circulating sFLT1 to PlGF [441], measuring closer to the onset of symptoms [442], or by combining the assessment of PlGF with maternal serum screening markers [443, 444]. Moreover, although somewhat debated, these angiogenic markers appear to have less predictive value for normotensive FGR than for PE [445-450], while accumulating evidence also suggests that sFLT1, sENG, and PlGF may in fact be predicting the presence of common maternal vascular malperfusion lesions in the delivered placentas [451-454], not the maternal and fetal disease symptoms themselves. In Toronto, measuring PlGF levels for the prediction of preeclampsia has been recently implemented, while its utilization Canada-wide is currently under consideration [455].

A wide range of additional molecular biomarkers have been proposed for both PE and FGR. These include molecules related to metabolism (ex. leptin), hormone activity (ex. placental protein 13 (PP13)), oxidative stress (ex. malondialdehyde, a product of free radical attack), and immune activity (ex. C-reactive protein) [456-468]. Additionally, some placental nucleic acids shed into the maternal circulation (cell-free fetal DNA, mRNAs, and miRNAs) demonstrate reasonable predictive value for PE and/or FGR development early in gestation [460, 469-471], while several markers of maternal status, linked to renal or hematological dysfunction, have also been explored with moderate success [472, 473]. However, systematic reviews of potential biomarkers for PE and FGR failed to find even a single molecular molecule with sufficient accuracy across the spectrum of cases for recommended use in clinical practice, citing

heterogeneity of the sample sets and inconsistent study designs as the culprits [450, 474]. As such, further investigation and additional possible biomarkers are required.

1.5.2 Imaging and clinical biomarkers

Ultrasound is the primary method of placental and fetal imaging during pregnancy (**Figure 6**). Fetal biometry, including head circumference, abdominal circumference, and femur length, are commonly employed indications of an SGA infant [475-477], although perhaps not overly accurate ones [478], while first trimester placental thickness has been demonstrated to be lower in future SGA pregnancies and higher in future PE pregnancies than in controls [479]. Additionally, Doppler ultrasound can be employed to assess blood flow to the placenta and fetus during pregnancy, particularly in the uterine and umbilical arteries. Relevant to the current thesis, this can be measured using the pulsatility index (PI), which is related to the velocity of blood flow, and the presence or absence of unilateral/bilateral uterine artery notching, indicating an increase in uterine artery resistance. In a non-pregnant woman, uterine artery PIs are high, and notching is present, restricting blood flow to the uterus. In healthy pregnancies, uterine and umbilical PIs are expected to decrease throughout gestation [480, 481], and uterine notching should disappear. As such, elevated uterine PIs and the presence of notching are signs of abnormal blood flow and have been linked to both PE and FGR. In a large study of 11,667 women, increased uterine artery PI in the second trimester was able to predict 59% of early-onset PE and 60% of early-onset FGR [482]. Unfortunately, however, these are some of the highest percentages observed. In a meta-analysis of 55,974 pregnancies, the sensitivity of abnormal uterine artery waveforms for identifying early-onset PE was only 48% (26% for all PE) and was even lower for early-onset FGR (39%; 15% for all FGR) [483]. Uterine artery notching is less frequently assessed, and may or may not improve prediction of PE or FGR (35-76% sensitivity) [444, 483-487]. These uterine Doppler ultrasound metrics are, therefore, insufficient for the discovery of all high-risk pregnancies [150], although it has also been proposed that, like the angiogenic biomarkers sFLT1, sENG, and PlGF, uterine artery PI is actually a strong predictor of maternal vascular malperfusion lesions in the resulting placenta, just not the diagnosis of PE or FGR itself [488, 489].

In contrast to the uterine arteries, umbilical artery blood flow has been considerably less studied as a biomarker. There is some evidence suggesting that elevated umbilical artery PI may have

predictive value for FGR [490-492]; however, the clinical utility is usually confined to situations where absent or reversed end-diastolic flow (AEDF/REDF) is observed, as this is significantly linked to poor fetal outcomes (**Figure 6**) [493, 494]. As such, current imaging techniques often miss a large portion of high-risk pregnancies. Recently, new methods of magnetic resonance imaging (MRI) have been proposed, which may be able to more accurately measure blood flow and oxygen delivery to the fetus [495]. Specifically, MRI measurements of the fetal superior vena cava and umbilical vein may provide new imaging biomarkers for FGR [496].

Furthermore, in the past few years, a number of additional clinical maternal measurements have also been suggested to have predictive potential in pregnancy, especially for PE. Several changes in maternal hemodynamics have been found to occur well before the onset of clinical symptoms, such as increased total peripheral resistance, increased augmentation index (a measure of arterial stiffness), increased blood pressure, decreased endothelial function, and decreased skin capillary density [497-501]. Interestingly, in one study, cardiac output at 14 weeks had predictive value for FGR, while stroke volume identified those at highest risk of PE development [502]. The inclusion of blood pressure measurements could also improve these predictions [502]. However, a large study with >3500 women found that 39 known risk factors at 14-16 weeks of gestation, including maternal age, BMI, blood pressure, family history, prior miscarriage, and cigarette smoking, could only predict 20-27% of future PE patients at a 5% false positive rate (FPR) [503], in line with the values observed in other cohorts [504]. As such, similar to the molecular studies, none of these individual imaging or clinical metrics can identify all women and fetuses at risk of PE and FGR.

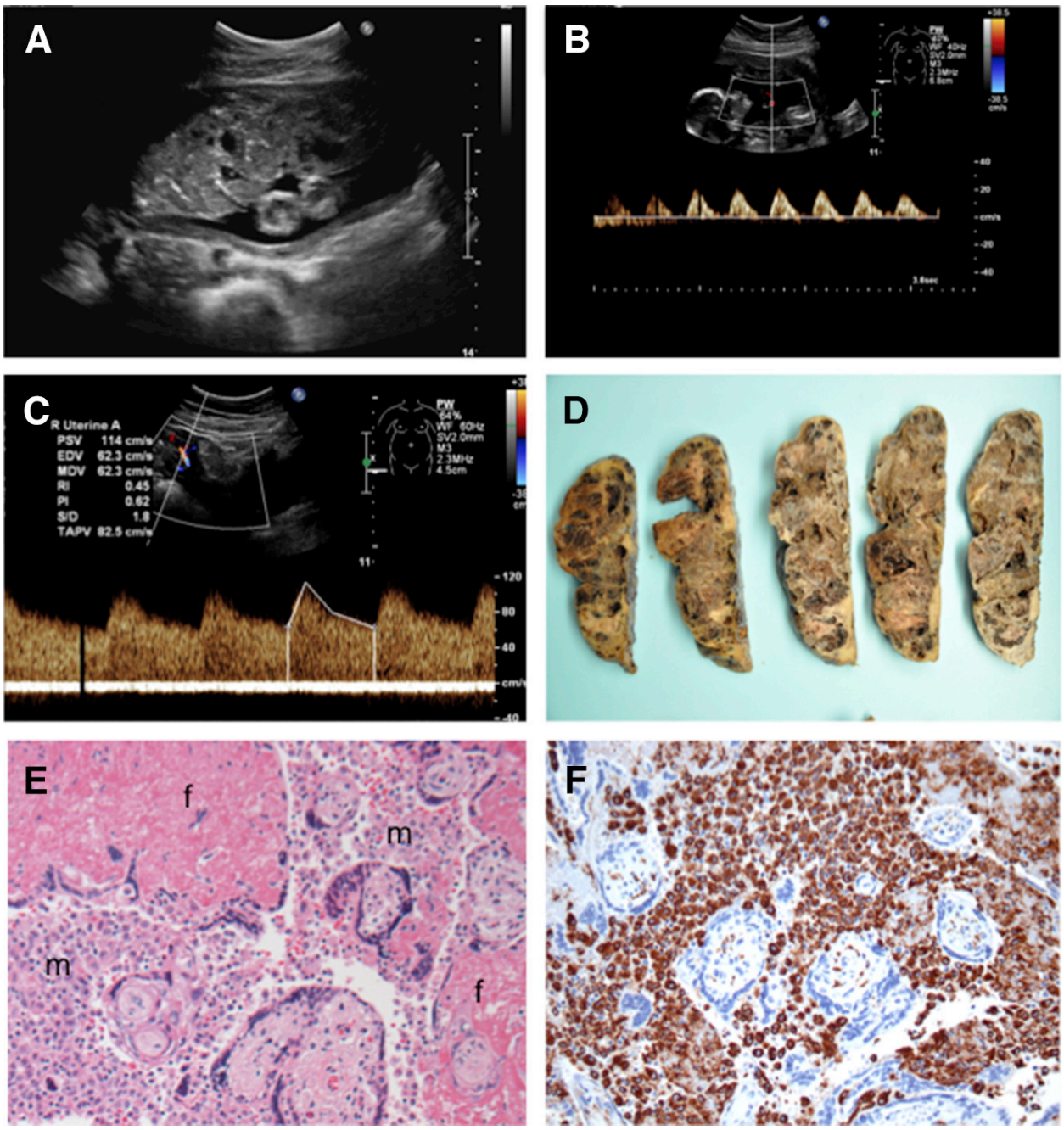

Figure 6 – Example Doppler ultrasound and histopathological data. (**A**) An ultrasound identified an fetus at 28 weeks with suspected FGR. Doppler waveforms revealed (**B**) absent end-diastolic flow (AEDF) in the umbilical arteries, but (**C**) normal uterine artery blood flow. (**D**) Gross pathology noted extensive fibrin replacement of the villous tissue, which was then confirmed by histology (**E** and **F**). (**E**) Massive perivillous fibrin deposition (MPFD) and chronic intervillositis were diagnosed. Fibrin deposition is indicated by pink staining and the letter "f", while the letter "m" marks regions with infiltrating histiocytes (tissue macrophages) into the intervillous space. (**F**) CD68 staining confirms that the infiltrating cells are histiocytes/macrophages. This is a clear example of a non-canonical clinical case. This figure is published in [150] and is reused here with permission from the publisher (**Appendix D**).

1.5.3 Integrated multi-level prediction

To improve the prediction of pregnancies with the greatest likelihood of complications, the combined assessment of multiple clinical, molecular, and imaging markers has been suggested. A study in 2012 in low-risk nulliparous women found that a multivariable model that included African American race, systolic blood pressure, BMI, and first-trimester PAPP-A and PlGF levels could only identify 46% of women that would develop PE at a 20% false positive rate [505]. The SCOPE consortium came to a similar conclusion in 2013 when they established an improvement for PE prediction with PlGF added to clinical factors, but the sensitivity was still only 45% at a 5% FGR [506]. It does, however, appear that the prediction of PE can be ameliorated by separating patients into early and late delivery windows. Integrated prediction at 11-13 weeks using maternal characteristics with uterine artery Doppler, mean arterial pressure (MAP), serum PlGF, and PAPP-A or sFLT1 can discover 89-96% of PE requiring delivery before 34 weeks at a 10% FPR [507, 508]. Prediction was much less successful for late-onset PE or all PE grouped together. Likewise, screening at 19-24 weeks with a combination of maternal factors, fetal head circumference, abdominal circumference, and femur length, along with uterine artery PI, has the capacity to identify 90% of SGA infants (birth weight $<5^{th}$ percentile) that will deliver before 32 weeks at a FDR of 10%, but only 68% of those that will deliver between 32-36 weeks and only 44% of those not requiring delivery until after 37 weeks [509]. Therefore, in general, prediction of more imminent outcomes is, understandably, significantly more accurate [504, 509]. However, this does not necessarily provide sufficient leeway for therapeutic administration.

1.5.4 Vasodilator treatment

Even if FGR and PE could be robustly predicted, the establishment of effective interventions for pregnancies pathologies is exceptionally complex. Given that both PE and FGR are associated with impaired blood flow, involving malperfusion of the placenta and increased resistance within the fetal capillaries, it is not surprising that vasodilation, specifically nitric oxide (NO) vasodilation, is a common target for PE and FGR treatment. NO is involved in vascular tone in both the maternal and fetal vessels [274] and is synthesized from L-arginine (an amino acid). As such, maternal supplementation of L-arginine has been shown to prevent growth restriction in underfed animals [510] and those exposed to hypoxic conditions [511]. Additionally, in several

small clinical studies, L-arginine supplementation has been reasonably successful, increasing fetal weights and decreasing maternal blood pressures [512, 513], while targeted delivery of another NO donor (SE175) to the uteroplacental vasculature has also been proposed [514]. However, the most commonly studied vasodilator for pregnancy pathologies is sildenafil citrate, which functions by prolonging NO's actions on the vasculature [426]. Sildenafil has been shown to increase vasodilation in an FGR model [515], and reduce the levels of sFLT1 and sENG, decrease blood pressure, and increase fetal growth in models of PE [516, 517]. Unfortunately, a large clinical trial assessing the utility of sildenafil for severe FGR (STRIDER trial) recently concluded that this drug is not effective [518].

1.5.5 Anticoagulant treatment

In 1979, AJ Crandon and DM Isherwood published a study showing that women who had taken aspirin or aspirin-containing compounds regularly during pregnancy were four times less likely to develop preeclampsia [519]. Since PE is associated with infarction and coagulation changes, aspirin is thought to help by inhibiting platelet activation [519]. However, more recently, it has been discovered that aspirin is also able to induce NO release from the endothelium [520]. In the intervening 39 years since the original study, a substantial number of clinical trials, as well as meta-analyses, have been performed investigating the ability of aspirin to improve pregnancy outcomes. Overall, these reveal similar results: aspirin intervention is affiliated with a moderate decrease in preterm PE development; the likelihood of PE prevention is much higher when treatment is commenced prior to 16 weeks gestation and when confined to a high-risk population; and the utility of aspirin does not extend to term PE [521-524]. Although not as extensively explored, the findings are comparable for FGR/SGA [522, 523]. Therefore, aspirin may have considerable benefit for particular groups of pregnant women, but is not effective against all PE and FGR. Regardless, given its low cost and good safety profile, it is currently recommended for pregnancies with at least moderately elevated risk of PE and/or FGR [22, 525].

Heparin is another drug that was initially proposed to reduce infarctions in the placenta [526]. However, further investigation into its mechanism of action revealed that heparin has a number of other functions, including as both an anti-inflammatory and a pro-angiogenic molecule [527, 528]. In clinical studies, heparin, or more specifically low-molecular-weight heparin (LMWH), has been shown to increase levels of PlGF in maternal serum, as well as decrease the

sFLT1/PlGF ratio [529], and may improve maternal endothelial function and vascular dilation [530]. Although early trials demonstrated a reduction in PE and FGR development with LMWH [531, 532], there has been considerable heterogeneity in clinical findings, and heparin's many cellular activities, as well as its potential long-term side effects, have not been fully elucidated [533-537]. Its current utilization is usually restricted to pregnancies with maternal indications, such as previous thrombosis or antiphospholioid antibody syndrome.

1.5.6 Antioxidant treatment

Oxidative stress is one of the hallmarks of both PE and FGR pregnancies; therefore, antioxidant treatment has also been thoroughly explored. In a small trial with only 283 women, vitamin C and E supplementation was found to reduce the rates of PE development in a high-risk population from 17% to 8% [538]. However, unfortunately, in two larger clinical trials with >2000 women each (VIP and INTAPP trials), vitamin C and E treatment did not affect PE development, but did result in a higher proportion of fetal loss and low birth weight infants [539, 540]. As such, vitamin C and E supplementation is no longer under investigation for pregnancy pathologies [426]. A different possibility is melatonin, a hormone known for its role in the circadian cycle, that can also act as an antioxidant [426]. Currently, two Phase I clinical trials are underway to determine melatonin's utility for reducing oxidative stress and improving clinical outcomes in both preterm PE and preterm FGR [541, 542].

1.5.7 Anti-rejection treatment

A few drugs have also been attempted in cases where recurrent pregnancy loss has indicated a likely immunological source of the pathology [222, 406]. One of these is intravenous immunoglobulin (IVIG), which consists of pooled immunoglobulin G (IgG) from the plasma of at least 1000 blood donors, that has been shown to improve outcomes in renal transplant recipients with HLA incompatibility issues [543]. Several clinical trials have assessed IVIG treatment for an unselected population of women with recurrent miscarriage, with little to no avail [544, 545]. However, in women with clear indications of abnormal immune function, such as antiphospholipid antibodies, increased NK cell activity, and/or histological signs of MPFD/MFI/chronic intervillositis, IVIG has been shown to have a considerable positive effect on the rate of live birth [546-548]. In cases where IVIG is insufficient for the prevention of MPFD/MFI, pravastatin has been proposed [549]. Pravastatin is a cholesterol-lowering agent

that, based on animal models [550, 551], is also capable of decreasing sFLT1 and sENG levels, as well as increased PlGF and VEGF concentrations, although the underlying mechanism for these angiogenic actions is not yet identified [549]. Pravastatin has been successfully employed in a number of cases of maternal antiphospholipid syndrome or recurrent miscarriage with MPFD/MFI [549, 552], and, unlike most statins, demonstrates a promising safety profile [553]. Other therapies involving the addition of VEGF or the removal of sFLT1 are also being explored [554, 555]. Overall, most of this clinical trial and case study data suggest that several of these investigated interventions may be highly effective in certain subpopulations of PE and FGR pregnancies, but that the prophylactic effects become masked when applied to the full clinical spectrum of patients. Increasing homogeneity in the patient groups assessed should, therefore, improve the utility and applicability of these treatments.

1.6 Heterogeneity in PE and SGA/FGR

As discussed above, the appearance of both PE and FGR is quite diverse in the clinical population, varying by time of disease onset, the severity of complications, associated placental pathologies, and aberrant transcriptional pathways. Additionally, although the placenta is widely considered to be the primary source of the pathology, a number of fetal, maternal, and even paternal factors are also likely involved in both their development and the modulation of disease severity. As such, the fact that no one biomarker or treatment has been found to robustly predict or prevent these pathologies is not necessarily surprising. This simply fits with the accumulating evidence that heterogeneity is at the epicenter of the PE/FGR clinical problem.

1.6.1 Differences between PE and FGR pregnancies

Although preeclampsia and fetal growth restriction frequently co-occur in the same pregnancy, especially in early-onset severe disease [556], it is also possible for an FGR infant to be associated with a normotensive mother and a PE women to give birth to an average-sized infant [557, 558]. This is inevitable given that these two pathologies are affiliated with a number of different risk factors. PE is more robustly linked to several maternal predisposing conditions and states, such as obesity, renal disease, chronic hypertension, and a prior hypertensive pregnancy, while the previous delivery of a low birth weight infant is a specific risk factor for FGR, along

with certain congenital infections [558, 559]. Placentas only associated with PE tend to be thicker in the first trimester [479], and may exhibit differences in growth trajectories [560] and increased syncytiotrophoblast shedding and apoptosis compared to normotensive FGR placentas [353, 561]. In contrast, FGR trophoblasts show higher expression of an oxidative stress marker, 8-hydroxy-2'-deoxy-guanosine (8-OHdG) [562]. This may result in some maternal vascular alterations even in FGR women who maintain a normotensive state [563], although likely not to the same degree as in PE cases, fitting with the finding that normotensive FGR is not as well predicted by angiogenic markers [445]. Furthermore, PE shows a greater affinity for the histopathological identification of maternal vascular malperfusion lesions, while FGR is more robustly linked to fetal vascular malperfusion pathology [558, 564].

1.6.2 Heterogeneity within the spectrum of PE

Within studies that attempted to investigate PE patients or placentas as a cohesive group, considerable heterogeneity was also observed. In one low-risk cohort, MVM lesions were found in only 25% of PE placentas [388]. In the largest placental transcriptional study performed before 2013, with 23 PE patients, approximately 86% of the variance in gene expression could not be explained by the sample classification of “control” versus “PE”, even when fetal sex and the effect of labor were also considered [363]. In another study, 46% of women who developed PE had consistently low PLGF throughout pregnancy, while the remaining 54% had levels similar to the normotensive controls [565]. Within the cohort of 2,023 PE women used to develop and validate the fullPIERS model for the prediction of adverse maternal outcomes, only 13% (261/2023) demonstrated maternal complications at any point after hospital admission [78]. Interestingly, in a recent study, seven maternal SNPs were found to associate with the development of particular symptoms during a PE pregnancy, such as visual disturbances or nausea [566]. A worldwide assessment by the World Health Organization (WHO) involving >6000 PE pregnancies showed that only 34% were linked to a low birth weight infant, 44% of PE women suffered coagulation dysfunction, and 24% demonstrated hepatic or cardiovascular dysfunction [567]. While all of these features are certainly more common in PE than normotensive pregnancies, no one metric, other than the maternal hypertension required for a PE diagnosis, is found in all pregnancies annotated as having this disorder. Even then, blood pressure can be severe (over 160/110 mmHg) or mild (between 140/90 mmHg and 160/110 mmHg) [77].

In general, early-onset PE is considered the "placental" disorder, while late-onset PE is thought to be associated with a more significant "maternal" contribution to the pathology [568]. As such, these two subgroups have been affiliated with different risk factors and fetal outcomes [27, 569]. Additionally, early-onset PE demonstrates reduced placental perfusion by MRI, higher uterine artery PIs, increased MVM lesions, augmented activation of placental stress response pathways, and increased syncytial shedding compared to LOPE [403, 568, 570-573]. Different maternal hemodynamic states have also been observed, with EOPE patients showing elevated maternal vascular resistance, while high BMIs are more frequently noted in women with late-onset PE [574]. As mentioned above, early-onset PE is much better predicted by the majority of the clinical, imaging, and molecular biomarkers identified thus far [507, 508]. However, this separation into two PE subgroups based solely on gestational age at the time of symptom appearance still does not fully explain the considerable heterogeneity observed in this hypertensive disorder. Furthermore, in studies involving both EOPE and LOPE, the findings can be categorized into three groups: those where LOPE shows a similar pathology to EOPE, just not as severe [403, 573, 575], those where LOPE cannot be distinguished from controls [571], and those where the aberrations discovered in LOPE are in the opposite direction or are completely different to those seen in the EOPE patients [27, 572, 574]. As such, it is still quite unclear if LOPE is a milder form of EOPE, a different pathology altogether, or both.

1.6.3 Heterogeneity within the spectrum of SGA and FGR

A large portion of the heterogeneity observed within the range of small fetuses and infants is due to the lack of consistency across studies regarding FGR and SGA sample definitions. While some datasets assess both disorders independently but simultaneously [473, 562], many others are either vague or incorrect in their sample terminology [432, 576-578]. This is highly problematic, since the majority of SGA infants are constitutionally small with little or no signs of pathology [104], their inclusion in a study aimed at pathological FGR will underestimate or even eliminate significant differences. Unfortunately, reliable methods of separating these two patient populations, especially in cases with a paucity of maternal demographic and fetal growth trajectory information, do not currently exist. Furthermore, the accurate identification of fetuses that are small-for-gestational-age is not necessarily a given, as a number of the different formulas for estimating fetal weight have significant error [146].

Even amongst studies that were thought to be focusing on pathological FGR, the findings were still not applicable to all subjects. In one study, only 10% of FGR fetuses resulted in poor fetal outcomes, with low Apgar scores, NICU transfer, and necrotizing enterocolitis [579]. VUE has been noted in 26% of FGR placentas [580], while it has been stated that 25% of FGR placentas have no histopathological abnormalities [556]. In a study of early-onset FGR, 10% of the FGR pregnancies demonstrated completely normal uterine artery blood flow [488]. These women delivered later than those with high uterine artery PIs, and the placentas displayed more chronic intervillositis and MPFD, and less maternal vascular malperfusion lesions [488]. A different cohort revealed a similar result with only 71% of early-onset FGR placentas exhibiting signs of MVM lesions [387]. In late-onset FGR, this number is even lower, with only 57% annotated as having MVM features [387]. Additionally, as discussed above, symmetrical and asymmetrical FGR are associated with different risk factors, clinical outcomes, and long-term sequelae [113]. As such, FGR appears to be just as heterogeneous as PE.

1.6.4 Support from animal models

Further evidence of PE and FGR heterogeneity comes from the many animal models of these disorders. Maternal PE-like symptoms can be induced based on acute and chronic placental hypoxia [581-583], dietary changes [584, 585], angiogenic profile alterations [321, 323, 586], maternal immune system modulation [587], maternal fluid retention [588, 589], a genetic predisposition to hypertension exacerbated by pregnancy [590], and trophoblast hyperplasia [591]. This indicates that multiple different causative insults can all ultimately lead to the endothelial dysfunction required for the development of maternal hypertension in pregnancy. Growth restriction can be observed in animal models as a result of the modification of genes involved in blood vessel formation and function [592, 593], occlusion of uterine blood flow [594], exposure to hypoxic conditions [595], maternal food restriction [596], and many others [597]. Overall, these models are invaluable tools for understanding the individual contributing factors to PE and FGR. However, no one animal model can replicate the entire clinical spectrum of either pathology.

1.6.5 Lessons from other heterogeneous human pathologies

Other multi-factorial pathologies, such as cancer, have taken a particular, highly successful approach towards resolving this heterogeneity problem: patient subtyping. Predominately, this is

performed using transcriptomics data, as this type of information provides an excellent, easily quantifiable overview of the tissue's activities at the time of sampling. However, it is important to analyze this gene expression data employing a method that does not force a comparison of a binary set of states (ex. "PE" versus "control"), but instead groups samples based on similar transcriptional patterns before investigating correlations to clinical attributes; the "unsupervised" clustering approach to data analysis [598]. In this way, hidden groups of patients with increased homogeneity can be revealed (**Figure 7**).

For example, in a 2002 seminal paper published by van't Veer et al. [599], gene expression microarrays were performed on 78 sporadic lymph-node-negative breast cancer tumors. Application of clustering methods to this data resulted in an expression profile of 70 genes that were able to accurately predict patients with poor prognosis. Until then, 70-80% of breast cancer patients were unnecessarily treated with chemotherapy or hormonal therapy [599], and this discovery led to the development of a clinical tool [600] that considerably improved treatment selection and management of breast cancer. Another example involved microarray data from 62 primary prostate tumors and 41 normal prostate samples [601]. Unsupervised clustering was able to separate the tumors from the normal samples and then further split the tumors into three subtypes based on gene expression. Two markers with significant differential expression between subtype 1 and subtypes 2/3 were found to be strong predictors of tumor recurrence in an independent set of 225 primary prostate cancers [601]. Similar success has also been observed with clustering in other diseases, such as ovarian cancer, lung cancer, and lymphoma [602-604].

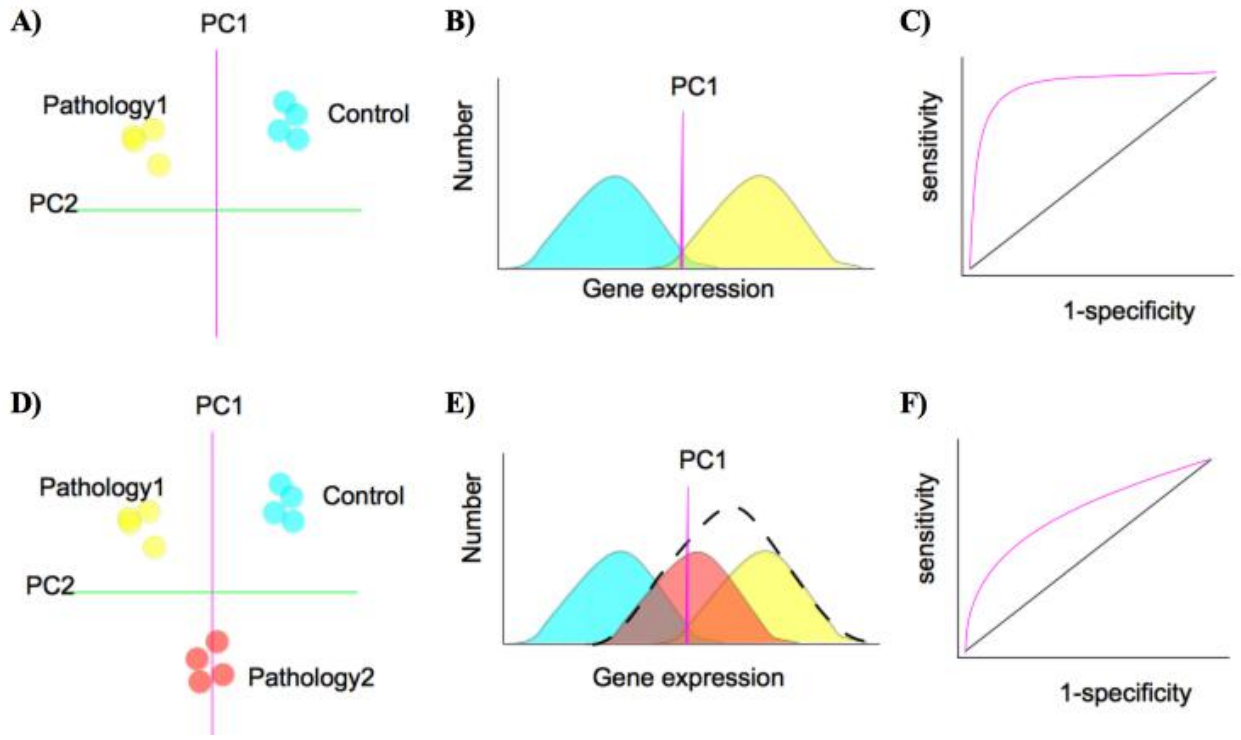

Figure 7 – The hidden class problem. The investigation of placental diseases performed by comparing a single pathology group to a group of controls assumes that only one kind of pathology exists and that it is distinct from these healthy samples (**A-C**). In this case, these two phenotype groups would (**A**) easily separate on a principal component analysis (PCA) plot and (**B**) demonstrate little overlap in gene expression on a density plot. This would lead to high sensitivity and specificity on a receiver operator characteristic (ROC) curve (**C**) when these genes were employed to distinguish the pathology group. However, if there were in fact two different subtypes of pathology, including one with more similarity to controls (**D**), then the gene expression of a single merged "pathology" group (dotted line) would show considerable overlap with the controls on a density plot (**E**), and identification of the pathology would be weak (**F**). ROC curves for biomarkers of preeclampsia and fetal growth restriction much more closely resemble the plot in (**F**) than the plot in (**C**). Therefore, there are likely multiple hidden subtypes of patients within these pathologies that need to be discovered and distinguished. This figure is a model (not real data) and is modified from one produced by Dr. Brian Cox (unpublished). It is reused here with permission.

1.6.6 Subtypes of pregnancy pathologies

In 2011, Dr. Brian Cox tested the theory that subtypes of preeclampsia also exist and can be found using unsupervised clustering techniques. Using the placental microarray dataset published by Sitras et al. (N=17 severe PE) [367], he first enriched for genes expressed by the

trophoblast and then clustered using unsupervised methods [605]. This revealed three molecular subtypes of preeclamptic placentas, demonstrating dysfunction in different underlying pathways: angiogenesis (subtype 1), MAPK signaling (subtype 2), and hormone biosynthesis and metabolism (subtype 3). Furthermore, only subtypes 1 and 3 displayed elevated levels of FLT1 and ENG, while samples in subtype 2 instead exhibited overexpression of GNA12 [605]. GNA12 has been implicated in blood pressure regulation and was found to correlate with PE superimposed on maternal chronic hypertension in an independent set of placenta samples [605]. This paper by Cox et al., therefore, demonstrated the potential for PE subtyping using microarray data, and also suggests the importance of including patients with known maternal predisposing factors, like CH [605]. However, one of its main limitations is that the 26 control samples were not included as unique samples in the clustering, making it difficult to determine how these three PE subtypes compare to a healthy placenta. Additionally, all non-trophoblast-enriched genes were removed, eliminating the important contributions of the other cells types in the placenta. Validating and improving upon this 2011 study, and extending it to FGR, is the basis of the current thesis.

1.7 Bioinformatic Methods of Unsupervised and Transcriptional Analysis

1.7.1 Genome-wide gene expression microarrays

To identify placental subtypes, genome-wide gene expression data must first be procured. Since RNA is relatively unstable, it is important that placentas that will be assessed transcriptionally are processed quickly, preferably within 30-60 minutes of delivery [263, 606]. Optimally, tissue for RNA analysis is snap-frozen in liquid nitrogen (the standard method) or preserved using commercial solutions (ex. RNAlater™, a newer and potentially improved method [606]) after sampling; however, it is possible to obtain reasonable quality RNA from fixed tissue [607, 608]. The overall integrity of the RNA can be measured using the RIN (RNA integrity number) [609], although RNA degradation can preferentially occur in certain transcripts even in overall intact samples [610].

In 2012/2013, when this project was initiated, the decision was made to employ microarrays for gene expression assessment, instead of alternative methods such as RNA sequencing. The main

advantage of microarrays is that the bioinformatics tools required to analyze the data are well established and can be implemented on standard computers [371, 611], but reduced cost and the availability of previously published cohorts also contributed to this decision. Microarrays involve reverse transcribing the RNA to complementary DNA (cDNA) and hybridizing this cDNA to the array, which contains a multitude of positions, each with a DNA probe that has the complementary sequence to the gene of interest in that particular location [612]. With most array platforms, multiple probes are included for each gene, such that an average expression value can be calculated [371]. Unbound cDNA is then washed off, the array is scanned, and an image of the fluorescence intensity at each location on the array, which depends on the amount of cDNA binding to that spot, is used to quantify expression [613].

1.7.2 Data pre-processing

Although the pre-processing steps can differ depending on the array platform used, the general pipeline is usually similar [371]. Initially, background correction is performed to remove the background noise caused by scanning/non-specific hybridization [614]. This can be done by deconvolving the signal and noise distributions observed on the array [615]. Additionally, the data is often log transformed such that upregulated and downregulated genes are treated similarly [616], and the data becomes normally (Gaussian) distributed, simplifying analysis. Next, normalization for differences in starting RNA quantities or hybridization efficiencies across the separate array chips is conducted, thus allowing samples to be directly compared [614, 616]. A number of normalization methods exist [617], but in the current thesis, quantile normalization is performed, which results in the same range of probe values for each sample [617]. Probe sets associated with the same gene are then collapsed to a single (average) expression metric [615]. Furthermore, once individual datasets are pre-processed, statistical methods now exist to merge smaller microarray cohorts into larger aggregate cohorts, allowing gene expression values across multiple original datasets, assessed on different platforms, to be compared and analyzed simultaneously [618]. These algorithms rely on batch correction for aggregation. Of the possible batch correction techniques, an Empirical Bayes (EB) method is commonly employed in this situation, as it is considered more robust to outliers and small sample size [619]. Batch correction can also be employed within individual datasets if necessary, although experimental designs that do not add additional confounding factors (ex. RNA extracted by different people, arrays run years apart, etc.) are significantly more reliable [620].

1.7.3 Methods of unsupervised clustering and subtype discovery

The goal of an unsupervised clustering analysis is to group samples based solely on similarities or dissimilarities in gene expression (or histological/proteomic/metabolomic, etc.) profiles, independent of clinical diagnosis or characteristics. A common algorithm is multivariate model-based clustering [621], which compares the (Gaussian distributed) data to defined models that represent possible multivariate distributions with certain volumes and shapes. This is done using an expectation-maximization algorithm, producing likelihood values for each of the models and number of clusters to determine their fit to the data at hand [621]. The Bayesian Information Criterion (BIC) is then employed, rewarding models that fit the data well while penalizing overly complicated models with a lot of parameters to avoid over-fitting the data [621]. This optimal model and cluster number produces a maximum on the BIC curve, and as such, the number of clusters and the cluster assignments for each sample are established in an unsupervised manner. However, for data that is not normally distributed, different clustering algorithms need to be utilized, such as hierarchical clustering. Hierarchical agglomerative clustering treats each sample as their own cluster and then, based on distance metrics, successively merges pairs of similar clusters until the entire cohort is one cluster, forming a hierarchical tree (dendogram) [622]. This dendogram formation is unsupervised; however, the decision of where to cut the tree to split off the clusters is often supervised, although this can be improved by assigning statistical values of certainty to the groups observed within the tree [623].

1.7.4 Methods of data reduction and subtype visualization

Furthermore, a number of data reduction techniques exist such that redundancy in the expression values of thousands of genes can be minimized and the important information can be visualized in two or three-dimensional space. A method employed in this thesis is PCA [624, 625]. PCA converts the gene expression data into new independent weighted variables called “principal components” (PCs). Genes with highly linearly correlated expression and responsible for the most variance in the data will contribute the most to the first principal component (PC1). Those weighted strongly in principal component 2 (PC2) are those that contribute the second greatest to the data variance and exhibit a significant linear correlation to each other, but are independent of PC1. This continues for PC3 onwards, depending on the number of samples. Once the contribution of each gene to each principal component is determined, these are used in

combination with the original expression values to calculate a weighted score for each sample for each component. Plotting these weighted values for the first two or three principal components usually results in good separation of the samples, either based on a technical batch effect or biologically meaningful clusters. PCA, like model-based clustering, is a multivariate metric that takes into consideration the relationships between the genes and has been previously performed on placental datasets [365, 626, 627].

A more recently developed alternative to PCA is t-distributed stochastic neighbor embedding (t-SNE) [628], a non-linear method of data reduction. t-SNE works by calculating distance-based similarity scores between all the samples in high-dimensional space and then randomly projecting the sample points onto a two or three-dimensional plot. With each iteration, a given sample is moved closer to other samples with high similarity scores and farther from those with low similarity scores until the relationships between the points (i.e. the matrix of similarity scores) in low-dimensional space reflects the relationships between the points in the original high-dimensional space, or the set maximum number of iterations is reached. t-SNE is considered an improvement on the original SNE method as it employs the t-distribution instead of the Gaussian distribution to assess the associations between samples in low dimensional space, thus reducing crowding [628]. In this way, t-SNE is thought to significantly preserve both the local and global structures of the original data [628].

1.7.5 Methods for investigating the underlying pathology

Once clusters have been identified, the primary goal is to ascertain if they have any biological significance. One way of doing this is pathway enrichment analysis, which determines whether genes that are differentially expressed between groups are involved in similar functions or pathways [371, 629]. Sets of genes with a pre-established commonality are obtained from resources such as the Gene Ontology (GO) Consortium [630] or the Kyoto Encyclopedia of Genes and Genomes (KEGG) [631], where they are organized in a hierarchical manner (ex. genes involved in DNA initiation, DNA priming, and DNA unwinding are all also categorized as involved in DNA replication [630]). In this field, gene-set enrichment analysis (GSEA) is a popular method of testing for pathway enrichments [632]. With GSEA, all available genes are first ranked based on their degree of differential expression between the phenotype/cluster groups in question. Then, for each gene set of interest, an enrichment score is calculated

indicating whether the members of this gene set are grouped closer to the top or bottom of the ranked list, or are just dispersed evenly. Next, to generate a null distribution for comparison purposes, either the phenotype or the gene labels are permuted, and the enrichment score is calculated again. This is repeated 100-1000 times, and the true enrichment score is then compared to this null distribution to determine statistical significance. Since a huge number of tests are being performed, it is critical that p-values are adjusted for multiple hypothesis testing [632].

An alternative method of pathway enrichment analysis that has been proposed to improve upon GSEA is sigPathway [633]. This approach assesses two separate hypotheses to test if a gene set is significant in a given group comparison. Initially, instead of a ranked list, association scores are calculated for all the genes with the group of interest using t-tests. The first hypothesis (Q1) then determines whether the association scores observed for the genes belonging to a given gene set is statistically different than one would expect from a random sample of associations. In this case, the null distribution is determined by permuting the gene labels on the association scores. The second hypothesis (Q2) compares the association scores of genes in the gene set when the group labels are correct to when they are incorrect. In this case, permutation is done on the group labels. In this manner, a gene set with tightly correlated gene expression, but otherwise unimportant, can appear significant if only Q1 is tested. In contrast, when a high fraction of genes is affiliated with the group of interest, a large gene set can appear significant by chance if only Q2 is tested. Therefore, by using both, gene sets deemed significant are more likely to be biologically meaningful. Multiple hypothesis correction is also essential in this method [633]. Furthermore, correlative analysis with available clinical, imaging, and/or histopathology data will also contribute substantially to understanding the underlying pathology in any identified cluster or patient subtype.

1.7.6 Targeted gene expression analysis

In many microarray studies, a targeted gene expression investigation, using quantitative polymerase chain reaction (qPCR) analysis, is also performed to confirm significant findings [365, 634]. Additionally, qPCR is a less expensive, more clinically applicable method for classifying samples [635, 636]. Therefore, once clusters have been established and underlying pathology has been elucidated, qPCR may help to improve the clinical utility of these results. In

the current thesis, qPCR was performed using TaqMan® methods [637], employing a primer-probe set, where the primer is specific to the gene of interest and the probe is an oligonucleotide with a fluorescent reporter dye on the 5' end and a quencher dye on the 3' end. RNA is reverse transcribed to cDNA and then amplified in the presence of this primer-probe set. While the probe is intact, the quencher stops the reporter from emitting much fluorescence. However, once bound to the target, the extension of the primer by DNA polymerase cleaves the probe and separates the two dyes, releasing signal. With each PCR cycle, more and more fluorescence is released, proportional to the amount of the target gene in the sample, which can then be quantified with a C_T value. Genes with a lower C_T value were amplified sooner, and were, therefore, present at a greater concentration in the original mixture. Important technical considerations for qPCR include the amount of loaded cDNA, as well as differences in amplification efficiency across different plates [638].

1.8 Hypothesis

The primary hypothesis of this project was that large cohort unsupervised multi-scale (transcriptional and histopathological) analyses of PE and FGR placentas, with corresponding detailed clinical data, could allow for the identification of biologically and clinically relevant placental subtypes of these two pathologies. Once these were discovered, the second goal was to establish a set of gene expression differences that could separate the subtypes using qPCR.

1.9 Specific Aims (Figure 8)

Aim 1 (Chapter 2): Investigate the possibility that a large cohort unsupervised clustering analysis of placental gene expression can identify subtypes of PE placentas.

Aim 2 (Chapter 3): Expand upon the transcriptional results from Aim 1 and determine the utility of added clinical information in the assessment of PE subtypes and placental clusters.

Aim 3 (Chapter 4): Incorporate histological information and investigate the relationships between the three data types in the PE-focused cohort.

Aim 4 (Chapter 5): Perform a transcriptional, clinical, and histopathological analysis of normotensive and hypertensive SGA placentas associated with suspected FGR, and assess relationships between PE and SGA/FGR.

Aim 5 (Chapter 6): Develop and utilize a qPCR panel of markers to validate the gene expression differences between the transcriptional clusters and classify unknown samples.

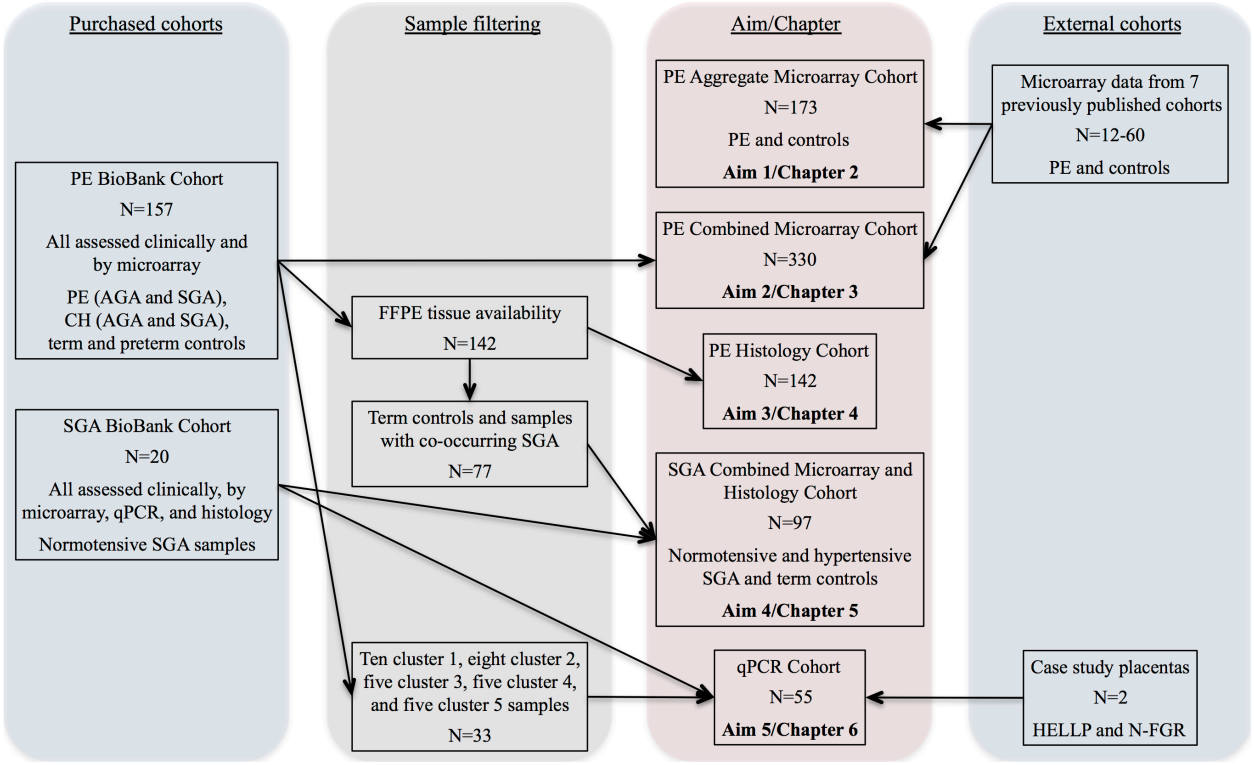

Figure 8 – An overview of the datasets and cohorts employed in this thesis, and their uses in each of the Aims/Chapters. The two cohorts that were purchased from the RCWIH BioBank for the purpose of this project are shown on the left, while samples obtained from external sources are on the right. PE = preeclampsia, AGA = average-for-gestational-age, SGA = small-for-gestational-age, CH = chronic hypertension, FFPE = formalin-fixed paraffin-embedded; HELLP = hemolysis, elevated liver enzymes, low platelet count syndrome; FGR = fetal growth restriction.

2 Chapter 2 – Unsupervised Clustering Analysis of a Large Aggregate Microarray Dataset Reveals Multiple Molecular Subtypes of Preeclamptic Placentas

Content in this chapter is published in:

Leavey K, Bainbridge SA, Cox BJ. (2015). Large Scale Aggregate Microarray Analysis Reveals Three Distinct Molecular Subclasses of Human Preeclampsia. *PloS one*. 10(2): e0116508. [639]

Co-authors' contributions are described in the methods section.

2.1 Introduction

Preeclampsia (PE) is a heterogeneous, multi-system disorder of pregnancy, affecting 3-8% of all pregnancies and responsible for >60,000 maternal deaths worldwide each year [3]. To date, PE has no cure short of the removal of what is thought to be the causative organ, the placenta, which may necessitate a preterm delivery and result in both acute and chronic health risks to the child. The incidence of PE has risen relentlessly [10] and effective screening tools and/or treatments have yet to be discovered.

These challenges have led researchers to apply genome-wide profiling techniques, such as microarray analysis, in cases of PE in order to better understand the etiology of placental dysfunction in this disorder. The primary anticipated outcome of all microarray studies performed prior to 2013 was the identification of differentially expressed genes in the PE placentas, as a cohesive group, compared to a control group. However, in the largest study performed [363] (N=23 PE patients), considerable variability was observed and ~80% of the gene expression variance in the dataset could not be explained by the binary clinical classification of "control" versus "PE" and other covariates. This has led us [605], and others [212, 278, 640], to hypothesize that multiple placental subtypes of preeclampsia exist and are driven by the deregulation of different molecular pathways.

Previous large-scale microarray analysis (N>70) in other multi-factorial, heterogeneous diseases, such as cancer [599, 601], has been beneficial for discovering molecular subtypes of disease. Furthermore, statistical methods now exist to merge smaller microarray datasets into larger aggregate datasets [618]. Therefore, the primary aim of this chapter was to determine if unsupervised clustering of a large aggregate placental microarray dataset could identify molecular-based subtypes of PE patients.

2.2 Methods

2.2.1 Study selection

Previously published preeclampsia-associated placental gene expression datasets available on NCBI's Gene Expression Omnibus (GEO) [641] were reviewed using a set of inclusion and

exclusion criteria by Drs. Brian Cox and Shannon Bainbridge. Exclusion criteria were sampling at earlier stages of gestation (1st trimester), sampling of non-placental tissue, or sample set redundancy. Inclusion criteria were a minimum of three or more patient samples of a preeclamptic pathology (early and/or late onset types), an array platform with more than 15,000 gene features, and the availability of raw data tables. At the time of study selection (2013), a diagnosis of preeclampsia was defined as two or more episodes of hypertension (>140/90 mmHg) with proteinuria after the 20th week of pregnancy [642]. Proteinuria was not consistently defined between studies, as values ranged from 300mg-2g of protein in a 24 hour period or >2+ on a dipstick test (**Table 1**). Placentas obtained from non-PE pregnancies were labeled as "controls" for consistency with the original publications; however, whether or not these came from truly healthy pregnancies was not always clear.

2.2.2 Assembly of the aggregate microarray dataset

The seven identified placental microarray datasets were loaded into R 3.0.1 from GEO using the *GEOquery* library. Gene expression values were extracted from each GEO series and converted into log2 intensities. The GSE25906 dataset was batch corrected for the two indicated batches in the supplied annotation files, and eight samples with fetal growth restriction were removed from the GSE24129 dataset. The individual sample sets were then aggregated into one array, including Empirical Bayes batch correction, using the *virtualArray* package [618]. Finally, the merged dataset was unbiasedly filtered for genes with expression variance in the top quartile. This cut-off was chosen to select for those genes with the highest potential information content for clustering patients.

Table 1 – The seven previously published PE microarray datasets used in this chapter.

GEO ID	Platform	PE	Controls	Total	PE definition	Reference
GSE30186	Illumina HumanHT-12 V4.0 expression beadchip	6	6	12	Maternal systolic and diastolic blood pressure >140/90 mmHg on at least two occasions separated by 6 h after 20 weeks of gestation, with urinary protein >2+ on dipstick, or >0.3 g/day	365
GSE10588	AGI Human Genome Survey Microarray Version 2	17	26	43	Blood pressure of at least 160 mmHg (systolic) and/or 110 mmHg (diastolic), with proteinuria ≥2+ on dipstick, measured on at least two occasions 6 h apart, or HELLP syndrome, after the 20th week of gestation	367
GSE24129	Affymetrix Human Gene 1.0 ST Array	8	8	16	Blood pressure of higher than 140/90 mmHg, with proteinuria of >0.3g in a 24 hour collection	353
GSE25906	Illumina human-6 v2.0 expression beadchip	23	37	60	Systolic pressure ≥140 mmHg, diastolic pressure ≥90 mmHg, and proteinuria ≥0.3 g in a 24 hour collection	363
GSE43942	NimbleGen Homo sapiens HG18 090828 opt expr HX12	5	7	12	Systolic pressure ≥140 mmHg, diastolic pressure ≥90 mmHg, and proteinuria ≥0.3 g in a 24 hour collection	368
GSE4707	Agilent-012391 Whole Human Genome Oligo Microarray G4112A	10	4	14	Blood pressure of higher than 160/110 mmHg, with proteinuria of more than 2 g in a 24 h collection	366
GSE44711	Illumina HumanHT-12 V4.0 expression beadchip	8	8	16	New onset hypertension (diastolic BP of ≥90 mmHg, based on the average of at least two measurements) after 20 weeks with proteinuria (≥0.3g/d in a 24-hour urine collection or ≥30 mg/mmol urinary creatinine in a random urine sample) or one/more adverse maternal condition(s)	364
TOTAL:		**77**	**96**	**173**		

2.2.3 Clustering and covariate assessment

The PE and control samples were treated as a single dataset and subjected to unsupervised multivariate model-based clustering, using the *mclust* package [621] from CRAN. The optimal number of clusters was selected based on the Bayesian Information Criterion. Principal component analysis (PCA) was performed on the transpose of the expression matrix, which allowed for the visualization of the clusters in component space using the *rgl* library. Information about the clinical phenotype (PE or control), gestational age (25–40 weeks; binned), nationality (Canada, China, Finland, Japan, or USA), and occurrence of labor (yes, no, or unknown) was annotated for each sample. Fetal sex was typically not reported but was determined using *mclust* and the expression of two Y-chromosome genes: UTY and USP9Y. Fisher's exact tests were employed to test the significance of these patient variables on cluster membership. Finally, principal variance component analysis (PVCA, using the *pvca* library), an extension of PCA, was performed on the full aggregate dataset of samples and all genes in order to determine the main sources of variability within the data.

2.2.4 Expression of known PE markers

Soluble fms related tyrosine kinase 1 (sFLT1) and endoglin (sENG) are two of the most frequently studied potential biomarkers of PE, produced in the placenta and found elevated in the maternal serum early in pregnancy, prior to the signs and symptoms of PE, and until delivery [65, 440]. The differential placental expression of FLT1 and ENG was visualized with a three-dimensional PCA plot, using colour gradients to demonstrate increasing expression of FLT1 (green to orange) and ENG (green to blue). PlGF, another common biomarker, in delivered placentas is substantially more difficult to interrogate as pathological differences in expression are confounded by differences due to gestational age [65]. Additionally, a list of the top ten genes with significantly upregulated expression in the PE samples compared to the controls was obtained using linear modeling (*limma* library [643]), and the mean expression of these ten PE markers was calculated across each sample and visualized as a density plot, using the *sm.density.compare* function from the *sm* library [644]. The WEKA machine learning software package [645] was then employed to evaluate the ability of these ten genes to discriminate all PE samples from controls, and each PE subtype from controls, using a Naive Bayes classifier (which applies Bayes' theorem and assumes independence across the genes) and 10-fold cross-

validation. Marker performance was assessed by receiver operator characteristic (ROC) curves, which plot the true positive rate (TPR) against the false positive rate (FPR).

2.2.5 Assessment of trophoblast and endothelial markers

Given that many of the original studies reported obtaining their placenta samples from a single biopsy, and that the placenta is not a homogeneous structure [336, 646], sampling bias was investigated as a potential cause of the controls splitting. This was done by calculating the mean expression of 35 genes known to be significantly upregulated in endothelial cells as well as the mean expression of 20 genes significantly enriched in trophoblasts [605], across each of the controls. A scaled (0 mean and 1 variance) heatmap of these mean expression values was then produced using the *heatmap* function and reverse heat colors. This was also done for each gene individually.

2.2.6 Gene set enrichment analysis (GSEA)

To determine biologically significant transcriptional differences between the control subtypes, the PE subtypes, and the co-clustering PE and control samples in clusters 1 and 3, pathway enrichment analysis was performed using the Molecular Signatures Database (MsigDB) collections associated with the GSEA software v2.1.0 [632], comparing the groups of interest. All C5 GO gene sets (v4.0) with 10–1000 members were assessed, including those annotated to Biological Process, Cellular Component, and Molecular Function, as well as C2 Canonical Pathways gene sets (v4.0), which includes KEGG, Protein Interaction Database, and Reactome collections, among others. The recommended number of permutations (1000) was performed using the less stringent (gene set) permutation type against a background model of the 14,653 genes found in common across all original microarray platforms. Pathways were considered significant at a corrected false discovery rate (FDR) q-value <0.25. GSEA GO results were visualized in Cytoscape v2.8.3 using the two-colour Enrichment Map plugin [647], with a p-value cutoff of 0.01, a FDR q-value cutoff of 0.25, and an overlap coefficient of 0.5. Nodes were re-coloured to reflect the subtype in question, and networks of related ontologies were circled and assigned a group label. Additionally, placental trophoblast expression for each gene found to be significantly upregulated and belonging to the *response to virus* GO ontology was assessed using Human Protein Atlas [648], and the cell component(s) of expression was/were determined from the information contained in NCBI's Entrez Gene database [649].

2.2.7 Ethics

As all the patient data was de-identified and obtained from previously published reports, an ethics waiver from the University of Toronto Office of Research Ethics was obtained.

2.3 Results

2.3.1 Assembly of the aggregate dataset

The literature search discovered 38 previously published microarray studies examining gene expression within the PE placenta (as of 2013), seven of which were found to meet the inclusion and exclusion criteria [353, 363-368] (**Table 1**). After merging, the aggregate dataset contained 173 samples (77 PE and 96 controls) with expression values for 14,653 genes. Invariable genes were removed using an unbiased filtering, leaving those with expression variance in the top quartile and reducing the number of genes utilized for sample clustering to 3,663.

2.3.2 Clustering and covariate analysis

The combined set of PE samples and controls was treated as a single large dataset and analyzed by unsupervised multivariate model-based clustering. Clustering with the optimal model (VEI: diagonal, equal shape) revealed three distinct molecular groups of placental gene expression (**Figure 9a**). Significantly, cluster 2 was composed entirely of preeclamptic patients (**Figure 9b,c**). Surprisingly, the controls split between clusters 1 and 3, and each of these control subtypes co-clustered with PE samples, suggesting the existence of at least three placental subtypes of preeclampsia.

Differences in covariates may explain these unexpected results, as it has been reported that the occurrence of labor, gestational age, and fetal sex may impact placental gene expression [266, 650]. No associations between cluster membership and nationality, occurrence of labor, original study membership, or fetal sex, were observed as statistically supported by Fisher's exact tests ($p>0.30$; **Figure 10a-d**). Additionally, the few known late-onset PE samples included in the aggregate dataset showed no significant differential segregation compared to the remaining early-onset preeclamptics, although none of these late-onset samples were found in cluster 2

(**Figure 10e**). In contrast, a significant relationship between gestational age (GA) and cluster membership was noted, with younger samples (i.e. earlier GAs) generally gravitating towards clusters 2 and 3, and older samples often found in cluster 1 ($p<0.01$; **Figure 10f**).

To better understand the effects of covariates and the novel subgroups on gene expression, the full set of preeclamptic and control samples was subjected to PVCA. This analysis indicated that the covariates were responsible for very little of the transcriptional variation within the data (<5%; **Figure 11**), supporting the Fisher's exact test results. The exception was cluster membership, which was found to account for more than three times the variability in gene expression than the phenotypes of PE and control (13.9% versus 3.5%).

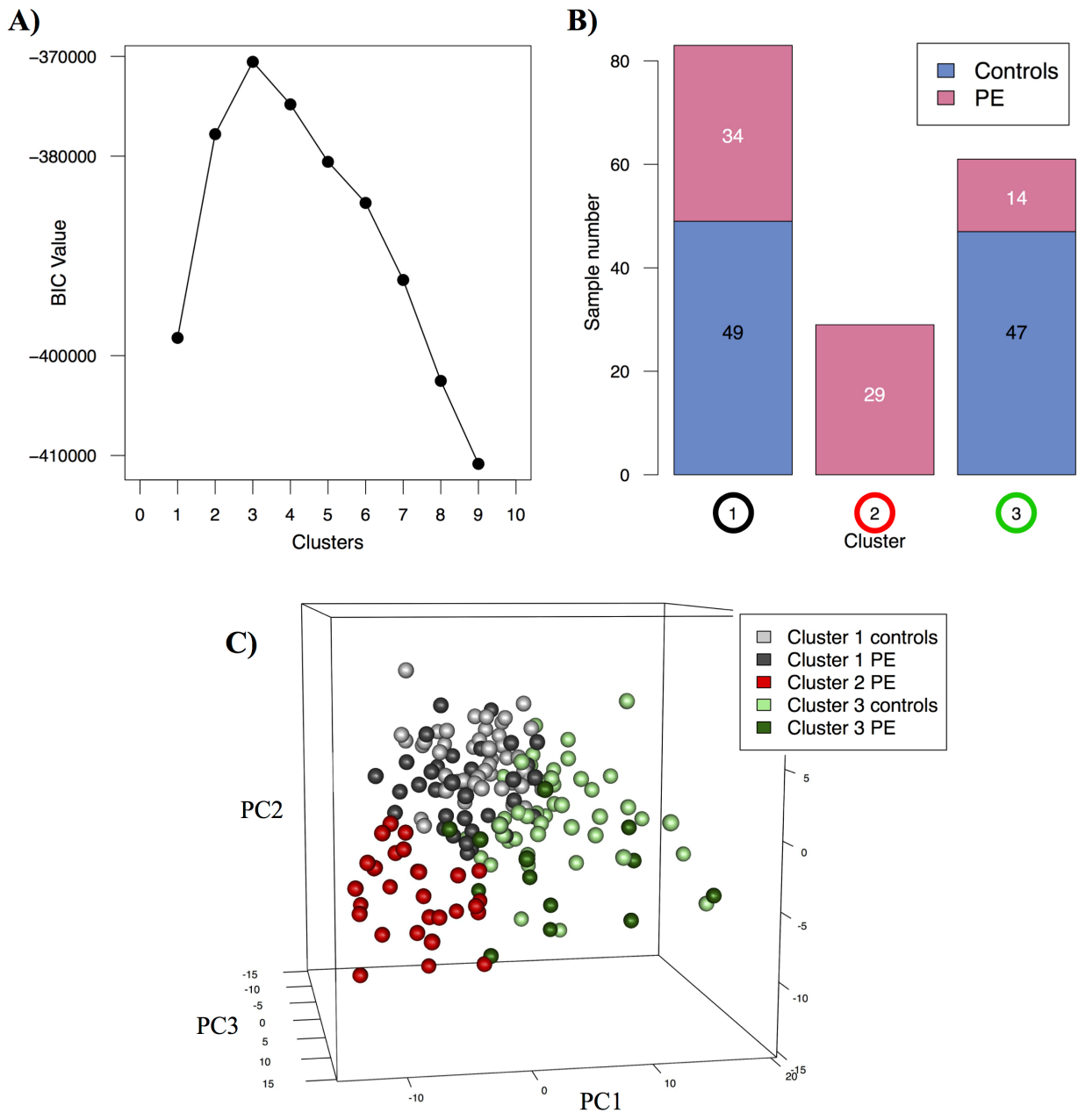

Figure 9 – Unsupervised multivariate model-based clustering of the aggregate dataset of 77 preeclamptics and 96 controls (N=173 total). (**A**) The Mclust model VEI (diagonal, equal shape) gave the best performance based on the Bayesian Information Criterion (BIC; y-axis) and an optimal cluster number of three was selected (x-axis). (**B**) Cluster 2 was composed entirely of PE samples (pink) while the remaining two clusters consisted of a mixture of preeclamptic and control samples (blue). (**C**) Principal component analysis (PCA) was performed on the data to allow for cluster visualization in component space. Under PCA, samples closer together demonstrate higher similarity in gene expression. PC1–3 are principal components 1–3, respectively, while colours indicate cluster membership (cluster 1: grey; cluster 2: red; cluster 3: green), with light shades denoting controls and dark shades indicating preeclamptics.

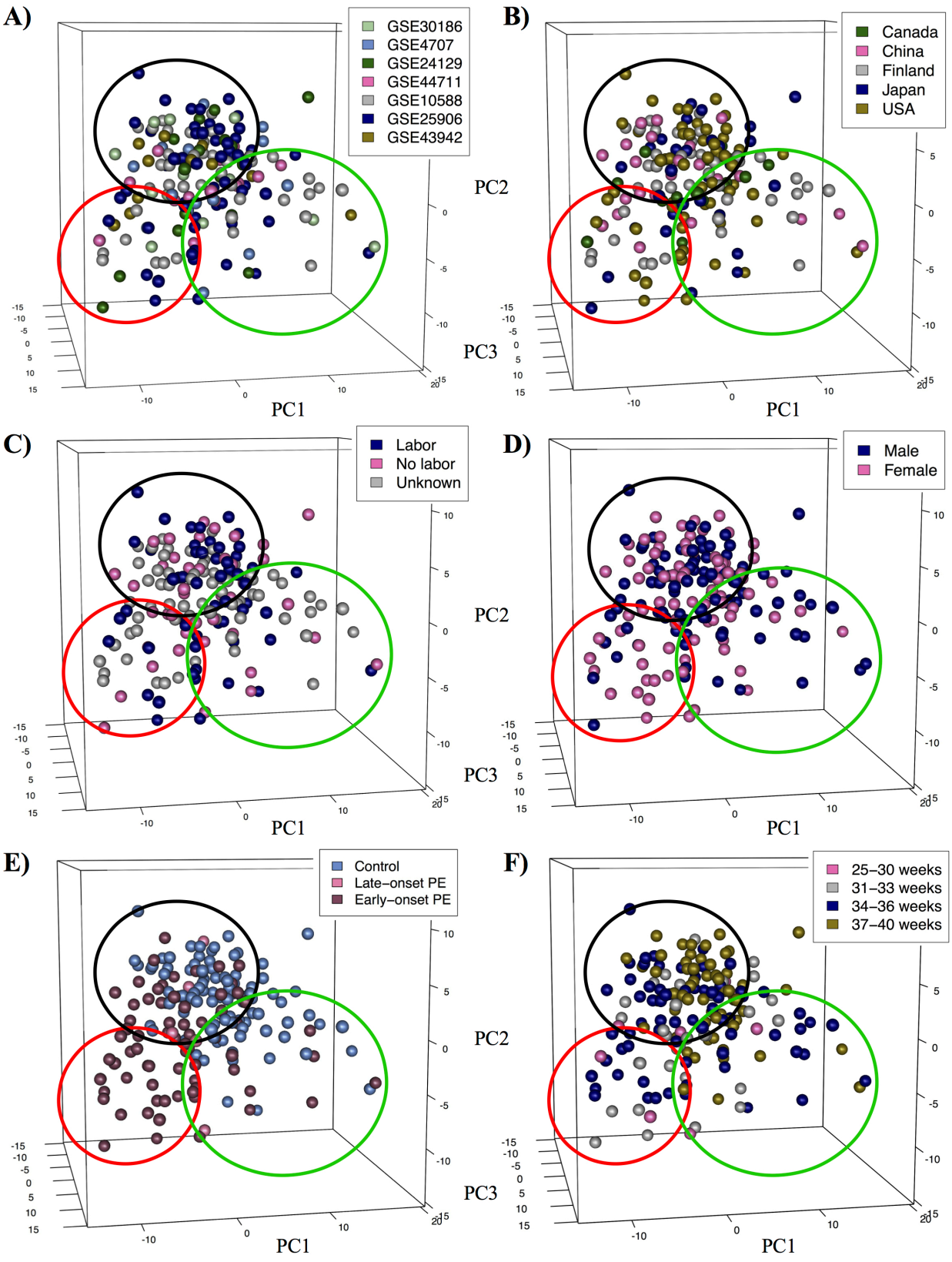

Figure 10 – Principal component analysis (PCA) of potential confounding factors of clustering. None of (**A**) original study membership, (**B**) nationality, (**C**) occurrence of labor, or

(**D**) fetal sex demonstrated differential segregation between cluster 1 (circled in black), cluster 2 (circled in red) and cluster 3 (circled in green). These observations were supported by Fisher's exact tests ($p>0.30$ for all). (**E**) No differential separation of late-onset PE samples was observed compared to the remaining early-onset preeclamptics. (**F**) The few identified preterm controls (<34 weeks) were found in cluster 3 (circled in green). The youngest identified PE samples (<30 weeks) were in cluster 2 (circled in red) while the oldest PE samples (>37 weeks) belonged to cluster 1 (circled in black).

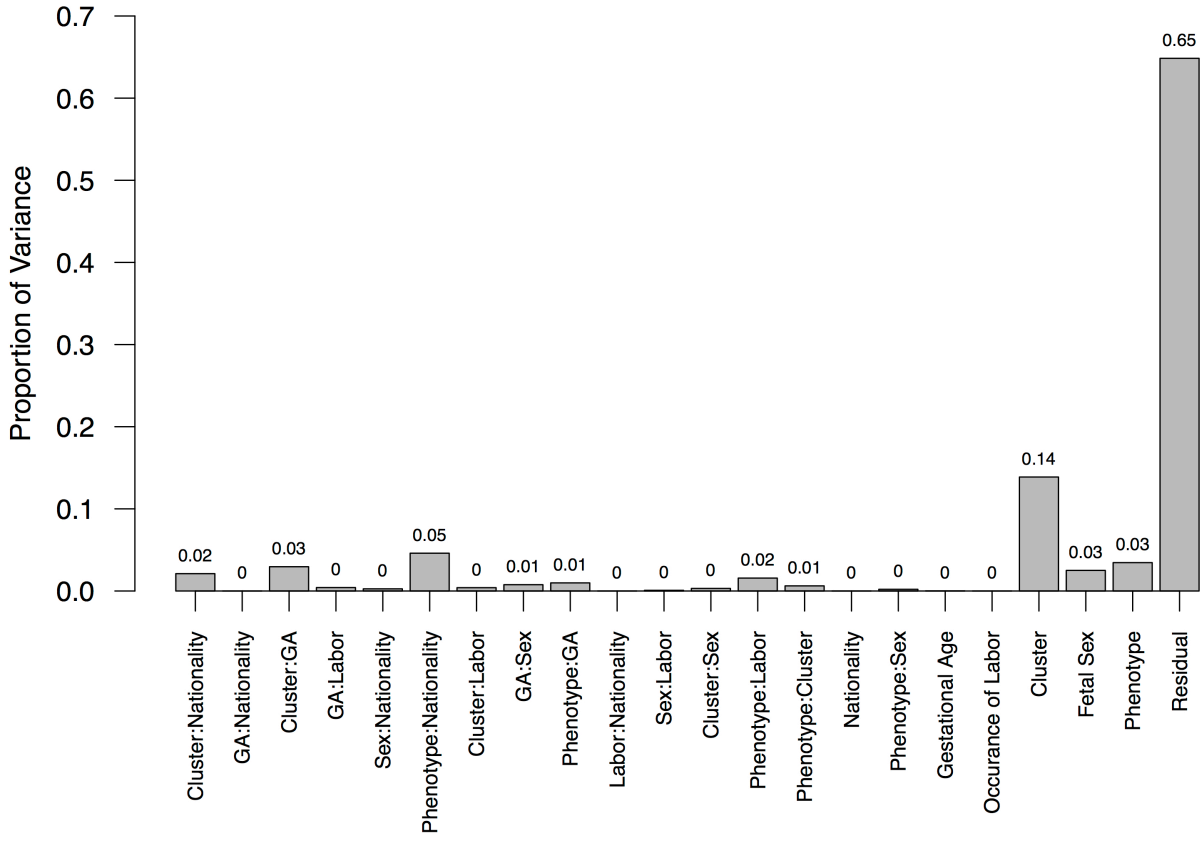

Figure 11 – Principal variance component analysis (PVCA). PVCA on the full dataset of preeclamptics and controls was performed to quantify the effect of each factor (and pairwise interactions between factors) on the gene expression variability within the dataset. Minimal contributions were observed from the covariates and most pairwise interactions. Importantly, however, cluster membership was found to be responsible for more than three times the transcriptional variation than the clinical diagnosis (13.9% versus 3.5%), indicating a diversity of molecular groups with common clinical presentation. The residual variability observed (65%) was likely due to additional covariates that could not be accounted for as well as underlying non-pathological heterogeneity amongst the human samples. Although this value is still high, it is significantly reduced compared to a previously published PVCA interrogation of placental gene expression (residual: 86%) [363], employing a binary clinical classification only.

2.3.3 Assessment of current PE biomarkers

On the basis of the results described above, we hypothesized that previous poor biomarker performance [440] may have been due to the existence of these different subtypes of PE. To investigate this, the expression of two of the most frequently studied markers of preeclampsia, FLT1 and ENG, were assessed. The samples in the PE-enriched cluster 2 demonstrated increased expression of both of these common markers, while the remaining two clusters displayed much lower levels, barely above control values of expression (**Figure 12a**).

Encouraged by this result, the ability of PE markers to distinguish between the controls and the preeclamptic samples as a cohesive group, as well as split into PE subtypes, was tested. Using a subjective binary comparison employed by most typical analyses of this disease, a list of the top ten genes with increased expression in the preeclamptics compared to the controls (LEP, HTRA4, FSTL3, LHB, TREM1, ENG, PAPPA2, FLT1, INHBA, and INHA) was obtained, all of which had been previously identified as potential markers of PE [375]. Visualization of the mean expression value of these ten genes in control samples revealed a normal distribution (**Figure 12b**). In contrast, the PE samples showed a higher mean expression and a bimodal distribution (**Figure 12b**). When the mean expression was plotted for the preeclamptic placentas split into their three subtypes, the PE-enriched cluster 2 had the highest expression and was well separated from the controls, while the PE samples in clusters 1 and 3 displayed a somewhat higher but strongly overlapping "PE signature" with the controls (**Figure 12b**).

Furthermore, using only the expression values of these ten markers, Naive Bayes methods of classification and prediction was able to correctly separate more than 95% of the cluster 2 PE samples from the controls at a 5% FPR (**Figure 12c**). In contrast, only ~50% and ~40% of the preeclamptics in clusters 1 and 3, respectively, could be accurately categorized at this FPR. Combining all samples, these markers have a general ability to correctly identify 70% of all the PE samples as preeclamptic at a 5% FPR (**Figure 12c**).

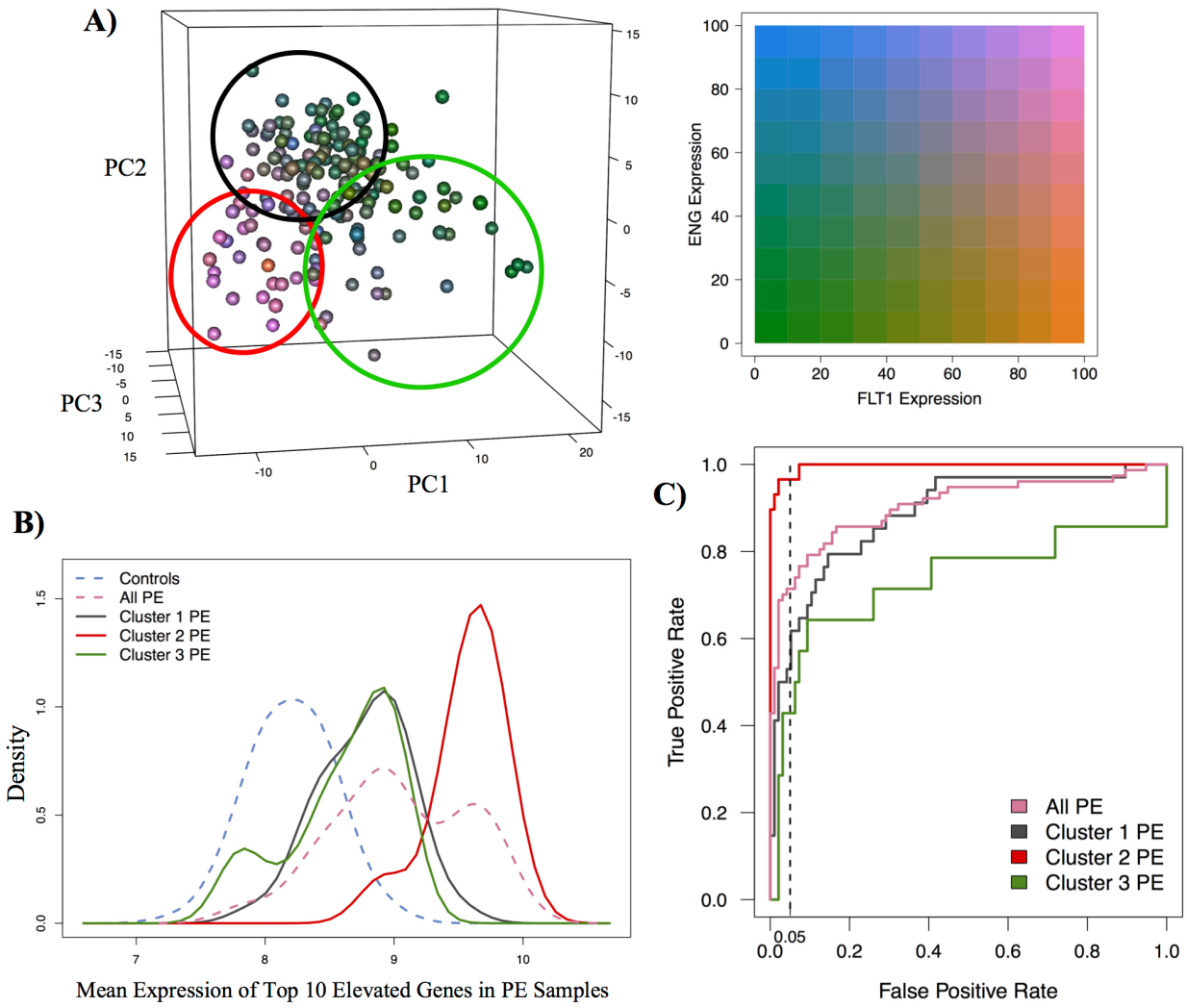

Figure 12 – Markers of preeclampsia. (**A**) Only the samples in the PE-enriched cluster 2 (circled in red) demonstrated highly increased expression of the two most frequently studied markers of PE, FLT1 and ENG (pink), while the remaining preeclamptics in clusters 1 (circled in black) and 3 (circled in green) displayed lower levels of both of these markers (green), more in line with control values of expression. (**B**) Density plots of the mean expression of the top 10 genes significantly elevated in the preeclamptics compared to the controls. Considerable overlap in expression was observed between the controls (dashed blue) and the preeclamptics as a cohesive group (dashed pink). However, when the PE placentas were split into their three subtypes, cluster 2 PE samples (solid red) were easily separated from the controls, while the preeclamptics in clusters 1 (solid grey) and 3 (solid green) still demonstrated considerable overlap. (**C**) Naive Bayes classification using these 10 PE markers was able to distinguish >95% of the PE samples in cluster 2 (red) from the controls at a 5% false positive rate (dashed black line), while only ~50% and ~40% of the preeclamptics in clusters 1 (grey) and 3 (green), respectively, could be correctly categorized. This led to an overall ability of these markers to correctly identify approximately 70% of all the PE samples as preeclamptic (pink).

2.3.4 Investigation into the splitting of the control samples

To determine why the control samples split into two clusters, the placentas were initially investigated for a sampling bias. Based on sets of genes previously established as enriched to either trophoblast or endothelial cells [605], a general upregulation of trophoblast marker expression was observed in cluster 1 controls, compared to an increased expression of endothelial genes in controls belonging to cluster 3 (both $p<0.01$; **Figure 13**). This was also consistent with a statistically significant difference in the expression of GCM1, a transcription factor localized to the trophoblast and involved in syncytialization [244, 651], between cluster 1 and cluster 3 controls (8.81 versus 8.52; $p<0.01$). A sampling bias may, therefore, be involved in the formation of the two control subtypes.

Next, GSEA was used to test if these two control groups demonstrate underlying physiological or pathological differences. This assessment revealed an over-representation of genes generally involved in reproduction and pregnancy in cluster 1 controls, along with genes involved in normal pregnancy processes such as intracellular transport, organelle function, and protein modification and activity (**Figure 14**) [639]. In contrast, cluster 3 controls demonstrated an abundance of genes involved in specific signaling and metabolic pathways, as well as terms related to homeostasis, organ development, and extracellular matrix structure (**Figure 14**) [639]. However, the most surprising finding was a significant enrichment of immune response terms to cluster 3 controls, including inflammatory response, defense response, cytokine activity, and response to wounding. Further investigation into this over-representation of immune pathways revealed an enrichment of genes associated with graft-versus-host disease and allograft rejection in cluster 3 controls, many of which belong to HLA class II. These results, therefore, indicate that the controls likely split into two subtypes predominately due to an underlying pathology difference.

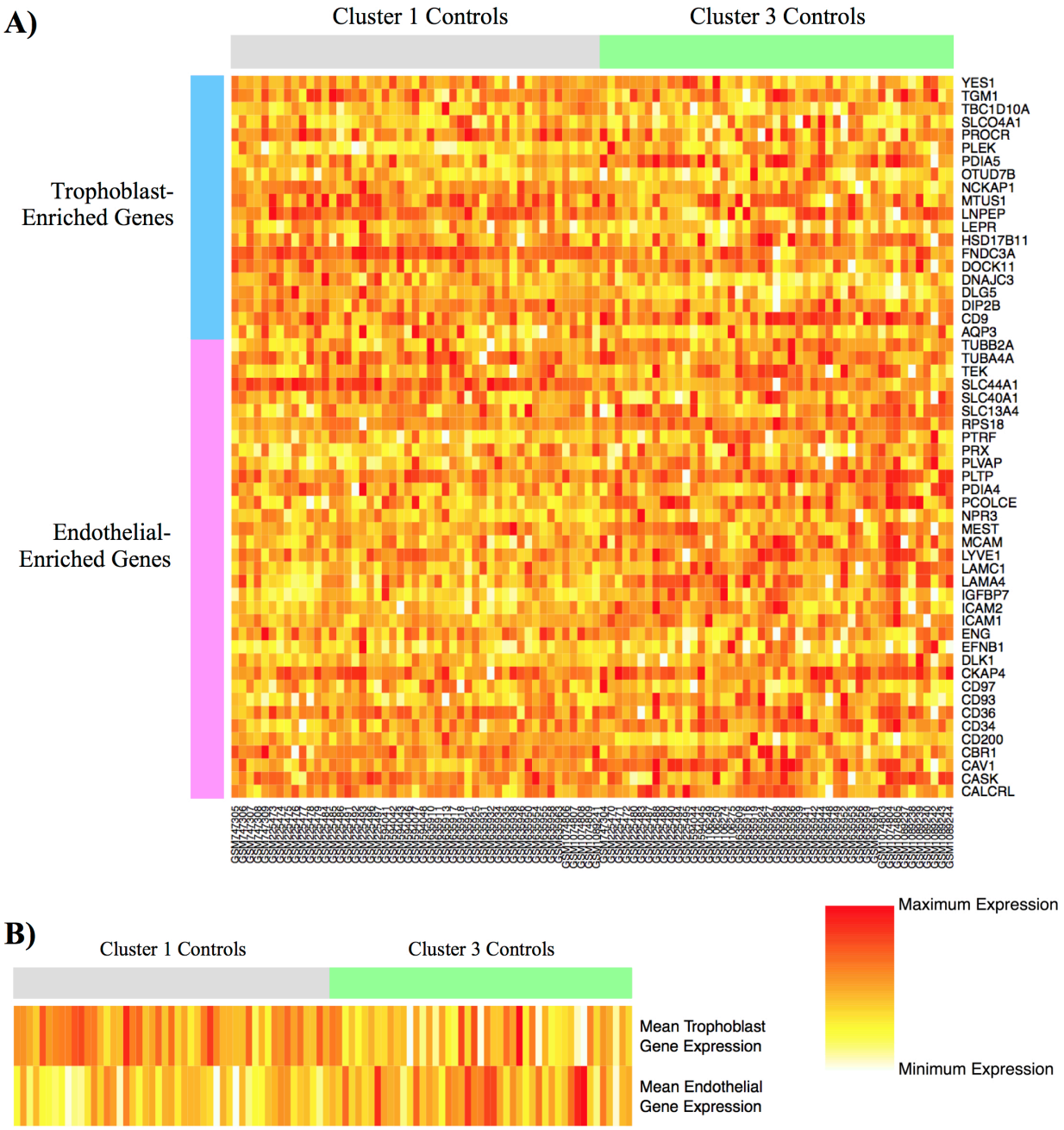

Figure 13 – Trophoblast and endothelial markers for the investigation of a sampling bias in cluster 1 (grey) and cluster 3 (green) controls. Heatmaps of (**A**) individual known markers of placental trophoblasts (N=20; blue) and endothelial cells (N=35; magenta) and (**B**) the mean expression of these genes in each of the control samples. A general upregulation of trophoblast marker expression was observed in cluster 1 controls ($p<0.01$), and increased expression of endothelial genes was shown in controls belonging to cluster 3 ($p<0.01$), implying that a sampling bias may be involved in the formation of the two control subtypes. Samples with high gene expression are colored red, with a gradient of decreasing expression down to white.

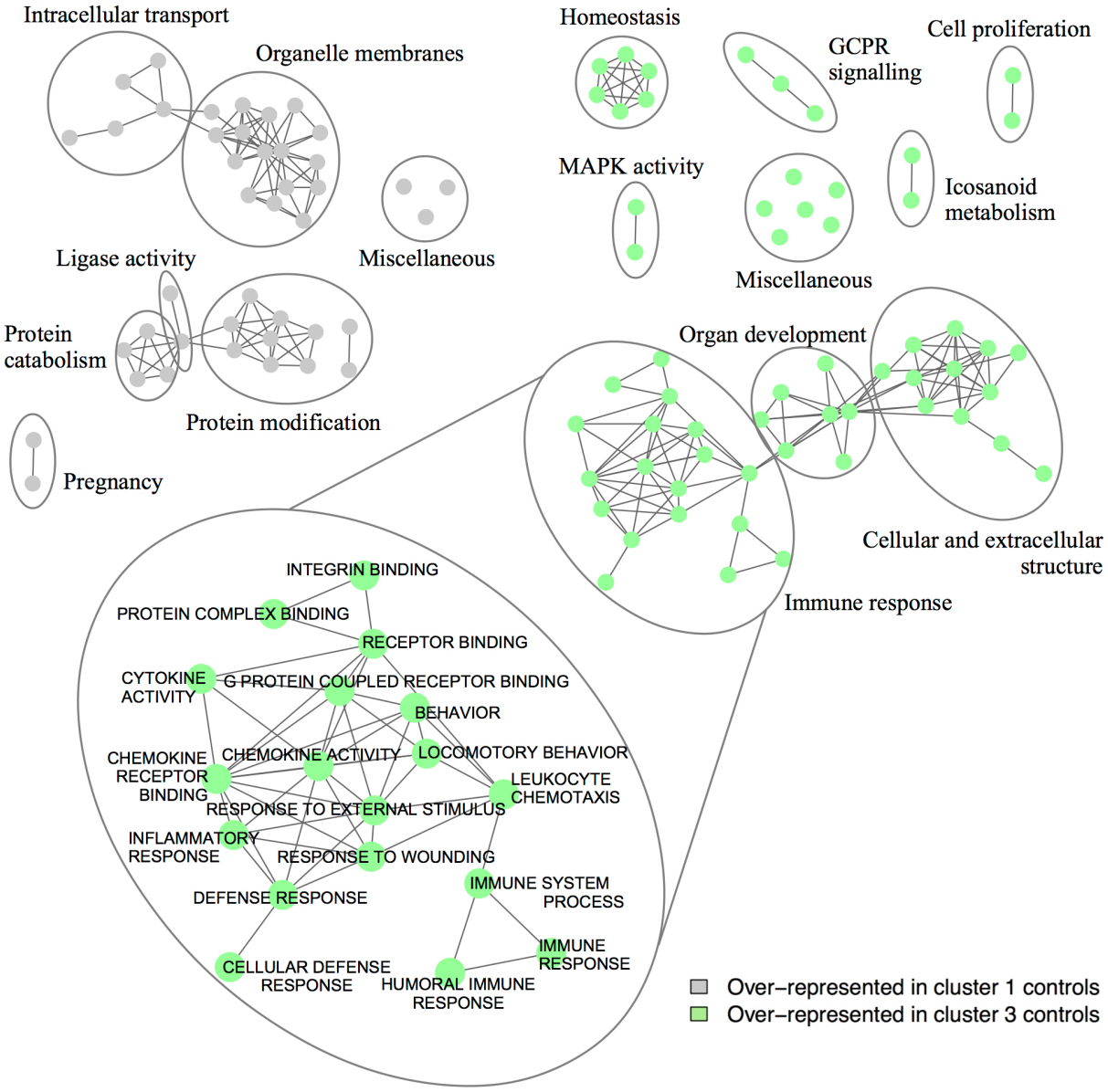

Figure 14 – Gene-set enrichment analysis (GSEA) comparison of the controls in clusters 1 and 3. Cluster 1 controls (grey) revealed a significant over-representation of genes generally involved in pregnancy and normal pregnancy processes, while cluster 3 controls (green) demonstrated an increase in genes related to organ development and extracellular matrix structure, as well as an abundance of terms associated with immune response (enlarged). Results were visualized in Cytoscape and networks of related ontologies (shown as colored nodes connected by grey edges, representing common genes between gene sets) were circled and assigned a group label. Ontologies labeled as "miscellaneous" did not share genes with any of the networks.

2.3.5 Characterization of the PE subtypes

In the absence of detailed patient and placental data, GSEA was employed to characterize the differences in molecular pathology between the three subtypes of PE patients (**Figure 15**). Compared to cluster 2 and cluster 3 PE samples, the preeclamptics in cluster 1 were found to be enriched in few gene sets, most of which were related to organelle membranes and envelopes, as well as protein catabolism (**Figure 15**) [639]. Downregulated were ontologies involved in immune response, cell signaling, and tissue development and structure.

On the other hand, the preeclamptics in cluster 2 displayed a substantial over-representation of genes involved in feeding behaviour, B-cell activation, interferon-gamma production, and hormone activity and secretion, as well as an under-representation of genes associated with oxidative phosphorylation (**Figure 15**) [639]. Additional enrichments to this PE subtype were the hypoxia-inducible factor-1 (HIF-1) and -2 (HIF-2) pathways, which were mostly significant due to the elevated expression of known PE markers involved in these pathways, such as ENG (HIF-1 pathway) and FLT1 (HIF-2 pathway).

Cluster 3 PE samples demonstrated an upregulation of genes involved in homeostasis, organ development, and extracellular matrix structure, as well as numerous terms affiliated with immune response, such as inflammatory response, defense response, cytokine activity, and response to wounding (**Figure 15**) [639]. Further investigation also revealed an over-representation of genes linked to graft-versus-host disease and allograft rejection, which was driven, once again, by the upregulation of HLA class II genes. Gene sets specific to the PE samples of cluster 3 were DNA damage response signal transduction resulting in induction of apoptosis, response to other organism, and response to virus. Downregulated ontologies were involved in female pregnancy, organelle function and membranes, and intra-cellular transport.

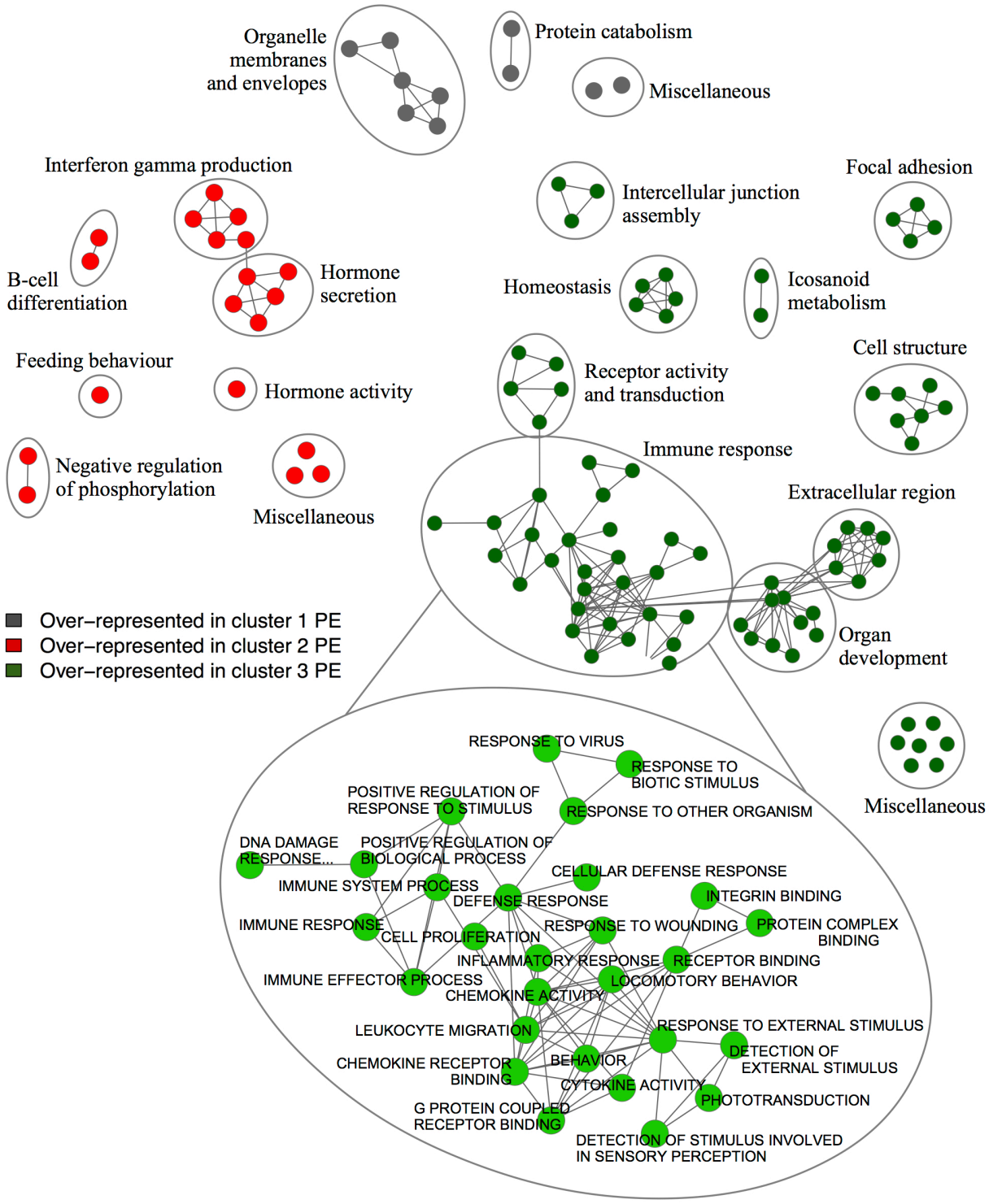

Figure 15 – Gene set enrichment analysis (GSEA) results for the comparison of the PE subtypes. In contrast to the other two PE subtypes, the preeclamptics in cluster 1 (grey) were found to be enriched in few gene sets, most of which were related to organelle membranes and envelopes; the preeclamptics in cluster 2 (red) displayed upregulation of genes associated with feeding behavior, hormone activity, and hormone secretion; and the PE samples in cluster 3

(green) demonstrated an over-representation of genes involved in organ development and extracellular matrix structure, as well as numerous terms associated with immune response. An enlarged version of the immune response network enriched to cluster 3 PE samples, including the *response to virus* ontology, is also shown. GSEA outputs were visualized in Cytoscape and networks of related ontologies (shown as colored nodes connected by grey edges, representing common genes between gene sets) were circled and assigned a group label. Ontologies labeled as "miscellaneous" did not share genes with any of the networks.

2.3.6 Assessment of co-clustering controls and PE patients

Lastly, the preeclamptic samples in clusters 1 and 3 were investigated for their ability to be transcriptionally separated from their co-clustering controls. Initial assessment of differential gene expression revealed few individual genes (six and 15, respectively) reaching statistical significance (FDR $q<0.01$) in the PE samples compared to the control samples in both clusters. Furthermore, no gene sets were found to be significant by GSEA between the preeclamptics and controls in cluster 1 at a false FDR of 25%, whereas, in cluster 3, eight gene sets were over-represented in PE placentas versus the controls at this same FDR. This included regulation of hormone secretion and feeding behaviour, which are terms previously observed as enriched to the cluster 2 PE samples (**Figure 15**). However, as expected from the GSEA results described above (**Figure 14, Figure 15**), the preeclamptics in cluster 3 also exhibited elevated expression of genes involved in the response to a virus. The 20 significant genes annotated to this viral gene set are listed in **Table 2**.

Table 2 – The list of the 20 genes annotated to the GO ontology *response to virus* and found to be upregulated in the preeclamptics of cluster 3 compared to their co-clustering controls.

Gene[a]	Protein Expression in Trophoblast[b]	Cell Component
ABCE1	High	Cytoplasm, membrane, mitochondria
BNIP3	Medium	Mitochondrial membrane
BNIP3L	Medium	Endoplasmic reticulum, mitochondrial membrane
CCL8	---	Secreted
CREBZF	None	Nucleus
FGR	None[c]	Plasma membrane
IFI44	Low	Cytoplasm
IFNAR1	Medium[c]	Plasma membrane
IFNAR2	--[c]	Plasma membrane
IFNGR1	None[c]	Plasma membrane
IFNGR2	Medium	Plasma membrane
IFNW1	---	Secreted
IRF7	High	Nucleus
ISG20	---	Nucleus
PTPRC	None	Plasma membrane
RSAD2	Low	Endoplasmic reticulum
SPACA3	None	Extracellular region, secretory granule, lysosome
TLR8	None	Membranes
TNF	---	Secreted
TRIM22	Medium	Cytoplasm

[a]The genes in bold were also enriched in comparison to the other PE subtypes
[b]As detected by antibody staining of term placenta histology samples on Human Protein Atlas. A dashed line indicates that no trophoblast expression results were available for this gene
[c]Modified from its original result in 2014 when checked again in 2018

2.4 Discussion

We hypothesized that previously observed heterogeneity in preeclampsia, leading to a lack of robust predictive biomarkers and effective treatments for this disorder, was due to the existence of multiple molecular forms of PE. To explore this, we performed an aggregate analysis involving seven previously published PE microarray datasets, and clustered the samples based on gene expression alone, without accounting for clinical diagnosis. This unbiased approach led to the discovery of three patient clusters, all of which contained PE samples, which were found to better explain transcriptional differences among the samples than the binary clinical classification of PE or control by PVCA. Therefore, the primary aim of this chapter (to determine if unsupervised clustering can identify molecular placental subtypes of PE patients) was successful.

Further investigation into the three uncovered preeclampsia subtypes revealed that current PE biomarkers are excellent at finding cluster 2 patients, but are inadequate for the recognition of cluster 1 and cluster 3 PE samples. Thus, when all three subtypes are grouped together, the true gene expression differences are underestimated, resulting in density plots and ROC curves that are closer to **Figure 7e,f** than **Figure 7b,c**. Additionally, each of these subtypes displayed different previously published phenotypes of PE: cluster 2 PE samples fit with the classic, "canonical" understanding of preeclampsia [2, 6], demonstrating an over-representation of known PE markers and genes associated with hypoxia and hormone production and secretion; PE samples of cluster 3 are enriched in genes related to immune response [41, 44, 652, 653]; and cluster 1 PE samples likely represent a poor maternal response to pregnancy that presents without overt placental pathology, a group that is often overlooked in the literature [212]. What is unique about this study is that these subtypes have clustered apart from each other, strongly indicating the existence of multiple causative sources of preeclampsia, and revealing molecular pathways that may mark each group.

The surprising observation in this analysis was the discovery of both PE and control samples in clusters 1 and 3. We propose the following potential explanations that, when combined, may account for this unexpected finding. First, it is possible that some of the PE patients, particularly in cluster 1, may have been misdiagnosed as preeclamptic, and were really afflicted with another maternal hypertensive disorder, such as gestational hypertension or chronic hypertension [20].

This is supported by the GSEA and gestational age comparisons, which indicate that cluster 1 is largely composed of the healthiest term placentas in this dataset. Furthermore, it is known that gestational hypertension does not cause the same increases in ENG and FLT1 levels as PE [65, 654]. Therefore, it is also anticipated that their global placental gene expression would have more similarities to the healthy controls of cluster 1 than the canonical preeclamptics of cluster 2.

An additional explanation is poor or advantageous maternal adaptation to pregnancy. Pregnancy leads to many physiological changes in the mother [271], such as reduced vascular resistance and increased cardiac output. A failure of the mother's adaptive processes could result in the symptoms of PE despite a normal placenta, which would also explain the co-clustering of the cluster 1 PE samples with the healthy controls. The converse could also occur where the mother adapts to an abnormal placenta, reducing the severity of the symptoms and improving the outcome. This is possibly the case for the controls in cluster 3, where an earlier poor placental event may have been resolved or compensated for by the maternal system but left a mark of increased immune response.

Lastly, and with the strongest argument for the phenotype mixture in cluster 3, is the likelihood that despite the aggregation of seven microarray datasets, the final sample size of 173 may still be too underpowered to identify all existing clusters. Evidence for this explanation is the cluster 2 PE-related gene sets found to be significantly enriched to the PE samples in cluster 3 compared to their co-clustering controls. This overlap may be anticipated from the PCA plot of cluster membership as most of the PE cluster 3 samples are near the border of cluster 2 while the control samples are farther away. Therefore, a further increase in sample size may allow for cluster 3 to resolve into a control subgroup and a preeclampsia subgroup, demonstrating a milder but still existent canonical PE phenotype. Additional support for this theory exists in the enrichment of viral response genes to the cluster 3 PE samples only.

Of the 20 significant genes annotated to this response to virus ontology, most are known to be expressed in the placental trophoblast based on Protein Atlas database records [648] (**Table 2**), and form a contiguous cellular pathway, spanning the plasma membrane, cytoplasm, and nucleus based on Entrez annotation [648, 649]. The inclusion of six genes usually not expressed in healthy placentas may indicate either immune cell invasion or aberrant ectopic expression, although the immune cell invasion theory is also supported by the observation of elevated TNF

expression, a molecule that is known to be involved in the macrophage-induction of trophoblast apoptosis [291-294]. Additionally, these 20 genes appear to be involved in a general viral response, associated with a range of different viruses, and not specific to any single infectious entity [649]. This indicates the possibility of a plurality of viral infection types occurring among the cluster 3 PE samples, such that responses to specific viruses are not apparent. Potential culprits are cytomegalovirus (CMV) [40, 41], human papilloma virus (HPV) [44], and adeno-associated virus-2 (AAV-2) [42], as these are all known to be capable of infecting placental trophoblasts and have been linked to PE [41, 44].

Furthermore, cluster 3 samples demonstrated an over-representation of genes associated with allograft rejection and graft-versus-host disease (GVHD), compared to the samples in clusters 1 and 2. These ontologies have been previously affiliated with poor pregnancy outcome and the development of preeclampsia [652, 653]. However, the majority of the significant genes annotated to these gene sets, including the HLA class II molecules, are not usually expressed in placental cells [655-657]. This enrichment, therefore, may be due to an increased infiltration of maternal immune cells, which do express these genes, into the placenta. Although this may simply be a component of the GVHD response, maternal leukocyte infiltration can also occur in the placental response to a virus [658, 659]. Additionally, viral infection and specific combinations of HLA isotypes have been shown to have compounding effects on pregnancy outcome, including preeclampsia development [60]. Therefore, while it is evident that the PE samples in cluster 3 demonstrate a heightened immune response relative to the remaining samples, it is unclear if this is a true viral infection, an allograft rejection, or multiple, potentially compounded, immunologically regulated events. Regrettably, as direct access to alternate preparations of these previously published patient samples were not available, it was not possible to investigate these theories, or any of these results, with targeted assays in this chapter.

Although the use of deposited and archived gene expression data is an excellent resource, this chapter also highlights the necessity of having detailed clinical records available for all human patient studies such that a more complete covariate examination can be performed and gene to phenotype relationships can be tested. Additionally, given possible sampling bias observed within the control placentas, this study emphasizes the importance of obtaining multiple biopsies per placenta in order to control for the high degree of variability in gene expression frequently observed across the same tissue [336]. Finally, this chapter also indicates the requirement of

having sufficient sample size in order to be able to distinguish biologically meaningful subgroups within a heterogeneous human population. Although this was the largest dataset of PE samples analyzed before 2015, it is highly probable that a further increase in placental number would identify additional clusters, representing rarer but important pathological and physiological characteristics.

3 Chapter 3 – Robust Gene Expression Clusters of Preeclamptic Placentas are Strongly Associated with a Number of Clinical Attributes

Content in this chapter is published in:

Leavey K, Benton SJ, Grynspan D, Kingdom JC, Bainbridge SA, Cox BJ. (2016). Unsupervised Placental Gene Expression Profiling Identifies Clinically Relevant Subclasses of Human Preeclampsia. *Hypertension*. 68: 137-147. [660]

Co-authors' contributions are described in the methods section.

3.1 Introduction

Preeclampsia (PE) is a potentially life-threatening, systemic, hypertensive disorder affecting 3-8% of all pregnancies. Apart from expectant management and delivery of the infant and the placenta, there currently exists no cure or effective treatments for PE. We [371, 605, 639], and others [278, 640, 661], have proposed that the lack of robust biomarkers and interventions for PE is due to the multifactorial nature of this disease, a notion supported by considerable evidence within the human literature [30, 652, 662, 663]. As such, past placental microarray studies with small and highly selected patient cohorts, predominately assessed using a binary classification system (of PE versus control), do not accurately reflect the true clinical presentation of patients. Even the separation of women into early-onset (diagnosis before 34 weeks) and late-onset PE groups [30, 663] still does not fully explain the heterogeneity observed in this disorder. Although these studies are likely uncovering valid information about PE disease, these findings are not applicable to the full range of PE patients and, thus, do not result in substantial clinical progress in prediction and treatment. A more complete molecular understanding of preeclampsia, therefore, requires both a large broad sample set representing the high variation of patients seen in a clinical setting and an unbiased analysis.

As a first step toward class discovery of PE pathology, we performed an aggregated analysis of seven previously published human PE placental microarray datasets [353, 363-368] using unbiased/unsupervised multivariate clustering techniques (Chapter 2). Our novel application of these techniques to preeclampsia identified three molecular subtypes of PE placentas, exhibiting distinct alterations in disease pathways and varying expression of commonly accepted PE markers. However, this analysis was limited by the paucity of matched clinical information, as well as the lack of access to these samples for follow-up analyses, thus restricting our ability to truly comprehend these different molecular groups.

In this chapter, the previously assessed PE microarray studies were combined with a new PE-focused microarray dataset, which was both highly annotated and accessible. We postulated that this robust dataset, with clinical information ranging from pre-pregnancy to delivery, would illuminate not only clinical differences between subtypes of PE, but also yield insight into potential contributions of individual maternal factors to the development of specific types of preeclampsia.

3.2 Methods

3.2.1 BioBank sample selection

A total of 157 placenta samples were purchased from the patient sample set at the Research Centre for Women's and Infants' Health BioBank (Mount Sinai Hospital, Toronto, Canada) by Drs. Brian Cox and Shannon Bainbridge. Samples were selected to span multiple distinct clinical classification groups of non-PE and PE patients, including women with chronic hypertension as an example of a likely maternal contribution to disease (**Figure 16**). Although the goal was to collect at least 15 samples per clinical group, based on power analysis performed by Dr. Cox (PowerAtlas [664] and the Benjamini-Hocherg framework for multiple testing), this was not feasible for all groups. At the time of sample collection and purchase (2013), PE was defined as the onset of systolic pressure ≥140 mmHg and/or diastolic pressure ≥90 mmHg after the 20th week of gestation, accompanied by proteinuria (greater than 300 mg protein/day, or at least 2+ by dipstick) [71]. Chronic maternal hypertension was defined as systolic pressure ≥140 mmHg and/or sustained diastolic ≥90 mmHg before the 20^{th} week of gestation. Within these groups, there was an approximately balanced representation of fetal sex and co-morbidities of preterm (<34 weeks gestation) and small-for-gestational-age infants (SGA; neonatal birth weight <10th percentile for gestational age and sex, based on a Canadian growth reference [169]). Patients with diabetes (pre-existing or gestational), sickle cell anemia, and/or morbid obesity (BMI ≥ 40) were excluded, and all samples came from singleton pregnancies. Some samples were also associated with HELLP (hemolysis, elevated liver enzymes, low platelets (thrombocytopenia, <100,000/ul)) syndrome.

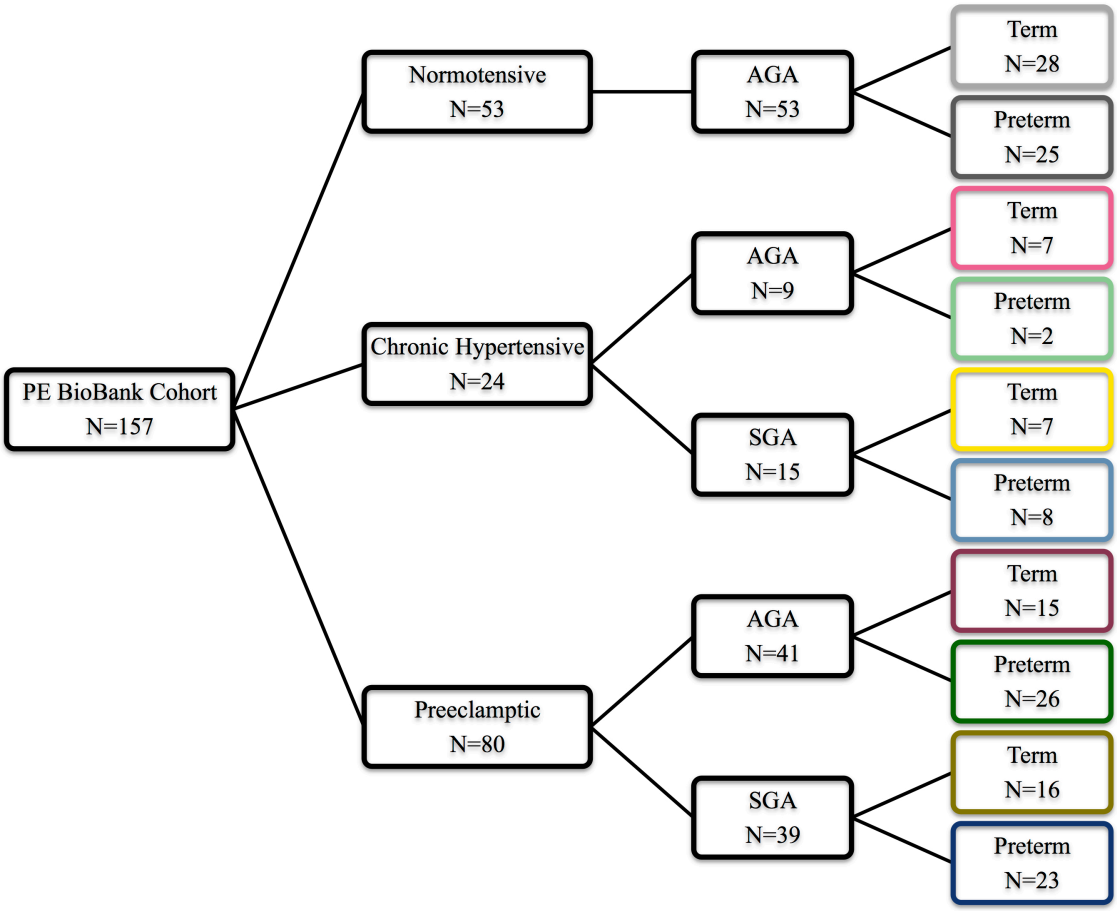

Figure 16 – Phenotype breakdown of the 157 placenta samples purchased from the RCWIH BioBank (PE-focused BioBank cohort, used in Chapters 3-6). AGA = average-for-gestational-age, SGA = small-for-gestational-age, preterm = delivered before 34 weeks.

3.2.2 Placental sampling and microarrays

Placental sampling was performed by the BioBank, utilizing a standardized procedure in which four tissue biopsies (one sample/quadrant, excluding the chorionic plate) are collected per placenta [665], rinsed in PBS to remove contaminating maternal blood, pooled, snap-frozen in liquid nitrogen, and crushed into a powder. This is a significant improvement over prior studies that only obtained 1-2 biopsies per placenta, given the considerable known heterogeneity within this tissue. mRNA was extracted from each of these pooled placental samples using Trizol and

RNAeasy spin columns by Drs. Brian Cox and Shannon Bainbridge, assessed for quality by an Agilent Bioanalyzer, and sent to the Princess Margaret Genomics Centre (Toronto, Canada) for hybridization against Human Gene 1.0 ST Array chips (Affymetrix). These particular arrays contain 11-20 probes per gene of interest, each 25 bases long. The resulting microarray data is available from the Gene Expression Omnibus (GEO) database under the accession number GSE75010.

3.2.3 Assembly and clustering of the combined dataset

The 157 BioBank microarray CEL files (PE "BioBank" samples) were processed, normalized, converted into log2 values, and probes sets were collapsed into a robust average expression value in R 3.0.1 using the *Affy* library [614]. In order to increase the cohort size, these samples were merged with the seven previously published datasets from Chapter 2 (PE "Aggregate" samples) using the *virtualArray* package [618], which employs Empirical Bayes methods of normalization and batch correction. For this step, the BioBank files were split into three random groups, as *virtualArray* cannot handle datasets as large as 157 samples.

This combined set of BioBank and Aggregate samples was then unbiasedly assessed as previously described in Chapter 2. Briefly, the expression data was filtered for genes with variances in the top quartile, and subjected to unsupervised multivariate model-based clustering, using the *mclust* package [621], as well as principal component analysis (PCA), using the *rgl* library. The stability of the clusters was investigated using the *clusterboot* function [666], with 1000 bootstrap resamples of the data and the "noisemclustCBI" cluster method. This function works by clustering the resampled data and then computing the Jaccard similarity between each of the original clusters and the most similar cluster in the resampled set. Clusters that are consistently re-discovered are considered stable. Additionally, the center of cluster 1 by PCA was utilized as being representative of "normal" for the identification of a gradient of birth weight z-scores in cluster 3 and sample selection for array-based comparative genomic hybridisation (aCGH; see below).

3.2.4 Gene set enrichment analysis (GSEA)

Each of the complete clusters 2-5 were compared separately to the "normal" cluster 1 using the Molecular Signatures Database (MsigDB) associated with the GSEA software v2.1.0 [632],

similar to previously described in Chapter 2. Briefly, all GO gene sets (v4.0), Hallmark gene sets (v5.0), and Positional gene sets (v5.0) with 10–1000 members were assessed against a background model of the 14,651 genes found in common across all original microarray platforms. The recommended number of permutations (1000) was performed with the less stringent (gene set) permutation type. Pathways were considered significant at a corrected false discovery rate (FDR) q-value <0.25. Over-represented GO ontologies were visualized in Cytoscape v2.8.3 using the two-color Enrichment Map plugin [647], with a raw p-value cutoff of 0.01, a FDR q-value cutoff of 0.25, and an overlap coefficient of 0.5. Nodes were re-colored to reflect the cluster in question, and networks of related ontologies were circled and assigned a group label. Furthermore, expression differences in specific genes of interest were confirmed by t-tests and ANOVA, as appropriate.

3.2.5 Organization of the clinical information

The BioBank samples were accompanied by a significant amount of maternal and fetal clinical information (gestational age, ethnicity, fetal sex, pregnancy history, method of delivery, etc.), as well as details about the placentas themselves (weight, dimensions, and umbilical cord information). Assistance in interpreting the clinical data was obtained from Dr. John Kingdom. While most clinical attributes were known for all BioBank samples, others (such as blood work, paternal ethnicity, and Doppler ultrasound data) were not complete. This clinical data was merged with the gene expression dataset in R. Covariates were converted (if necessary) to either a continuous numeric or a categorical variable for analysis. In cases where multiple measurements over pregnancy were available per patient (ex. blood pressure or Doppler ultrasound pulsatility index), the mean, maximum, and/or minimum value was calculated and utilized, as appropriate. Placental weight z-scores were computed based on normal weight charts for male and female fetuses [667] and blood work and blood pressure results obtained on the day of delivery were removed to avoid potential confounding with the effect of labor or cesarean section surgery. While the Aggregate data was included in the initial clustering and PCA visualization for statistical power, all detailed clinical phenotyping of the clusters was performed on the BioBank samples only, as these were the samples where this information was available and more consistently collected. Statistical analysis was performed using Mann–Whitney–Wilcoxon tests, Fisher's exact tests, Kruskal–Wallis rank-sum tests, Student's t-tests, and Pearson correlations in R 3.1.3, as appropriate.

3.2.6 Quantitative polymerase chain reaction (qPCR)

Human TaqMan primer/probes sets were purchased from Life Technologies for cytomegalovirus (*UL132* gene, Pa03453400_s1), human papillomavirus 16 (*E1* gene, Pa03453396_s1), and Epstein–Barr virus (*IR1* gene, Pa03453399_s1), which have been shown to be capable of infecting trophoblasts and have been associated with PE [40, 44, 45]. RNA from three cluster 3 samples was converted into complementary DNA (cDNA) using reagents purchased from Invitrogen (catalog numbers 48190011 and 18064014), ThermoScientific (material number R0192), and New England BioLabs (U.S. product codes M0297S1 and M0303S1) (**Appendix A**). Samples were run in triplicate (using the TaqMan Universal PCR Master Mix (Life Technologies, catalog number 4304437)) on a qPCR machine owned by Dr. Patricia Brubaker (MJ Research PTC-200 Thermal Cycler with a Bio-Rad Chromo 4 Continuous Fluorescence Detector head).

3.2.7 Array-based comparative genomic hybridization (aCGH)

To investigate chromosomal copy numbers, DNA was isolated (Promega Wizard® Genomic DNA Purification Kit) from the eight cluster 5 BioBank samples that plotted the furthest from the center of cluster 1 on principal component 3 (PC3), and subjected to aCGH analysis (Princess Margaret Genomics Centre (Toronto, Canada); Agilent Human 8x60K Array), compared to a pooled reference sample of the ten cluster 1 BioBank term controls that were closest to the center of cluster 1 (based on PC1-3). In this case, DNA from each cluster 5 sample and the pooled cluster 1 reference sample are differentially labeled with fluorescent dyes (typically cyanine-3 and cyanine-5), combined, and co-hybridized to a microarray containing probes for different genomic regions. The sample and reference competitively bind to the spots and the resulting fluorescence intensity ratios are reflected by their relative quantities. The raw intensity aCGH data was background-subtracted and normalized using the *CGHnormaliter* package in R, and the results were analyzed and visualized using the *KCsmart* library [668], with a kernel width of 6Mb, a median probe distance of 41Kb, and 1000 permutations. Significance was assigned to regions achieving a Bonferroni corrected p-value <0.05. The mean fold changes across the probes on chromosome 19 in cluster 5 samples versus the pooled reference sample were calculated and utilized in an algebraic formula ((1.5 fold change x estimated portion of cells with

a trisomy) + (1 fold change x (1 – estimated portion of cells with a trisomy)) = mean fold change) to estimate the number of biopsied placental cells with a potential trisomy.

3.2.8 Ethics

Ethics approval for this study was granted from the Research Ethics Boards of Mount Sinai Hospital (#13-0211-E), the University of Toronto (#29435), and the Ottawa Health Science Network (#2011623-01H). All women provided written informed consent for the collection of biological specimens and medical information.

3.3 Results

3.3.1 Formation of the combined dataset and clustering

Merging of the 157 highly annotated placenta samples purchased from RCWIH BioBank with the seven previous published datasets from our prior aggregate analysis (Chapter 2) resulted in a final combined PE-focused cohort of 330 placentas (157 PE (including superimposed on chronic hypertension (CH)), 24 CH without preeclampsia, and 149 controls) with expression values for 14,651 genes found in common across all original microarray platforms. Unsupervised multivariate clustering of this combined dataset, using only the top quartile of most variable genes (N=3,663), identified five patient clusters as the optimal number based the Bayesian Information Criterion (**Figure 17a**). Visualization of these clusters by principal component analysis revealed two larger clusters (clusters 1 and 2) at the center of the plot with three smaller clusters (clusters 3–5) radiating away from them (**Figure 17b**). Of these, clusters 1, 2, and 4 were stable (>75% similarity between the bootstrapped reclusters), while cluster 3 was somewhat less so (55% similarity) and cluster 5 was relatively unstable (40%) (**Figure 17c**). In general, the cluster 1 and 2 Aggregate samples from Chapter 2 distributed similarly in this larger-scale analysis; however, patients that previously belonged to cluster 3 were found to split across clusters 1, 3, 4, and 5 in the present study (**Table 3**). No significant batch effects were observed across the clusters (**Table 4**).

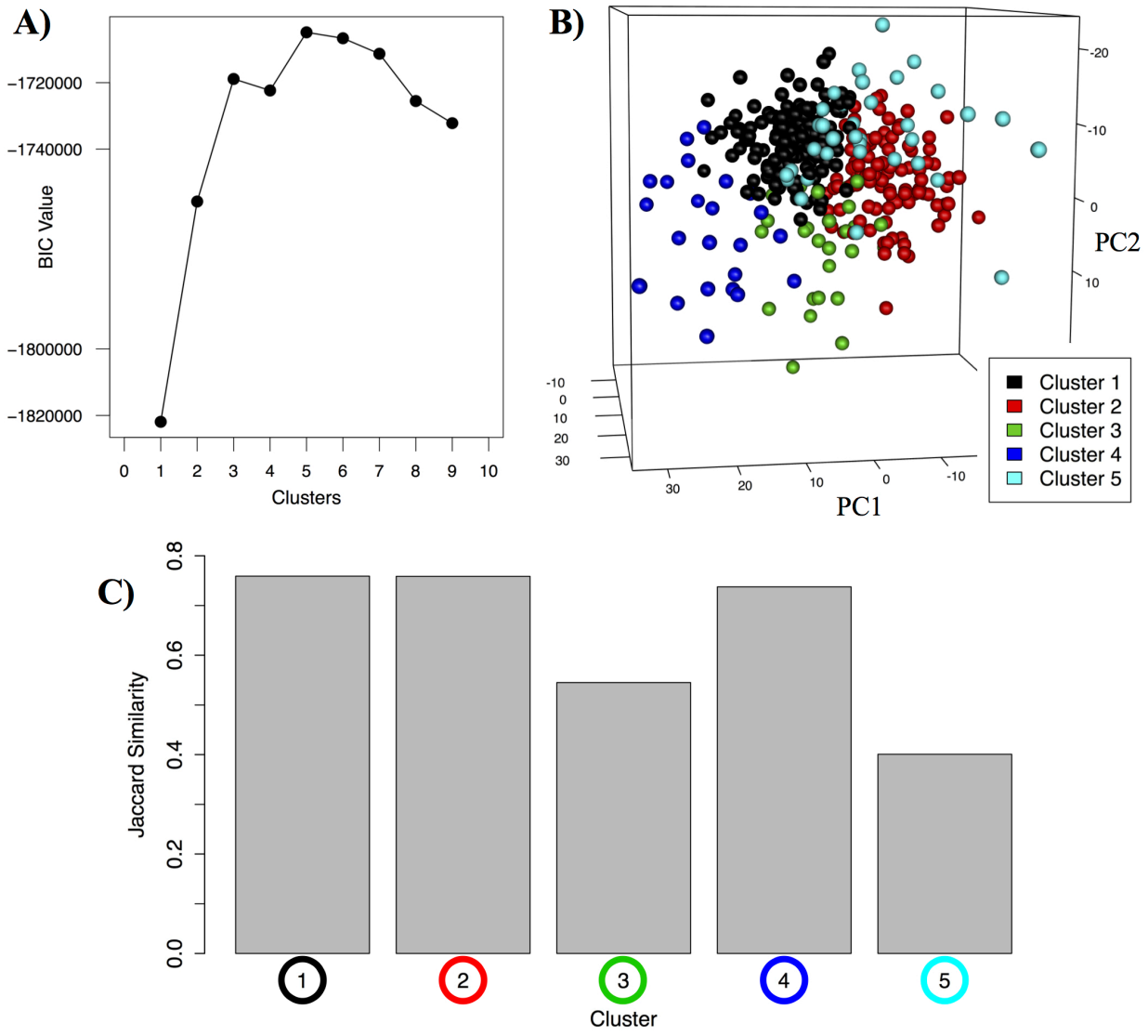

Figure 17 – Unsupervised clustering of the combined dataset of 157 BioBank samples and 173 Aggregate samples (N=330) revealed five clusters of placental gene expression. (**A**) The Mclust model VEI (diagonal, equal shape) gave the best performance based on the Bayesian Information Criterion (BIC; y-axis) and an optimal cluster number of five was selected (clusters; x-axis). (**B**) Principal component analysis (PCA) of the full combined dataset showed the two largest clusters (clusters 1 (black) and 2 (red)) at the center of the plot with three smaller clusters (clusters 3 (green), 4 (blue), and 5 (cyan)) radiating away from them. (**C**) A barplot of the average Jaccard similarities from the *clusterboot* analysis revealed that clusters 1, 2, and 4 were stable (>75% similarity between the bootstrapped reclusters), while cluster 3 was less stable (55% similarity) and cluster 5 was relatively unstable (40%).

Table 3 – Aggregate (previously published/external) sample cluster inclusion in Chapter 2 (clusters 1-3) versus this chapter (clusters 1-5).

	Cluster 1	**Cluster 2**	**Cluster 3**	**Cluster 4**	**Cluster 5**
Cluster 1	60	18	1	0	4
Cluster 2	0	28	0	0	1
Cluster 3	22	0	16	9	14

Table 4 – Contribution of each dataset/batch to the five clusters identified in this chapter. For merging, the BioBank samples were split into three random groups. There was no significant differential distribution of the batches across the clusters (p=0.74).

Dataset	**Cluster 1**	**Cluster 2**	**Cluster 3**	**Cluster 4**	**Cluster 5**	**Total**
GSE30186	5	4	1	2	0	12
GSE10588	22	12	2	3	4	43
GSE24129	9	3	1	1	2	16
GSE25906	28	14	10	1	7	60
GSE43942	5	5	0	2	0	12
GSE4707	5	3	2	0	4	14
GSE44711	8	5	1	0	2	16
BioBank subgroup 1	20	19	3	5	5	52
BioBank subgroup 2	22	18	4	4	4	52
BioBank subgroup 3	18	19	4	5	7	53
Total	**142**	**102**	**28**	**23**	**35**	**330**

3.3.2 Clinical group distributions

The clusters were first assessed for the inclusion of the different PE and non-PE clinical groups (**Figure 18a**). Cluster 1 contained mostly controls from both preterm (<34 weeks) and term deliveries (**Figure 18b**). Similar to the observations in Chapter 2, cluster 1 also contained some PE samples, generally associated with term deliveries and average-for-gestational-age (AGA) infants. Cluster 2 was composed predominately of PE samples, either delivered preterm or term with small-for-gestational-age (SGA) infants (**Figure 18b**), as well as a portion of the BioBank samples from women with chronic hypertension (CH) but without PE who delivered prematurely. Clusters 3 and 5 contained a mixture of PE and non-PE samples, whereas cluster 4 was mostly composed of preterm controls (**Figure 18b**). The clustering results, therefore, imply the existence of at least four molecular-based PE subtypes in this combined cohort (in clusters 1, 2, 3, and 5), demonstrating molecular separation far more complex than the simple distinction between "term/late-onset" versus "preterm/early-onset", and also more complex that the distribution observed in Chapter 2 with only 173 samples.

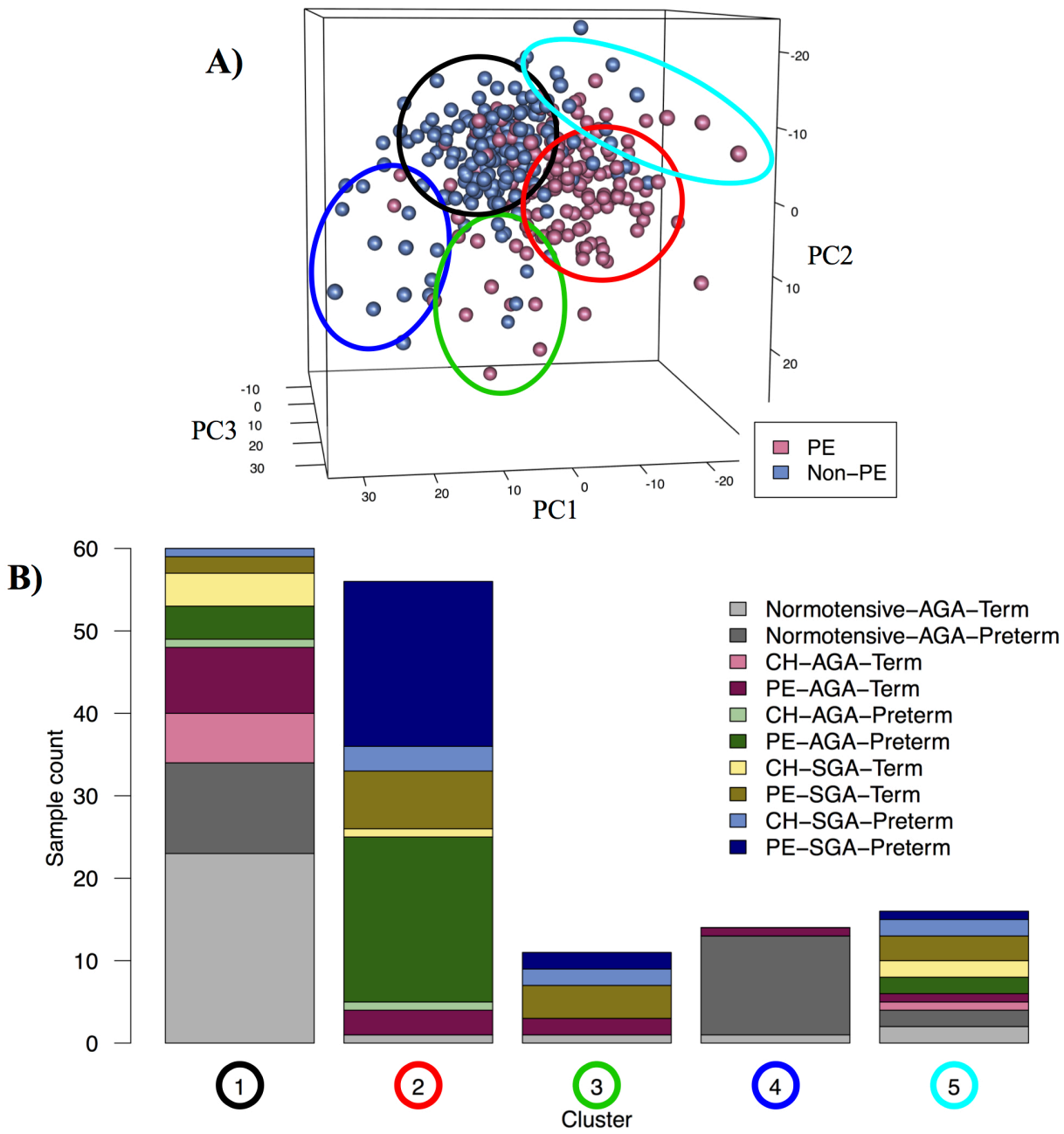

Figure 18 – Phenotype breakdown of the five clusters. (**A**) Principal component analysis (PCA) of the full combined dataset showed that each of the five clusters (cluster 1 circled in black, cluster 2 in red, cluster 3 in green, cluster 4 in blue, and cluster 5 in cyan) demonstrated varying numbers of preeclamptic (PE; pink) and non-PE (blue) samples. (**B**) Barplot displaying the clinical group distributions across the clusters for the BioBank samples only. Cluster 1 contained most of the BioBank term control samples, as well as half of the preterm (delivery <34 weeks) controls and some PE and chronic hypertensive (CH) samples that were generally associated with average-for-gestational-age (AGA) infants. Cluster 2 was composed predominately of preeclamptics (with AGA and small-for-gestational-age (SGA) infants), in addition to some of the preterm CH patients. Both clusters 3 and 5 contained a mixture of PE and non-PE samples, whereas cluster 4 was primarily composed of the remaining preterm controls. CH and PE samples are color matched, with darker shades indicating the more severe PE diagnosis.

3.3.3 GSEA compared to cluster 1

To characterize the different clusters at a molecular level, gene-set enrichment analysis (GSEA) was applied to the full combined set of Aggregate and BioBank samples [660]. Given that cluster 1 is consistently the healthiest group of placentas in our dataset, this analysis was performed comparing clusters 2-5 to this cluster. In contrast to cluster 1, the PE-enriched cluster 2 demonstrated an over-representation of genes involved in hormone secretion and activity, hypoxia, and glycolysis ($q<0.25$; **Figure 19**). Cluster 3 revealed an enrichment of numerous genes involved in immune and inflammatory responses, cytokine/interferon signaling, the extracellular space, apoptosis, and hypoxia ($q<0.25$; **Figure 19**). Additionally, of particular interest in cluster 3 were genes associated with allograft rejection and viral reproduction (**Figure 19**). These findings in clusters 2 and 3 are highly consistent with the results in Chapter 2.

Compared with cluster 1, the newly discovered cluster 4 demonstrated increased expression of genes involved in normal cell processes, such as metabolism, cell proliferation, cell cycle, and chromosome organization, in addition to genes involved in DNA damage and inflammation ($q<0.25$; **Figure 19**). Cluster 5 revealed an over-representation of genes involved in hormone secretion, response to nutrients, and ion channel activity, as well as numerous genes annotated to neurological processes, such as olfactory transduction and signaling ($q<0.25$; **Figure 19**). Clusters 2 to 4 each demonstrated few significant under-represented gene sets compared with cluster 1, whereas cluster 5 exhibited decreased expression of genes involved in the cell cycle and an inflammatory response.

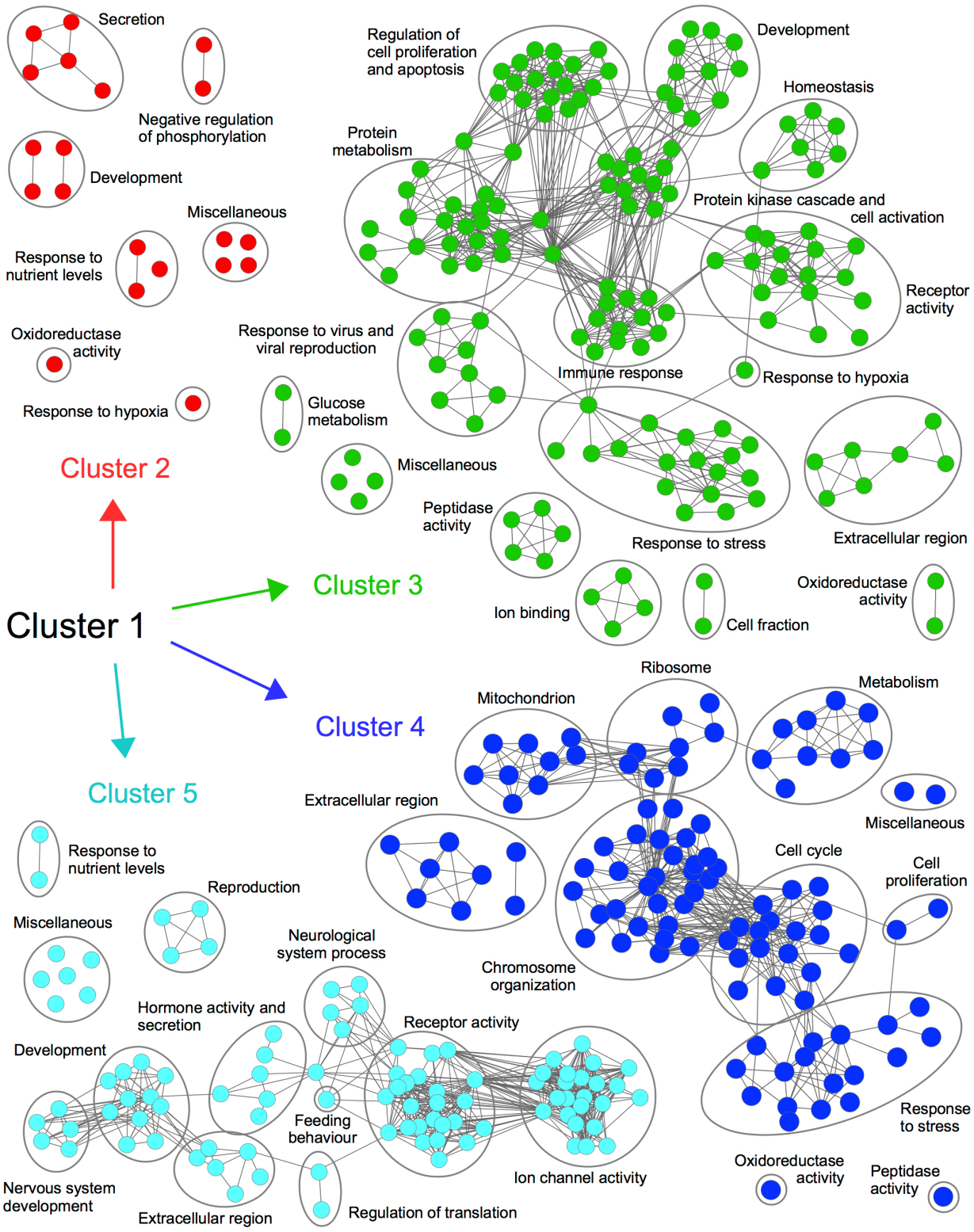

Figure 19 – Over-represented GO ontologies in clusters 2 to 5 compared with the healthy cluster 1 by gene-set enrichment analysis (GSEA). The preeclampsia (PE)-enriched cluster 2 (red) demonstrated an over-representation of genes associated with hormone secretion, response

to hypoxia, and response to nutrient levels. Cluster 3 (green) revealed an enrichment of terms involved in immune and inflammatory responses, such as viral reproduction and cytokine/interferon signaling. Cluster 4 (blue) demonstrated an abundance of genes associated with metabolism, cell proliferation, and cell cycle in addition to genes involved in the response to stress and DNA damage. Cluster 5 (cyan) revealed an over-representation of terms involved in hormone secretion and ion channel activity, as well as genes annotated to nervous system development and neurological system processes. Common genes between gene sets are indicated by gray edges, with networks of related ontologies circled and assigned a group label. Ontologies labeled as miscellaneous did not share genes with any of the networks.

3.3.4 Inter-cluster clinical comparisons

Since extensive maternal, fetal, and placental clinical information was available for the BioBank samples, these characteristics were compared across the five identified molecular clusters, as well as across the four discovered PE subtypes in clusters 1, 2, 3, and 5 (**Tables 5-8, Figure 20**). Overall, cluster 1 samples, including those diagnosed with preeclampsia, demonstrated the healthiest Doppler ultrasound values and placental weights, leading to infants born at later gestational ages ($p<0.01$ across the clusters and $p<0.01$ across the PE subtypes) with the highest Apgar scores at 1 minute ($p<0.01$ and $p=0.28$) (**Table 5, Table 7, Figure 20a**). The preterm controls belonging to this cluster were generally those with gestational ages between 30 and 34 weeks (**Figure 20a**), delivered for reasons such as cholestasis of pregnancy or placental abruption. In comparison to the other clusters and PE groups, cluster 1 contained few newborns born SGA ($p<0.01$ and $p=0.02$) and the lowest percentage requiring transfer to the neonatal intensive care unit (NICU) after delivery ($p<0.01$ and $p=0.09$) (**Table 6, Table 8, Figure 20b**).

In contrast to cluster 1, the high rate of PE diagnosis (89%) in cluster 2 was strongly associated with low-weight placentas ($p<0.01$ across the clusters and $p=0.05$ across the PE subtypes) and abnormal uterine and umbilical Doppler ultrasound waveforms (ex. mean uterine pulsatility index of 1.81, $p=0.03$ and $p=0.02$), with all infant birth weights below the 50^{th} percentile (**Table 5, Table 7, Figure 20b**). Additionally, most of the cluster 2 infants were born preterm by non-laboring Cesarean section, due to non-reassuring fetal and/or maternal status, often resulting in infant transfer to the NICU (**Table 6, Table 8, Figure 20a**). PE disease appeared to be more severe in this cluster as it included women with the highest maternal blood pressures ($p<0.01$ and $p<0.72$) in the last four weeks of pregnancy (**Table 5, Table 7**). Moreover, a number of samples

also associated with HELLP syndrome were dispersed throughout this cluster (**Table 6, Table 8, Figure 20c**). Infants born to mothers diagnosed with HELLP syndrome were usually delivered preterm (86%), but were often AGA (68%) and associated with higher placental weight z-scores compared to the non-HELLP patients in this cluster (-0.98 versus -1.38, p=0.06), suggesting that the maternal state is primarily responsible for the early delivery of these fetuses.

Cluster 3 samples were generally delivered between 30 and 37 weeks from older women (p=0.02 across the clusters and p=0.09 across the PE subtypes) of a non-Caucasian ethnicity (**Tables 5-8, Figure 20a**). Placental weight z-scores were dramatically reduced (p<0.01 and p=0.05) with narrower umbilical cords (p<0.01 and p=0.01), especially among the PE patients (**Table 5, Table 7**). Additionally, a significant gradient of fetal growth restriction severity (p<0.01) was observed in cluster 3 samples (**Figure 21**), along with the highest frequency of SGA infants (p<0.01 and p=0.02) (**Figure 20b**).

Cluster 4 members were preterm controls from younger mothers (p=0.02 across the clusters) delivered before 30 weeks with AGA infants, as well as a few large infants (>90th percentile) (**Table 5, Table 6, Figure 20a**). Most of these women went into spontaneous labor with some infants delivered by Cesarean section due to breech presentation or arrest of decent (**Table 6**). Additionally, accompanying clinical data reported signs of infection (predominately chorioamnionitis) in 10 out of 12 preterm control placentas in this cluster (**Table 6, Figure 20d**). This was in contrast to only 3 (out of 11) preterm controls belonging to cluster 1 that showed signs of infection, and these were found to plot on the border of cluster 1, near cluster 4, by PCA (**Figure 20d**). Understandably, cluster 4 patients also displayed the highest white blood cell (WBC) counts in the second and third trimesters (p<0.02) (**Table 5**).

Cluster 5 consisted of samples from a range of gestational ages at delivery, placental and infant weights, and PE or non-PE diagnoses (**Tables 5-8, Figure 20**). No clinical variables were found to be statistically significant or clinically relevant in describing this molecular subtype.

Table 5 – Continuous clinical characteristics across the clusters.

	Cluster 1 N=60	Cluster 2 N=56	Cluster 3 N=11	Cluster 4 N=14	Cluster 5 N=16	
Clinical Attribute	**Mean (SD)[a]**					**P-value[b]**
Parental demographics						
Maternal age (years)	32.6 (4.8)	33.8 (6.1)	35.9 (4.2)	29.2 (6.4)	34.8 (5.4)	0.02
Paternal age (years)	35.4 (3.5)	36.3 (4.1)	--	31.3 (8.6)	--	0.40
Maternal BMI (kg/m^2)	25.1 (6.3)	26.5 (4.3)	25.6 (5.0)	25.2 (6.2)	23.8 (3.3)	0.16
Maternal height (cm)	162 (6)	162 (7)	161 (5)	160 (5)	164 (8)	0.45
Uteroplacental blood flow/Ultrasound data						
Mean uterine artery PI[c]	1.23 (0.46)	1.81 (0.48)	1.65 (0.47)	1.16 (0.25)	1.79 (0.56)	0.03
Max uterine artery PI[c]	1.56 (0.68)	2.17 (0.60)	2.16 (0.66)	1.36 (0.40)	2.21 (0.99)	0.12
Mean umbilical artery PI[c]	1.16 (0.37)	1.51 (0.42)	1.52 (0.55)	1.07 (0.12)	1.38 (0.17)	<0.01
Max umbilical artery PI[c]	1.29 (0.43)	1.67 (0.51)	1.69 (0.48)	1.13 (0.12)	1.50 (0.25)	<0.01
Blood pressure						
Mean systolic blood pressure (mmHg)[d]	130 (23)	154 (20)	148 (23)	122 (15)	140 (22)	<0.01
Max systolic blood pressure (mmHg)[d]	136 (27)	167 (23)	157 (24)	125 (15)	154 (31)	<0.01
Mean diastolic blood pressure (mmHg)[d]	82 (16)	98 (11)	93 (15)	74 (12)	86 (14)	<0.01
Max diastolic blood pressure (mmHg)[d]	85 (18)	106 (14)	96 (15)	77 (12)	95 (16)	<0.01
Blood/urine analysis						
Max proteinuria (dipstick)[d]	+1.5 (1.3)	+2.8 (1.2)	+2.1 (1.1)	+0.9 (1.4)	+1.8 (1.7)	<0.01
2^{nd} trimester hemoglobin (g/L)	120 (8)	123 (12)	115 (12)	115 (8)	119 (11)	0.08
3^{rd} trimester hemoglobin (g/L)	134 (91)	126 (13)	120 (9)	104 (1)	121 (11)	0.02
2^{nd} trimester WBC ($x10^3/mm^3$)	10.0 (2.1)	11.3 (2.6)	9.8 (2.0)	12.8 (2.7)	11.6 (3.3)	0.01
3^{rd} trimester WBC ($x10^3/mm^3$)	11.3 (2.9)	11.4 (2.7)	8.9 (0.9)	12.4 (0.0)	11.4 (1.8)	0.02
2^{nd} trimester creatinine (mmol/L)	48 (12)	58 (10)	52 (9)	42 (6)	63 (28)	0.05
3^{rd} trimester creatinine (mmol/L)	53 (11)	62 (12)	65 (12)	--	54 (8)	0.01
2^{nd} trimester platelets ($x10^9/L$)	211 (55)	214 (60)	233 (42)	249 (40)	254 (44)	0.02
3^{rd} trimester platelets ($x10^9/L$)	216 (55)	199 (63)	180 (55)	260 (21)	219 (38)	0.22
2^{nd} trimester ALT (U/L)	40 (69)	46 (83)	12 (4)	11 (2)	17 (13)	0.01
3^{rd} trimester ALT (U/L)	23 (24)	28 (24)	21 (20)	--	25 (31)	0.17
2^{nd} trimester AST (U/L)	41 (66)	37 (54)	15 (3)	15 (6)	23 (18)	0.06
3^{rd} trimester AST (U/L)	26 (18)	29 (14)	31 (28)	--	20 (12)	0.02
2^{nd} trimester uric acid (umol/L)	253 (64)	339 (100)	263 (23)	205 (75)	280 (108)	0.10

3rd trimester uric acid (umol/L)	312 (82)	390 (84)	361 (62)	--	376 (52)	<0.01
PAPPA (MoM)	1.03 (0.60)	0.87 (0.74)	0.85 (0.94)	1.21 (0.67)	0.81 (0.34)	0.50
AFP (MoM)	1.17 (0.62)	1.70 (0.72)	1.35 (0.56)	1.41 (0.98)	0.90 (0.22)	<0.01
hCG (MoM)	1.73 (2.25)	2.73 (3.50)	2.23 (3.14)	2.23 (1.75)	1.14 (0.56)	0.69
Inhibin A (MoM)	1.55 (1.56)	2.16 (1.03)	2.97 (2.45)	2.20 (0.81)	1.37 (0.64)	0.22
Unconjugated estriol (MoM)	0.96 (0.24)	0.89 (0.17)	0.72 (0.19)	0.84 (0.12)	0.77 (0.16)	0.20
Fetal demographics						
GA at delivery (weeks)	36 (4)	32 (3)	34 (4)	29 (4)	33 (4)	<0.01
Newborn weight z-score	-0.13 (1.01)	-1.33 (0.74)	-1.46 (0.89)	0.34 (0.95)	-0.85 (1.15)	<0.01
Apgar score at 1 minute (/10)	8.3 (1.2)	7.2 (2.0)	7.4 (2.1)	7.0 (1.7)	7.0 (2.4)	<0.01
Apgar score at 5 minutes (/10)	8.9 (0.4)	8.7 (0.8)	8.8 (0.4)	8.1 (2.3)	8.3 (1.2)	0.24
Placental and umbilical cord data						
Placental weight z-score	-0.37 (0.99)	-1.25 (0.76)	-1.31 (1.16)	0.72 (1.37)	-0.98 (0.79)	<0.01
Placental thickness (cm)	2.60 (0.72)	2.28 (0.96)	2.05 (0.59)	2.44 (0.50)	2.22 (0.49)	0.05
Placental asymmetry (ratio)	0.13 (0.09)	0.16 (0.11)	0.15 (0.10)	0.15 (0.07)	0.19 (0.18)	0.42
Placental efficiency (ratio)	5.12 (0.99)	4.37 (1.01)	4.77 (0.96)	3.49 (0.97)	4.61 (0.93)	<0.01
Cord insertion distance from placental margin (cm)	3.85 (1.49)	2.88 (1.11)	3.21 (1.79)	3.11 (1.45)	3.43 (1.27)	0.03
Cord diameter (cm)	1.31 (0.38)	1.12 (0.34)	0.93 (0.31)	1.22 (0.26)	1.21 (0.27)	0.01

[a]Only noted and used if values were available for at least two samples in the cluster
[b]Calculated by Kruskal–Wallis rank-sum tests
[c]PI = pulsatility index
[d]Within the last four weeks of gestation

Table 6 – Categorical clinical characteristics across the clusters.

	Cluster 1 N=60	Cluster 2 N=56	Cluster 3 N=11	Cluster 4 N=14	Cluster 5 N=16	
Clinical Attribute	**Percentage of Cluster (n/N)[a]**					**P-value[b]**
Parental demographics						
Nulliparous	50.0 (30/60)	66.1 (37/56)	36.4 (4/11)	50.0 (7/14)	37.5 (6/16)	0.14
Previous miscarriage	28.3 (17/60)	26.8 (15/56)	27.3 (3/11)	7.1 (1/14)	25.0 (4/16)	0.58
Previous termination	20.0 (12/60)	19.6 (11/56)	27.3 (3/11)	14.3 (2/14)	12.5 (2/16)	0.91
Previous hypertensive pregnancy	30.8 (8/26)	53.3 (8/15)	28.6 (2/7)	20.0 (1/5)	50.0 (3/5)	0.52
Maternal ethnicity						0.09
Caucasian	66.7 (38/57)	44.6 (25/56)	27.3 (3/11)	64.3 (9/14)	66.7 (10/15)	--
Black	8.8 (5/57)	23.2 (13/56)	36.4 (4/11)	14.3 (2/14)	0 (0/15)	
Asian	17.5 (10/57)	21.4 (12/56)	27.3 (3/11)	7.1 (1/14)	20.0 (3/15)	
East Indian	5.3 (3/57)	7.1 (4/56)	9.1 (1/11)	7.1 (1/14)	0 (0/15)	
Paternal ethnicity						0.03
Caucasian	87.5 (21/24)	36.9 (7/19)	40.0 (2/5)	71.4 (5/7)	100 (5/5)	--
Black	4.2 (1/24)	31.6 (6/19)	20.0 (1/5)	14.3 (1/7)	0 (0/5)	
Asian	4.2 (1/24)	15.8 (3/19)	40.0 (2/5)	0 (0/7)	0 (0/5)	
East Indian	4.2 (1/24)	5.3 (1/19)	0 (0/5)	14.3 (1/7)	0 (0/5)	
Maternal blood type						0.22
A	21.7 (13/60)	41.8 (23/55)	45.5 (5/11)	28.6 (4/14)	18.8 (3/16)	--
B	26.7 (16/60)	21.8 (12/55)	36.4 (4/11)	21.4 (3/14)	12.5 (2/16)	
O	48.3 (29/60)	30.9 (17/55)	18.2 (2/11)	42.9 (6/14)	56.3 (9/16)	
AB	3.3 (2/60)	5.5 (3/55)	0 (0/11)	7.1 (1/14)	12.5 (2/16)	
Rh positive	88.3 (53/60)	98.1 (53/54)	90.9 (10/11)	85.7 (12/14)	87.5 (14/16)	0.13
BMI >25 kg/m^2	37.3 (22/59)	66.7 (30/45)	44.4 (4/9)	45.5 (5/11)	40.0 (6/15)	0.05
Asthma	10.6 (5/47)	17.4 (8/46)	0 (0/8)	10.0 (1/10)	16.7 (2/12)	0.75
History of STDs	4.3 (2/47)	4.3 (2/46)	0 (0/8)	10.0 (1/10)	0 (0/12)	0.78
Renal problems	2.1 (1/47)	4.3 (2/46)	12.5 (1/8)	0 (0/10)	8.3 (1/12)	0.34
Anxiety/depression	8.5 (4/47)	13.0 (6/46)	12.5 (1/8)	20.0 (2/10)	25.0 (3/12)	0.45
Chronic hypertension	23.3 (14/60)	30.4 (17/56)	36.4 (4/11)	0 (0/14)	37.5 (6/16)	0.07
Ultrasound data						
Placenta position on ultrasound						0.83
Anterior	31.6 (6/19)	48.3 (14/29)	66.7 (4/6)	42.9 (3/7)	33.3 (2/6)	--
Posterior	63.2 (12/19)	55.2 (16/29)	16.7 (1/6)	57.1 (4/7)	50.0 (3/6)	

Amniotic fluid deficiency	16.7 (2/12)	29.2 (7/24)	66.7 (4/6)	62.5 (5/8)	33.3 (1/3)	0.11
Medications						
H1N1 vaccine	20.0 (12/60)	10.1 (6/56)	9.1 (1/11)	14.3 (2/14)	18.9 (3/16)	0.67
Prenatal vitamins	60.0 (36/60)	51.8 (29/56)	45.5 (5/11)	50.0 (7/14)	43.8 (7/16)	0.73
Folic acid	10.0 (6/60)	12.5 (7/56)	0 (0/11)	7.1 (1/14)	0 (0/16)	0.61
Acetaminophen treatment	8.3 (5/60)	35.7 (20/56)	9.1 (1/11)	14.3 (2/14)	18.8 (3/16)	<0.01
Aspirin treatment	0 (0/60)	5.4 (3/56)	9.1 (1/11)	7.1 (1/14)	6.3 (1/16)	0.12
Morphine treatment	5.0 (3/60)	7.1 (4/56)	0 (0/11)	35.7 (5/14)	6.3 (1/16)	0.02
Antibiotic treatment	43.3 (26/60)	42.9 (24/56)	36.4 (4/11)	71.4 (10/14)	56.3 (9/16)	0.28
Anti-hypertensive treatment	28.3 (17/60)	83.9 (47/56)	63.6 (7/11)	21.4 (3/14)	62.5 (10/16)	<0.01
Steroid administration	18.3 (11/60)	71.4 (40/56)	36.4 (4/11)	64.3 (9/14)	43.8 (7/16)	<0.01
Diagnoses						
Preeclampsia diagnosis	23.3 (14/60)	89.3 (50/56)	72.7 (8/11)	7.1 (1/14)	43.8 (7/16)	<0.01
HELLP diagnosis	1.7 (1/60)	32.1 (18/56)	9.1 (1/11)	0 (0/14)	12.5 (2/16)	<0.01
Chorioamnionitis diagnosis	6.7 (4/60)	0 (0/56)	0 (0/11)	71.4 (10/14)	12.5 (2/16)	<0.01
Labor and Delivery						
Spontaneous labor	30.0 (18/60)	3.6 (2/56)	0 (0/11)	92.9 (13/14)	6.7 (1/15)	<0.01
Attempted vaginal delivery	50.0 (30/60)	30.4 (17/56)	9.1 (1/11)	100 (14/14)	43.8 (7/16)	<0.01
Vaginal delivery	38.3 (23/60)	12.5 (7/56)	9.1 (1/11)	64.3 (9/14)	18.8 (3/16)	<0.01
Delivery <34 weeks	28.3 (17/60)	78.6 (44/56)	36.4 (4/11)	85.7 (12/14)	43.8 (7/16)	<0.01
Delivery <37 weeks	43.3 (26/60)	91.1 (51/56)	72.7 (8/11)	92.9 (13/14)	75.0 (12/16)	<0.01
Fetal demographics						
Male fetus	51.7 (31/60)	57.1 (32/56)	45.5 (5/11)	57.1 (8/14)	43.8 (7/16)	0.85
AGA (10-90th percentile)	85.0 (51/60)	44.6 (25/56)	36.4 (4/11)	78.6 (11/14)	50.0 (8/16)	<0.01
SGA (<10th percentile)	11.7 (7/60)	55.4 (31/56)	63.6 (7/11)	0 (0/14)	50.0 (8/16)	<0.01
5 minute Apgar score <7	0 (0/56)	4.3 (2/47)	0 (0/9)	11.1 (1/9)	18.8 (3/16)	0.01
NICU transfer	18.3 (11/60)	51.8 (29/56)	36.4 (4/11)	42.9 (6/14)	37.5 (6/16)	<0.01

[a]All available data was utilized, however, information was missing for some samples for some characteristics
[b]Calculated by Fisher's exact tests

Table 7 – Continuous clinical characteristics across the PE subtypes.

	Cluster 1 PE N=14	Cluster 2 PE N=50	Cluster 3 PE N=8	Cluster 5 PE N=7	
Clinical Attribute	**Mean (SD)[a]**				**P-value[b]**
Parental demographics					
Maternal age (years)	30.5 (4.5)	33.4 (6.2)	35.4 (3.9)	36.0 (4.7)	0.09
Paternal age (years)	34.3 (3.3)	36.3 (4.1)	--	--	0.30
Maternal BMI (kg/m^2)	26.7 (9.4)	26.8 (4.2)	26.6 (4.9)	24.3 (4.3)	0.38
Maternal height (cm)	163 (5)	162 (7)	162 (5)	167 (10)	0.22
Uteroplacental blood flow/Ultrasound data					
Mean uterine artery PI[c]	0.97 (0.43)	1.81 (0.48)	1.50 (0.27)	--	0.02
Max uterine artery PI[c]	1.05 (0.39)	2.15 (0.59)	2.05 (0.46)	--	0.04
Mean umbilical artery PI[c]	1.11 (0.22)	1.46 (0.36)	1.44 (0.61)	1.47 (0.13)	0.04
Max umbilical artery PI[c]	1.24 (0.28)	1.62 (0.46)	1.60 (0.54)	1.53 (0.19)	0.08
Blood pressure					
Mean systolic pressure (mmHg)[d]	151 (19)	155 (19)	148 (17)	155 (14)	0.72
Max systolic pressure (mmHg)[d]	162 (18)	168 (22)	158 (14)	168 (21)	0.64
Mean diastolic pressure (mmHg)[d]	95 (10)	100 (10)	96 (12)	94 (10)	0.13
Max diastolic pressure (mmHg)[d]	101 (10)	108 (11)	99 (10)	103 (7)	0.02
Blood/urine analysis					
Max proteinuria (dipstick)[d]	+2.5 (0.9)	+2.9 (1.2)	+2.4 (1.0)	+3.2 (1.0)	0.43
2^{nd} trimester hemoglobin (g/L)	125 (8)	122 (12)	113 (9)	119 (8)	0.42
3^{rd} trimester hemoglobin (g/L)	121 (8)	124 (12)	119 (10)	122 (14)	0.30
2^{nd} trimester WBC ($x10^3/mm^3$)	10.4 (1.5)	11.1 (2.6)	9.1 (0.6)	10.0 (3.5)	0.51
3^{rd} trimester WBC ($x10^3/mm^3$)	12.0 (3.7)	11.5 (2.8)	8.7 (0.8)	11.6 (1.8)	0.02
3^{rd} trimester creatinine (mmol/L)	55 (12)	63 (12)	67 (11)	57 (7)	0.07
2^{nd} trimester platelets ($x10^9/L$)	178 (55)	210 (61)	236 (58)	228 (17)	0.48
3^{rd} trimester platelets ($x10^9/L$)	191 (38)	199 (56)	170 (49)	205 (34)	0.50
3^{rd} trimester ALT (U/L)	30 (32)	29 (25)	22 (21)	33 (41)	0.56
3^{rd} trimester AST (U/L)	33 (24)	30 (15)	33 (28)	21 (15)	0.23
3^{rd} trimester uric acid (umol/L)	341 (92)	398 (82)	360 (67)	373 (37)	0.13
PAPPA (MoM)	1.01 (0.22)	0.88 (0.77)	0.46 (0.41)	0.71 (0.36)	0.19
AFP (MoM)	1.61 (0.93)	1.74 (0.75)	1.48 (0.60)	0.92 (0.32)	0.25
hCG (MoM)	1.23 (0.73)	2.73 (3.50)	3.37 (3.94)	1.45 (0.74)	0.96
Inhibin A (MoM)	1.19 (0.68)	2.16 (1.03)	3.38 (2.82)	1.73 (0.83)	0.42
Unconjugated estriol (MoM)	1.05 (0.41)	0.89 (0.17)	0.74 (0.21)	0.64 (0.11)	0.29

Fetal demographics					
GA at delivery (weeks)	35 (3)	31 (3)	35 (3)	33 (4)	<0.01
Newborn weight z-score	-0.48 (0.67)	-1.26 (0.69)	-1.64 (0.87)	-1.05 (1.13)	<0.01
Apgar score at 1 minute (/10)	7.9 (1.2)	7.2 (1.7)	7.6 (2.1)	6.3 (2.4)	0.28
Apgar score at 5 minutes (/10)	8.8 (0.6)	8.8 (0.6)	8.7 (0.5)	8.0 (1.4)	0.28
Placental and umbilical cord data					
Placental weight z-score	-0.59 (0.87)	-1.20 (0.76)	-1.33 (1.32)	-1.11 (0.72)	0.05
Placental thickness (cm)	2.71 (0.75)	2.31 (0.99)	2.26 (0.42)	2.17 (0.49)	0.29
Placental asymmetry (ratio)	0.18 (0.11)	0.16 (0.11)	0.17 (0.10)	0.13 (0.11)	0.66
Placental efficiency (ratio)	4.96 (1.04)	4.34 (0.95)	4.77 (1.06)	4.22 (0.75)	0.11
Cord insertion distance from placental margin (cm)	3.23 (1.64)	2.81 (1.11)	2.83 (0.66)	2.98 (0.66)	0.66
Cord diameter (cm)	1.45 (0.54)	1.13 (0.35)	0.86 (0.25)	1.24 (0.22)	0.01

[a]Only noted and used if values were available for at least two samples in the cluster. Attributes without sufficient data in at least two PE subtypes were eliminated
[b]Calculated by Kruskal–Wallis rank-sum tests
[c]PI = pulsatility index
[d]Within the last four weeks of gestation

Table 8 – Categorical clinical characteristics across the PE subtypes.

	Cluster 1 PE N=14	Cluster 2 PE N=50	Cluster 3 PE N=8	Cluster 5 PE N=7	
Clinical Attribute	**Percentage of Cluster (n/N)[a]**				**P-value[b]**
Parental demographics					
Nulliparous	71.4 (10/14)	64.0 (32/50)	37.5 (3/8)	57.1 (4/7)	0.46
Previous miscarriage	14.3 (2/14)	28.0 (14/50)	0 (0/8)	14.3 (1/7)	0.30
Previous termination	35.7 (5/14)	20.0 (10/50)	25.0 (2/8)	28.6 (2/7)	0.58
Previous hypertensive pregnancy	100 (4/4)	53.3 (8/15)	40.0 (2/5)	50.0 (1/2)	0.34
Maternal ethnicity					0.22
Caucasian	84.6 (11/13)	46.0 (23/50)	37.5 (3/8)	100 (6/6)	--
Black	7.7 (1/13)	24.0 (12/50)	37.5 (3/8)	0 (0/6)	
Asian	0 (0/13)	20.0 (10/50)	12.5 (1/8)	0 (0/6)	
East Indian	7.7 (1/13)	6.0 (3/50)	12.5 (1/8)	0 (0/6)	
Paternal ethnicity					0.33
Caucasian	100 (7/7)	36.8 (7/19)	50.0 (2/4)	100 (4/4)	--
Black	0 (0/7)	31.6 (6/19)	25.0 (1/4)	0 (0/4)	
Asian	0 (0/7)	15.8 (3/19)	25.0 (1/4)	0 (0/4)	
East Indian	0 (0/7)	5.3 (1/19)	0 (0/4)	0 (0/4)	
Maternal blood type					0.04
A	14.3 (2/14)	42.9 (21/49)	62.5 (5/8)	14.3 (1/7)	--
B	7.1 (1/14)	20.4 (10/49)	12.5 (1/8)	0 (0/7)	
O	78.6 (11/14)	30.6 (15.49)	25.0 (2/8)	71.4 (5/7)	
AB	0 (0/14)	6.1 (3/49)	0 (0/8)	14.3 (1/7)	
Rh positive	92.9 (13/14)	97.9 (47/48)	87.5 (7/8)	71.4 (5/7)	0.03
BMI >25 kg/m^2	42.9 (6/14)	70.7 (29/41)	42.9 (3/7)	50.0 (3/6)	0.18
Asthma	7.7 (1/13)	18.6 (8/43)	0 (0/6)	25.0 (1/4)	0.58
History of STDs	15.4 (2/13)	4.7 (2/43)	0 (0/6)	0 (0/4)	0.50
Renal problems	0 (0/13)	4.7 (2/43)	16.7 (1/6)	25.0 (1/4)	0.17
Anxiety/depression	15.4 (2/13)	14.0 (6/43)	16.7 (1/6)	50.0 (2/4)	0.30
Chronic hypertension	14.3 (2/14)	24.0 (12/50)	25.0 (2/8)	14.3 (1/7)	0.88
Ultrasound data					
Placenta position on ultrasound					0.85
Anterior	33.3 (2/6)	46.2 (12/26)	60.0 (3/5)	50.0 (1/2)	--
Posterior	66.7 (4/6)	57.7 (15/26)	20.0 (1/5)	50.0 (1/2)	

Amniotic fluid deficiency	20.0 (1/5)	29.2 (7/24)	60.0 (3/5)	0 (0/2)	0.54
Medications					
H1N1 vaccine	28.6 (4/14)	12.0 (6/50)	12.5 (1/8)	28.6 (2/7)	0.29
Prenatal vitamins	64.3 (9/14)	50.0 (25/50)	62.5 (5/8)	42.9 (3/7)	0.72
Folic acid	7.1 (1/14)	12.0 (6/50)	0 (0/8)	0 (0/7)	0.91
Acetaminophen treatment	21.4 (3/14)	40.0 (20/50)	12.5 (1/8)	28.6 (2/7)	0.36
Aspirin treatment	0 (0/14)	6.0 (3/50)	12.5 (1/8)	0 (0/7)	0.66
Morphine treatment	7.1 (1/14)	8.0 (4/50)	0 (0/8)	0 (0/7)	1
Antibiotic treatment	42.9 (6/14)	46.0 (23/50)	25.0 (2/8)	71.4 (5/7)	0.38
Anti-hypertensive treatment	64.3 (9/14)	86.0 (43/50)	62.5 (5/8)	85.7 (6/7)	0.15
Steroid administration	21.4 (3/14)	72.0 (36/50)	25.0 (2/8)	42.9 (3/7)	<0.01
Diagnoses					
Preeclampsia diagnosis	100 (14/14)	100 (50/50)	100 (8/8)	100 (7/7)	--
HELLP diagnosis	7.1 (1/14)	36.0 (18/50)	12.5 (1/8)	28.6 (2/7)	0.12
Chorioamnionitis diagnosis	7.1 (1/14)	0 (0/50)	0 (0/8)	0 (0/7)	0.37
Labor and Delivery					
Spontaneous labor	0 (0/6)	6.3 (1/16)	0 (0/1)	0 (0/4)	1
Attempted vaginal delivery	42.9 (6/14)	32.0 (16/50)	12.5 (1/8)	57.1 (4/7)	0.29
Vaginal delivery	42.9 (6/14)	12.0 (6/50)	12.5 (1/8)	28.6 (2/7)	0.05
Delivery <34 weeks	28.6 (4/14)	80.0 (40/50)	25.0 (2/8)	42.9 (3/7)	<0.01
Delivery <37 weeks	50.0 (7/14)	94.0 (47/50)	75 (6/8)	100 (7/7)	<0.01
Fetal demographics					
Male fetus	50.0 (7/14)	56.0 (28/50)	50.0 (4/8)	28.6 (2/7)	0.63
AGA (10-90th percentile)	85.7 (12/14)	46.0 (23/50)	25.0 (2/8)	42.9 (3/7)	0.02
SGA (<10th percentile)	14.3 (2/14)	54.0 (27/50)	75.0 (6/8)	57.1 (4/7)	0.02
5 minute Apgar score <7	0 (0/14)	2.4 (1/41)	0 (0/7)	28.6 (2/7)	0.10
NICU transfer	21.4 (3/14)	54.0 (27/50)	25.0 (2/8)	28.6 (2/7)	0.09

[a]All available data was utilized, however, information was missing for some samples for some characteristics
[b]Calculated by Fisher's exact tests

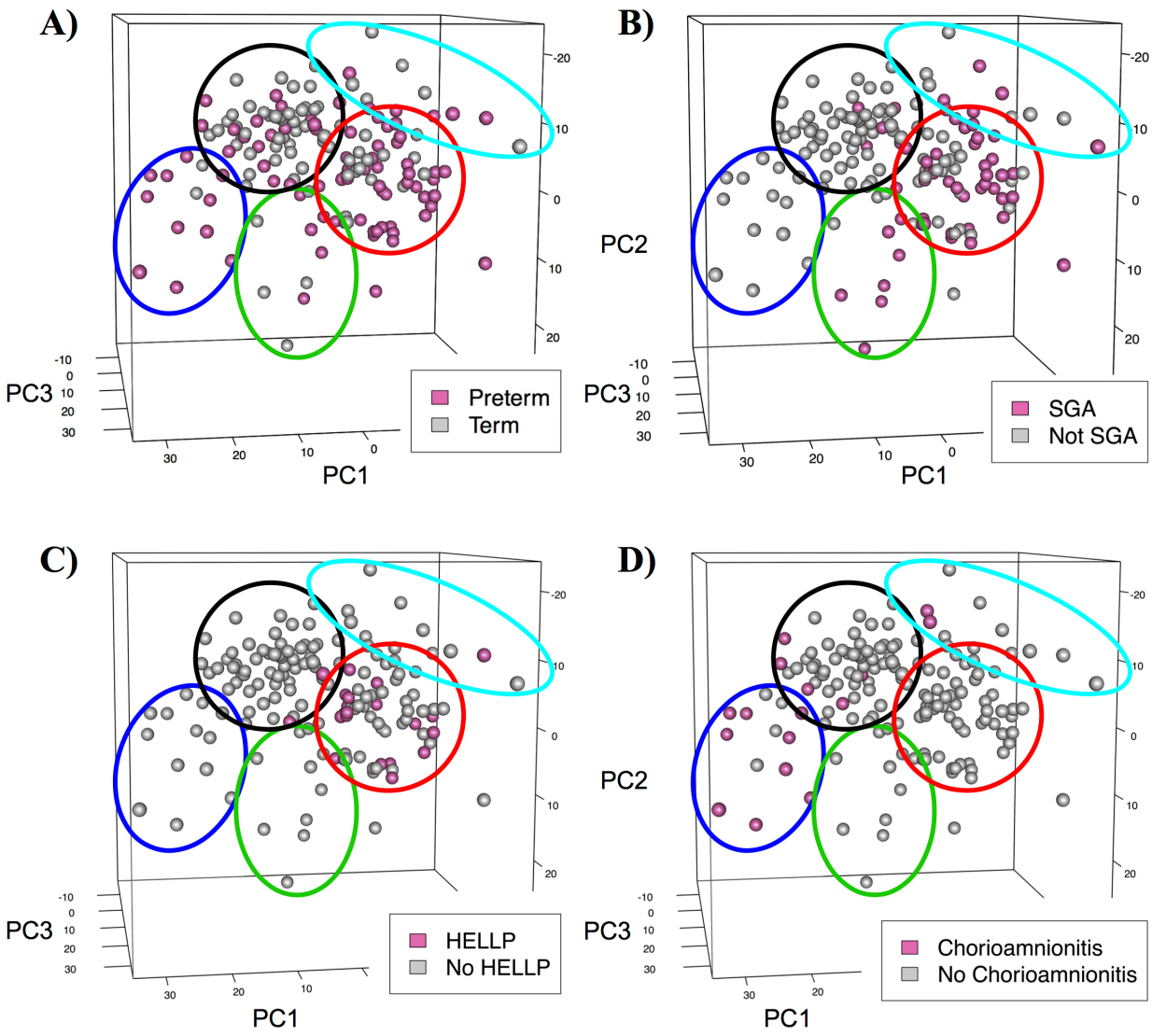

Figure 20 – Principal component analysis (PCA) plots for the visualization of significant clinical attributes in the BioBank samples only. Cluster 1 is circled in black; cluster 2 is circled in red; cluster 3 is circled in green; cluster 4 is circled in blue; and cluster 5 is circled in cyan. (**A**) Placentas in clusters 4 and 2 were the youngest, while most samples in cluster 1 were delivered at or close to term (preterm: <34 weeks). (**B**) Two main groups of samples associated with small-for-gestational-age (SGA) infants were identified in clusters 2 and 3, in addition to some samples in clusters 1 and 5. (**C**) Most placentas linked to hemolysis, elevated liver enzymes, low platelets (HELLP) syndrome were found dispersed throughout cluster 2. (**D**) Ten out of 12 preterm control placentas in cluster 4 reported signs of infection (predominately chorioamnionitis). This was in contrast to only three (out of 11) preterm controls belonging to cluster 1 that showed signs of infection, and these were found to plot on the outskirts of cluster 1, bordering cluster 4.

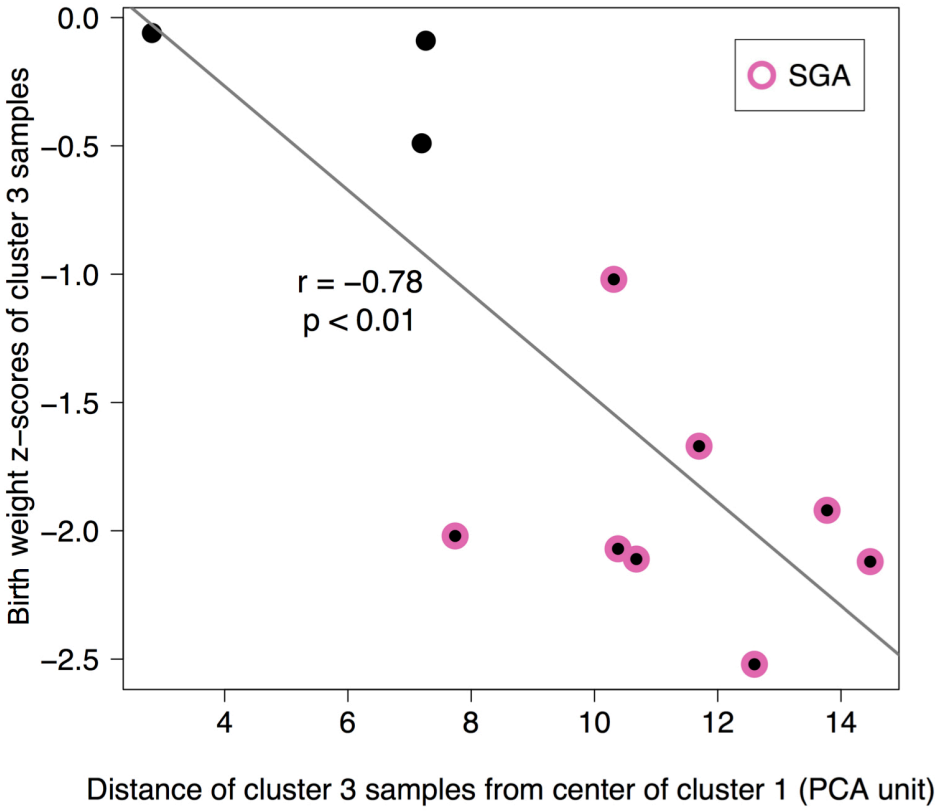

Figure 21 – Assessment of growth restriction in cluster 3 samples. Cluster 3 BioBank samples that plotted the furthest from the center of cluster 1 (i.e. the center of healthy) in principal component analysis (PCA) units (x-axis) demonstrated the lowest birth weight z-scores (y-axis), producing a significant gradient of growth restriction severity ($r=-0.78$, $p<0.01$). Most of these were clinically annotated as small-for-gestational-age (SGA; circled in pink). Samples closer to cluster 1, however, did not exhibit this reduced fetal growth.

3.3.5 Intra-cluster maternal clinical differences between PE and non-PE patients

Of the five identified clusters, four (clusters 1, 2, 3, and 5) contained varying but significant proportions of samples with a diagnosis of preeclampsia, suggesting that maternal factors may protect or promote PE development in each of these groups of molecularly similar placentas. To address this, the available pre-pregnancy maternal clinical information was compared between the BioBank PE cases (including those with superimposed PE disease on CH) and non-PE cases (normotensive controls and patients with preexisting CH who did not develop PE) in each of these four clusters. Interestingly, all 14 PE patients in cluster 1 were either nulliparous ($p=0.13$) or had experienced a prior hypertensive pregnancy ($p<0.01$; **Table 9**). Cluster 2 non-PE women almost exclusively had chronic hypertension ($p<0.01$), whereas the preeclamptic patients demonstrated a trend toward higher maternal BMIs ($p=0.13$; **Table 10**). Surprisingly, in cluster 3, the three women without PE had all experienced a previous miscarriage and were all B blood type (**Table 11**). This was in contrast to the eight cluster 3 PE subjects, none of whom had experienced a miscarriage ($p<0.01$) and the majority of whom were A blood type ($p<0.05$) (**Table 8, Table 11**). Cluster 5 PE and non-PE patients revealed no remarkable maternal differences (**Table 12**).

Table 9 – Intra-cluster pre-pregnancy maternal differences between preeclamptics and non-preeclamptics in cluster 1.

	Non-PE N=46	**PE N=14**	
Clinical Attribute	**Mean (SD)**		**P-value[a]**
Maternal age (years)	33 (5)	31 (4)	0.06
BMI (kg/m^2)	24.7 (5.0)	26.7 (9.4)	0.71
Clinical Attribute	**Percentage of Phenotype (n/N)[b]**		**P-value[c]**
Nulliparous	43.4 (20/46)	71.4 (10/14)	0.13
Previous miscarriage	32.6 (15/46)	14.3 (2/14)	0.31
Previous termination	15.2 (7/46)	35.7 (5/14)	0.13
Previous hypertensive pregnancy	18.2 (4/22)	100 (4/4)	<0.01
Maternal Ethnicity			0.29
Caucasian	61.3 (27/44)	84.6 (11/13)	--
Black	9.1 (4/44)	7.7 (1/13)	
Asian	22.7 (10/44)	0 (0/13)	
East Indian	4.5 (2/44)	7.7 (1/13)	
Maternal blood type			0.09
A	23.9 (11/46)	14.3 (2/14)	--
B	32.6 (15/46)	7.1 (1/14)	
O	39.1 (18/46)	78.6 (11/14)	
AB	4.3 (2/46)	0 (0/14)	
Rh positive	87.0 (40/46)	92.8 (13/14)	1
BMI >25 kg/m^2	35.6 (16/45)	42.8 (6/14)	0.75
Chronic hypertension	26.1 (12/46)	14.3 (2/14)	0.48

[a]Calculated by Mann–Whitney–Wilcoxon tests
[b]Information was not available for all patients for all attributes
[c]Calculated by Fisher's exact tests

Table 10 – Intra-cluster pre-pregnancy maternal differences between preeclamptics and non-preeclamptics in cluster 2.

	Non-PE N=6	**PE N=50**	
Clinical Attribute	**Mean (SD)**		**P-value[a]**
Maternal age (years)	36 (4)	33 (6)	0.29
BMI (kg/m^2)	23.3 (3.8)	26.8 (4.2)	0.12
Clinical Attribute	**Percentage of Phenotype (n/N)[b]**		**P-value[c]**
Nulliparous	83.3 (5/6)	64.0 (32/50)	0.65
Previous miscarriage	16.6 (1/6)	28.0 (14/50)	1
Previous termination	16.6 (1/6)	20.0 (10/50)	1
Previous hypertensive pregnancy	--	53.3 (8/15)	--
Maternal Ethnicity			0.69
Caucasian	40.0 (2/5)	46.0 (23/50)	--
Black	20.0 (1/5)	24.0 (12/50)	
Asian	40.0 (2/5)	20.0 (10/50)	
East Indian	20.0 (1/5)	6.0 (3/50)	
Maternal blood type			0.90
A	33.3 (2/6)	42.8 (21/49)	--
B	33.3 (2/6)	20.4 (10/49)	
O	33.3 (2/6)	30.6 (15/49)	
AB	0 (0/6)	6.1 (3/49)	
Rh positive	100 (6/6)	97.9 (47/48)	1
BMI >25 kg/m^2	25.0 (1/4)	70.7 (29/41)	0.10
Chronic hypertension	83.3 (5/6)	24.0 (12/50)	0.01

[a]Calculated by Mann–Whitney–Wilcoxon tests
[b]Information was not available for all patients for all attributes
[c]Calculated by Fisher's exact tests

Table 11 – Intra-cluster pre-pregnancy maternal differences between preeclamptics and non-preeclamptics in cluster 3.

	Non-PE N=3	**PE N=8**	
Clinical Attribute	**Mean (SD)**		**P-value[a]**
Maternal age (years)	37 (6)	35 (4)	0.54
BMI (kg/m^2)	22.1 (4.6)	26.6 (4.9)	0.66
Clinical Attribute	**Percentage of Phenotype (n/N)[b]**		**P-value[c]**
Nulliparous	33.3 (1/3)	37.5 (3/8)	1
Previous miscarriage	100 (3/3)	0 (0/8)	0.01
Previous termination	33.3 (1/3)	25.0 (2/8)	1
Previous hypertensive pregnancy	0 (0/2)	40.0 (2/5)	1
Maternal Ethnicity			0.56
Caucasian	0 (0/3)	37.5 (3/8)	--
Black	33.3 (1/3)	37.5 (3/8)	
Asian	66.7 (2/3)	12.5 (1/8)	
East Indian	0 (0/3)	12.5 (1/8)	
Maternal blood type			0.05
A	0 (0/3)	62.5 (5/8)	--
B	100 (3/3)	12.5 (1/8)	
O	0 (0/3)	25.0 (2/8)	
AB	0 (0/3)	0 (0/8)	
Rh positive	100 (3/3)	87.5 (7/8)	1
BMI >25 kg/m^2	50.0 (1/2)	42.9 (3/7)	1
Chronic hypertension	66.7 (2/3)	25.0 (2/8)	0.49

[a]Calculated by Mann–Whitney–Wilcoxon tests
[b]Information was not available for all patients for all attributes
[c]Calculated by Fisher's exact tests

Table 12 – Intra-cluster pre-pregnancy maternal differences between preeclamptics and non-preeclamptics in cluster 5.

	Non-PE N=9	**PE N=7**	
Clinical Attribute	**Mean (SD)**		**P-value[a]**
Maternal age (years)	34 (6)	36 (5)	0.13
BMI (kg/m^2)	23.5 (2.7)	24.3 (4.3)	0.86
Clinical Attribute	**Percentage of Phenotype (n/N)[b]**		**P-value[c]**
Nulliparous	22.2 (2/9)	57.1 (4/7)	0.30
Previous miscarriage	33.3 (3/9)	14.3 (1/7)	0.58
Previous termination	0 (0/9)	28.6 (2/7)	0.18
Previous hypertensive pregnancy	50.0 (2/4)	50.0 (1/2)	1
Maternal Ethnicity			0.15
Caucasian	44.4 (4/9)	100 (6/6)	--
Black	0 (0/9)	0 (0/6)	
Asian	33.3 (3/9)	0 (0/6)	
East Indian	0 (0/9)	0 (0/6)	
Maternal blood type			0.78
A	22.2 (2/9)	14.3 (1/7)	--
B	22.2 (2/9)	0 (0/7)	
O	44.4 (4/9)	71.4 (5/7)	
AB	11.1 (1/9)	14.3 (1/7)	
Rh positive	100 (9/9)	71.4 (2/7)	0.18
BMI >25 kg/m^2	33.3 (3/9)	50.0 (3/6)	0.62
Chronic hypertension	55.6 (5/9)	14.3 (1/7)	0.15

[a]Calculated by Mann–Whitney–Wilcoxon tests
[b]Information was not available for all patients for all attributes
[c]Calculated by Fisher's exact tests

3.3.6 Investigation into the cluster 3 immune signature

Given that we had access to the original snap-frozen tissue for the BioBank samples, cluster 3 patients could be further assessed to determine the most likely source of the observed immune-enriched transcriptional pattern in these placentas: allograft rejection or viral infection. Quantitative polymerase chain reaction (qPCR) for signs of cytomegalovirus, human papillomavirus 16, and/or Epstein–Barr virus in cluster 3 samples were all negative. Alternatively, cluster 3 placentas showed a consistent upregulation of a number of known rejection markers, such as CXCL10 [406, 669], CD3E [670, 671], CXCL13 [672], and TAP1 [673], as well as HLA-G, the non-classical MHC class I molecule linked to the promotion of immune tolerance [224-226] (all $p<0.01$ compared to the other clusters). Additionally, TNF, a gene involved in trophoblast apoptosis [292], was again upregulated in cluster 3, similar to the findings in Chapter 2 ($p=0.04$ compared to cluster 1).

3.3.7 Investigation into cluster 5

Given the lack of clinical cohesion in the cluster 5 patients, the observed enrichment in olfactory receptor genes [674], and a suggestion from Dr. Gary Bader, we hypothesized that this group may exist due to chromosomal abnormalities in these samples, leading to common changes in gene expression [675]. Since no genetic anomalies were observed in the infants, these samples were tested for confined placental mosaicism (CPM) [331]. A comparison of clusters 2-5 to cluster 1 with GSEA for chromosome positional enrichments based on the gene expression data identified 91 statistically significant gains or losses of chromosome regions in cluster 5 samples at a FDR q-value cut-off of 0.05 (**Table 13**). Chromosomal differences were not observed to nearly the same extent (<8 regions at $q<0.05$) in clusters 2, 3, or 4 [660].

To confirm this placental mosaicism in cluster 5 samples, eight cluster 5 BioBank samples were subjected to array-based comparative genomic hybridization (aCGH) analysis compared with a pooled reference sample of ten BioBank cluster 1 term controls. Gains in cluster 5 samples were confirmed on chromosomes 1, 6, 16, 17, and 22, with the greatest gains identified on chromosome 19 (adjusted $p<0.05$; **Figure 22a**). Significant losses were also noted on chromosomes 4, 5, 13, and 21 in cluster 5 samples (adjusted $p<0.05$; **Figure 22b**). The mean fold change observed on chromosome 19 in cluster 5 samples compared with the reference sample (1.05– 1.10) suggests mosaicism in ~10-20% of biopsied placental cells.

Table 13 – Significant (q<0.05) chromosome regions in cluster 5 samples compared to cluster 1 samples based on gene expression.

Chromosome region	Gene set size	Uncorrected p-value	FDR q-value
Over-represented regions/gene sets			
CHR19P13	408	0.00	0.00
CHR17Q25	132	0.00	0.00
CHR16P13	190	0.00	0.00
CHR22Q11	94	0.00	0.00
CHR1P36	235	0.00	0.00
CHR11Q13	214	0.00	0.00
CHR17Q12	67	0.00	0.00
CHR9Q34	173	0.00	0.00
CHR19Q13	565	0.00	0.00
CHR16Q24	65	0.00	0.00
CHR16P11	69	0.00	0.00
CHR17P13	174	0.00	0.00
CHR8Q24	120	0.00	0.00
CHR20Q13	138	0.00	0.00
CHR22Q13	143	0.00	0.00
CHR16Q13	35	0.00	0.00
CHR11P15	184	0.00	0.03
CHR20Q11	89	0.00	0.03
CHR11P11	39	0.00	0.04
CHR20P13	47	0.00	0.04
Under-represented regions/gene sets			
CHR4Q21	68	0.00	0.00
CHR3Q26	40	0.00	0.00
CHR1P31	57	0.00	0.00
CHR5Q12	29	0.00	0.00
CHR4Q32	21	0.00	0.00
CHR15Q21	61	0.00	0.00
CHR14Q22	47	0.00	0.00
CHR6Q22	43	0.00	0.00
CHR2Q33	70	0.00	0.00
CHR8Q22	56	0.00	0.00
CHR5P13	40	0.00	0.00
CHR13Q14	60	0.00	0.00
CHR4Q31	52	0.00	0.00
CHR4Q24	14	0.00	0.00
CHR18Q11	22	0.00	0.00
CHR14Q23	32	0.00	0.00
CHR2Q31	64	0.00	0.00
CHR4P15	30	0.00	0.00
CHR4Q22	24	0.00	0.01
CHR8Q21	40	0.00	0.01
CHR4Q25	27	0.00	0.01
CHR3Q25	37	0.00	0.01
CHR1Q25	48	0.00	0.01
CHR1Q24	33	0.00	0.01
CHR14Q21	31	0.00	0.01
CHR12P12	33	0.00	0.01
CHR2Q22	15	0.00	0.01

CHR5Q14	28	0.00	0.01
CHR6Q21	45	0.00	0.01
CHR4Q23	11	0.00	0.01
CHR3Q13	58	0.00	0.01
CHR1P21	25	0.00	0.01
CHR2P24	37	0.00	0.01
CHR12P11	25	0.00	0.01
CHR6P22	80	0.00	0.01
CHR4Q28	24	0.00	0.01
CHR9P24	31	0.00	0.01
CHR12Q22	22	0.00	0.01
CHRXQ21	28	0.00	0.01
CHR5Q11	26	0.01	0.01
CHR5Q21	19	0.01	0.01
CHR1P22	54	0.00	0.01
CHRXQ26	36	0.00	0.02
CHR13Q22	12	0.01	0.02
CHR14Q13	21	0.01	0.02
CHR10P14	14	0.01	0.02
CHR3P24	30	0.01	0.02
CHR6Q14	28	0.00	0.02
CHR11Q14	32	0.01	0.02
CHR5Q15	16	0.01	0.02
CHR8Q23	19	0.02	0.02
CHR12Q23	52	0.00	0.03
CHR8Q13	31	0.01	0.03
CHR9P22	17	0.02	0.03
CHRXQ22	52	0.01	0.03
CHR7Q31	61	0.01	0.03
CHR5Q22	16	0.01	0.04
CHR2P16	22	0.02	0.04
CHR11P13	33	0.01	0.04
CHR21Q21	10	0.02	0.04
CHR9Q21	38	0.01	0.04
CHR13Q13	22	0.03	0.05
CHR6Q23	33	0.01	0.05
CHR4Q26	12	0.04	0.05
CHR2P22	34	0.01	0.05
CHR18Q21	58	0.01	0.05
CHR7Q21	58	0.00	0.05
CHR4Q12	23	0.02	0.05
CHR10P13	16	0.02	0.05
CHR12Q21	27	0.03	0.05
CHR5Q13	38	0.01	0.05

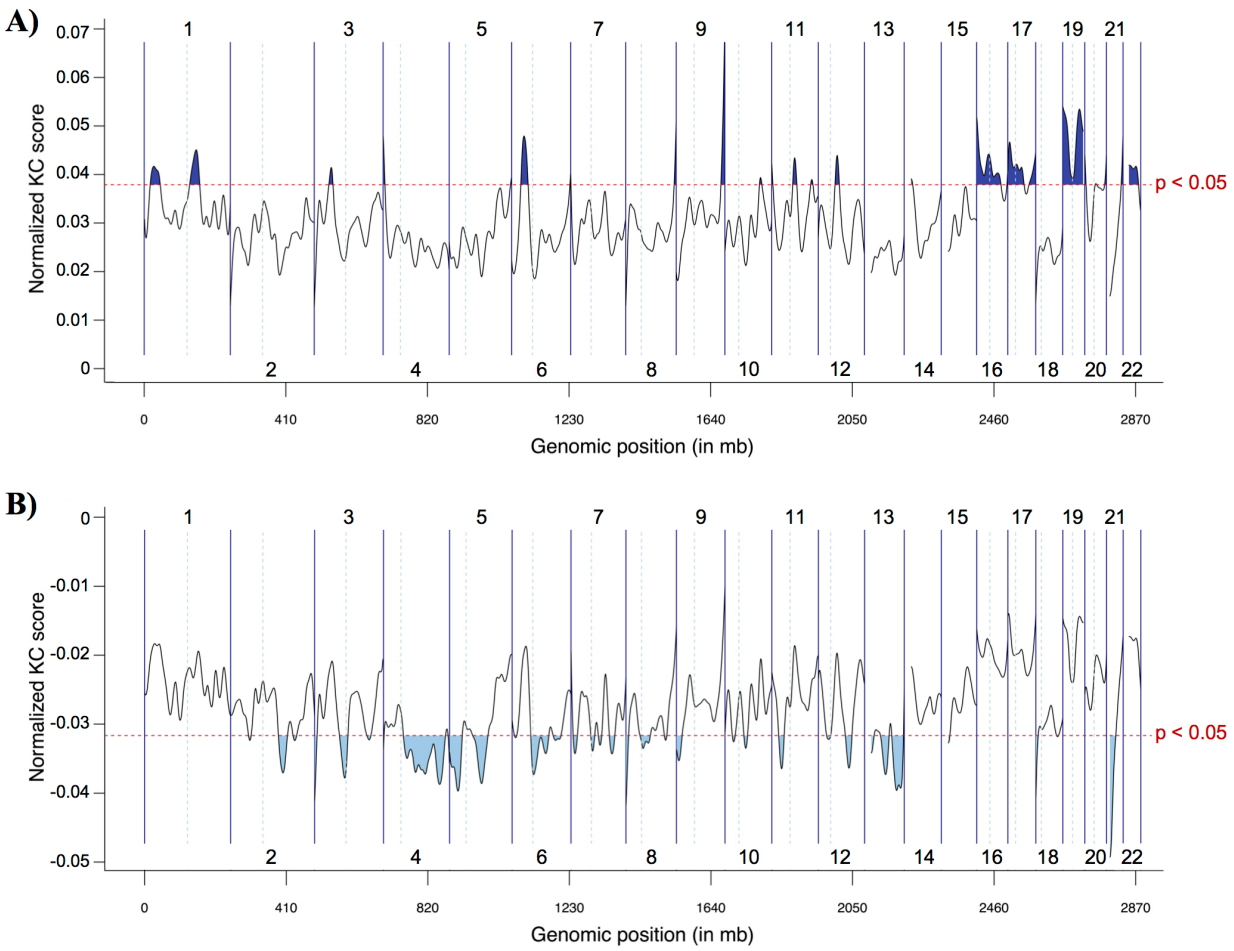

Figure 22 – Array-based comparative genomic hybridization (aCGH) analysis of eight cluster 5 samples compared with a pooled reference sample of ten cluster 1 term controls. At a significance threshold associated with a Bonferroni corrected p-value of 0.05 (dotted line), (**A**) gains in cluster 5 samples were identified predominately on chromosomes 16, 17, 19, and 22 and regions of chromosomes 1 and 6 (dark blue), while (**B**) significant losses in cluster 5 samples were noted on chromosomes 4, 5, 13, and 21 (light blue). The normalized KC score (y-axis) is a Kernel Smoothed Estimate accounting for the strength of a probe's signal, its local genomic environment, and the signal distribution across multiple samples.

3.4 Discussion

In this chapter, we extended the power of the prior analysis in Chapter 2 by the inclusion of an additional 157 placenta samples drawn from a single BioBank and representing a range of hypertensive and normotensive states. Importantly, corresponding detailed clinical information associated with these PE-focused BioBank samples demonstrated significant correlations to the majority of the identified molecular subtypes of placentas, indicating distinct pathophysiology and influence of maternal factors on the presence of PE.

Prior studies have revealed the existence of a late-onset (>34 weeks) preeclampsia pathology that is affiliated with a milder presentation of disease and less fetal growth restriction [663]. Consistent with this literature, PE cases in cluster 1 were dominated by placentas from term and near-term delivery of AGA infants, with known maternal risk factors of nulliparity or a prior hypertensive pregnancy [30]. Given that these placentas appear globally normal by gene expression, PE development in cluster 1 is likely predominately driven by underlying maternal cardiovascular disease susceptibility in these subjects (i.e., a "maternal" PE), either due to common risk factors or persistent endothelial damage from a previous pregnancy [100, 101]. Therefore, the acquisition of maternal samples, such as endothelial cells or plasma, will be required to comprehend the PE pathology observed in this subtype.

The more severe early onset (<34 weeks) form of preeclampsia is linked to growth restriction and other signs of systemic maternal pathology, such as HELLP syndrome [663]. Samples belonging to cluster 2 were highly enriched in PE, demonstrating smaller placental weights, early deliveries, and co-existing classifications of SGA or HELLP syndrome [374]. GSEA identified enrichment of hypoxia, glycolysis, and secretion ontologies in this cluster, all of which have been previously reported in the analysis of PE [297, 366, 367, 374, 375]. This supports a PE pathogenesis arising from poor trophoblast invasion and spiral artery remodeling in this cluster (i.e., a classic, "canonical" PE). The co-clustering of early-onset PE and HELLP placentas is also consistent with the prior finding of similar transcriptional profiles in placentas associated with these two diagnoses [374].

As in Chapter 2, a second molecular group of preeclamptic samples was identified in cluster 3 with a severe, but somewhat later-onset, form of the pathology. Interestingly, although these placentas were linked to poor fetal outcomes, similar to cluster 2, the observed maternal

parameters of disease severity, such as blood pressure and proteinuria levels, were not as dramatically increased in this cluster. This slightly milder maternal disease is likely responsible for the longer mean gestation (by four weeks) observed in cluster 3 compared to cluster 2. Furthermore, GSEA of cluster 3 samples discovered enriched expression of genes related to immune and inflammatory response [652], in addition to elevated levels of rejected organ markers [406, 669-673]. These findings suggest an "immunological" PE in this cluster, and, in combination with negative results for PE-associated viruses, favor an interpretation of this immune response as a maternal–fetal incompatibility/allograft rejection, rather than a viral infection, although further investigation is necessary. Additionally, the notable observation of upregulated HLA-G expression in these samples may be a compensatory response, trying to restore immune tolerance [676, 677], and its unexpected expression within the sampled villi may help to prevent cell lysis [224].

Moreover, an interesting correlate in the clusters, particularly in cluster 3, was maternal blood type and pregnancy history to the presence or absence of a PE diagnosis. Blood type A, common in cluster 3 PE patients, has been affiliated with an increase in inflammatory markers and co-existing events of SGA infants and PE [678]. Conversely, blood type B, observed in all three non-PE subjects in cluster 3, has not been linked to this increased risk for PE [678]. Further investigation into this relationship will require matched placental and maternal samples to assess changes in immune cell activity. Additionally, although the observation of a previous miscarriage in all non-PE cluster 3 subjects and none of the cluster 3 PE subjects is certainly of interest, it is difficult to interpret without complete pregnancy history information, specifically concerning partner changes between pregnancies [661], which, unfortunately, is not available for these patients.

An important consideration for research in this field is the use of preterm controls. Within our dataset, early preterm control placentas (<30 weeks) uniquely generated cluster 4. Clinically, these were predominately recorded as exhibiting signs of infection, mostly chorioamnionitis. Molecularly, cluster 4 demonstrated an over-representation of genes associated with development, due to their young age, and damage, as a consequence of this active infection. Although some previous PE studies have employed preterm controls for gestational age matching [364], others have used term placentas to eliminate confounding molecular changes caused by preterm pathologies [353, 365, 368], while yet others have grouped all normotensive

controls together [363]. In our study, by including both term and preterm controls and performing an unbiased analysis, a significantly larger gene expression difference was noted between the similarly aged preterm controls and PE samples than between the term controls and preeclamptics. This may suggest that preterm PE samples have prematurely aged, resulting in more molecular similarity to term controls [359]. It also suggests that preterm normotensive samples exhibit a distinct underlying pathology, resulting in significant changes in placental gene expression, independent of PE. As such, direct comparisons between early-onset PE samples and preterm controls likely overestimate transcriptional differences and this experimental design would, therefore, not be recommended.

Finally, the increased power gained from the addition of the BioBank samples to the Aggregate samples led to the identification of cluster 5. This cluster contained a mixture of non-PE and PE samples with no differential enrichment of maternal or fetal attributes. However, significant gains (on chromosomes 1, 6, 16, 17, 19, and 22) and losses (on chromosomes 4, 5, 13, and 21) were observed in this cluster by both gene expression and aCGH. Interestingly, these chromosomal abnormalities are frequently observed in cancer [679, 680] and, therefore, imply possible biological significance associated with increased invasion and proliferation that could benefit a PE placenta. Alternatively, these chromosomal anomalies may be a common, but confined, occurrence as the placenta is a large organ composed of redundant clonally derived units. The observation of only 10-20% affected placental cells may result from the BioBank's strategy of biopsying four sample sites per placenta, as this would discover these abnormal sites more frequently than a single site biopsy procedure [332, 681]. Additionally, as our samples are pooled biopsies of multiple placental cell types, it is not possible to establish which type of CPM has been identified in these placentas. Future efforts should be directed toward determining the frequency of mosaicism in the human placenta and its possible aggravating or protective role in pathologies.

Another improvement in this dataset compared to our aggregate analysis (Chapter 2) is the addition of several samples with co-occurring and confounding pathologies of preeclampsia. For example, chronic hypertension with preterm delivery demonstrated similar placental gene expression to the cluster 2 preeclamptics, and CH placentas without PE were found in all four PE-enriched clusters (1, 2, 3 and 5). Although it is possible that several of these non-PE CH samples may be diagnosed as preeclamptic under the new broader guidelines [1], it is also likely

that maternal factors can act to protect or exacerbate the transition to PE from a CH state. As such, analysis of maternal samples may yield biomarkers to predict PE development in CH women and distinguish between a diagnosis of preeclampsia and chronic hypertension. Additionally, given that two subtypes of non-PE preterm labor were identified in clusters 1 and 4 and four subtypes of PE-SGA were observed in clusters 1, 2, 3, and 5, this confirms that other common pregnancy-related pathologies are likely as heterogeneous as PE and would, therefore, also benefit from an unbiased/unsupervised analysis in a larger, focused set of samples.

Although this study represents substantial progress toward understanding PE disease, it is not without limitations. The results in this chapter and in Chapter 2 are dependent on the reliability of the microarray data collected in the seven other employed studies, as well as the assumption that biases in their initial sample selection, for example in ethnicity and gestational age, did not have a significant impact on the bioinformatic aggregation of the studies and the resulting combined dataset. Additionally, while these findings confirm and expand on the results from Chapter 2, considerable clinical outcome heterogeneity is still observed within these clusters (especially in clusters 1, 3, and 5), and the clinical utility and feasibility of this post-delivery transcriptional clustering is unclear. Therefore, these placentas will also need to be assessed by more clinically relevant methods, such as histology and targeted qPCR.

4 Chapter 4 – Histopathological Concordance and Discordance with Gene Expression Data in Transcriptional Subtypes of Preeclampsia

Part of this chapter's content is published in:

Leavey K, Benton SJ, Grynspan D, Kingdom JC, Bainbridge SA, Cox BJ. (2016). Unsupervised Placental Gene Expression Profiling Identifies Clinically Relevant Subclasses of Human Preeclampsia. *Hypertension*. 68: 137-147. [660]

Part of this chapter's content is under review:

Benton SJ*, Leavey K*, Grynspan D, Cox BJ, Bainbridge SA. High Degree of Concordance Between Placental Gene Expression and Histopathology in Subtypes of Preeclampsia. *AJOG*.

* Co-first authorship

Co-authors' contributions are described in the methods section.

4.1 Introduction

Preeclampsia (PE) is a potentially life-threatening disorder of pregnancy, characterized by maternal hypertension and end organ dysfunction [1]. After decades of research into the etiology and pathophysiology of PE, much is still not understood about this disorder, and no effective interventions exist other than the delivery of the placenta, which is thought to be the causative organ. Further complicating our understanding of PE is the heterogeneity observed among pregnancies in terms of clinical presentation, disease severity, and placental pathology, and accumulating evidence suggests that this is because PE is a disorder encompassing several disease subtypes [371, 605, 639, 640, 682].

In this vein, we used genome-wide microarray analysis to generate transcriptional profiles of 157 placentas from PE and control pregnancies in Chapter 3. Unsupervised clustering of this data (merged with the additional previously published data from Chapter 2) identified five distinct groups of placental gene expression, including three clinically significant subtypes of PE: "maternal" PE patients with relatively normal placental gene expression profiles and healthier clinical outcomes (cluster 1); "canonical" PE patients with preterm deliveries, severe maternal symptoms, and high placental expression of FLT1 and ENG, and genes related to hypoxia and altered hormone secretion (cluster 2); and "immunological" PE patients exhibiting dramatically reduced fetal growth and an over-representation of immune and inflammatory genes (cluster 3). An additional group of PE patients was also discovered in this analysis, with no strong clinical or epigenetic [683] associations, and further investigation determined this cluster to be the likely result of chromosomal abnormalities consistent with confined placental mosaicism (cluster 5). The control patients included in the study primarily split into two clusters, with the healthy term controls clustering alongside the "maternal" PE patients (cluster 1), and approximately half of the preterm control samples (delivery <34 weeks) forming a unique cluster defined by the over-representation of genes related to cell proliferation and stress response, along with clinical annotations of chorioamnionitis (cluster 4).

However, clinical outcome heterogeneity was still observed within these groups (especially clusters 1, 3, and 5) and patients located at the periphery of a cluster were often ill-defined. For example, some average-for-gestational-age (AGA) infants were found in cluster 3, which was partially characterized by severely reduced fetal growth, while some cluster 1 samples with

clinical indications of chorioamnionitis where found on the border of cluster 4. These findings suggest that: 1) in some women, multiple pathophysiologies may be contributing to the development of PE; and/or 2) placental gene expression profiling on its own may be insufficient to identify all possible subtypes of PE pathophysiology. Therefore, in this chapter, these pre-defined transcriptional subtypes of PE were further characterized using detailed histopathology. In addition to offering complimentary insight into the underlying placental pathologies observed across the transcriptional clusters, the additional contextual information provided through clinical histology offered the possibility of discovering smaller, more subtle subtypes of PE placental pathophysiology.

4.2 Methods

4.2.1 Patient cohort

Details pertaining to the patient cohort used in this chapter have been described in Chapter 3. Briefly, 157 women with singleton normotensive pregnancies (N=53), pregnancies with chronic hypertension (CH) (N=24), or pregnancies with PE (N=80) were selected from the Research Centre for Women's and Infants' Health (RCWIH) BioBank. PE was defined as the onset of hypertension (systolic pressure ≥140 mmHg and/or diastolic pressure ≥90 mmHg) after 20 weeks' gestation with proteinuria (>300 mg protein/day, or ≥2+ by dipstick) according to diagnostic guidelines at the time of the study [642]. Chronic maternal hypertension was defined as systolic pressure ≥140 mmHg and/or sustained diastolic ≥90 mmHg before 20 weeks gestation. Average-for-gestational-age (AGA) was defined as a neonatal birth weight >10th percentile for gestational age and sex, and small-for-gestational-age (SGA) was defined as a neonatal birth weight <10th percentile for gestational age and sex, based on a Canadian growth reference [169].

4.2.2 Placental histopathology scoring

Additional placental tissue biopsies and corresponding historical placental pathology reports for each available sample included in the microarray study (N=142/157) were purchased from the RCWIH BioBank. For each placenta, four tissue biopsies were excised midway between the umbilical cord insertion and the periphery of the placental disc, fixed in formalin, and embedded

in paraffin wax. The FFPE tissue was then sectioned (5μm thick) and four sections per placenta (one section per biopsy) were sent to Dr. Shannon Bainbridge's laboratory at the University of Ottawa, where it was stained with hematoxylin and eosin [684] and scanned to a digital image using an Aperio® ScanScope by Dr. Bainbridge's post-doctoral fellow Dr. Samantha Benton. Dr. David Grynpan, an experienced perinatal pathologist, examined and graded the digital images, blinded to the microarray results (transcriptional cluster membership) and clinical outcomes (excluding gestational age at delivery). This was done for 30 pathological lesions [385, 393, 394, 404, 685] on a scale of 0-1 (absence/presence), 0-2, or 0-3 (absence/presence and degree of severity), according to a pre-specified rubric developed by Drs. Benton, Grynspan, and Bainbridge (**Appendix B**), an extension of their prior histological analysis of a separate cohort of placentas [454]. Individual lesions were also grouped according to eight broad placental pathology categories: features of maternal vascular malperfusion, fetal vascular malperfusion, placental villous maldevelopment, chronic inflammation, implantation site abnormalities, chorioamnionitis, chronic utero-placental separation, and maternal-fetal interface disturbance. Gross anatomy (ex. placental weight, umbilical cord length) was obtained from the accompanying placental pathology reports, in addition to several microscopic lesions (ex. placental infarction), as the tissue biopsies were collected from areas that appeared grossly normal and only included villous tissue (i.e., maternal decidua was not sampled). Resulting histology scores were then sent to us for analysis.

4.2.3 Visualization and clustering analysis of histopathology data

Graded scores for the 30 individual placental lesions in the 142 samples were loaded into R 3.1.3, and scored sums for each broad pathology category as well as a total overall pathology score (sum of all 30 lesions) were calculated for each placenta. Individual histological features and category sums (on at least a 0-2 scale) were investigated for (Kendall) correlations with the continuous clinical data from Chapter 3. The p-values were adjusted for multiple comparisons by the Bonferroni method and the *tau* coefficients were plotted as a red-blue heatmap. Kendall correlations were also employed to assess linear relationships between the maternal vascular malperfusion lesions and FLT1 and ENG placental expression. Histological differences across the previously identified transcriptional clusters 1-5 were investigated using Kruskal-Wallis rank sum tests, and the global associations between all 142 placentas based on the histology information alone were visualized using t-distributed stochastic neighbor embedding (t-SNE)

[628] with a perplexity of 13. Histology scores for the samples belonging to each individual transcriptional cluster were subjected to hierarchical clustering, and the results were plotted as phylogenetic trees, using the *ape* package [686].

4.2.4 Concordance between placental histopathology and gene expression findings

Using gene set enrichment analysis, over-represented biological pathways and possible underlying placental pathophysiology have been previously characterized for each transcriptional cluster (Chapter 3). This information was then utilized to determine the degree of concordance between the transcriptional and histopathology profiling across our sample set: samples in cluster 1 were classified as "concordant" when they showed little or no pathology, in line with these placentas demonstrating the healthiest transcriptional profiles; concordant cluster 2 placentas had a high score (3+) for maternal vascular malperfusion lesions, fitting with the transcriptional observation of hypoxia in these "canonical" PE samples; in the "immunological" cluster 3, concordance was assigned to placentas showing signs of a maternal-fetal interface disturbance and/or chronic inflammation, in agreement with the enrichment of immune response genes; and concordant cluster 4 samples were associated with histological chorioamnionitis, which is strongly linked to preterm delivery and has already been noted in the clinical charts associated with these samples. Cluster 5 had no clear defining features (outside of the identified chromosomal abnormalities); therefore, all placentas in this cluster were classified as "discordant".

The principal component analysis (PCA) plot of the gene expression data from Chapter 3 was restricted to the 142 placenta samples assessed in this chapter, and was re-plotted and re-colored to demonstrate the transcriptional relationships between samples with concordant and discordant histological features. In this case, sphere transparency was achieved by setting the *plot3d* alpha to 0.2. The center of each transcriptional cluster on the PCA plot was calculated, based on principal components 1-3 and the 142 samples with available histology, and the relative locations of various concordant and discordant groups were compared by Wilcoxon rank sum tests.

4.2.5 Ethics

Ethics approval for this study was granted from the Research Ethics Boards of the Ottawa Health Science Network (#2011623-01H), Mount Sinai Hospital (#13-0211-E), and the University of

Toronto (#29435). All women provided written informed consent for the collection of biological specimens and medical information.

4.3 Results

4.3.1 Clinical and transcriptional correlations with histological lesion severity

Of the 157 samples included in our original microarray study, 142 (90%) had matched formalin-fixed paraffin-embedded (FFPE) placental tissue available for histological assessment. Of these, 49 were normotensive controls (term and preterm), 18 were associated with a diagnosis of chronic hypertension, and 75 were preeclamptic. To investigate general relationships between the presence of histology lesions and clinical attributes, the individual placental features and category sums with a minimum range of 0-2 initially underwent correlative analysis with clinical characteristics in the 142 patients. The summed maternal vascular malperfusion (MVM) score, as well as the individual MVM lesions distal villous hypoplasia, placental infarction, and syncytial knots, showed strong positive relationships (adjusted $p<0.05$) to maternal blood pressure and umbilical and uterine pulsatility indices, as well as strong negative relationships to gestational age at delivery, newborn weight z-score, Apgar score at 1 minute, and placental weight z-score (**Figure 23, Figure 24**). Furthermore, the summed MVM score demonstrated significant positive correlations ($p<0.01$) with the placental expression of both FLT1 and ENG genes (**Figure 25**). The summed histological chorioamnionitis score, and its specific maternal and fetal inflammation lesions, generally showed the opposite linear clinical relationships to the MVM features, with negative correlations (adjusted $p<0.05$) with maternal blood pressure and positive correlations with newborn and placental z-scores (**Figure 23**). However, histological chorioamnionitis lesions were also strongly affiliated with earlier gestational ages (negative relationship), similar to the MVM pathology.

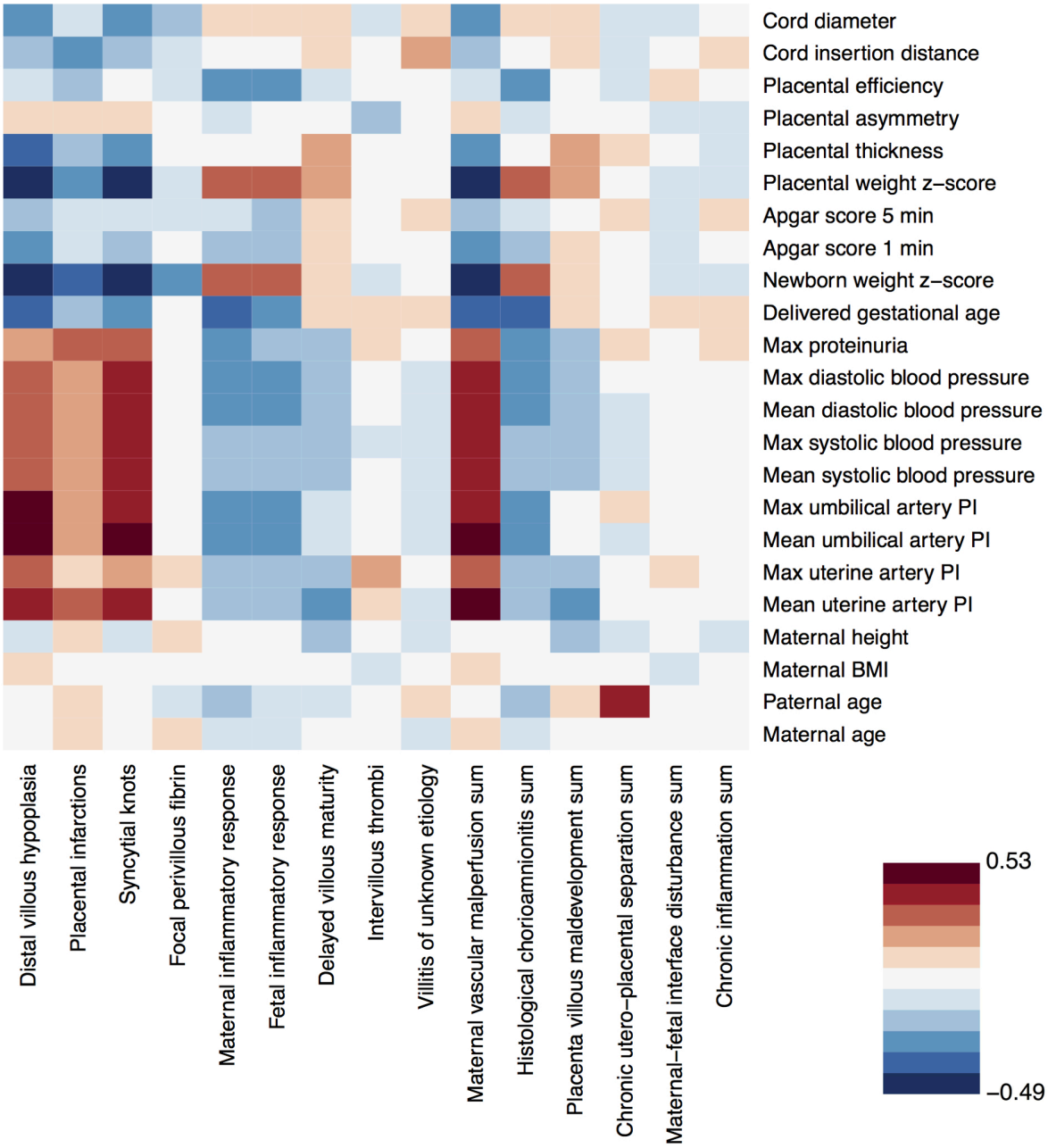

Figure 23 – Heatmap of Kendall's *tau* coefficients for correlations between individual histological features and category sums (on at least a 0-2 scale) and available continuous clinical data. Strong negative relationships are shown in dark blue, while strong positive relationships are in dark red. BMI = body mass index; PI = pulsatility index.

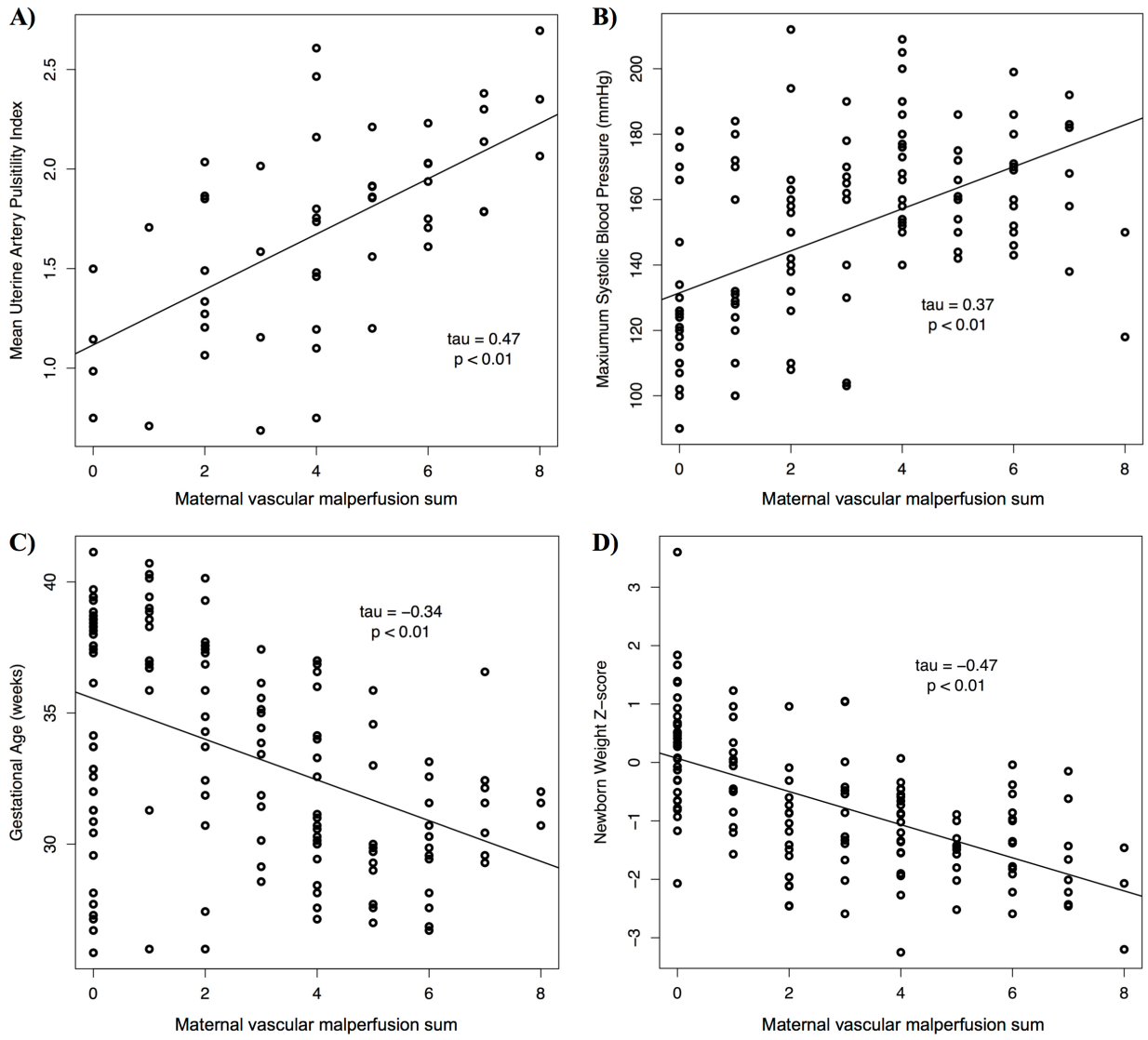

Figure 24 – Correlation plots between the severity of maternal vascular malperfusion lesions and clinical attributes. Maternal vascular malperfusion features were the most common in our cohort; therefore, its score sum demonstrated the largest discrete range and the most linear associations with the clinical information. This included strong positive relationships to (**A**) mean uterine artery pulsatility indices and (**B**) maximum systolic blood pressure, as well as strong negative relationships to (**C**) gestational age at delivery and (**D**) newborn weight z-scores. P-values and *tau* values were obtained from Kendall's tests.

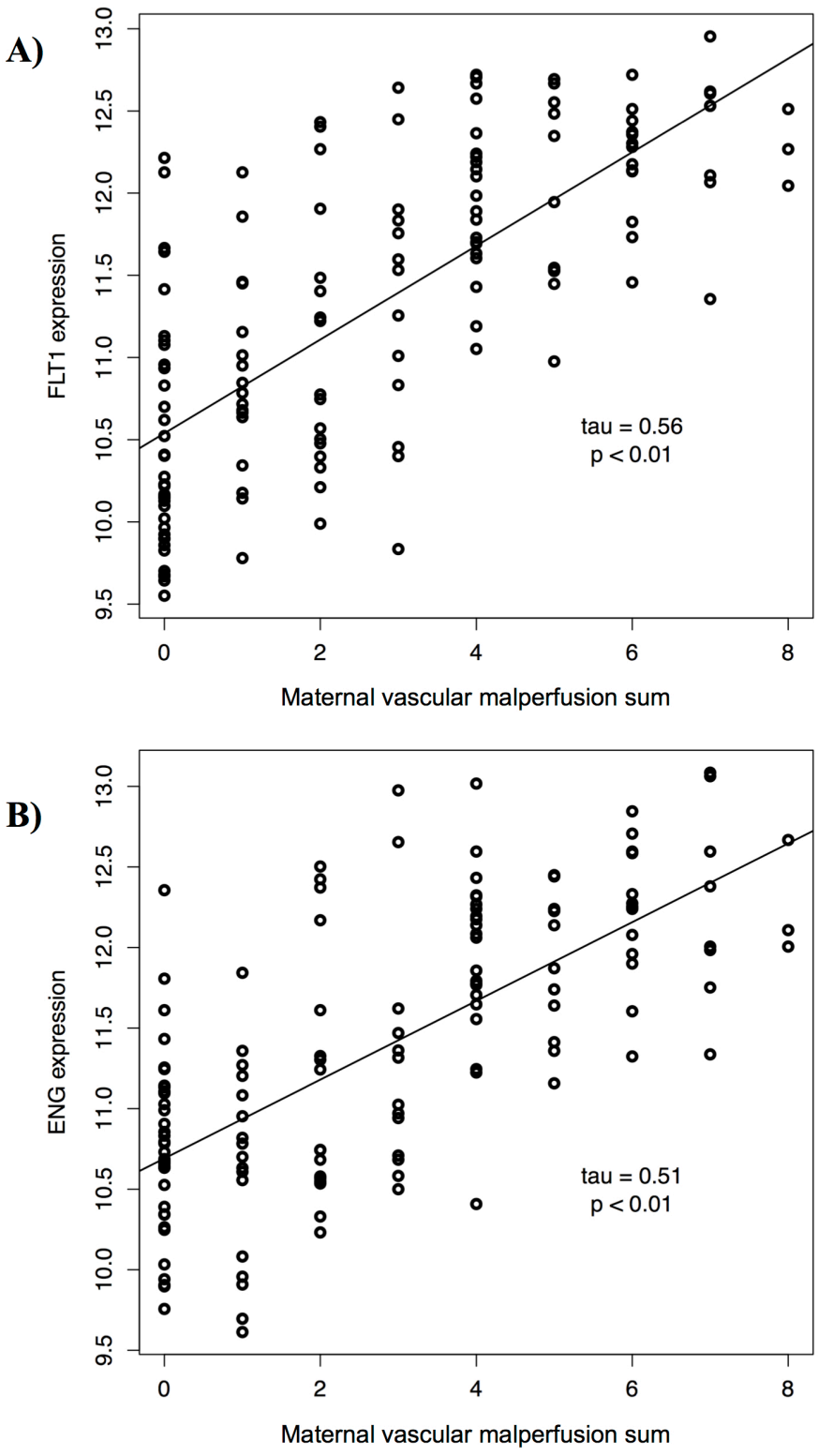

Figure 25 – Placental severity of maternal vascular malperfusion lesions and the expression of anti-angiogenic markers (A) FLT1 and (B) ENG revealed a strong positive correlation. P-values and *tau* values were obtained from Kendall's tests.

4.3.2 Defining histological features of each transcriptional cluster

To further characterize each of the original transcriptional clusters, histological findings were compared across the five groups (**Table 14**). Placentas from transcriptional cluster 1 demonstrated minimal evidence of placental histopathology, with the lowest mean cumulative pathology score (2.44; $p<0.01$ across the clusters). The most severe observations of placenta pathology were in transcriptional cluster 2 samples (mean cumulative pathology score of 5.40; $p<0.01$), including the three placentas with the highest overall scores in the entire cohort (9.00). Histopathology findings enriched in cluster 2 samples were maternal vascular malperfusion lesions ($p<0.01$), such as distal villous hypoplasia, placental infarctions, advanced villous maturity, and syncytial knots (**Figure 26**). Placentas from cluster 3 also demonstrated significant evidence of placental histopathology (mean cumulative pathology score of 4.91; $p<0.01$), with the presence of lesions consistent with a maternal-fetal interface disturbance ($p=0.01$), such as massive perivillous fibrin deposition (MPFD), maternal floor infarct, and/or intervillous thrombi (**Figure 26**), as well as several individual MVM and chronic inflammation features. Placentas belonging to transcriptional cluster 4 displayed distinct lesions of histological chorioamnionitis ($p<0.01$), while no evident enrichment of particular placental features was identified in samples with transcriptional cluster 5 membership.

Table 14 – Histological lesion comparison across the transcriptional clusters.

	Cluster 1 N=52	**Cluster 2 N=52**	**Cluster 3 N=11**	**Cluster 4 N=13**	**Cluster 5 N=14**	
Histopathology lesion (N=number of samples with a non-zero score)[a]	**Mean (SD)**					**P-value[b]**
Maternal vascular malperfusion lesions						
Distal villous hypoplasia (N=66)	0.25 (0.48)	1.23 (0.73)	0.36 (0.50)	0 (0)	0.71 (0.83)	<0.01
Placental infarctions (N=58)	0.19 (0.44)	1.02 (0.80)	0.27 (0.47)	0.23 (0.60)	0.79 (0.80)	<0.01
Advanced villous maturity (N=75)	0.33 (0.47)	0.87 (0.34)	0.45 (0.52)	0.08 (0.28)	0.50 (0.52)	<0.01
Syncytial knots (N=81)	0.44 (0.57)	1.15 (0.61)	0.55 (0.69)	0.08 (0.28)	0.64 (0.63)	<0.01
Focal perivillous fibrin (N=21)	0.10 (0.30)	0.25 (0.44)	0.64 (0.81)	0.08 (0.28)	0.21 (0.43)	0.02
Villous agglutination (N=3)	0 (0)	0.06 (0.24)	0 (0)	0 (0)	0 (0)	0.26
Decidual vasculopathy (N=14)	0.06 (0.24)	0.13 (0.34)	0.18 (0.40)	0 (0)	0.14 (0.36)	0.37
Category sum (N=104)	**1.37 (1.66)**	**4.71 (1.90)**	**2.45 (1.51)**	**0.46 (0.78)**	**3.00 (2.48)**	**<0.01**

Implantation site abnormalities lesions						
Microscopic accreta (N=1)	0 (0)	0 (0)	0 (0)	0 (0)	0.07 (0.27)	0.06
Increased basement membrane fibrin (N=1)	0 (0)	0.02 (0.14)	0 (0)	0 (0)	0 (0)	0.79
Category sum (N=2)	**0 (0)**	**0.02 (0.14)**	**0 (0)**	**0 (0)**	**0.07 (0.27)**	**0.35**
Histological chorioamnionitis lesions						
Maternal inflammation (N=14)	0.13 (0.53)	0 (0)	0 (0)	1.46 (1.20)	0.14 (0.53)	<0.01
Fetal inflammation (N=12)	0.08 (0.27)	0 (0)	0 (0)	0.62 (0.65)	0.08 (0.27)	<0.01
Vessel thrombosis (N=1)	0 (0)	0 (0)	0 (0)	0.08 (0.28)	0 (0)	0.04
Category sum (N=14)	**0.21 (0.77)**	**0 (0)**	**0 (0)**	**2.15 (1.72)**	**0.21 (0.80)**	**<0.01**
Placenta villous maldevelopment lesions						
Chorangiosis (N=4)	0.02 (0.14)	0.02 (0.14)	0.09 (0.30)	0 (0)	0.07 (0.27)	0.53
Chorangiomas (N=2)	0 (0)	0.04 (0.19)	0 (0)	0 (0)	0 (0)	0.48
Delayed villous maturity (N=19)	0.15 (0.36)	0.02 (0.14)	0.45 (0.52)	0.38 (0.65)	0.07 (0.27)	<0.01
Category sum (N=24)	**0.17 (0.38)**	**0.08 (0.27)**	**0.55 (0.69)**	**0.38 (0.65)**	**0.14 (0.36)**	**0.02**
Fetal vascular malperfusion lesions						
Avascular fibrotic villi (N=4)	0 (0)	0 (0)	0.18 (0.40)	0.15 (0.38)	0 (0)	<0.01
Thrombosis (N=8)	0.02 (0.14)	0.10 (0.30)	0.09 (0.30)	0.08 (0.28)	0 (0)	0.40
Intramural fibrin deposition (N=0)	0 (0)	0 (0)	0 (0)	0 (0)	0 (0)	--
Category sum (N=12)	**0.02 (0.14)**	**0.10 (0.30)**	**0.27 (0.47)**	**0.23 (0.44)**	**0 (0)**	**0.01**
Chronic utero-placental separation lesions						
Chorionic hemosiderosis (N=5)	0.04 (0.19)	0.02 (0.14)	0.09 (0.30)	0 (0)	0.07 (0.27)	0.66
Retroplacental hematoma (N=8)	0.02 (0.14)	0.10 (0.30)	0.18 (0.40)	0 (0)	0 (0)	0.10
Laminar necrosis (N=4)	0.02 (0.14)	0.06 (0.24)	0 (0)	0 (0)	0 (0)	0.58
Category sum (N=15)	**0.08 (0.27)**	**0.17 (0.51)**	**0.27 (0.47)**	**0 (0)**	**0.07 (0.27)**	**0.21**
Maternal-fetal interface disturbance lesions						
Massive perivillous fibrin deposition (N=5)	0 (0)	0.02 (0.14)	0.27 (0.47)	0.08 (0.28)	0 (0)	<0.01
Maternal floor infarction pattern (N=1)	0 (0)	0 (0)	0.09 (0.30)	0 (0)	0 (0)	0.02
Intervillous thrombi (N=23)	0.17 (0.38)	0.13 (0.34)	0.45 (0.69)	0.08 (0.28)	0.14 (0.36)	0.31
Category sum (N=25)	**0.17 (0.38)**	**0.15 (0.41)**	**0.82 (0.98)**	**0.15 (0.55)**	**0.14 (0.36)**	**0.01**
Chronic inflammation lesions						
Infectious villitis (N=0)	0 (0)	0 (0)	0 (0)	0 (0)	0 (0)	--
Villitis of unknown etiology (N=9)	0.15 (0.50)	0.02 (0.14)	0.18 (0.60)	0.08 (0.28)	0.08 (0.27)	0.57
Chronic intervillositis (N=2)	0 (0)	0.02 (0.14)	0.09 (0.30)	0 (0)	0 (0)	0.21
Chronic deciduitis (N=15)	0.12 (0.32)	0.10 (0.30)	0.18 (0.40)	0.15 (0.38)	0 (0)	0.60
Category sum (N=20)	**0.27 (0.69)**	**0.13 (0.40)**	**0.45 (0.93)**	**0.23 (0.60)**	**0.07 (0.27)**	**0.60**
Additional features						
Meconium histiocytes/ macrophages within membranes (N=11)	0.15 (0.36)	0.02 (0.14)	0.09 (0.30)	0 (0)	0.07 (0.27)	0.10
Meconium-induced myonecrosis (N=1)	0 (0)	0.02 (0.14)	0 (0)	0 (0)	0 (0)	0.79
Cumulative Pathology Score						
Overall sum (N=132)	**2.44 (1.83)**	**5.40 (1.95)**	**4.91 (2.34)**	**3.62 (1.45)**	**3.79 (2.29)**	**<0.01**

[a]Out of 142 possible samples
[b]Based on non-parametric Kruskal-Wallis rank sum tests

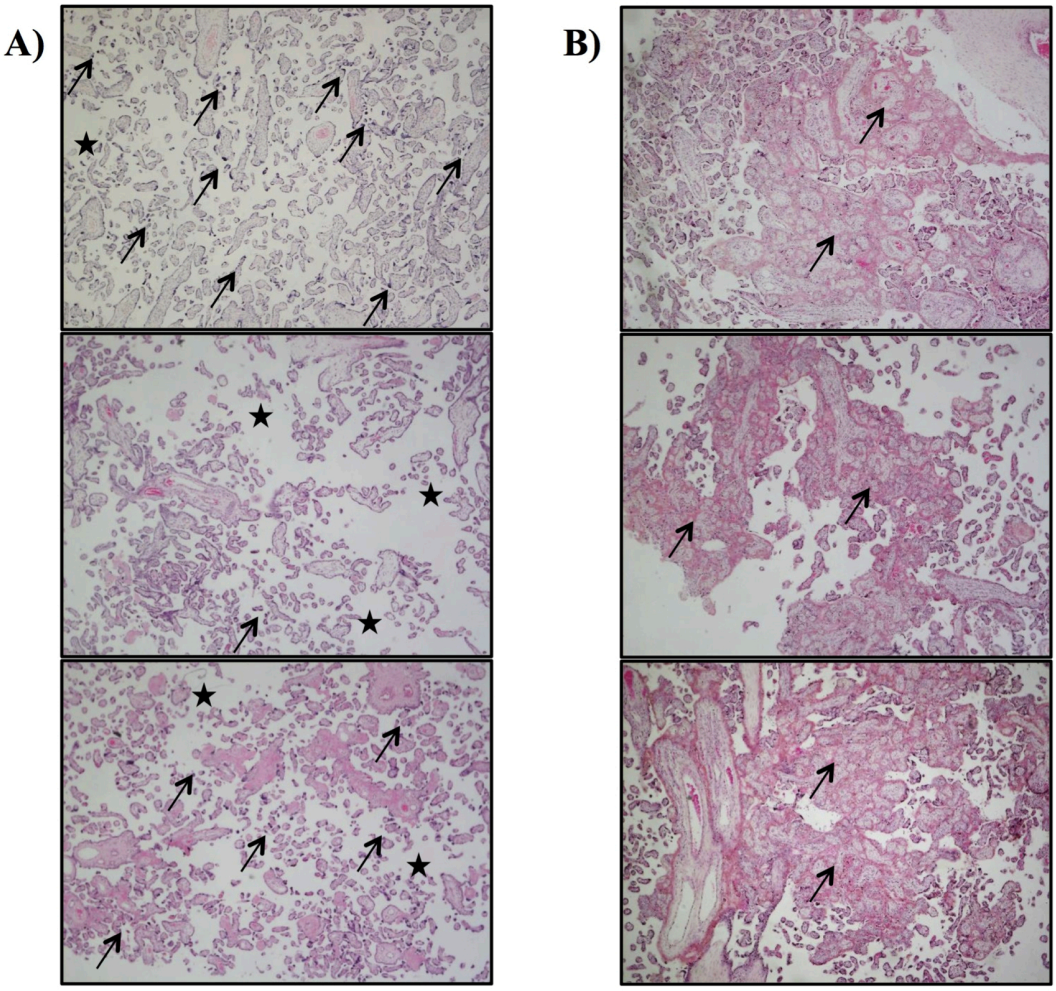

Figure 26 – Histological comparison of a transcriptional cluster 2 placenta and a transcriptional cluster 3 placenta, both associated with preeclamptic mothers and small-for-gestational-age infants. (A) In this representative cluster 2 placenta, placental villi exhibit distal villous hypoplasia as shown by sparsely distributed and small distal villi with thin intermediate villi (indicated with stars). Increased syncytial knots (indicated with arrows) are also seen and are consistent with pathological features of maternal vascular malperfusion. (**B**) In this representative cluster 3 placenta, a massive perivillous fibrin deposition pattern is observed as expansive fibrin within the intervillous space (white areas), occupying a significant proportion of the overall intervillous space (indicated by arrows). This figure was produced by Dr. Samantha Benton after histological scoring by Dr. David Grynspan.

4.3.3 Sample relationships based on histopathology findings

To determine relationships between the samples based solely on the histopathology profiling results, the histology data for the 142 placentas was subjected to t-SNE visualization. This revealed an overall congruency in the grouping of patients to those originally identified through transcriptional clustering, particularly for the samples belonging to transcriptional clusters 2 and 4 (**Figure 27a**). Interestingly, however, several subsets of samples with similar clinical outcomes of maternal hypertensive state, infant birth weight, and gestational age at delivery (ex. normotensive/AGA/preterm) grouped together by histology regardless of their placental gene expression profile, while other clinical phenotypes (ex. PE/SGA/term) were more spread throughout the plot (**Figure 27b**), demonstrating no histological cohesion. In general, samples with increasingly elevated scores for maternal vascular malperfusion lesions plotted on the lower half of the t-SNE plot (**Figure 27c**), while placentas with histological chorioamnionitis formed a group on the top left of the figure (**Figure 27d**). Samples with maternal-fetal interface disturbance and/or chronic inflammation lesions were predominately found along the right side of the plot (**Figure 27e,f**).

A)

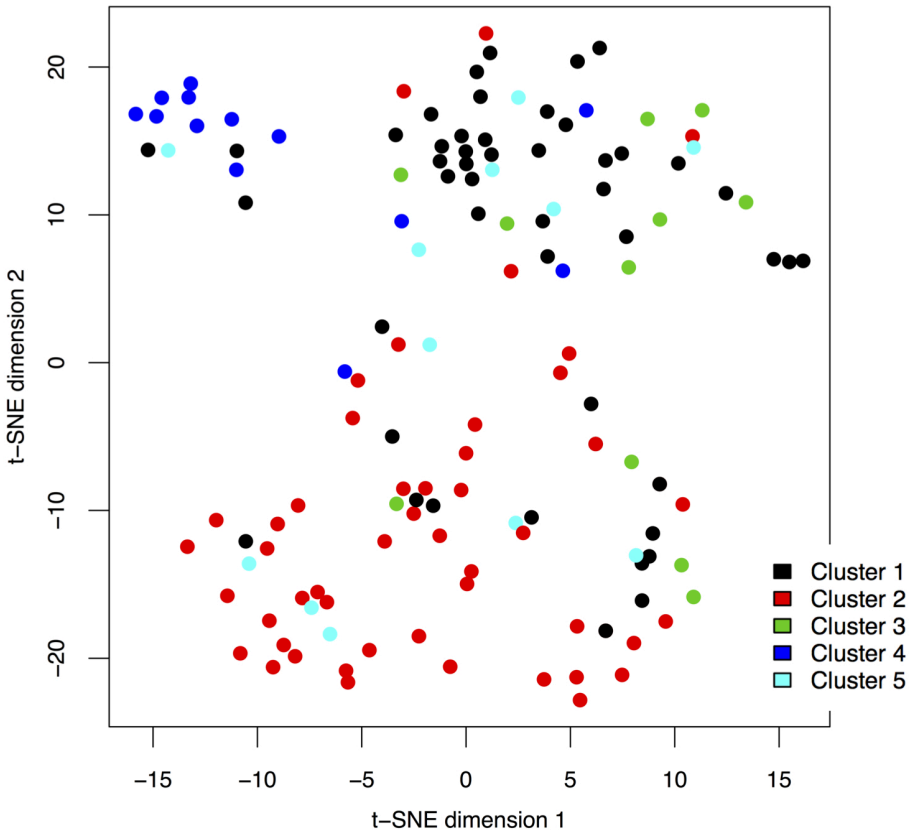
t–SNE dimension 2
20
10
0
–10
–20
–15
–10
–5
0
5
10
15
t–SNE dimension 1
Cluster 1
Cluster 2
Cluster 3
Cluster 4
Cluster 5

B)

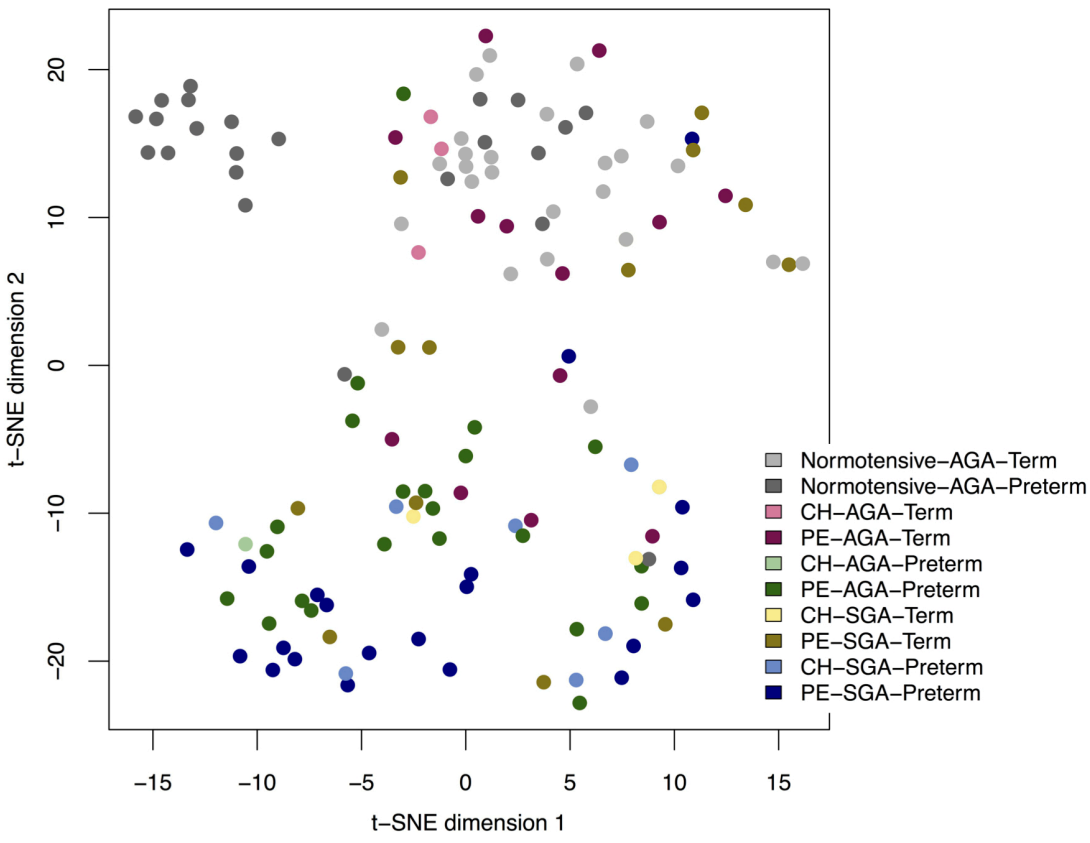
t–SNE dimension 2
20
10
0
–10
–20
–15
–10
–5
0
5
10
15
t–SNE dimension 1
Normotensive–AGA–Term
Normotensive–AGA–Preterm
CH–AGA–Term
PE–AGA–Term
CH–AGA–Preterm
PE–AGA–Preterm
CH–SGA–Term
PE–SGA–Term
CH–SGA–Preterm
PE–SGA–Preterm

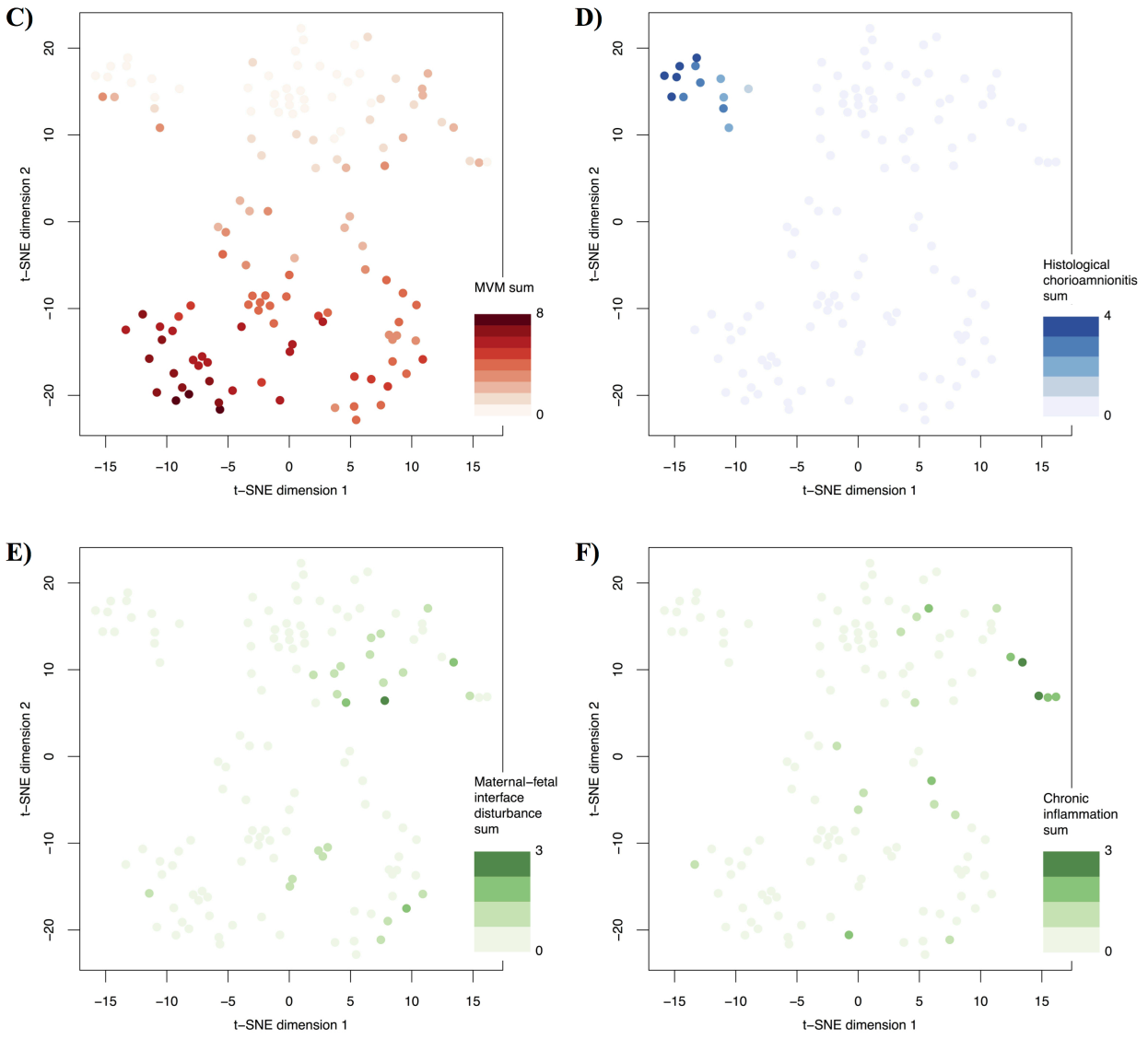

Figure 27 – t-SNE of the 142 samples and 30 individual histology lesion scores. (**A**) Overall, the grouping of patients by histology demonstrated a general congruency to those originally identified through transcriptional clustering (cluster 1, black; cluster 2, red; cluster 3, green; cluster 4, blue; cluster 5, cyan). (**B**) However, several subsets of samples with similar clinical features such as maternal hypertensive state (normotensive, chronic hypertensive (CH), or preeclamptic (PE)), infant birth weight (average-for-gestational-age (AGA) or small-for-gestational-age (SGA)), and gestational age at delivery (preterm (<34 weeks) or term) grouped together by histology regardless of their placental gene expression profile, while other clinical phenotypes were spread throughout the plot. (**C**) Samples with increasingly elevated maternal vascular malperfusion (MVM) lesions (range 0-8, light to dark red) plotted on the lower half of the t-SNE plot, (**D**) while the group of placentas on the top left of the plot was driven by the presence of histological chorioamnionitis features (range 0-4, light to dark blue). Samples with maternal-fetal interface disturbance (**E**) and/or chronic inflammation (**F**) lesions were predominately found along the right side of the plot (both range 0-3, light to dark green).

4.3.4 Identification of histology subgroups within each transcriptional cluster

Given the observed histological heterogeneity within the transcriptional clusters (especially clusters 1, 3, and 5), further hierarchical clustering of the histopathology scores within each individual transcriptional cluster was performed to identify intra-cluster histology subgroups (**Figure 28**). Within transcriptional cluster 1, placentas from healthy pregnancies demonstrated histopathology driven subgroups with: little to no pathology; meconium histiocytes/macrophages within membranes; or villitis of unknown etiology (VUE) (**Figure 28a**). The PE samples in transcriptional cluster 1 (N=14) split into three histopathology subgroups based on the severity of maternal vascular malperfusion lesions present: placentas with a score of 0-2 clustered with the healthy samples; placentas with a score of 3-4 formed a subgroup associated with term deliveries; and placentas with a score of 4-6 formed a small subgroup with preterm deliveries. Approximately half of the preterm normotensive samples included in this transcriptional cluster formed their own histopathology subgroup, driven by the presence of lesions consistent with histological chorioamnionitis.

Transcriptional cluster 2 placentas were fairly cohesive by histology, with subgroup formation based on the severity of overall and specific maternal vascular malperfusion lesions and co-occurrence of chronic deciduitis (chronic inflammation of the decidua) (**Figure 28b**). Additionally, a subgroup of samples in this cluster (N=6, N=3 PE) exhibited little or no evidence of MVM histopathology. The samples associated with co-occurring HELLP syndrome in this cluster did not demonstrate any distinct histological lesions.

In transcriptional cluster 3, the 11 samples clustered into three main histopathology subgroups: one with dominant features of MPFD or maternal floor infarct and/or chronic inflammation, with clinical outcomes of PE, term delivery, and SGA; a second with signs of maternal vascular malperfusion, delivered preterm with maternal hypertension and SGA; and the third with overall low histopathology (**Figure 28c**). Within this third subgroup, two PE/AGA/Term associated placentas showed evidence of a different maternal-fetal interface disturbance lesion, intervillous thrombi. Furthermore, a single PE/SGA/preterm placenta displayed features of both maternal vascular malperfusion and MPFD, and clustered between the first two histopathology-driven subgroups.

Within transcriptional cluster 4, the majority of the placentas demonstrated overt signs of histological chorioamnionitis (**Figure 28d**). However, a small subgroup of samples (N=4) exhibited either minimal evidence of placental histopathology or maternal-fetal interface disturbance/chronic inflammation lesions.

Finally, transcriptional cluster 5 samples, previously characterized as having chromosomal abnormalities likely due to confined placental mosaicism (Chapter 3), split into three subgroups by histology: one with little to no pathology, linked to term deliveries; one with severe features of maternal vascular malperfusion, composed of placentas associated with preterm hypertensive pregnancies; and a single normotensive preterm placenta with evidence of histological chorioamnionitis (**Figure 28e**).

A) Cluster 1:

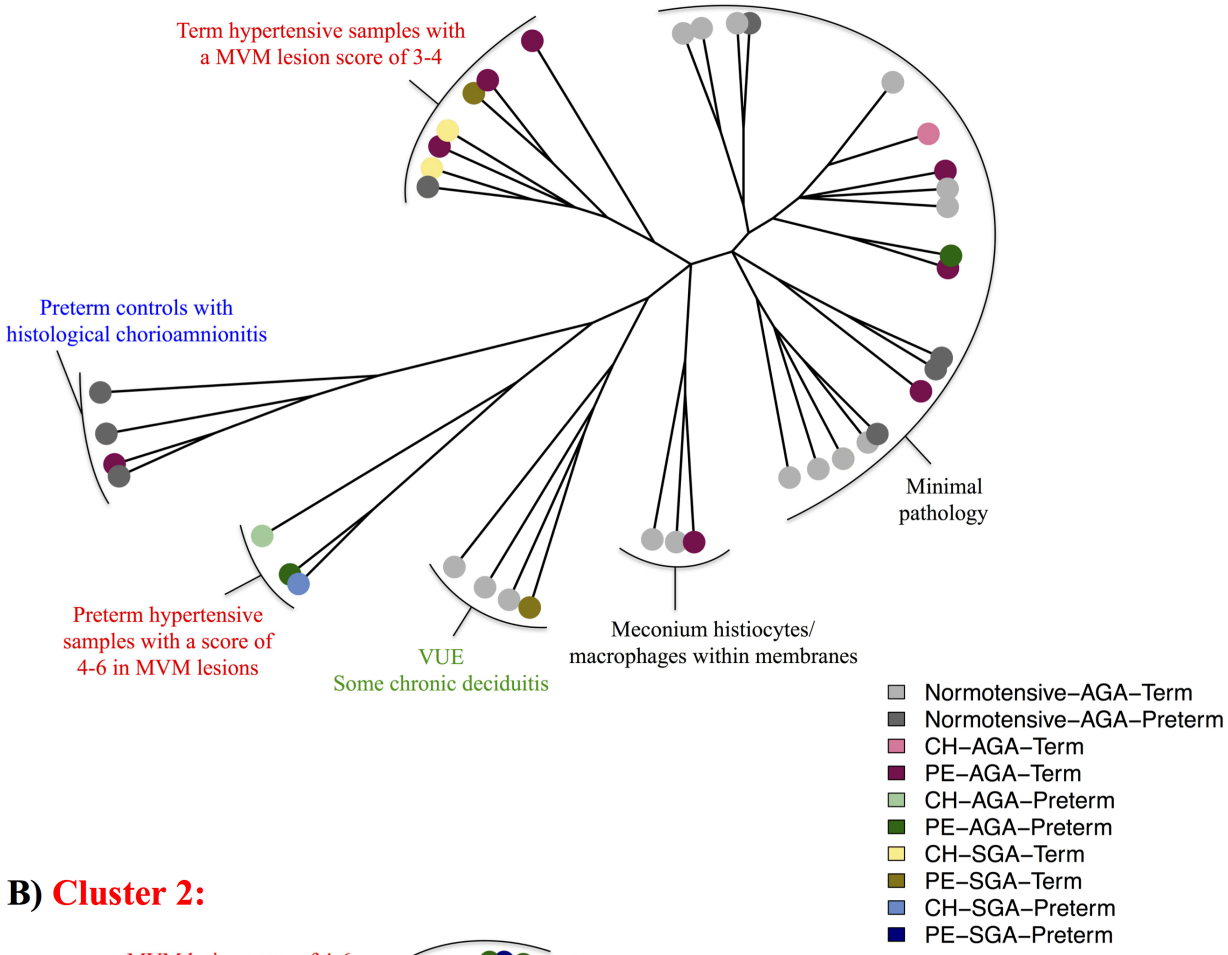

B) Cluster 2:

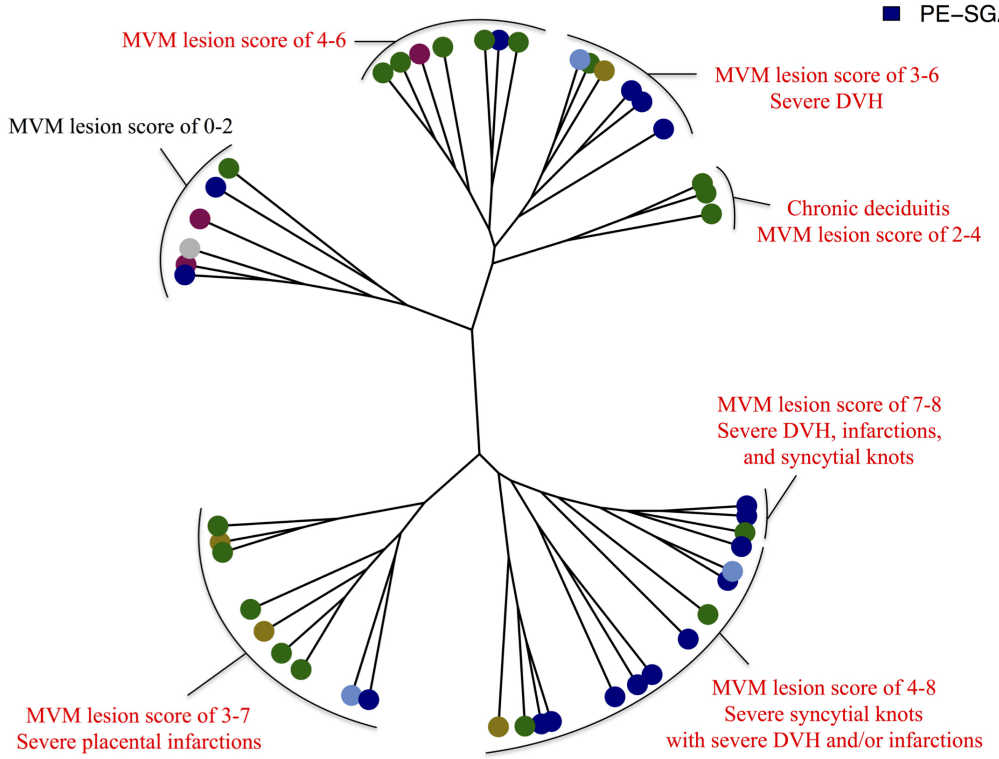

C) Cluster 3:

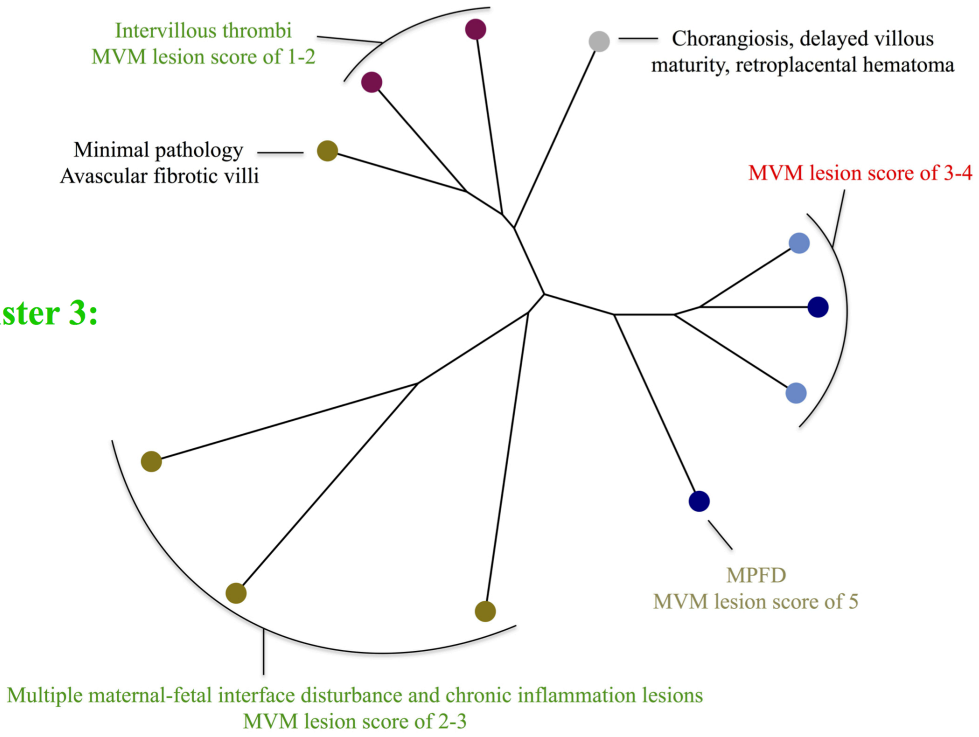

D) Cluster 4:

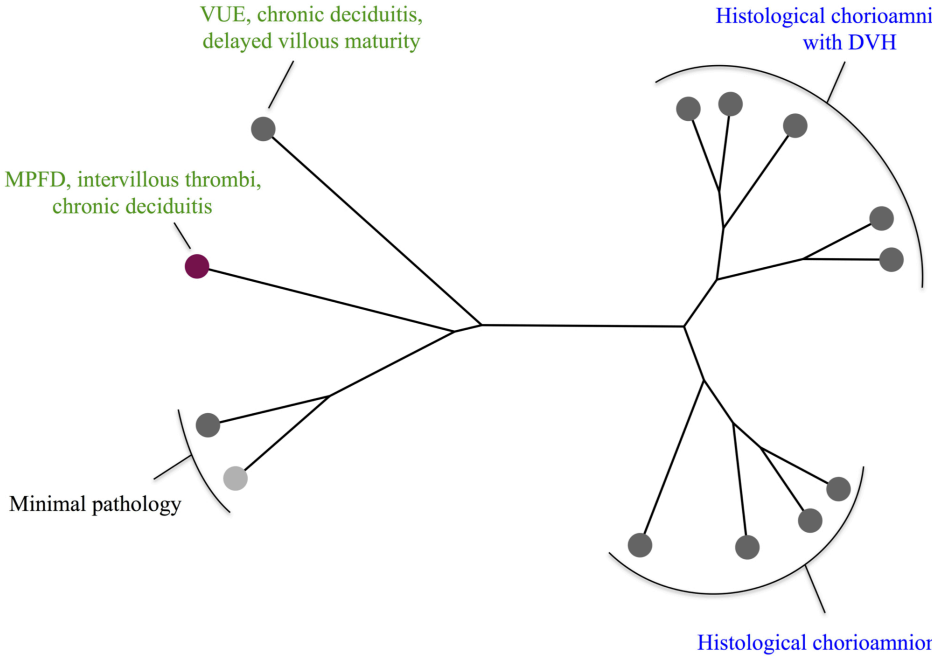

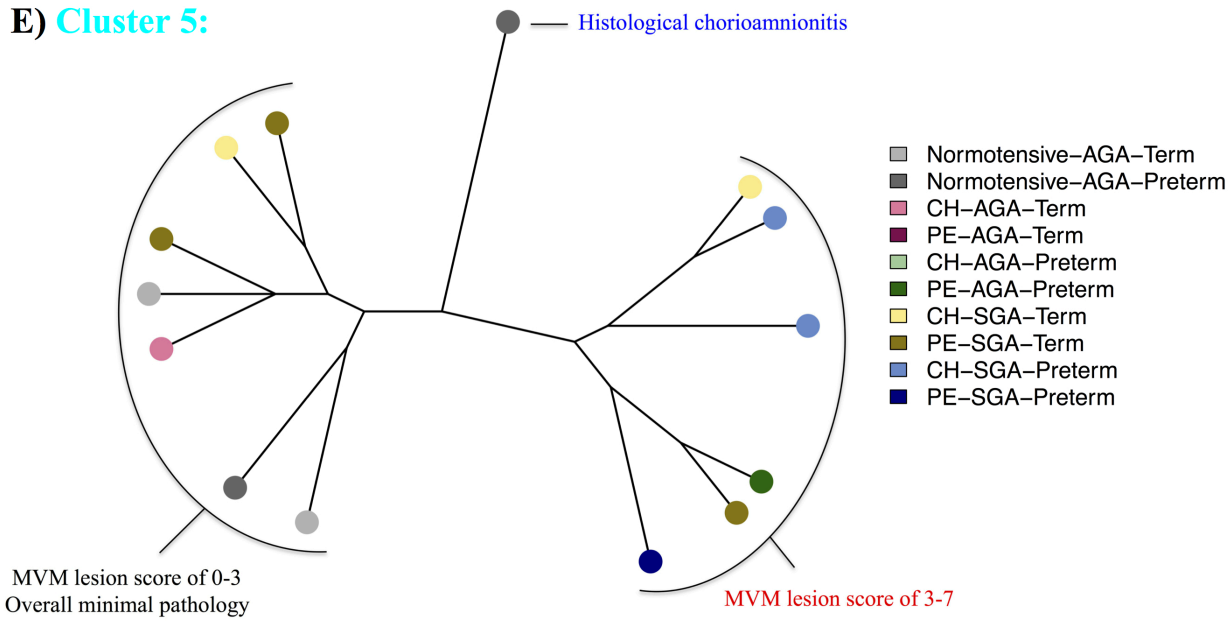

Figure 28 – Trees of the histology clustering results within transcriptional (A) cluster 1, (B) cluster 2, (C) cluster 3, (D) cluster 4, and (E) cluster 5. Tips are colored based on clinical outcome. Each subgroup of placentas identified was assigned a group label with writing color based on the transcriptional cluster that the subgroup most closely resembled histologically (cluster 1, black; cluster 2, red; cluster 3, green; cluster 4, blue). MVM = maternal vascular malperfusion; VUE = villitis of unknown etiology; DVH = distal villous hypoplasia; MPFD = massive perivillous fibrin deposition.

4.3.5 Concordance between placental histopathology and gene expression findings

Overall, the degree of concordance between transcriptional classification and histopathology phenotype was 65% (93/142 samples) (**Figure 28**). By individual cluster, 62% (32/52) of cluster 1 placentas demonstrated transcriptional-histological concordance, with normal/healthy placental gene expression profiles and no evidence of significant placental histopathology. These concordant samples were centered in cluster 1 on the PCA plot of gene expression (**Figure 29a,c**) and separated distinctly from the other transcriptional clusters. Transcriptional-histological discordant samples in cluster 1 demonstrated placental lesions characteristic of transcriptional cluster 2 (maternal vascular malperfusion), cluster 3 (chronic inflammation), or cluster 4 (histological chorioamnionitis). These samples with MVM or chorioamnionitis lesions plotted on the periphery of cluster 1, bordering clusters 2 ($p=0.01$) and 4 ($p=0.01$), respectively (**Figure 29b,d**). However, the placentas with chronic inflammation (specifically VUE) did not plot significantly closer to transcriptional cluster 3 ($p=0.51$).

Within cluster 2 (88% concordant, 46/52) and cluster 4 (69% concordant, 9/13) themselves, transcriptional-histological concordant samples plotted further away from cluster 1 (**Figure 29a,c**), while the discordant samples were located closer to cluster 1 ($p=0.10$ and $p=0.33$, respectively) (**Figure 29b,d**). In transcriptional cluster 3 (55% concordant, 6/11), the discordant preterm hypertensive patients with high maternal malperfusion lesions formed a group bordering cluster 2 ($p=0.56$) (**Figure 29b,d**). Lastly, transcriptional cluster 5 had no clear defining histological features; however, placentas with little to no pathology plotted closer to the center of principal component 1 (PC1), in line with cluster 1, while those with features of maternal vascular malperfusion plotted along the negative axis of PC1, similar to cluster 2 ($p=0.03$) (**Figure 29b,d**). These patterns indicate the existence of blended or intermediate phenotype samples on the cluster borders.

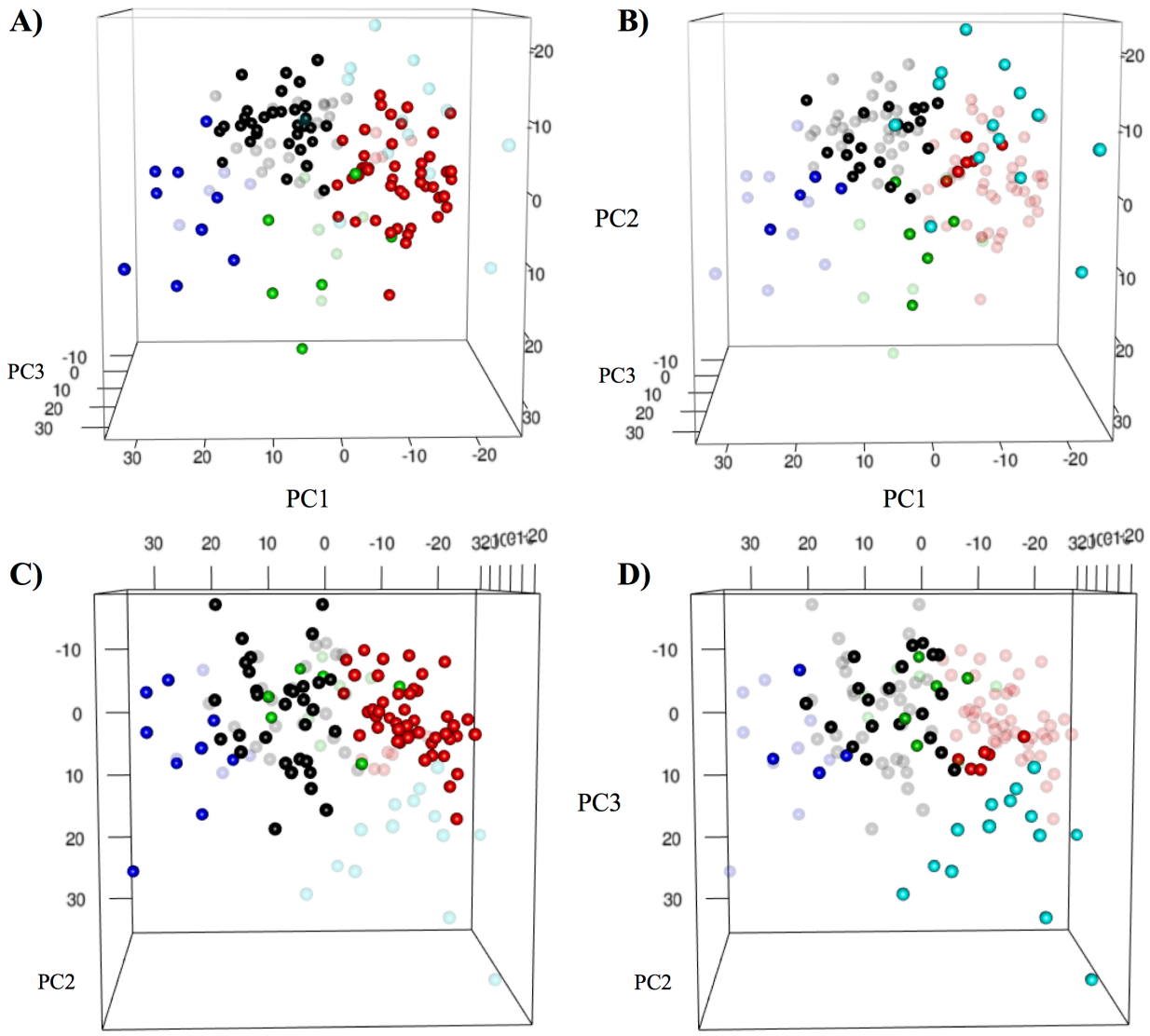

Figure 29 – PCA plots of placental gene expression from Chapter 3 in the 142 samples colored by original transcriptional cluster (cluster 1 – black; cluster 2 – red; cluster 3 – green; cluster 4 – blue; cluster 5 – cyan). Placentas with concordant transcriptional-histological features are shown in (**A**) (from the front) and (**C**) (from the top), while samples with discordant transcriptional-histological features are shown in (**B**) (front) and (**D**) (top). Concordant patients form tighter groups by gene expression, plotting further away from the borders, while discordant samples generally plot near the cluster with more similar histological features.

4.4 Discussion

In the current chapter, we initially employed detailed placental histopathology to further characterize the five transcriptional clusters of placental gene expression identified in Chapter 3, including the three clinically significant subtypes of PE (within transcriptional clusters 1-3). Overall, general concordance between the gene expression and histology data was discovered (~65%), with transcriptional clusters 2-4 each dominated by a single category of histopathology lesions, globally fitting with the prior molecular results and gene enrichment findings (Chapters 2 and 3). Transcriptional cluster 1 samples, which appeared the healthiest by gene expression, exhibited the lowest overall pathology of the clusters, including nine term controls with absolutely no observed lesions. Samples belonging to transcriptional cluster 2 displayed histopathology features consistent with maternal vascular malperfusion of the placenta, which is most commonly associated with "canonical" preterm PE patients [451] and is in line with the over-expression of hypoxia-mediated gene sets in this group. The severity of these maternal malperfusion features in the entire cohort was also shown to demonstrate strong linear relationships with maternal blood pressure, newborn and placental weights, and placental FLT1 and ENG expression, in addition to gestational age at delivery, fitting with prior findings and confirming the clinical basis for the timing of intervention/delivery [359, 400-402, 451]. Transcriptional cluster 3 placentas exhibited an increased likelihood of maternal-fetal interface disturbance and chronic inflammation lesions, in agreement with the observed enrichment of immune response and inflammatory gene sets in this group [406, 415]. Furthermore, placentas belonging to transcriptional cluster 4, primarily made up of preterm control samples, were robustly affiliated with histological chorioamnionitis. This is not surprising given the known relationship between chorioamnionitis and preterm delivery [424], as well as the clinical annotations of infection in these samples described in Chapter 3. Additionally, the almost exclusive finding of chorioamniontis in these cluster 4 samples (also associated with preterm deliveries, normotensive mothers, and normally-grown infants) drove the observed correlations between these lesions and gestational age at delivery (negative), maternal blood pressure (negative), and newborn weight (positive) in the full cohort.

The second goal of this chapter was to determine if pathology offers the ability to further refine the multiple disease processes underlying preeclampsia. Multiple histological subgroups of placentas within each individual transcriptional cluster were identified, some of which revealed

the expected pathological features described above (transcriptional-histological concordant) and some of which showed features more strongly associated with other transcriptional clusters (transcriptional-histological discordant). Concordant subgroups within each molecular cluster, with agreement between gene expression and histopathology findings, often demonstrated subtle differences in the severity of observed placental lesions and/or co-occurrence of additional placental features, and plotted near the center of the cluster by PCA of the microarray data. Transcriptional-histological discordant samples, on the other hand, were found at the cluster periphery by PCA, near the neighboring transcriptional cluster with phenotypically similar histopathology. This indicates that these intermediate phenotypes were contained within the prior transcriptional analysis (Cluster 3), but the additional contextual information gathered through detailed histopathology was required to distinguish these samples. Most importantly, these concordant and discordant subgroups demonstrated increased homogeneity for several clinical outcome characteristics (i.e., time of delivery, fetal growth), further improving on the prior transcriptional analysis. As such, matched molecular and histopathological assessment is essential for identifying and comprehending placental subtypes of preeclampsia, especially those that may have contributions from multiple different core pathologies.

In particular, the addition of the histological information has been especially informative for samples belonging to transcriptional clusters 1, 3, and 5, which are the most clinically and histologically heterogeneous groups in our cohort. In the initial transcriptional analysis (Chapter 3), cluster 1 PE patients exhibited globally normal placental gene expression, initially indicating minimal placental involvement and likely significant maternal contribution to PE development. In actuality, the majority of the late-onset PE patients found within this placental cluster did, in fact, demonstrate some histological evidence of maternal vascular malperfusion, suggesting that this subtype may instead be a somewhat exaggerated maternal response to a milder form of the hypoxic "canonical" disease phenotype observed in the transcriptional cluster 2 PE patients. It is important to note, however, that five PE patients in cluster 1 (~6% of all PE samples) demonstrated limited evidence of placental pathology, through both transcriptional profiling and histopathology, identifying a population of PE patients with truly healthy placentas. These patients likely represent a subtype of PE pathophysiology driven almost exclusively by maternal constitutive factors (i.e. endothelial damage/subclinical cardiovascular dysfunction) [100, 319],

and may perhaps be the PE patients at highest risk of cardiovascular disease across their lifetime [93, 97, 101].

Within cluster 3, the core group of transcriptional-histological concordant PE patients demonstrated histological findings consistent with profound immune activation, such as massive perivillous fibrin deposition. This histological feature has been previously linked to a poor maternal tolerance of the fetal-placental unit [406, 548], and therefore, confirms that the source of the immune response in cluster 3 is likely an allograft rejection, not a viral infection. This is also supported by the identification of no infectious villitis pathology in any of these placentas, as well as the known relationship between apoptosis, a significant cluster 3 gene set (Chapters 2 and 3), and fibrin deposition [399]. Interestingly, these cluster 3 samples also had the greatest frequency and severity of focal perivillous fibrin deposition, which is generally considered to be a MVM lesion [385], but showed a stronger relationship to the immunological-associated placental features in this study. Therefore, it may be worth re-considering the classification of this lesion. Additionally, a significant discordant subgroup of hypertensive patients was also discovered within cluster 3, demonstrating dominant maternal malperfusion histological features despite gene expression profiles suggesting immune activation. Whether these are intermediate phenotypes of PE with mixed pathophysiology, or the result of external factors, such as increased infiltration of maternal immune cells into these placentas, is unclear. Assessing differences in immune cell populations in cluster 3 placentas, compared to the other transcriptional clusters, is one of our future goals.

Lastly, the histological analysis also significantly improved our understanding of transcriptional cluster 5. This cluster was associated with confined placental mosaicism (Chapter 3), but we have otherwise observed no clear clinical, histological, or epigenetic [683] features in these placentas. In this chapter, histology sub-clustering revealed subgroups of cluster 5 samples with similar pathology and clinical outcomes to concordant transcriptional cluster 1, cluster 2, and cluster 4 placentas. These results imply that this cluster is composed of members that, in all probability, should have belonged to the other molecular clusters but grouped together solely due to global mosaicism-induced transcriptional differences.

Given the known sub-optimal inter-observer reliability in histological assessment [384], the main limitation of this study is that scoring of these placentas was only done by one pathologist. The

degree of concern is somewhat mitigated, however, by the general concordance observed between the histological information and the objective transcriptional information, as well as the use of a blinded scoring metric. Furthermore, there likely exists some bias in our initial sample selection that may have minimized the identification of concordant cluster 3 (immune-driven) PE patients. The cases originally selected for transcriptional analysis were limited to those with live births, and, given that the histological features characteristic of cluster 3 PE patients (massive perivillous fibrin deposition and maternal floor infarct) are often lethal and observed earlier in pregnancy [390, 405, 407, 408], we have probably excluded the more severe and common form of this pathology. Additionally, considerable overlap between the PE and CH placentas was once again observed in terms of their scored histological features, similar to the prior transcriptional analysis (Chapter 3). This confirms that these two hypertensive states are indistinguishable at the placental level, and matched maternal samples, which unfortunately were not available for these patients, will be required to understand the transition from a CH to a PE diagnosis. Lastly, it is possible that some of the transcriptional-histological discordance observed is due to sampling limitations. The placenta is a redundant structure composed of hundreds of terminal villi over a large surface area. While four biopsies randomly drawn from each quadrant of the placenta were utilized, the histological and molecular specimens were collected from different biopsies. It is conceivable that sampling could have occurred in regions of the placenta that have slightly different pathology or cellular composition. The use of four biopsies should help to minimize this effect, but higher sampling rates could be warranted in future studies.

Collectively, this integrated histological and transcriptional analysis has discovered core and intermediate subtypes of preeclampsia, with increased clinical significance and decreased heterogeneity, and further emphasizes the importance of clinical histopathology in cases of placental dysfunction. With further investigation, the histological features characterizing each PE subtype could help to estimate pathology risks in subsequent pregnancies as well as potential long-term consequences for both the mother and the child. Immediate future work should focus on the development of a cheaper and more accessible tool for the molecular classification of placentas, such that integrated multi-scale analysis can be performed in a clinical setting.

5 Chapter 5 – Integrated Transcriptional, Histological, and Clinical Analysis Identifies Placental Subtypes of Suspected Fetal Growth Restriction

Content in this chapter is under review:

Gibbs I*, Leavey K*, Benton SJ, Grynspan D, Bainbridge SA, Cox BJ. Placental Subtypes of Suspected Fetal Growth Restriction and Relationships to Maternal Hypertensive State. *AJOG*.

*Co-first authorship

Co-authors' contributions are described in the methods section.

5.1 Introduction

Fetal growth restriction (FGR) is associated with an increased risk of stillbirth and neonatal mortality [106, 107, 178], and the consequences for infants who survive are extensive [109, 110, 180]. Despite decades of research into the pathology of FGR, progress in comprehension and prediction has been limited, and no established treatments exist aside from the delivery of the infant to reduce the risk of stillbirth. This lack of significant progress is likely due to two fundamental issues in FGR research: 1) an inability to accurately distinguish within the range of small-for-gestational-age (SGA) infants those that are simply constitutionally small from those that show pathological FGR [146, 153, 687]; and 2) the continued assessment of FGR samples as a single cohesive group, despite considerable evidence of heterogeneity and the likely existence of multiple subtypes of this pathology [152, 153, 556, 688].

Preeclampsia (PE) is another heterogeneous placenta-centric pathology of pregnancy that has been suggested to share several pathological features with FGR [563, 689]. In our previous work on PE (Chapters 2-4), we found that by using unsupervised clustering techniques, novel molecular subtypes of this hypertensive disorder could be identified [639, 660]. Specifically, within a large cohort of 330 placentas representing a wide range of PE clinical presentations and co-occurring complications (SGA, chronic hypertension (CH), and preterm labor), unsupervised clustering revealed five patient groups based solely on placental gene expression, including four subtypes of PE samples. Using a combined transcriptional (Chapter 2/3), clinical (Chapter 3), epigenetic [683], and histopathological (Chapter 4) approach, we have been able to further describe each of these distinct PE placental subtypes: cluster 1 PE samples demonstrated molecular similarity to healthy term controls and minimal placental pathology, suggesting this may be a “mild” placental or partially “maternal” PE subtype driven by pre-existing, sub-clinical, maternal cardiovascular disease; cluster 2 PE was termed “canonical”, with overwhelming evidence of maternal vascular malperfusion and placental hypoxia, along with increased expression of several hallmark markers of preeclampsia; cluster 3 contained a less prevalent “immunological” subtype of PE, exhibiting evidence of heightened immune response at the maternal-fetal interface, similar to an allograft rejection [406, 409]; and, finally, a subtype of PE placentas with chromosomal abnormalities was discovered in cluster 5, but showed no strong clinical, epigenetic, or histological association. Notably, patients with both maternal hypertension (PE or CH) and SGA split across all four of these clusters.

Motivated by these findings, in the current chapter, a similar molecular profiling approach was applied to test the hypothesis that subtypes of normotensive FGR placentas also exist, and span the spectrum of placental dysfunction described for PE. To accomplish this, a combined placental SGA-focused microarray dataset was assembled, consisting of placentas from normotensive and hypertensive pregnancies with suspected FGR, in addition to healthy control placentas. This microarray dataset was then subjected to unsupervised clustering, and each cluster was assessed for enriched ontological, clinical, and histological features. This analysis should separate the SGA pregnancies that arose as a result of placentally-mediated growth restriction (FGR) from those that were constitutionally small. Additionally, this unbiased assessment should split the true cases of FGR into etiological subtypes, possibly related to those observed for PE, and may also uncover the patients at the greatest risk of pathology recurrence in subsequent pregnancies.

5.2 Methods

5.2.1 Placenta sample collection

Matched snap-frozen and formalin-fixed, paraffin-embedded (FFPE) placental tissue from 20 normotensive pregnancies with SGA infants (N-SGA) were purchased from the Research Centre for Women's and Infants' Health (RCWIH) BioBank (Mount Sinai Hospital, Toronto, Canada) by Dr. Shannon Bainbridge. SGA was defined as birth weight <10th percentile for gestational age (GA) and sex, based on a Canadian growth reference [169]. All samples came from singleton live births occurring after 34 weeks of gestation, and were flagged by the BioBank as suspected FGR; however, not all of these pregnancies showed robust signs of placental insufficiency (such as abnormal shape/size of the placenta, abnormal umbilical artery blood flow, abnormal uterine artery blood flow, or sonographic signs of placental injury) based on their clinical charts, and two were missing ultrasound values entirely. Therefore, these pregnancies will be referred to as SGA, as this phenotype is confirmed, and will be investigated further for evidence of FGR. Placentas associated with maternal smoking, diabetes (pre-existing or gestational), sickle cell anemia, and/or morbid obesity (BMI $\geq$ 40), and/or clear evidence of a fetal cause of reduced growth (ex. genetic anomaly), were excluded. Additionally, insufficient fetal measurements were

available to determine if these were suspected symmetrical or asymmetrical FGR, but since they appear to be late-onset, the assumption is that they are asymmetrical.

5.2.2 Microarray gene expression assessment

Similar to our prior PE profiling study (Chapter 3), placental sampling for mRNA assessment was performed by the BioBank, such that one biopsy was collected, midway between the umbilical cord insertion and disc periphery, from each quadrant in the placenta. All four biopsies from each placenta were immediately rinsed in PBS, pooled, snap-frozen in liquid nitrogen, and crushed into a powder. mRNA was extracted from the 20 N-SGA snap-frozen tissues using Trizol and RNAeasy spin columns by Dr. Bainbridge's technician Jeremiah Gaudet, as well as from four average-for-gestational-age (AGA) term control placentas previously purchased and utilized in the PE study (Chapter 3) to serve as technical replicates. Extracted mRNA for all 24 placentas were hybridized against Human Gene 1.0 ST Array chips (Affymetrix) by the Princess Margaret Genomics Centre (Toronto, Canada). The generated microarray dataset for the 20 new N-SGA samples is available on the Gene Expression Omnibus (GEO), under the accession number GSE100415.

5.2.3 Dataset aggregation

To investigate relationships between normotensive and hypertensive suspected FGR pregnancies, relevant samples from our prior PE cohort with available matched microarray, histological, and clinical information (Chapters 3 and 4) were also included in the current analysis (N=77). These consisted of samples classified as preeclamptic and SGA (PE-SGA, N=37), chronic hypertensive and SGA (CH-SGA, N=14), or normotensive term AGA controls (N-AGA, N=26). Most of these SGA infants were also flagged as suspected FGR, but in some cases, limited antenatal data was available. At the time of the original sample collection, PE was defined as the onset of systolic pressure ≥140 mmHg and/or diastolic pressure ≥90 mmHg after the 20th week of gestation, accompanied by proteinuria (greater than 300 mg protein/day, or at least 2+ by dipstick) [642]. Chronic hypertension was defined as systolic pressure ≥140 mmHg and/or sustained diastolic ≥90 mmHg before the 20th week of gestation, and SGA was defined as above. Given the previous identification of similar placental gene expression and histological profiles between cases of PE and CH (Chapters 3 and 4), these two phenotypes were frequently analyzed together

as a single hypertensive group (H-SGA; N=51). Microarray data for these original 77 samples is available under the GEO accession number GSE75010.

Using the *oligo* library [690], raw probe level microarray data from both cohorts (the N-SGA cohort (N=24, including the four technical replicate controls) and the previous PE cohort (N=77)) were read into R 3.2.1 and normalized using the *rma* function from *Affy* [614]. Empirical Bayes batch correction and conversion of probe level annotations to human gene symbols were performed using the *virtualArray* package [618]. The four control technical replicates were removed from the combined SGA dataset after confirming they aligned with the original samples on a t-distributed stochastic neighbor embedding (t-SNE) plot [628] following batch correction (**Figure 30**). Genes with a mean expression in the bottom quartile were considered to be indistinguishable from background noise and were, therefore, filtered out. The basis of this decision is described in Chapter 6.

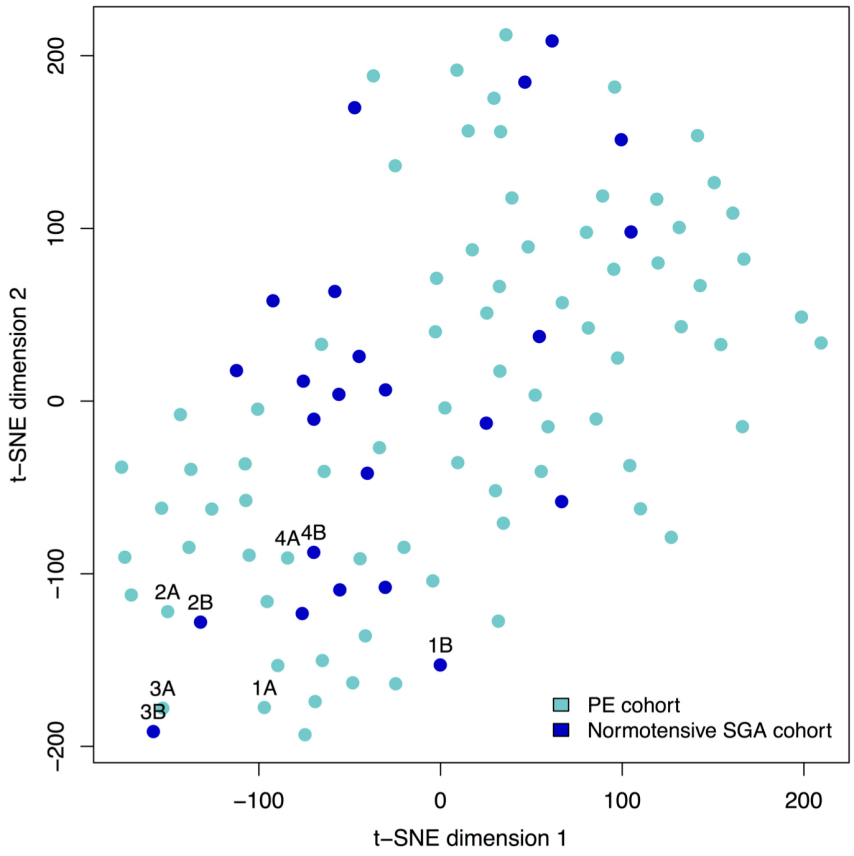

Figure 30 – Visualization of the technical replicates by t-distributed stochastic neighbor embedding (t-SNE). t-SNE was performed on all 101 originally aggregated samples (N = 97 + 4 technical replicates) and the top quartile of variable genes to obtain a two-dimensional representation of the molecular similarities between placentas. As expected, the technical replicates (four healthy term controls from our prior PE-focused cohort (cyan) and the second assessment of these samples as part of our SGA-focused cohort (blue)) plotted beside each other, indicating that batch correction was successful.

5.2.4 Unsupervised clustering and cluster stability

To identify potential subtypes of placental disease in pregnancies with suspected FGR, unsupervised mixture-model based clustering (*mclust*) [691] was applied to the top quartile of most variable genes in the 97 unique placenta samples, as previously described in Chapters 2 and 3. The optimal number of patient clusters was automatically selected based on the Bayesian Information Criterion, and visualized by principal component analysis (PCA), using the *rgl* library. The stability of the clusters was investigated using the *clusterboot* function [666], with 1000 bootstrap resamples of the data and the "noisemclustCBI" cluster method.

5.2.5 Pathway enrichment analysis

To determine the likely underlying biological mechanisms responsible for the gene expression clustering observed, pathway enrichment analysis was performed comparing each of the N-SGA subtypes to the cluster 1 N-AGA controls, and the co-clustering N-SGA and H-SGA placentas within each of the clusters. This was done using all 14,038 possible genes and the *sigpathway* package [633], as this method has been shown to be more statistically robust than the GSEA method employed in the previous chapters based on a literature assessment by our summer student Isaac Gibbs [633, 692, 693]. The Hallmark and GO gene sets (v6.1) were downloaded from the Molecular Signatures Database (MsigDB) [694, 695], and pathways with 10–1000 members were tested with 1000 permutations. Gene sets were considered significant when they achieved a q-value <0.05 for both tested hypotheses (Q1 and Q2).

5.2.6 Histopathological analysis

Matched FFPE tissue and historical placenta pathology reports obtained from the RCWIH BioBank for the 20 N-SGA samples underwent detailed histopathology evaluation, as described in Chapter 4. Briefly, placenta tissue biopsies were collected from each quadrant of the placenta, fixed in formalin, embedded in paraffin wax, and sectioned at a thickness of 5μm. One section per biopsy (four per placenta) was stained with hematoxylin and eosin [684] by Dr. Samantha Benton. Digital images of each slide were examined by Dr. David Grynspan, an experienced placental pathologist, blinded to transcriptional results and clinical information (excluding gestational age at delivery). Placentas were assessed for 30 well-defined pathological features

[385, 393, 394, 404, 685] and scored on a scale of 0-1 (absence/presence), 0-2, or 0-3 (assessing degree of severity) where appropriate.

Individual lesions were each categorized into one of the eight broad pathology categories of biological significance determined by Drs. Benton, Grynspan, and Bainbridge (Chapter 4, **Appendix B**), and then sent to us. Graded scores for the 30 individual placental lesions in the 20 new N-SGA samples were loaded into R, and sums for each category were calculated for each placenta. These scores were then merged with the scores for the 77 placentas obtained from our prior PE cohort (Chapter 4). Kruskal-Wallis rank sum tests were employed to assess histological differences across the three transcriptional clusters (and seven significant subtype groups) in the current study.

5.2.7 Clinical analysis

Similar to the PE cohort study (Chapter 3), more than 50 clinical variables were analyzed as either a continuous numeric or a categorical feature. The initial organization and formatting of the clinical data associated with the 20 new N-SGA patients for analysis in R was done by Isaac Gibbs. In cases where multiple measurements over pregnancy were available per patient (ex. umbilical artery pulsatility indices (PIs)), the mean, maximum, and/or minimum value across gestation was calculated, as appropriate. Only blood pressure measurements within the last four weeks of gestation but prior to the day of delivery were assessed to avoid confounding with labour or cesarean section surgery. Placental weight z-scores were computed based on normal weight charts for male and female infants [667] and measured uterine and umbilical artery PIs were compared to reference ranges for gestational age [480, 481]. Estimated fetal weight percentiles were calculated using the Hadlock standard [148]. Assessed signs of placental insufficiency by ultrasound were uterine artery notching, uterine artery PI above the 95th percentile for gestational age, umbilical artery PI above the 95th percentile for gestational age, abnormal umbilical artery blood flow (absent end-diastolic velocity, reverse end-diastolic velocity, and/or increased resistance), as well as other indications, such as non-concordant placental grading (ex. placental grade III at 35 weeks), placental lakes, echogenic cysts, wedge infarcts, signs of a "wobbly" placenta, and/or abnormal placental size, shape, or texture, some of which have been shown to correlate with specific histological features [150]. Clinical differences

across the clusters and subtypes were performed using Kruskal-Wallis rank sum tests, Fisher's exact tests, and Mann-Whitney-Wilcoxon tests, as appropriate.

5.2.8 Ethics

Ethics approval for this study was granted from the Research Ethics Boards of Mount Sinai Hospital (#13-0211-E), the Ottawa Health Science Network (#2011623-01H), and the University of Toronto (#29435). All women provided written informed consent for the collection of biological specimens and medical information.

5.3 Results

5.3.1 Unsupervised clustering and cluster stability

After successful batch correction (**Figure 30**) and removal of the technical replicates and low expression genes, the final combined SGA dataset for analysis contained 97 samples and 14,038 genes. Unsupervised clustering of these 97 samples based on the expression profiles of the top quartile of most variable genes (N=3,510) identified three placental clusters as the optimal number (VEI model) (**Figure 31a**). Of these, clusters 1 and 2 were highly stable (>80% similarity between the bootstrapped reclusters), while cluster 3 was somewhat less stable (67% similarity; **Figure 31b**). Cluster 1 contained the majority (92%) of the normotensive AGA controls, along with half (10/20) of the N-SGA samples and some of the PE-SGA and CH-SGA placentas (14%) (**Figure 31c, Table 15**). The remaining half of the N-SGA patients split between clusters 2 (7/20; 35%) and 3 (3/20; 15%), co-clustering with the majority of the hypertensive (PE and CH) SGA samples (**Figure 31c, Table 15**). This implies the existence of three molecular N-SGA subtypes, and three hypertensive SGA (H-SGA) subtypes, in this cohort, one in each of clusters 1-3.

Visualization of this transcriptional data by principal component analysis (PCA) revealed that within clusters 2 and 3, the N-SGA samples appear to integrate in well with the rest of the cluster (**Figure 31a,c**). However, within cluster 1, the majority of the N-SGA placentas formed a distinct group, along with the cluster 1 H-SGA samples, at the border of cluster 2, separate from the healthy controls (**Figure 31a,c**).

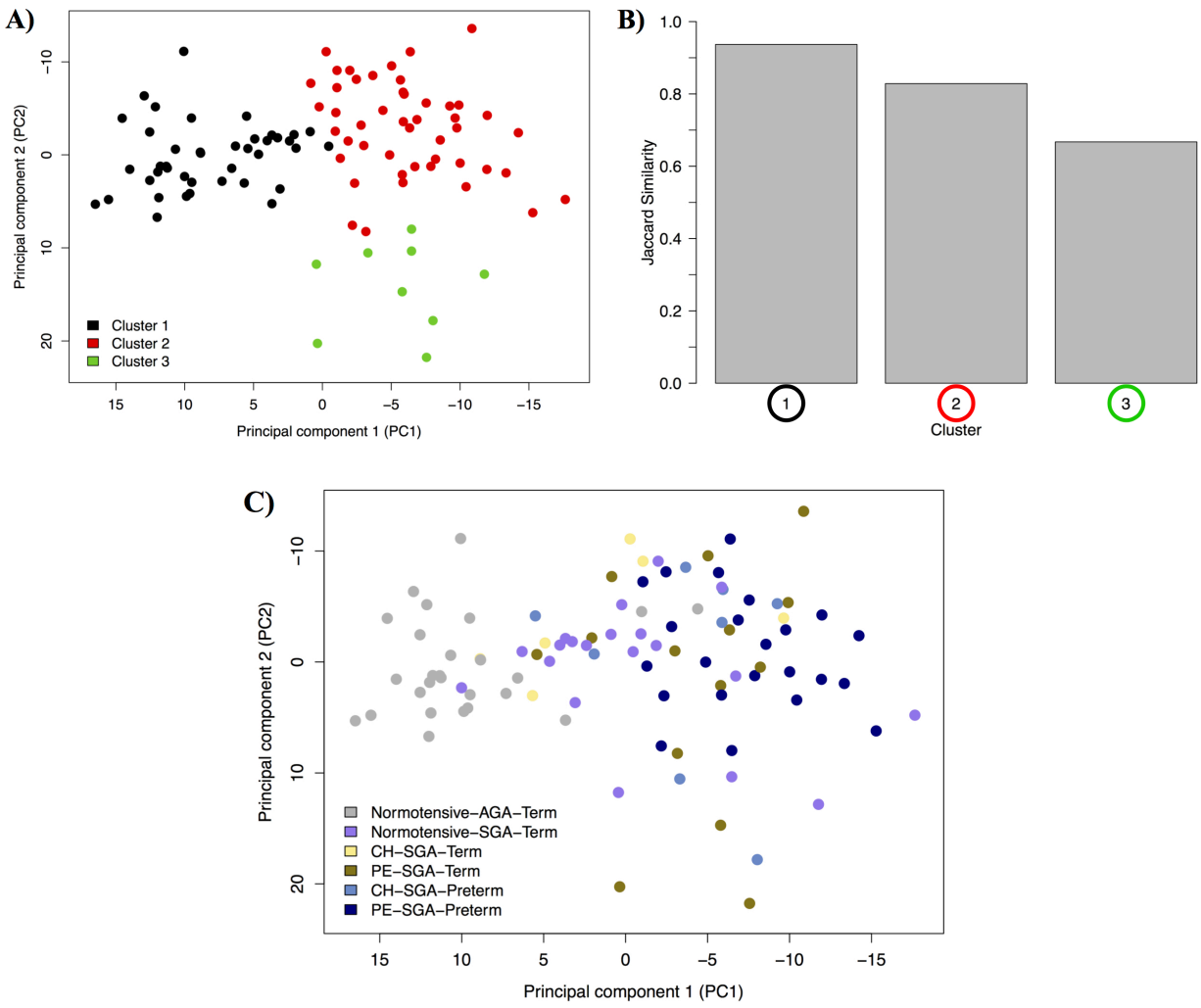

Figure 31 – Principal component analysis (PCA) visualization of the stability and composition of the three patient clusters identified by unsupervised clustering of the placental gene expression. A) Cluster 1 (black) separated from cluster 2 (red) and cluster 3 (green) across principal component 1 (PC1), while cluster 2 and 3 samples showed differences along principal component 2 (PC2). **B**) A barplot of the average Jaccard similarities from the *clusterboot* analysis revealed that all three clusters were relatively stable, although cluster 3 was somewhat less so (<80% similarity between the bootstrapped reclusters). **C**) Normotensive average-for-gestational-age (AGA) term controls (grey) were found to populate the exterior edge of cluster 1. The portion of cluster 1 closest to cluster 2, as well as both clusters 2 and 3, contained a mix of normotensive small-for-gestational-age (SGA) samples (purple), chronic hypertensive (CH) SGA samples (yellow and blue), and preeclamptic (PE) SGA samples (gold and navy). Preterm was defined as a gestational age at delivery before 34 weeks.

Table 15 – Cluster composition by neonatal size and maternal hypertensive state.

Phenotype	Cluster 1	Cluster 2	Cluster 3
Normotensive AGA[a] controls (N = 26)	24 (92%)	2 (8%)	0 (0%)
Normotensive SGA[a] (N = 20)	10 (50%)	7 (35%)	3 (15%)
Hypertensive SGA[a] (N = 51)	7 (14%)	38 (75%)	6 (12%)
CH-SGA[a] (N = 14)	5 (36%)	7 (50%)	2 (14%)
PE-SGA[a] (N = 37)	2 (5%)	31 (84%)	4 (11%)
Total (N = 97)	41 (42%)	47 (48%)	9 (9%)

[a]AGA = average-for-gestational-age; SGA = small-for-gestational-age; CH = chronic hypertensive; PE = preeclamptic

5.3.2 Comparison to prior clusters

For the 77 placentas obtained from our prior PE cohort (Chapter 3), cluster inclusion was compared between the former analysis and the current investigation. Samples previously belonging to clusters 1-3 retained highly similar cluster memberships, while those with prior cluster 5 inclusion predominately collapsed into cluster 2 (**Figure 32**). Samples with cluster disagreement between the two molecular analyses (Chapter 3 and current) plotted on the border of the two possible clusters by PCA (**Figure 32**). Almost all of these patients that switched transcriptional clusters were annotated as transcriptional-histological discordant in Chapter 4, thereby suggesting that these are intermediate phenotype placentas without a clear transcriptional cluster membership.

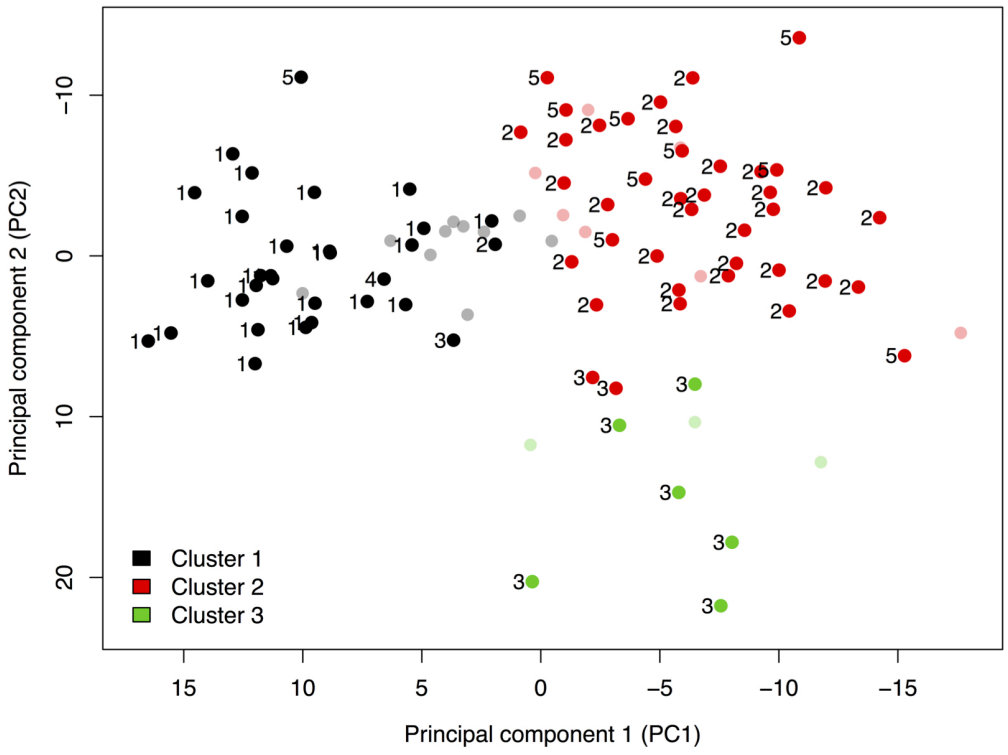

Figure 32 – Cluster inclusion comparison. For the 77 placentas obtained from our prior PE cohort (fully colored/non-transparent), cluster inclusion was compared between the previous analysis (Chapter 3; numbers 1-5 representing clusters 1-5) and the current assessment (colors black, red, and green representing clusters 1-3). Samples previously belonging to clusters 1-3 retained highly similar cluster memberships, while those with prior cluster 5 inclusion predominately collapsed into cluster 2. The 20 new normotensive small-for-gestational-age (N-SGA) samples are shown in semi-transparent colors.

5.3.3 Pathway enrichment analysis

To characterize the underlying molecular differences driving the formation of the three N-SGA placental subtypes, pathway enrichment analysis was performed. Given that almost all of the healthy term control (N-AGA) samples in this study were found together in cluster 1, these placentas were considered to be representative of "normal" gene expression and the N-SGA samples in clusters 1-3 were initially compared to these cluster 1 controls. Understandably, pathway enrichment analysis found only a small number of significant gene sets ($q<0.05$) between the cluster 1 N-SGA and control samples (N=1 Hallmark sets and N=51 GO sets; **Table 16, Appendix C**). The few enriched pathways in the N-SGA samples were associated with carbohydrate metabolism and hypoxia, while the underexpressed gene sets were involved in immune response.

In contrast, many significant pathway differences were observed in the cluster 2 N-SGA (N=5 Hallmark sets and N=219 GO sets) and cluster 3 N-SGA (N=14 Hallmark sets and N=365 GO sets) samples when assessed against the cluster 1 controls. Cluster 2 N-SGA placentas exhibited an upregulation of genes associated with metabolism, hormone activity and secretion, feeding behaviour, and hypoxia, and a depletion of genes involved in immune response and cell proliferation (**Table 17, Appendix C**). Cluster 3 N-SGA samples demonstrated a significant enrichment in immune, inflammatory, cytokine activity, and allograft rejection genes, as well as some hypoxia and apoptosis pathways, and a downregulation of protein metabolism and secretion pathways (**Table 18, Appendix C**).

Furthermore, to determine if there were any biologically meaningful transcriptional differences between the normotensive and hypertensive placentas within a given cluster, the N-SGA and H-SGA samples in each cluster were also compared by pathway enrichment analysis. Within clusters 1 and 2, almost no significant gene sets were identified between the normotensive and hypertensive SGA samples. However, in cluster 3, a few significant pathways were discovered (N=0 Hallmark sets and N=6 GO sets), with the N-SGA placentas exhibiting an overexpression of gene sets involved in epigenetic functions, such as demethylation, chromatin organization, and transcription factor activity (**Table 19**).

Table 16 – Significant (q<0.05) Hallmark pathway for the cluster 1 normotensive SGA samples compared to the cluster 1 controls.

Pathway	Set Size	NTk Stat	NTk q-value	NTk Rank	NEk Stat	NEk q-value	NEk Rank
HALLMARK HYPOXIA	179	8.41	0.00	1	3.28	0.00	1

Table 17 – Significant (q<0.05) Hallmark pathways for the cluster 2 normotensive SGA samples compared to the cluster 1 controls.

Pathway	Set Size	NTk Stat	NTk q-value	NTk Rank	NEk Stat	NEk q-value	NEk Rank
HALLMARK HYPOXIA	179	7.16	0.00	1	3.09	0.02	2
HALLMARK UV RESPONSE DN	134	-4.77	0.00	3	-3.08	0.01	4
HALLMARK KRAS SIGNALING UP	150	-3.42	0.00	5	-3.09	0.02	2
HALLMARK MITOTIC SPINDLE	186	-4.14	0.00	4	-2.65	0.03	6
HALLMARK GLYCOLYSIS	171	3.26	0.00	6	2.75	0.03	5

Table 18 – Significant (q<0.05) Hallmark pathways for the cluster 3 normotensive SGA samples compared to the cluster 1 controls.

Pathway	Set Size	NTk Stat	NTk q-value	NTk Rank	NEk Stat	NEk q-value	NEk Rank
HALLMARK INTERFERON GAMMA RESPONSE	169	16.25	0.00	1	5.22	0.00	2
HALLMARK INTERFERON ALPHA RESPONSE	81	13.86	0.00	2	5.89	0.00	1
HALLMARK INFLAMMATORY RESPONSE	156	11.65	0.00	3	5.09	0.00	3
HALLMARK TNFA SIGNALING VIA NFKB	168	11.31	0.00	4	4.03	0.00	7
HALLMARK ALLOGRAFT REJECTION	138	10.61	0.00	5	4.42	0.00	6
HALLMARK COMPLEMENT	159	8.89	0.00	7	4.91	0.00	4
HALLMARK IL6 JAK STAT3 SIGNALING	70	7.42	0.00	8	4.66	0.00	5
HALLMARK HYPOXIA	179	10.34	0.00	6	3.09	0.00	11.5
HALLMARK P53 PATHWAY	176	6.15	0.00	9	3.3	0.00	9
HALLMARK COAGULATION	97	5.25	0.00	10	3.18	0.00	10
HALLMARK CHOLESTEROL HOMEOSTASIS	64	4.95	0.00	12	3.85	0.00	8
HALLMARK GLYCOLYSIS	171	5.06	0.00	11	3.09	0.00	11.5
HALLMARK APOPTOSIS	132	4.13	0.00	14	2.88	0.01	13
HALLMARK IL2 STAT5 SIGNALING	170	4.11	0.00	15	2.41	0.04	14

Table 19 – Significant (q<0.05) GO pathways for the cluster 3 normotensive SGA samples compared to the cluster 3 hypertensive SGA samples.

Pathway	Set Size	NTk Stat	NTk q-value	NTk Rank	NEk Stat	NEk q-value	NEk Rank
DEMETHYLATION	42	3.72	0.00	53	2.74	0.00	3
REGULATION OF CHROMATIN ORGANIZATION	130	3.40	0.00	83	2.56	0.00	10
TRANSCRIPTION FACTOR ACTIVITY PROTEIN BINDING	495	3.44	0.00	80	2.31	0.00	33
DIOXYGENASE ACTIVITY	65	3.09	0.05	137	2.60	0.00	6
NEGATIVE REGULATION OF ERK1 AND ERK2 CASCADE	41	3.09	0.05	137	2.59	0.00	8
POSITIVE REGULATION OF POTASSIUM ION TRANSMEMBRANE TRANSPORTER ACTIVITY	12	3.09	0.05	137	2.38	0.00	21

5.3.4 Histopathological analysis

The three N-SGA subtypes were next investigated for differences in their histopathological profiles compared to the controls, each other, and their co-clustering H-SGA placentas. Overall, the cluster 1 N-SGA samples demonstrated the least histopathology, with almost identical cumulative severity scores to the cluster 1 N-AGA controls (1.80 versus 1.83, p=0.94) (**Table 20**). However, the types of lesions observed were different: the cluster 1 controls showed some signs of delayed villous maturity, intervillous thrombi, villitis of unknown etiology (VUE), and/or meconium histiocytes, covering a range of different categories of biological significance (as observed in Chapter 4), whereas the few lesions observed in the cluster 1 N-SGA placentas were associated with maternal vascular malperfusion (MVM) pathology, such as syncytial knots and advanced villous maturity (AVM) (MVM sum 1.70 in the N-SGA placentas versus 0.50 in the controls, p=0.01) (**Table 20**). Included in these two phenotype groups were the ten placentas in this cohort (seven cluster 1 controls and three cluster 1 N-SGA samples) with no observed histological lesions. The H-SGA samples belonging to cluster 1 also showed MVM features almost exclusively, although to a somewhat more severe degree than the normotensive placentas (3.29 versus 1.70, p=0.05) (**Table 20**).

In cluster 2, both the N-SGA and H-SGA samples exhibited some thrombosis and intervillous thrombi lesions; however, once again, the majority of the observed histopathology in this cluster consisted of maternal vascular malperfusion features (**Table 20**). Further, the cluster 2 H-SGA placentas revealed the highest MVM score sums in the entire cohort (4.87), with the cluster 2 N-SGA samples in second (3.43) ($p<0.01$ across the cohort, $p=0.15$ to each other) (**Table 20**). Cluster 3 samples uniquely demonstrated increased frequency and severity of histopathology lesions consistent with a maternal-fetal interface disturbance ($p=0.01$), such as massive perivillous fibrin deposition ($p<0.01$), as well as evidence of chronic inflammation ($p=0.05$), such as chronic intervillositis ($p=0.03$) (**Table 20**). Additionally, both the N-SGA and H-SGA placentas in cluster 3 showed signs of maternal vascular malperfusion lesions, although the MVM pathology was again moderately more severe in the H-SGA samples (3.33 versus 1.00, $p=0.05$) (**Table 20**).

Table 20 – Histopathological comparison across the subtype groups.

	Cluster 1 N-AGA[a] N=24	**Cluster 1 N-SGA[a] N=10**	**Cluster 1 H-SGA[a] N=7**	**Cluster 2 N-SGA[a] N=7**	**Cluster 2 H-SGA[a] N=38**	**Cluster 3 N-SGA[a] N=3**	**Cluster 3 H-SGA[a] N=6**	
Histopathology lesion (N=number of samples with a non-zero score)	**Mean (SD)**							**P-value[b]**
Maternal vascular malperfusion lesions								
Distal villous hypoplasia (N=46)	0 (0)	0.30 (0.48)	1.14 (0.69)	0.57 (0.79)	1.29 (0.77)	0 (0)	0.50 (0.55)	<0.01
Placental infarctions (N=40)	0.12 (0.34)	0.30 (0.48)	0.29 (0.49)	0.57 (0.79)	1.03 (0.79)	0 (0)	0.33 (0.52)	<0.01
Advanced villous maturity (N=51)	0.04 (0.20)	0.40 (0.52)	0.71 (0.49)	0.71 (0.49)	0.84 (0.37)	0.33 (0.58)	0.50 (0.55)	<0.01
Syncytial knots (N=59)	0.21 (0.41)	0.50 (0.53)	1.00 (0.58)	0.71 (0.49)	1.18 (0.65)	0.33 (0.58)	0.83 (0.75)	<0.01
Focal perivillous fibrin (N=23)	0.12 (0.34)	0.10 (0.32)	0 (0)	0.29 (0.49)	0.34 (0.48)	0.33 (0.58)	0.83 (0.98)	0.10
Villous agglutination (N=3)	0 (0)	0 (0)	0 (0)	0.43 (0.79)	0.03 (0.16)	0 (0)	0 (0)	0.01
Decidual vasculopathy (N=11)	0 (0)	0.10 (0.32)	0.14 (0.38)	0.14 (0.38)	0.16 (0.37)	0 (0)	0.33 (0.52)	0.32
Category sum (N=75)	**0.50 (0.66)**	**1.70 (1.42)**	**3.29 (1.38)**	**3.43 (2.51)**	**4.87 (2.00)**	**1.00 (1.00)**	**3.33 (1.21)**	**<0.01**
Implantation site abnormalities lesions								
Microscopic accreta (N=1)	0 (0)	0 (0)	0 (0)	0.14 (0.38)	0 (0)	0 (0)	0 (0)	0.05
Increased basement membrane fibrin (N=0)	0 (0)	0 (0)	0 (0)	0 (0)	0 (0)	0 (0)	0 (0)	--
Category sum (N=1)	**0 (0)**	**0 (0)**	**0 (0)**	**0.14 (0.38)**	**0 (0)**	**0 (0)**	**0 (0)**	**0.05**
Histological chorioamnionitis lesions								
Maternal inflammation (N=0)	0 (0)	0 (0)	0 (0)	0 (0)	0 (0)	0 (0)	0 (0)	--
Fetal inflammation (N=0)	0 (0)	0 (0)	0 (0)	0 (0)	0 (0)	0 (0)	0 (0)	--
Vessel thrombosis (N=0)	0 (0)	0 (0)	0 (0)	0 (0)	0 (0)	0 (0)	0 (0)	--
Category sum (N=0)	**0 (0)**	**0 (0)**	**0 (0)**	**0 (0)**	**0 (0)**	**0 (0)**	**0 (0)**	**--**
Placenta villous maldevelopment lesions								
Chorangiosis (N=2)	0.08 (0.28)	0 (0)	0 (0)	0 (0)	0 (0)	0 (0)	0 (0)	0.43
Chorangiomas (N=2)	0 (0)	0 (0)	0 (0)	0 (0)	0.03 (0.16)	0.33 (0.58)	0 (0)	0.02
Delayed villous maturity (N=12)	0.29 (0.46)	0 (0)	0 (0)	0 (0)	0.05 (0.23)	0 (0)	0.50 (0.55)	<0.01
Category sum (N=15)	**0.38 (0.58)**	**0 (0)**	**0 (0)**	**0 (0)**	**0.08 (0.27)**	**0.33 (0.58)**	**0.50 (0.55)**	**0.01**

Fetal vascular malperfusion lesions								
Avascular fibrotic villi (N=2)	0 (0)	0 (0)	0 (0)	0 (0)	0.03 (0.16)	0 (0)	0.17 (0.41)	0.30
Thrombosis (N=7)	0.04 (0.20)	0 (0)	0 (0)	0.14 (0.38)	0.11 (0.31)	0 (0)	0.17 (0.41)	0.71
Intramural fibrin deposition (N=0)	0 (0)	0 (0)	0 (0)	0 (0)	0 (0)	0 (0)	0 (0)	--
Category sum (N=9)	**0.04 (0.20)**	**0 (0)**	**0 (0)**	**0.14 (0.38)**	**0.13 (0.34)**	**0 (0)**	**0.33 (0.52)**	**0.27**
Chronic utero-placental separation lesions								
Chorionic hemosiderosis (N=2)	0.04 (0.20)	0 (0)	0 (0)	0.14 (0.38)	0 (0)	0 (0)	0 (0)	0.34
Retroplacental hematoma (N=5)	0.04 (0.20)	0 (0)	0 (0)	0 (0)	0.08 (0.27)	0 (0)	0.17 (0.41)	0.73
Laminar necrosis (N=0)	0 (0)	0 (0)	0 (0)	0 (0)	0 (0)	0 (0)	0 (0)	--
Category sum (N=7)	**0.08 (0.28)**	**0 (0)**	**0 (0)**	**0.14 (0.38)**	**0.08 (0.27)**	**0 (0)**	**0.17 (0.41)**	**0.83**
Maternal-fetal interface disturbance lesions								
Massive perivillous fibrin deposition (N=5)	0 (0)	0 (0)	0 (0)	0 (0)	0.03 (0.16)	0.33 (0.58)	0.50 (0.55)	<0.01
Maternal floor infarction pattern (N=1)	0 (0)	0 (0)	0 (0)	0 (0)	0 (0)	0 (0)	0.17 (0.41)	0.02
Intervillous thrombi (N=19)	0.25 (0.44)	0 (0)	0.14 (0.38)	0.29 (0.49)	0.16 (0.37)	0.67 (0.58)	0.50 (0.84)	0.20
Category sum (N=21)	**0.25 (0.44)**	**0 (0)**	**0.14 (0.38)**	**0.29 (0.49)**	**0.18 (0.46)**	**1.00 (1.00)**	**1.17 (1.17)**	**0.01**
Chronic inflammation lesions								
Infectious villitis (N=0)	0 (0)	0 (0)	0 (0)	0 (0)	0 (0)	0 (0)	0 (0)	--
Villitis of unknown etiology (N=8)	0.21 (0.59)	0 (0)	0.29 (0.76)	0 (0)	0.05 (0.23)	0.67 (1.15)	0.33 (0.82)	0.40
Chronic intervillositis (N=3)	0 (0)	0 (0)	0 (0)	0 (0)	0.03 (0.16)	0.67 (1.15)	0.17 (0.41)	0.03
Chronic deciduitis (N=10)	0.08 (0.28)	0.10 (0.32)	0.14 (0.38)	0.14 (0.38)	0.05 (0.23)	0.33 (0.58)	0.33 (0.52)	0.38
Category sum (N=16)	**0.29 (0.81)**	**0.10 (0.32)**	**0.43 (0.79)**	**0.14 (0.38)**	**0.13 (0.41)**	**1.67 (2.08)**	**0.83 (1.17)**	**0.05**
Additional features								
Meconium histiocytes/macrophages within membranes (N=9)	0.29 (0.46)	0 (0)	0 (0)	0 (0)	0.03 (0.16)	0 (0)	0.17 (0.41)	0.01
Meconium-induced myonecrosis (N=1)	0 (0)	0 (0)	0 (0)	0 (0)	0.03 (0.16)	0 (0)	0 (0)	0.96
Cumulative Pathology Score								
Overall sum (N=85)	**1.83 (1.61)**	**1.80 (1.40)**	**3.86 (0.9)**	**4.29 (2.36)**	**5.53 (2.19)**	**4.00 (1.00)**	**6.50 (1.64)**	**<0.01**

[a]N = normotensive; H = hypertensive; AGA = average-for-gestational-age; SGA = small-for-gestational-age

[b]Based on non-parametric Kruskal-Wallis rank sum tests

5.3.5 Clinical characteristics

To determine if the three N-SGA placental subtypes were associated with different clinical presentations and/or outcomes, the clinical features of each of these groups were compared to each other, the cluster 1 controls, and the H-SGA samples. In general, the cluster 1 N-SGA patients appeared the healthiest of the N-SGA subtypes, with the least reduced birth weights (p=0.29 across the N-SGA subtypes), the latest gestational ages at delivery (p=0.14), and the most efficient placentas (p=0.19) (**Table 21, Table 22**). Of the nine (out of ten) pregnancies with available ultrasound data in this N-SGA subtype, 78% (7/9) demonstrated at least one ultrasound indication of placental insufficiency during pregnancy, although none of these were associated

with abnormal uterine artery blood flow to the placenta (ex. high uterine artery PI or notching) (**Table 22**). In contrast, cluster 2 and 3 N-SGA patients exhibited more severe clinical outcomes. These infants were delivered slightly earlier ($p=0.14$ across the N-SGA subtypes), and were associated with higher maximum uterine and umbilical pulsatility indices ($p=0.05$-0.09 across the N-SGA subtypes) (**Table 21**). Uterine artery notching was most commonly observed in cluster 2 N-SGA ($p=0.07$ across the N-SGA subtypes), while cluster 3 N-SGA patients exhibited peripherally inserted umbilical cords ($p=0.07$ across the N-SGA subtypes), and were most likely to have experienced a previous stillbirth ($p=0.17$ across the N-SGA subtypes) (**Table 21, Table 22**). Fitting with the prior findings in Chapter 3, two out of three of the cluster 3 N-SGA patients had experienced a miscarriage; however, in contradiction to the Chapter 3 results, these women were different blood types (**Table 21, Table 22**). Additionally, although still within normal range, the cluster 3 N-SGA patients exhibited borderline hypertensive maximum systolic blood pressures measurements later in pregnancy (135 mmHg versus 114 mmHg in the cluster 1 N-AGA controls, $p=0.02$) (**Table 21**). All N-SGA subjects with placentas belonging to clusters 2 and 3 and available ultrasound data (9/10) demonstrated clear evidence of placental insufficiency during pregnancy (**Table 22**).

Lastly, a number of clinical attributes were found to be significantly different between all three N-SGA subtypes compared to their hypertensive counterparts. Across the cohort, the N-SGA group demonstrated lower mean uterine artery PIs ($p<0.01$), lower mean umbilical artery PIs ($p<0.01$), fewer cesarean section deliveries ($p<0.01$), later gestational ages at delivery ($p<0.01$), healthier placental weight z-scores ($p=0.06$), higher 1 minute and 5 minute Apgar scores ($p<0.01$ and $p=0.04$, respectively), and lower rates of infant transfer to the NICU ($p=0.06$) compared to the H-SGA group (**Table 21, Table 22**). Furthermore, none of the N-SGA women had experienced a prior hypertensive pregnancy, in contrast to 58% of the possible (i.e. primiparous and multiparous) H-SGA patients ($p<0.01$; **Table 22**).

Table 21 – Continuous clinical characteristics across the subtype groups.

	Cluster 1 N-AGA[a] N=24	Cluster 1 N-SGA[a] N=10	Cluster 1 H-SGA[a] N=7	Cluster 2 N-SGA[a] N=7	Cluster 2 H-SGA[a] N=38	Cluster 3 N-SGA[a] N=3	Cluster 3 H-SGA[a] N=6	
Clinical Attribute	**Mean (SD)[b]**							**P-value[c]**
Parental demographics								
Maternal age (years)	32.8 (5.4)	31.3 (3.0)	33.6 (3.2)	35.3 (4.3)	34.0 (5.2)	33.3 (4.9)	37.7 (4.2)	0.15
Maternal BMI (kg/m^2)	25.3 (5.5)	23.5 (7.4)	25.2 (5.2)	25.2 (4.7)	25.6 (4.4)	--	26.9 (4.0)	0.53
Maternal height (cm)	163 (7)	161 (9)	160 (7)	167 (10)	163 (7)	160 (7)	159 (5)	0.63
Ultrasound data								
Mean uterine artery PI[d]	--	0.88 (0.11)	1.91 (0.23)	1.25 (0.46)	1.81 (0.43)	1.23 (0.36)	1.62 (0.57)	<0.01
Max uterine artery PI[d]	--	0.88 (0.11)	2.59 (0.54)	1.35 (0.42)	2.21 (0.55)	1.50 (0.62)	2.07 (0.70)	<0.01
Mean umbilical artery PI[d]	0.98 (0.08)	1.10 (0.15)	1.76 (0.65)	1.36 (0.35)	1.67 (0.40)	1.28 (0.07)	1.44 (0.32)	<0.01
Max umbilical artery PI[d]	1.07 (0.12)	1.26 (0.25)	1.94 (0.7)	1.57 (0.27)	1.83 (0.44)	1.63 (0.12)	1.63 (0.28)	<0.01
Last EFW[d] (percentile)[e]	50 (16)	3 (2)	14 (18)	5 (8)	1 (1)	3 (4)	1 (1)	< 0.01
Evidence of preeclampsia/hypertension								
Mean systolic blood pressure (mmHg)[e]	113 (12)	110 (16)	150 (11)	117 (11)	152 (20)	122 (20)	150 (18)	<0.01
Max systolic blood pressure (mmHg)[e]	114 (13)	122 (12)	163 (13)	123 (15)	165 (23)	135 (9)	160 (20)	<0.01
Mean diastolic blood pressure (mmHg)[e]	70 (9)	70 (9)	96 (10)	75 (9)	97 (13)	73 (8)	93 (7)	<0.01
Max diastolic blood pressure (mmHg)[e]	70 (9)	74 (12)	103 (9)	78 (11)	105 (14)	77 (11)	97 (7)	<0.01
Max proteinuria level (dipstick)[e]	+0.5 (0.6)	--	+1.2 (1.0)	--	+2.5 (1.4)	--	+1.7 (1.8)	<0.01
Fetal demographics								
Gestational age at delivery (weeks)	39 (1)	38 (1)	35 (4)	36 (1)	32 (3)	37 (1)	33 (4)	<0.01
Newborn weight z-score	0.27 (0.97)	-1.78 (0.29)	-1.73 (0.42)	-2.09 (0.66)	-1.87 (0.51)	-1.99 (0.55)	-1.89 (0.51)	<0.01
1 minute Apgar score (/10)	8.8 (0.4)	8.8 (0.4)	8.5 (0.5)	8.8 (0.4)	7.0 (2.0)	9.0 (0.0)	7.6 (1.5)	<0.01
5 minutes Apgar score (/10)	9.0 (0.0)	9.0 (0.0)	9.0 (0.0)	9.0 (0.0)	8.6 (0.8)	9.0 (0.0)	8.8 (0.4)	0.06
Placental and umbilical cord data								
Placental weight z-score	-0.04 (0.87)	-1.41 (0.58)	-1.74 (0.72)	-1.34 (0.58)	-1.61 (0.62)	-1.09 (1.28)	-1.73 (0.73)	<0.01
Placental thickness (cm)	2.91 (0.66)	2.72 (0.96)	2.17 (0.56)	2.71 (0.72)	2.25 (1.10)	2.53 (0.06)	1.90 (0.72)	<0.01
Placental asymmetry (ratio)	0.10 (0.05)	0.10 (0.06)	0.14 (0.12)	0.10 (0.07)	0.18 (0.12)	0.14 (0.13)	0.14 (0.08)	0.20
Placental efficiency (ratio)	5.34 (0.67)	5.49 (0.80)	5.45 (1.04)	4.60 (0.75)	4.49 (1.01)	4.70 (2.15)	4.70 (1.11)	0.01
Cord insertion distance from margin to longest placental dimension (ratio)	0.25 (0.08)	0.28 (0.08)	0.22 (0.05)	0.26 (0.12)	0.22 (0.09)	0.10 (0.08)	0.19 (0.09)	0.12
Cord diameter (cm)	1.29 (0.19)	1.68 (1.75)	1.00 (0.20)	1.33 (0.60)	1.04 (0.39)	1.07 (0.06)	0.85 (0.21)	0.02

[a]N = normotensive; H = hypertensive; AGA = average-for-gestational-age; SGA = small-for-gestational-age
[b]Only noted and used if values were available for at least two samples in the cluster
[c]Based on non-parametric Kruskal-Wallis rank sum tests
[d]PI = pulsatility index; EFW = estimated fetal weight
[e]Within the last four weeks of pregnancy

Table 22 – Categorical clinical characteristics across the subtype groups.

	Cluster 1 N-AGA[a] N=24	Cluster 1 N-SGA[a] N=10	Cluster 1 H-SGA[a] N=7	Cluster 2 N-SGA[a] N=7	Cluster 2 H-SGA[a] N=38	Cluster 3 N-SGA[a] N=3	Cluster 3 H-SGA[a] N=6	
Clinical Attribute	**Percentage of Group (n/N)[b]**							**P-value[c]**
Parental demographics								
Nulliparous	33 (8/24)	30 (3/10)	43 (3/7)	57 (4/7)	61 (23/38)	33 (1/3)	33 (2/6)	0.34
Previous miscarriage	29 (7/24)	30 (3/10)	29 (2/7)	29 (2/7)	29 (11/38)	67 (2/3)	33 (2/6)	0.93
Previous termination	17 (4/24)	20 (2/10)	14 (1/7)	0 (0/7)	18 (7/38)	33 (1/3)	33 (2/6)	0.75
Previous hypertensive pregnancy	7 (1/14)	0 (0/7)	50 (2/4)	0 (0/2)	64 (7/11)	0 (0/2)	50 (2/4)	0.01
Previous SGA[a] pregnancy	7 (1/14)	43 (3/7)	75 (3/4)	0 (0/2)	18 (2/11)	100 (2/2)	50 (2/4)	0.01
Previous stillbirth	0 (0/14)	0 (0/7)	25 (1/4)	0 (0/3)	9 (1/11)	50 (1/2)	25 (1/4)	0.09
Maternal ethnicity								0.04
Caucasian	65 (15/23)	50 (5/10)	57 (4/7)	100 (7/7)	53 (20/38)	50 (1/2)	17 (1/6)	--
Black	0 (0/23)	20 (2/10)	43 (3/7)	0 (0/7)	16 (6/38)	50 (1/2)	33 (2/6)	
Asian	30 (7/23)	10 (1/10)	0 (0/7)	0 (0/7)	24 (9/38)	0 (0/2)	33 (2/6)	
East Indian	0 (0/23)	20 (2/10)	0 (0/7)	0 (0/7)	3 (1/38)	0 (0/2)	17 (1/6)	
Maternal blood type								0.46
A	25 (6/24)	11 (1/9)	29 (2/7)	57 (4/7)	29 (11/38)	33 (1/3)	50 (3/6)	--
B	42 (10/24)	33 (3/9)	29 (2/7)	0 (0/7)	16 (6/38)	33 (1/3)	33 (2/6)	
O	29 (7/24)	56 (5/9)	29 (2/7)	43 (3/7)	50 (19/38)	33 (1/3)	17 (1/6)	
AB	4 (1/24)	0 (0/9)	14 (1/7)	0 (0/7)	5 (2/38)	0 (0/3)	0 (0/6)	
Rh positive	83 (20/24)	78 (7/9)	100 (7/7)	100 (7/7)	95 (35/37)	100 (3/3)	83 (5/6)	0.39
Evidence of placental insufficiency[d]								
Uterine artery notching	0 (0/1)	0 (0/4)	67 (2/3)	80 (4/5)	90 (19/21)	33 (1/3)	60 (3/5)	<0.01
Uterine artery PI[e] above the 95th percentile for gestational age	0 (0/1)	0 (0/5)	100 (3/3)	80 (4/5)	100 (21/21)	67 (2/3)	80 (4/5)	<0.01
Umbilical artery PI[e] above the 95th percentile for gestational age	0 (0/6)	75 (6/8)	100 (5/5)	83 (5/6)	83 (25/30)	100 (3/3)	100 (6/6)	<0.01
Abnormal umbilical artery blood flow[f]	0 (0/6)	29 (2/7)	60 (3/5)	67 (4/6)	84 (27/32)	67 (2/3)	50 (3/6)	<0.01
Other signs of placental insufficiency on ultrasound[g]	33 (1/3)	56 (5/9)	60 (3/5)	60 (3/5)	37 (10/27)	67 (2/3)	40 (2/5)	0.83
At least one of the above	17 (1/6)	78 (7/9)	83 (5/6)	100 (6/6)	94 (31/33)	100 (3/3)	100 (6/6)	<0.01
At least two of the above	0 (0/6)	44 (4/9)	83 (5/6)	100 (6/6)	82 (27/33)	100 (3/3)	67 (4/6)	<0.01
Diagnoses								
Chronic hypertension	0 (0/24)	0 (0/10)	71 (5/7)	0 (0/7)	37 (14/38)	0 (0/3)	50 (3/6)	<0.01
Preeclampsia diagnosis	0 (0/24)	0 (0/10)	29 (2/7)	0 (0/7)	82 (31/38)	0 (0/3)	67 (4/6)	<0.01
HELLP diagnosis	0 (0/24)	0 (0/10)	0 (0/7)	0 (0/7)	16 (6/38)	0 (0/3)	0 (0/6)	0.28
Labor and delivery								
Spontaneous labor	62 (5/8)	0 (0/6)	0 (0/2)	50 (2/4)	10 (1/10)	0 (0/2)	--	0.04
Attempted vaginal delivery	38 (9/24)	60 (6/10)	29 (2/7)	57 (4/7)	26 (10/38)	67 (2/3)	0 (0/6)	0.1
Vaginal delivery	29 (7/24)	60 (6/10)	14 (1/7)	57 (4/7)	13 (5/38)	67 (2/3)	0 (0/6)	<0.01
Delivery <34 weeks	0 (0/24)	0 (0/10)	29 (2/7)	0 (0/7)	68 (26/38)	0 (0/3)	50 (3/6)	<0.01
Delivery <37 weeks	8 (2/24)	20 (2/10)	71 (5/7)	43 (3/7)	89 (34/38)	67 (2/3)	100 (6/6)	<0.01
Fetal demographics								
Male fetus	58 (14/24)	40 (4/10)	43 (3/7)	43 (3/7)	55 (21/38)	33 (1/3)	17 (1/6)	0.61
Birth weight <5th percentile for gestational age and sex	0 (0/24)	60 (6/10)	29 (2/7)	83 (5/6)	55 (21/38)	100 (3/3)	83 (5/6)	<0.01
Birth weight <3rd percentile for gestational age and sex	0 (0/24)	30 (3/10)	29 (2/7)	67 (4/6)	42 (16/38)	33 (1/3)	67 (4/6)	<0.01
5 minute Apgar score <7	0 (0/22)	0 (0/10)	0 (0/6)	0 (0/6)	6 (2/33)	0 (0/2)	0 (0/5)	0.79
NICU transfer	0 (0/24)	10 (1/10)	43 (3/7)	29 (2/7)	42 (16/38)	33 (1/3)	67 (4/6)	<0.01

[a]N = normotensive; H = hypertensive; AGA = average-for-gestational-age; SGA = small-for-gestational-age

[b]All available data was utilized within these seven subtype groups, however, information was missing for some samples for some characteristics
[c]Based on Fisher's exact tests
[d]Ultrasound measurement across all of pregnancy were included
[e]PI = pulsatility index
[f]Such as absent end-diastolic velocity, reverse end-diastolic velocity, and/or increased resistance
[g]Descriptions of non-concordant placental grading, placental lakes, echogenic cysts, wedge infarcts, a "wobbly" placenta, and/or abnormal placental size, shape, or texture

5.4 Discussion

The concept that FGR is a multifactorial, heterogeneous disease has been around for decades [150, 387, 688]. Despite this, previous attempts to characterize the underlying pathophysiology of this disorder have generally focused on the binary comparison of a small infant/fetus group to a healthy control group of patients. In this chapter, we have instead assessed placental gene expression using unsupervised clustering methods, and have revealed three transcriptional clusters, each containing placentas from both normotensive and hypertensive pregnancies with confirmed SGA and suspected FGR. Overall, cluster 1 patients were the healthiest in this cohort, with the least severe clinical outcomes and the lowest placental histopathology scores; cluster 2 was affiliated with an enrichment in metabolic and hormone secretion genes, along with considerable evidence of hypoxia-related maternal vascular malperfusion; and cluster 3 samples demonstrated overwhelming transcriptional and histological indications of an immunological response. These findings are highly consistent with the previous descriptions of clusters 1-3 in our prior preeclampsia-focused cohort (Chapters 2-4), which is not surprising given that the majority of the current samples (77/97) were obtained from this established PE dataset and have distributed similarly in the present chapter. However, what is novel about the current investigation is that the new normotensive suspected FGR samples (purchased on the basis of their clinical outcome similarity) fell into all three of these clusters, implying the existence of at least three subtypes of N-SGA samples even within this small sample set of 20 placentas. Furthermore, these new suspected FGR samples did not form any unique groups, thereby confirming the considerable placental similarity between N-SGA and H-SGA patients [556, 689].

Placentas belonging to the first normotensive suspected FGR subtype in cluster 1 (10/20 N-SGA patients, 50%) demonstrated gene expression patterns between the healthy term controls and the cluster 2 samples, with either no histopathology or lesions indicative of mild maternal vascular malperfusion. These patients are perhaps the most difficult to manage clinically, with some demonstrating obvious signs of placental insufficiency on ultrasound examination, while others are inconsistent, resulting in no abnormal ultrasound data within the clinical files obtained from the BioBank. We propose that this group may contain both constitutionally small infants and infants that were somewhat growth restricted *in utero* due to placental insufficiency. It is also possible that some of these patients could be associated with an unknown fetal cause of growth restriction [116, 696], although these three possibilities are not readily distinguishable with the currently available information. However, we also suggest that these cluster 1 N-SGA patients are likely the least essential to correctly classify, as they are associated with the healthiest clinical outcomes.

In contrast, the second and third placental N-SGA subtypes, in clusters 2 and 3, respectively, were linked to more severe clinical features, such as earlier deliveries. These samples show clear signs of placental pathology, both transcriptionally and histologically, and exhibit consistent evidence of placental insufficiency by ultrasound. Additionally, some of these patients experienced mild increases in maternal blood pressure during pregnancy, which has been linked to reduced fetal growth even in normotensive women [697], and is further supported by the knowledge that normotensive FGR pregnancies can still be associated with some maternal subclinical vascular alterations [563]. Overall, we believe that clusters 2 and 3 identify two subtypes of pathological growth restriction: “canonical/hypoxic” FGR and “immunological” FGR. Cluster 2 “canonical” FGR (7/20 N-SGA patients, 35%) is characterized by poor uterine artery blood flow and substantial maternal vascular malperfusion lesions (ex. distal villous hypoplasia, advanced villous maturity, and syncytial knots), while cluster 3 “immunological” FGR (3/20 N-SGA patients, 15%) is linked to maternal-fetal interface disturbance lesions (ex. massive perivillous fibrin deposition and intervillous thrombi) and features of chronic inflammation (ex. VUE and chronic intervillositis). These FGR subtypes would, in all probability, present similarly during pregnancy, excluding some potentially relevant differences in uterine artery blood flow [488], and may be those most accurately identified by markers such as placental growth factor (PlGF) early in gestation [411, 454]. It is, however, critical that they

are distinguished during pregnancy, as these two groups would likely benefit from different therapeutic approaches [150, 549], as well as after delivery, as the immune-related cluster 3 pathology is known to have much higher rates of recurrence [150, 407, 409, 417, 419, 420, 698] than the MVM pathology observed in cluster 2. In fact, even with the limited obstetrical history available in this cohort, it was noted that cluster 3 N-SGA (now N-FGR) patients were most likely to have experienced a prior SGA pregnancy and/or stillbirth. Therefore, the ability to accurately separate placentas belonging to these two clusters after pregnancy (to mitigate recurrence) is our immediate goal.

An additional finding of interest was the co-clustering of placentas from normotensive and hypertensive suspected FGR pregnancies in each of clusters 1-3, suggesting similar underlying placental states in these groups, regardless of maternal hypertensive status. In all clusters, the clinical characteristics of the hypertensive patients were, understandably, more severe than the normotensive patients, including significantly more restricted uterine artery blood flow and earlier deliveries to avoid worsening maternal outcomes. Fitting with the previously identified relationship between mean uterine artery PI and maternal vascular malperfusion lesions (Chapter 4) [489, 556], as well as a prior study directly comparing H-FGR and N-FGR placentas [558], hypertensive samples also exhibited moderately more severe MVM histological features than their normotensive counterparts ($p=0.05$ in clusters 1 and 3, and $p=0.15$ in cluster 2). This was somewhat in contrast to the discovery of little to no significant transcriptional differences between the normotensive and hypertensive SGA placentas in each cluster.

We propose the following possible explanations for this observed discrepancy between the transcriptional and histological information. First, it is feasible that the borderline significant maternal vascular malperfusion histopathology differences discovered between the normotensive and hypertensive samples are not sufficiently severe to observe a corresponding transcriptional change. This is supported by the identification of a more significant difference in MVM lesions between the cluster 1 N-SGA samples and the cluster 1 controls ($p=0.01$), but only a few significant gene sets in the transcriptional comparison of these two groups. Stricter thresholds are also employed in our gene expression analysis than in our histopathological assessment (two adjusted q-values versus nominal p-values). Second, although four biopsies were taken from each placenta for each of the two kinds of tissue preparation (snap-frozen tissue for microarrays and FFPE for histopathology), these were not the exact same biopsies. As such, minor sampling

differences could have contributed to the mild discordance between the transcriptional and histological results, as mentioned in Chapter 4. Lastly, it is possible that some of the transcriptional changes linked to this maternal vascular malperfusion pathology in particular are no longer visible at the time of placental delivery and RNA sampling. For example, oxidative stress-induced syncytial knots are thought to be transcriptionally inactive [395], while distal villous hypoplasia has been associated with nuclear senescence [396, 433, 699, 700]. Altogether, it is, therefore, reasonable that this moderate discrepancy is observed between the gene expression and histological results when comparing the normotensive placentas to the hypertensive placentas. However, these placental differences are still relatively subtle, and are likely insufficient to explain the development of PE in some of these patients but not others. Therefore, we suspect that the maternal response to a given placental pathology is primarily responsible for the hypertensive or normotensive state [563], perhaps in combination with unmeasured distinctions in syncytiotrophoblast shedding [561]. Unfortunately, matched maternal samples were not available for these patients, but will be essential in subsequent studies to directly address this theory.

This study also has several other inherent limitations. The 97 samples included in this cohort represent a substantial, but still relatively small, dataset, especially given the considerable heterogeneity observed in these placental pathologies. A further increase in sample size, as well as the inclusion of preterm (GA <34 weeks) N-SGA placentas, might reveal additional subtypes of normotensive SGA/suspected FGR. Furthermore, although growth restriction often results in a newborn weight below the 10^{th} percentile for gestational age and sex, some infants with a large genetic growth potential can remain above this threshold, even with a pathological pregnancy [688]. Thus, future work that uses customized growth charts [160] to diagnosis fetal/newborn size may also reveal further FGR subtypes. Additionally, the almost exclusive assessment of samples annotated as suspected FGR likely limited the number of constitutionally small infants included in the current study. Utilizing an unselected/prospectively collected SGA population may improve our capacity to distinguish between constitutionally small and mild canonical pathology placentas within cluster 1. Finally, one of the primary limitations is the unbalanced sample distribution, with substantially more SGA placentas associated with hypertensive pregnancies than normotensive pregnancies. As such, the samples from our prior PE cohort may be disproportionally responsible for the formation of the clusters. Overall, the fact that no unique

placental N-SGA subtypes have been identified does not eliminate the possibility that they exist, simply that their potential discovery will require a further cohort expansion and a better balanced study design.

In general, this chapter provides novel insight into at least two pathological etiologies of normotensive FGR and a normotensive SGA subtype with mild "canonical" dysfunction, which may or may not represent a mild form of true pathological growth restriction. Additionally, a high degree of similarity was observed between normotensive and hypertensive placentas, indicating that it is feasible to maintain a maternal normotensive state until term (mean GA in the 10 N-FGR patients is 37 weeks) despite a highly pathological placenta. As such, future research should focus on each individual placental subtype of SGA, including an in-depth analysis of fetal versus maternal contributions to pregnancy outcome.

6 Chapter 6 – Quantitative Polymerase Chain Reaction (qPCR) for the Validation of Transcriptional Differences Between Clusters and the Classification of Unknown Samples

Part of this chapter's content is published in:

Leavey K, Benton SJ, Grynspan D, Kingdom JC, Bainbridge SA, Cox BJ. (2016). Unsupervised Placental Gene Expression Profiling Identifies Clinically Relevant Subclasses of Human Preeclampsia. *Hypertension*. 68: 137-147. [660]

Part of this chapter's content is under review:

Gibbs I*, Leavey K*, Benton SJ, Grynspan D, Bainbridge SA, Cox BJ. Placental Subtypes of Suspected Fetal Growth Restriction and Relationships to Maternal Hypertensive State. *AJOG*.

*Co-first authorship

Part of this chapter's content is in preparation:

Leavey K, Cox B, Cargill Y, Grynspan D. Recurrent Placental Transcriptional Profile with a Different Histological and Clinical Presentation: A Case Report.

Co-authors' contributions are described in the methods section.

6.1 Introduction

Maternal preeclampsia (PE) and fetal growth restriction (FGR) are heterogeneous states and consequences of pregnancy that often co-occur. In both cases, the placenta is considered the primary cause of the pathology. To investigate this heterogeneity, we have previously subjected placentas linked to PE pregnancies and small-for-gestational-age (SGA)/suspected FGR pregnancies to gene expression microarrays, analyzed this data using unsupervised clustering techniques, and compared these results to available matched clinical and histopathological features (Chapters 2-5). These studies revealed multiple placental subtypes of PE and suspected FGR: a "mild" pathology group with molecular similarity to healthy term control samples, where maternal factors may have considerable influence on PE development and SGA infants may be constitutionally small or also affiliated with a non-placental source of growth restriction; a "canonical" group with preterm deliveries, low placental weights, and evidence of hypoxic maternal vascular malperfusion (distal villous hypoplasia, placental infarctions, and syncytial knots); and an "immunological" group with a significant enrichment of immune response genes and histological signs of maternal rejection of the feto-placental unit. These "canonical" and "immunological" SGA pregnancies exhibited considerable evidence of placental insufficiency and pathology, thereby likely confirming a diagnosis of pathological FGR in these infants. An additional subtype of PE placentas with chromosomal abnormalities was also discovered in Chapter 3, but showed no strong clinical, histological, or epigenetic [683] association. These four PE and SGA subtypes belonged to transcriptional clusters 1, 2, 3, and 5, respectively, while cluster 4 in our prior PE analysis (Chapters 3 and 4) was composed of preterm control samples with histological chorioamnionitis.

The observation of multiple molecular clusters of placental samples with unique gene set enrichments, histopathology, and clinical correlations indicates that past and future research on PE and FGR may need to be re-evaluated in this new context. Additionally, the immune-related cluster 3 pathology is known to have much higher rates of recurrence [150, 407, 409, 417, 419, 420, 698] than the maternal malperfusion pathology observed in cluster 2, therefore necessitating the separation of these two groups even after delivery, as they likely require different post-partum counselling. Since microarrays and other genome-wide gene expression analyses are expensive for the classification of samples, the next goal was to identify candidate markers with the capacity to discriminate between these clusters and readily place placentas into groups. As

such, the primary aim of this chapter was to develop a panel of genes with the ability to classify samples using quantitative (real-time) polymerase chain reaction (qPCR) methods. This served to validate some of the observed transcriptional differences between the clustered placentas, and provided the opportunity to classify unknown samples.

6.2 Methods

6.2.1 Sample and gene selection with the PE (training) cohort

Samples from the PE BioBank cohort (Chapter 3) were used as a training set for the development of the qPCR panel. Ten cluster-by-cluster comparisons were performed using the microarray data and the *limma* package [643] in R 3.1.3 in order to determine the top differentially expressed genes between the full clusters 1-5 from Chapter 3. From these, 12 genes were selected (two genes for comparisons involving cluster 1, due to anticipated difficulties separating this cluster from all four bordering clusters, and one gene for the remaining comparisons). Human TaqMan primer/probes sets were purchased from Life Technologies for SNX10 (Hs00203362_m1), VPS54 (Hs00212957_m1), MAN1C1 (Hs00220595_m1), TPBG (Hs00272649 _s1), TAP1 (Hs00388675_m1), LIMCH1 (Hs00405524_m1), FSTL3 (Hs00610505_m1), MT1F (Hs00744661_sH), MORN3 (Hs00900107_g1), PIK3CB (Hs00927728_m1), SQRDL (Hs01126963 _m1), and METTL18 (Hs01851858_s1). Primer/probes sets were also obtained for two known PE markers, FLT1 (Hs01052961_m1) and ENG (Hs00923996_m1), and two reference genes, ACTB (Hs99999903_m1) and HPRT1 (Hs99999909_m1), as well as isolated RNA from a healthy placenta for use as a consistent external reference sample across all plates (catalog number AM7950).

Of the PE cohort BioBank placentas, 12 cluster 1 samples, eight cluster 2 samples, five cluster 3 samples, five cluster 4 samples, and five cluster 5 samples were randomly selected for qPCR using the *sample* function in R. The selected number of samples per cluster is approximately representative of the sample distribution in the full placental dataset, with the condition of a minimum of five samples per cluster. RNA from each of these 36 placentas (35 PE BioBank samples (previously extracted for the microarray analysis in Chapter 3) and one reference sample (purchased)) was converted into complementary DNA (cDNA) using reagents from Invitrogen

(catalog numbers 48190011 and 18064014), Thermo Scientific (material number R0192), and New England BioLabs (U.S. product codes M0297S1 and M0303S1) (**Appendix A**). For two cluster 1 samples, sufficiently concentrated cDNA could not be obtained, and these were consequently excluded.

6.2.2 Quantitative (real-time) polymerase chain reaction (qPCR)

Plates (Applied Biosystems MicroAmp Optical 384 well reaction plates with barcode) were loaded with 4.5µl diluted cDNA, 0.5µl primer/probe, and 5.0µl TaqMan Universal PCR Master Mix (Life Technologies, catalog number 4304437) by an Eppendorf epMotion® 5070 automated pipetting system, with all genes for a given sample assessed on the same plate. The qPCR reaction was performed by a Life Technologies QuantStudio™ 7 Flex Real-Time PCR System using default TaqMan cycling conditions (an initial denaturation step of 10 minutes at 95°C; and 40 cycles of 95°C (15 seconds) and 60°C (1 minute)). Targets were run in triplicate and averaged for analysis. Access to this qPCR machinery was provided by Dr. Michael Wheeler, with training obtained from his graduate student, Sean Froese.

6.2.3 Preliminary analysis and comparison to the microarray data

Mean C_T values were initially analyzed by the comparative C_T method [701] in order to obtain a fold change expression difference for each gene of interest in each sample of interest compared to the reference sample. The data was then loaded into R, log2 transformed, and compared to the log2 microarray results by Pearson's correlations. qPCR values for significantly correlating genes were assessed for their necessity and ability to differentiate between the five clusters using the WEKA machine learning software package [645] and receiver operator characteristic (ROC) curves, with Random Forest (decision tree) classification methods (1000 trees and 10-fold cross-validation).

6.2.4 Development of the initial qPCR decision tree

Attribute selection for the separation of clusters 1-4 only was performed by an exhaustive search with Correlation-based Feature Subset Selection, still using the log2 values obtained by the comparative C_T method. Correlation-based Feature Subset Selection establishes a subset of attributes that are highly correlated with class, but not with each other [702]. Simple differences in the mean C_T values for the three top genes identified by attribute selection were developed

into an initial qPCR panel/decision tree for the classification of samples into clusters 1, 2, 3, and 4, using J48 methods with 10-fold cross-validation in WEKA.

6.2.5 Testing of the initial qPCR decision tree

The 20 normotensive SGA BioBank samples from Chapter 5 were used as a testing cohort for the developed qPCR panel. Remaining available mRNA for these samples was converted into cDNA using Applied Biosystems/ThermoFisher's High-Capacity RNA-to-cDNA™ Kit, which requires a maximum input of 2µg of total RNA per reaction. Previously purchased TaqMan primer/probes sets for TAP1, LIMCH1, and FSTL3 were assessed using the Life Technologies QuantStudio™ 7 Flex Real-Time PCR System as above. Additionally, a new vial of the FSTL3 primer/probe (still Hs00610505_m1) was obtained from Life Technologies, and three N-SGA placentas (one from each of clusters 1-3, based on the microarray results from Chapter 5) were re-run with this original three-gene panel.

6.2.6 Development and validation of the second qPCR decision tree

All genes investigated by qPCR in our original PE cohort with the potential capacity to replace FSTL3 (i.e. distinguish PE samples) were identified, and C_T value differences between these genes and LIMCH1 were once again subjected to J48 methods with 10-fold cross-validation in WEKA. This resulted in a second developed three-gene qPCR panel for the classification of samples into clusters 1, 2, 3, and 4. Of the 20 normotensive SGA testing samples, 17 had available remaining tissue/RNA/cDNA for qPCR analysis. These 17 placentas were, therefore, subjected to this second qPCR panel, as described above. Samples were run in duplicate and averaged for analysis.

6.2.7 Application of the second qPCR panel to two new pathological placentas

Two newly acquired placentas from the same woman four years apart (2012 and 2016) were assessed for molecular cluster assignment using this second qPCR panel as part of a case study. These placentas were examined histologically by Dr. David Grynspan in the course of his clinical role as a perinatal pathologist at the Children's Hospital of Eastern Ontario in Ottawa, and curls from the formalin-fixed, paraffin-embedded (FFPE) tissues were obtained and sent to us.

RNA was extracted from the two FFPE samples using ThermoFisher's RecoverAll™ Total Nucleic Acid Isolation Kit for FFPE, quantified on a ThermoFisher Qubit® Fluorometer with the Qubit® RNA HS Assay Kit, and converted into cDNA with their High-Capacity RNA-to-cDNA™ Kit. Previously purchased Life Technologies Human TaqMan primer/probes sets for TAP1, LIMCH1, and FLT1, along with TaqMan Universal PCR Master Mix, were utilized for qPCR, performed by the Life Technologies QuantStudio™ 7 Flex Real-Time PCR System as above. Samples were run in triplicate and averaged for analysis. Differences in the mean C_T values for the three genes (TAP1, LIMCH1, and FLT1) within the same sample were used to classify the two FFPE placental tissues into molecular clusters, which were then compared to the histology results.

6.2.8 Ethics

Ethics approval for the use of the PE and SGA BioBank samples from Chapters 3-5 was granted from the Research Ethics Boards of Mount Sinai Hospital (#13-0211-E), the University of Toronto (#29435), and the Ottawa Health Science Network (#2011623-01H). Patient consent was obtained for the molecular assessment of the two case study placentas.

6.3 Results

6.3.1 Comparison of the qPCR and microarray results in the PE BioBank samples

To first confirm that the microarray results could be replicated at an individual gene level, a panel of 12 genes with significant differential expression between the five full clusters from Chapter 3 (**Table 23**), in addition to the frequently studied PE markers FLT1 and ENG, were selected for validation by qPCR in a subset of 33 PE cohort BioBank samples (ten from cluster 1, eight from cluster 2, five from cluster 3, five from cluster 4, and five from cluster 5). Of these 14 genes, 11 (including FLT1 and ENG) revealed moderate to strong correlations between the qPCR and the microarray values ($r=0.65–0.96$ and $p<0.01$) (**Figure 33**). Those that did not correlate (VPS54, SQRDL, and METTL18) had originally demonstrated mean expression in the bottom quartile of all genes by microarray (Chapter 3).

Table 23 – Gene selection for qPCR based on the microarray data. The full clusters (N=330, Chapter 3) were compared using *limma*.

Gene[a]	Log2 fold change	Mean expression[b]	t-statistic	P-value	Adj. p-value
Top five differentially expressed genes in cluster 1 versus cluster 2					
FSTL3	-2.08	11.42	-19.03	3.56E-55	5.22E-51
TPBG	-1.01	9.32	-18.22	5.73E-52	3.28E-48
INHA	-1.36	9.20	-18.20	6.88E-52	3.28E-48
CST6	-1.09	8.53	-18.16	9.76E-52	3.28E-48
SASH1	-1.26	10.27	-18.15	1.12E-51	3.28E-48
Top five differentially expressed genes in cluster 1 versus cluster 3					
TAP1	-1.16	8.97	-12.54	8.05E-30	1.18E-25
MT1F	-1.13	8.79	-11.88	2.18E-27	1.60E-23
SOD2	-0.97	8.33	-11.19	6.91E-25	3.37E-21
EMP3	-0.70	9.38	-11.06	1.99E-24	7.28E-21
CAPG	-0.99	7.82	-10.69	3.84E-23	1.13E-19
Top five differentially expressed genes in cluster 1 versus cluster 4					
MAN1C1	1.35	11.61	13.42	3.79E-33	5.55E-29
MORN3	1.05	8.72	12.20	1.49E-28	9.88E-25
CYP11A1	0.96	12.92	12.16	2.02E-28	9.88E-25
ALPP	1.29	12.07	11.89	1.96E-27	7.17E-24
GNE	0.87	10.97	11.83	3.25E-27	9.51E-24
Top five differentially expressed genes in cluster 1 versus cluster 5					
VPS54	0.49	7.66	11.31	2.50E-25	3.67E-21
METTL18	0.56	7.15	11.19	6.80E-25	4.98E-21
TRAPPC13	0.51	7.17	10.96	4.29E-24	2.09E-20
SELO	-0.56	8.58	-10.77	2.10E-23	7.70E-20
PPP2R3C	0.45	8.24	10.72	3.09E-23	8.22E-20
Top five differentially expressed genes in cluster 2 versus cluster 3					
SQRDL	-0.88	7.47	-11.56	3.19E-26	4.67E-22
PLEK	-1.03	8.53	-10.87	8.96E-24	6.56E-20
FCER1G	-0.96	9.53	-10.30	9.02E-22	4.40E-18
LCP2	-0.76	8.22	-10.22	1.61E-21	5.90E-18
CD53	-0.88	9.06	-10.16	2.68E-21	7.84E-18
Top five differentially expressed genes in cluster 2 versus cluster 4					
LIMCH1	2.08	10.20	18.52	3.85E-53	5.64E-49
CYP11A1	1.43	12.92	17.53	3.29E-49	1.84E-45
MAN1C1	1.81	11.61	17.51	3.76E-49	1.84E-45
PVRL4	2.14	10.03	17.12	1.35E-47	4.96E-44
PROCR	1.72	10.69	16.70	6.14E-46	1.80E-42
Top five differentially expressed genes in cluster 2 versus cluster 5					
PIK3CB	0.98	9.76	10.29	9.51E-22	8.27E-18
LIMCH1	0.98	10.20	10.27	1.13E-21	8.27E-18
ARSK	0.69	7.31	9.88	2.30E-20	1.01E-16
TMEM45A	1.32	8.88	9.86	2.77E-20	1.01E-16
PVRL4	1.03	10.03	9.70	9.38E-20	2.75E-16

Top five differentially expressed genes in cluster 3 versus cluster 4					
SNX10	1.17	10.01	10.81	1.46E-23	2.05E-19
HTRA1	1.45	12.81	10.73	2.80E-23	2.05E-19
EBI3	1.54	13.39	10.68	4.37E-23	2.14E-19
MCM3	-0.76	8.99	-9.97	1.13E-20	4.16E-17
CRH	2.61	12.17	9.92	1.75E-20	5.13E-17
Top five differentially expressed genes in cluster 3 versus cluster 5					
SQRDL	1.16	7.47	12.80	8.52E-31	1.25E-26
FPR3	1.48	6.99	11.56	3.26E-26	2.39E-22
DHRS7	1.07	8.22	11.32	2.27E-25	1.11E-21
PARP9	1.11	8.16	11.18	7.65E-25	2.80E-21
C1S	1.29	8.40	10.62	7.16E-23	2.10E-19
Top five differentially expressed genes in cluster 4 versus cluster 5					
MAN1C1	-1.52	11.61	-12.65	3.17E-30	2.83E-26
PRPS1	0.84	7.78	12.63	3.86E-30	2.83E-26
HPRT1	0.86	7.64	11.78	5.27E-27	2.20E-23
NPL	0.98	8.56	11.76	6.01E-27	2.20E-23
GMEB2	-0.84	8.69	-11.70	1.01E-26	2.96E-23

[a]Selected genes are in bold
[b]Within the two clusters in question

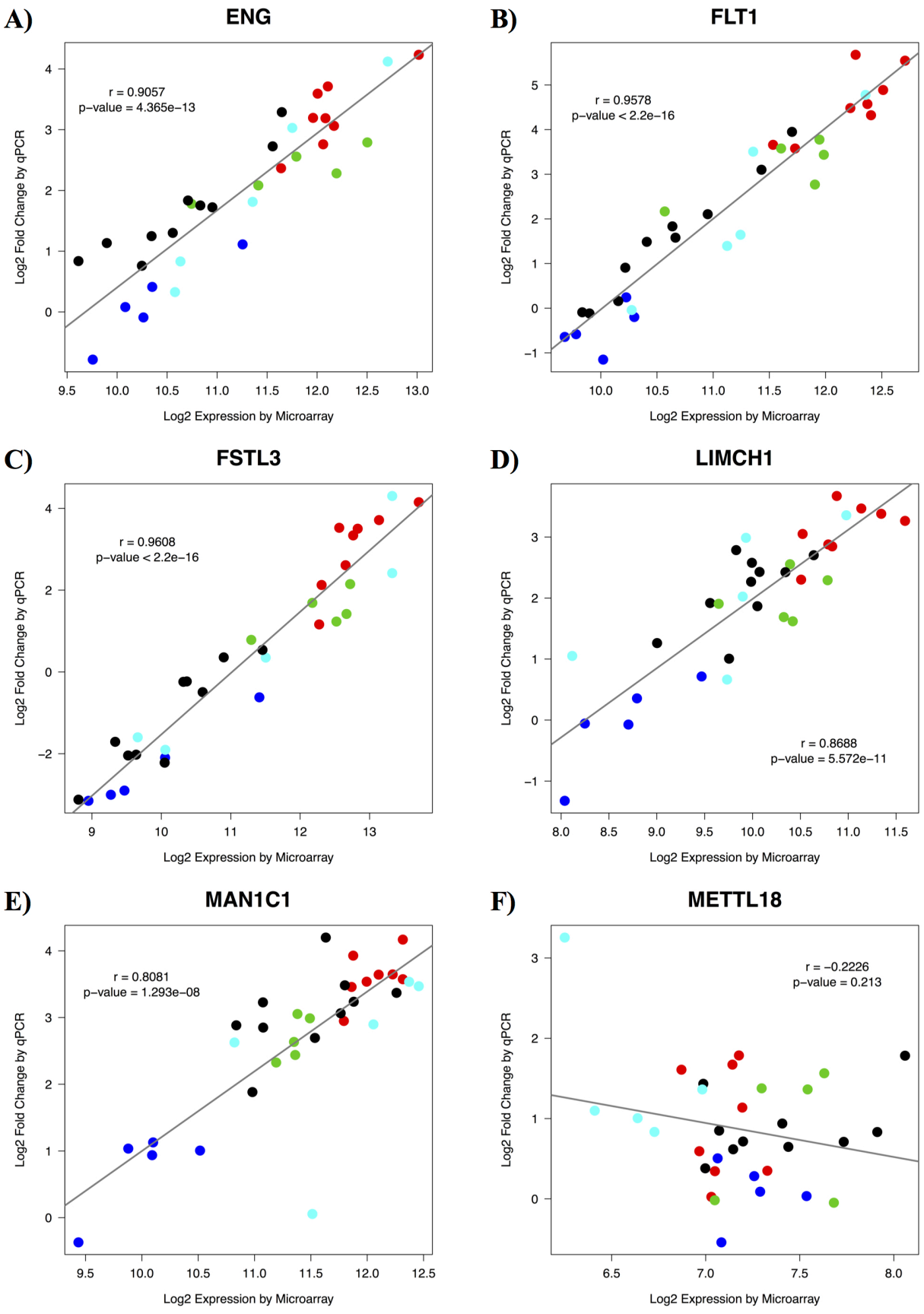
A)
ENG
r = 0.9057
p−value = 4.365e−13
Log2 Fold Change by qPCR
Log2 Expression by Microarray
B)
FLT1
r = 0.9578
p−value < 2.2e−16
Log2 Fold Change by qPCR
Log2 Expression by Microarray
C)
FSTL3
r = 0.9608
p−value < 2.2e−16
Log2 Fold Change by qPCR
Log2 Expression by Microarray
D)
LIMCH1
r = 0.8688
p−value = 5.572e−11
Log2 Fold Change by qPCR
Log2 Expression by Microarray
E)
MAN1C1
r = 0.8081
p−value = 1.293e−08
Log2 Fold Change by qPCR
Log2 Expression by Microarray
F)
METTL18
r = −0.2226
p−value = 0.213
Log2 Fold Change by qPCR
Log2 Expression by Microarray

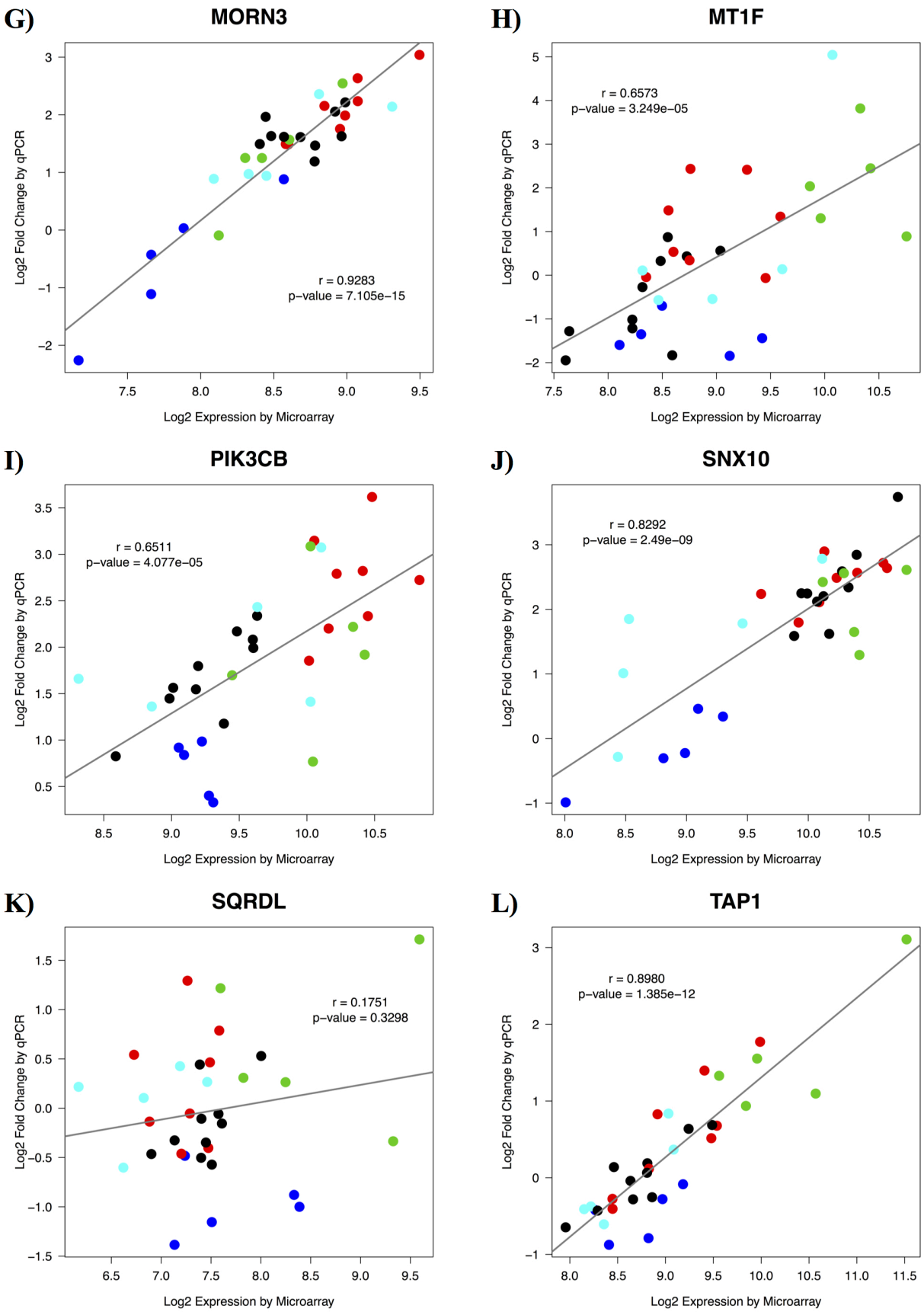
G)
MORN3
r = 0.9283
p−value = 7.105e−15
Log2 Fold Change by qPCR
Log2 Expression by Microarray
H)
MT1F
r = 0.6573
p−value = 3.249e−05
Log2 Fold Change by qPCR
Log2 Expression by Microarray
I)
PIK3CB
r = 0.6511
p−value = 4.077e−05
Log2 Fold Change by qPCR
Log2 Expression by Microarray
J)
SNX10
r = 0.8292
p−value = 2.49e−09
Log2 Fold Change by qPCR
Log2 Expression by Microarray
K)
SQRDL
r = 0.1751
p−value = 0.3298
Log2 Fold Change by qPCR
Log2 Expression by Microarray
L)
TAP1
r = 0.8980
p−value = 1.385e−12
Log2 Fold Change by qPCR
Log2 Expression by Microarray

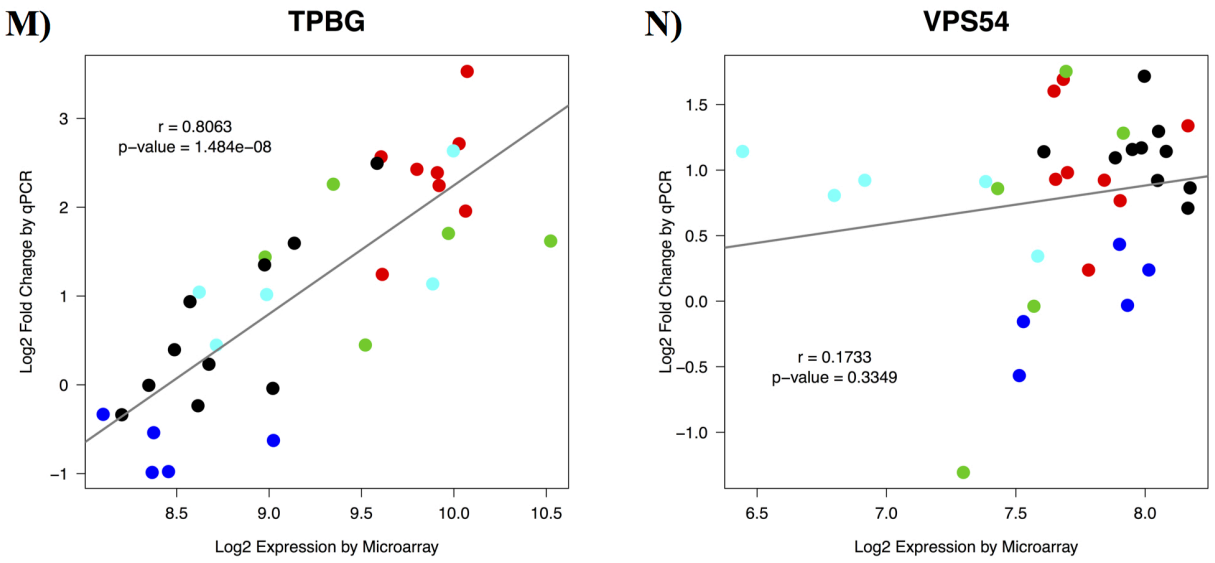

Figure 33 – Correlations between the log2 expression microarray data and the log2 fold-change-over-reference quantitative polymerase chain reaction (qPCR) data for the 14 genes and 33 samples assessed by qPCR. Cluster 1 samples – black; cluster 2 samples – red; cluster 3 samples – green; cluster 4 samples – blue; cluster 5 samples – cyan. Correlations and p-values were calculated by Pearson's correlations.

6.3.2 Assessment of the discriminatory potential of gene groups in the PE cohort

Expectedly, the PE samples in cluster 2 demonstrated the highest levels of FLT1 and ENG expression and could be easily distinguished from all the tested non-PE samples using only these two genes (**Figure 34a**). This was in contrast to the PE cases belonging to clusters 1, 3, and 5, which exhibited expression levels of these two markers closer to non-PE placentas and were consequently poorly identified (**Figure 34a**). Furthermore, the few non-PE samples with elevated FLT1 and ENG were from women with chronic hypertension. Next, the remaining nine genes with correlating qPCR values were assessed for their ability to discriminate between the five clusters using machine learning classification. Cluster 1, 2, 3, and 4 samples were predominately assigned correctly (area under the curve: 0.97, 0.86, 0.97, and 0.98, respectively); however, cluster 5 samples could not be identified with these genes (area under the curve: 0.48; **Figure 34b, Table 24**).

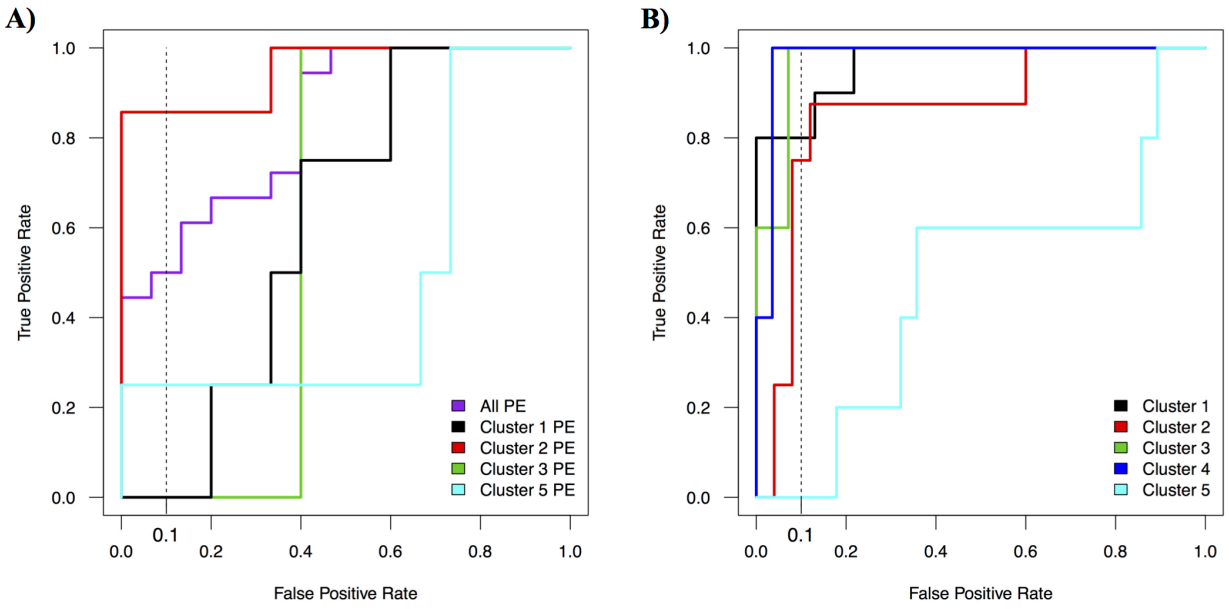

Figure 34 – Classification power of quantitative polymerase chain reaction (qPCR) data. (**A**) The preeclamptic (PE) samples in cluster 2 (red) demonstrated the highest levels of FLT1 and ENG by qPCR and could be easily distinguished from non-preeclamptics (>85%) at a 10% false-positive rate (FPR; black dotted line) using only these two genes. This was in contrast to the PE samples belonging to clusters 1 (black), 3 (green), and 5 (cyan), which exhibited expression levels closer to non-PE samples and were consequently poorly identified. This led to an overall ability of these two markers to differentiate ~50% of the PE samples from the non-PE samples (purple) at a 10% FPR. (**B**) qPCR data for nine genes (SNX10, MAN1C1, TPBG, TAP1, LIMCH1, FSTL3, MT1F, MORN3, and PIK3CB) with discriminatory potential were assessed for their ability to differentiate between the five clusters. Cluster 1 (black), cluster 2 (red), cluster 3 (green), and cluster 4 (blue) samples were predominately assigned correctly; however, cluster 5 (cyan) samples could not be identified with these markers.

Table 24 – Confusion matrix for the classification of cluster 1-5 samples using the qPCR data from nine genes (**Figure 34b**).

Classified as → Microarray cluster ↓	**Cluster 1**	**Cluster 2**	**Cluster 3**	**Cluster 4**	**Cluster 5**
Cluster 1	9	0	0	0	1
Cluster 2	0	7	1	0	0
Cluster 3	1	1	3	0	0
Cluster 4	0	0	0	5	0
Cluster 5	2	2	0	1	0

6.3.3 Development of a small qPCR panel for classification, using the PE cohort

To simplify the classification problem, machine learning attribute selection was employed to reduce the number of markers (from nine) needed to distinguish between clusters 1-4. This identified LIM and calponin homology domains 1 (LIMCH1), follistatin-like 3 (FSTL3), and transporter 1, ATP-binding cassette, subfamily B (TAP1) as the genes with the greatest potential for separating the clusters (**Table 25, Figure 33c,d,l**). Conveniently, differences in the measured qPCR mean C_T values for these three genes within a given sample (**Table 26**) were found to provide adequate information for successful cluster assignment in the majority (~85%) of cluster 1-4 cases (**Figure 35, Table 27**).

Since cluster 5 could not be identified as a cohesive group by targeted qPCR, this LIMCH1, FSTL3, and TAP1 panel for the discrimination of clusters 1-4 was applied to the five cluster 5 samples with available qPCR values to determine if their individual categorizations revealed any significant biological meaning. Two cluster 5 placentas were classified as cluster 1, two were classified as cluster 2, and one was classified as cluster 3 (**Table 26**, **Figure 35**). The samples allocated to cluster 1 exhibited healthier clinical characteristics, plotted in line with cluster 1 by PCA of the original microarray data from Chapter 3 (**Figure 36a,b**), and the sample with available histology (Chapter 4) demonstrated minimal pathology (**Figure 36c**). The two cluster 5 placentas classified as cluster 2 by qPCR were associated with more severe PE outcomes, plotted in line with cluster 2 by PCA (**Figure 36a,b**), and revealed high maternal malperfusion lesions (**Figure 36c**). Finally, the one sample allocated to cluster 3 showed some global molecular similarity to both clusters 1 and 3 by PCA (**Figure 36a,b**) and displayed low histopathology (**Figure 36c**).

Table 25 – Attribute selection for the separation of clusters 1-4 with the nine genes showing correlating microarray and qPCR values.

Attribute	Number of folds[a]	Percent	Selected[b]
FSTL3	10	100%	✔
LIMCH1	10	100%	✔
MAN1C1	5	50%	--
MORN3	7	70%	--
MT1F	2	20%	--
PIK3CB	0	0%	--
SNX10	0	0%	--
TAP1	9	90%	✔
TPBG	7	70%	--

[a]Number of folds where the gene was selected to classify samples into clusters 1-4, out of 10 folds

[b]Genes utilized at least 90% of the time were selected as those with the greatest discriminatory potential and were investigated further

Table 26 – Mean C_T values (and differences between them) for relevant genes in the original qPCR analysis of the 33 PE cohort samples from Chapters 3 and 4.

Microarray cluster	FSTL3	TAP1	LIMCH1	FLT1	FSTL3-LIMCH1	TAP1-LIMCH1	FLT1-LIMCH1
2	21.968	30.799	25.478	21.971	-3.510	5.321	-3.507
2	23.281	30.426	24.978	20.832	-1.697	5.448	-4.146
2	23.159	32.621	25.942	22.844	-2.783	6.679	-3.098
2	19.578	27.894	21.905	18.475	-2.327	5.989	-3.430
1	25.947	30.931	26.588	24.867	-0.641	4.343	-1.721
4	26.085	29.587	25.399	24.587	0.686	4.188	-0.812
2	18.128	26.421	21.816	18.952	-3.688	4.605	-2.864
1	27.793	31.984	26.131	26.225	1.662	5.853	0.094
1	22.007	28.088	22.462	20.257	-0.455	5.626	-2.205
2	19.486	28.914	22.522	20.235	-3.036	6.392	-2.287
1	26.382	32.104	26.165	23.195	0.217	5.939	-2.970
3	24.283	30.518	26.814	23.927	-2.531	3.704	-2.887
1	23.284	27.771	23.398	21.733	-0.114	4.373	-1.665
5	20.705	27.904	22.609	20.663	-1.904	5.295	-1.946
3	21.439	28.172	24.097	20.806	-2.658	4.075	-3.291
3	23.574	29.335	25.253	23.186	-1.679	4.082	-2.067
4	25.435	28.403	24.520	23.452	0.915	3.883	-1.068
5	26.609	31.017	25.660	24.477	0.949	5.357	-1.183
4	27.178	30.696	28.273	26.290	-1.095	2.423	-1.983
5	23.348	29.028	25.985	23.023	-2.637	3.043	-2.962
4	24.452	28.330	25.362	23.906	-0.910	2.968	-1.456
3	21.953	27.786	24.039	21.034	-2.086	3.747	-3.005
2	22.200	28.929	23.809	20.856	-1.609	5.120	-2.953
1	26.163	30.398	25.531	25.073	0.632	4.867	-0.458
4	25.230	30.378	27.429	25.436	-2.199	2.949	-1.993
5	26.529	30.666	26.247	25.528	0.282	4.419	-0.719
1	24.908	28.561	24.157	23.577	0.751	4.404	-0.580
2	21.508	28.353	23.945	20.498	-2.437	4.408	-3.447
3	20.960	24.771	23.321	19.826	-2.361	1.450	-3.495
1	25.657	29.114	23.685	23.196	1.972	5.429	-0.489
1	28.519	31.521	25.769	26.482	2.750	5.752	0.713
5	20.289	30.883	23.983	20.884	-3.694	6.900	-3.099
1	22.112	28.272	23.132	22.142	-1.020	5.140	-0.990

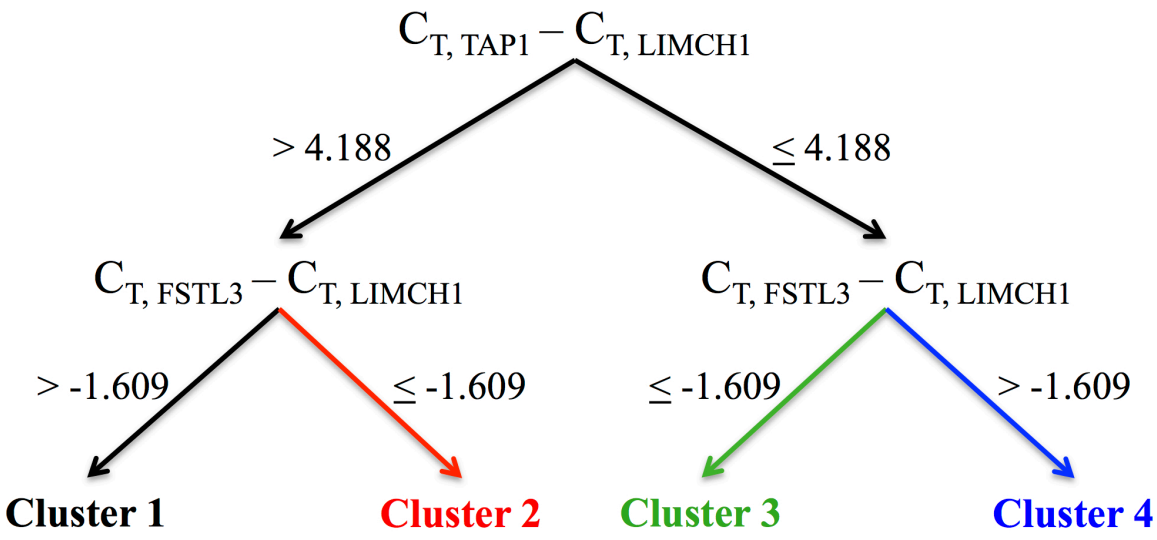

Figure 35 – The original qPCR panel. qPCR differences in the mean C_T values representing FSTL3, LIMCH1, and TAP1 gene expression were found to be sufficient for distinguishing between clusters 1 (black), 2 (red), 3 (green), and 4 (blue) 85% of the time. The immune-associated clusters 3 and 4 demonstrated more similar expression of TAP1 and LIMCH1 than the non-immune clusters 1 and 2, whereas the PE-enriched clusters 2 and 3 revealed elevated FSTL3 expression compared with LIMCH1.

Table 27 – Confusion matrix for the classification of cluster 1-4 PE cohort samples using the first three-gene (FSTL3, LIMCH1, and TAP1) qPCR panel (**Figure 35**).

Classified as → Microarray cluster ↓	**Cluster 1**	**Cluster 2**	**Cluster 3**	**Cluster 4**
Cluster 1	10	0	0	0
Cluster 2	1	7	0	0
Cluster 3	0	0	4	1
Cluster 4	1	0	1	3

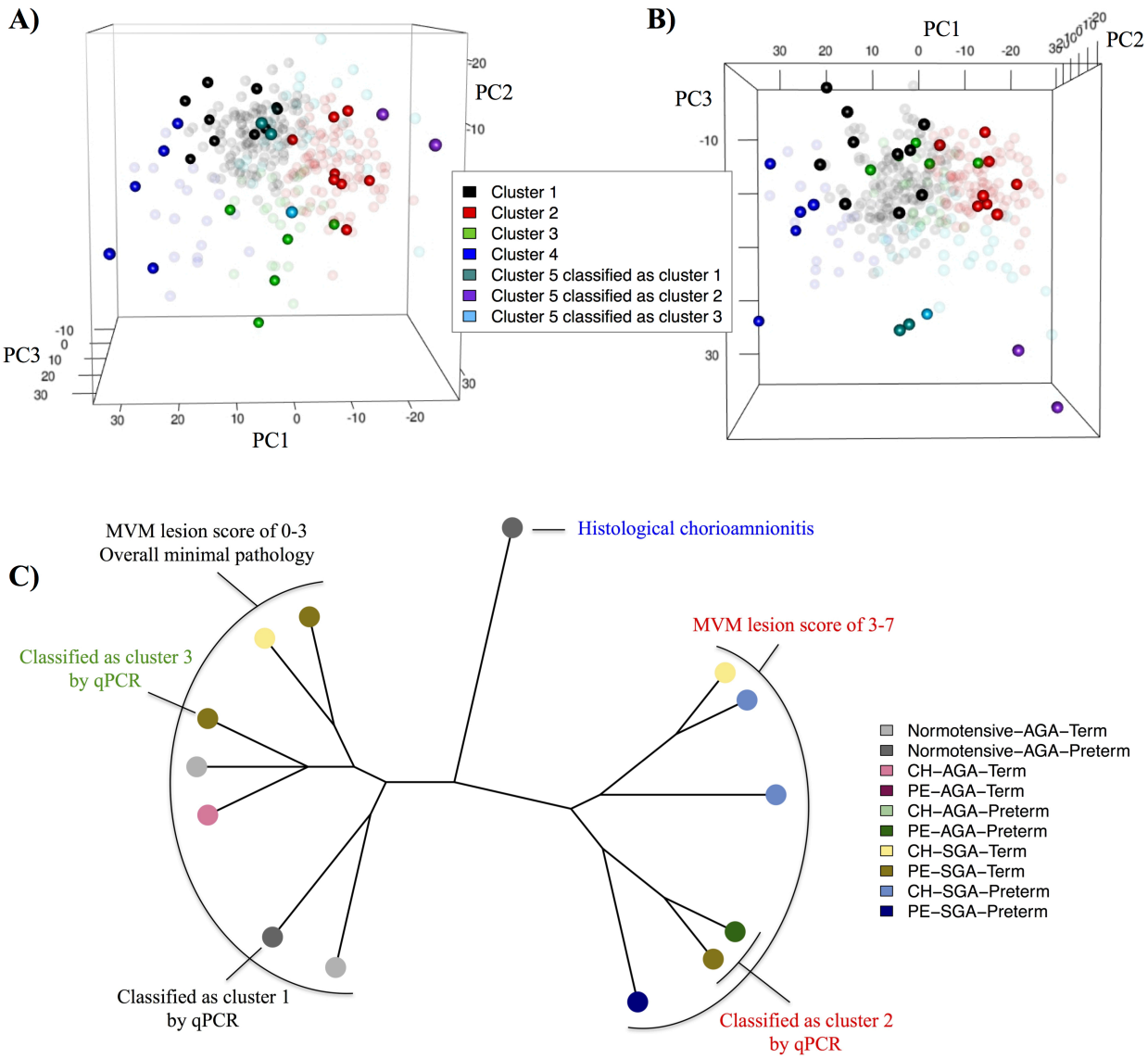

Figure 36 – Cluster 5. Of the five cluster 5 samples assessed by qPCR, two were classified as cluster 1, two as cluster 2, and one as cluster 3, based on the FSTL3, TAP1, and LIMCH1 qPCR panel. Principal component analysis (PCA) of the microarray data from Chapter 3 from the front (**A**) and the top (**B**) revealed that the cluster 5 samples that were classified as cluster 1 (dark cyan) were in line with cluster 1 (black) on the principal component 1 (PC1) axis. The cluster 5 samples allocated to cluster 2 (purple) were in line with cluster 2 (red) on the PC1 axis, while the cluster 5 sample assigned to cluster 3 (sky blue) demonstrated a more positive PC2 value, similar to cluster 3 (blue). Fully colored samples are those that were assessed by qPCR, while semi-transparent dots are samples that did not undergo qPCR analysis. (**C**) The phylogenetic tree of the histopathology data in cluster 5 placentas from Chapter 4. The samples allocated as cluster 2 by qPCR exhibited high maternal vascular malperfusion (MVM) lesions (red). Both the placenta classified as cluster 1 (black) (the other did not have available tissue for histology scoring) and the sample classified as cluster 3 (green) demonstrated overall low pathology.

6.3.4 Attempted validation of the qPCR panel, using the SGA cohort

The normotensive small-for-gestational-age (N-SGA) placentas from Chapter 5 were used to test the accuracy of the developed FSTL3, LIMCH1, and TAP1 qPCR panel. Based on the microarray data, ten should be classified as cluster 1, seven as cluster 2, and three as cluster 3. qPCR assessment of these three genes in all 20 N-SGA samples revealed the expected values and relationship between TAP1 and LIMCH1 expression (**Table 28**). However, the C_T values for FSTL3 were substantially higher (i.e. lower expression) than anticipated (**Table 28**). The first possible explanation for this discrepancy was that the FSTL3 primer/probe set had perhaps been compromised in the almost two years it had been sitting in the freezer, despite an acceptable expiry date. A new FSTL3 primer/probe set was, therefore, purchased and used to assess the expression of the three genes again in three of the N-SGA placentas (one from each of clusters 1-3). Unfortunately, similar results were observed (**Table 29**).

Table 28 – Mean C_T values (and differences between them) for the first test of the FSTL3, TAP1, and LIMCH1 qPCR panel in the 20 normotensive SGA placentas from Chapter 5.

Microarray cluster	FSTL3	TAP1	LIMCH1	FSTL3-LIMCH1	TAP1-LIMCH1
1	29.121	25.247	19.020	10.101	6.227
1	26.062	24.165	18.644	7.418	5.522
2	27.606	25.732	20.292	7.314	5.440
2	23.327	24.515	19.422	3.905	5.092
1	27.637	26.236	19.970	7.667	6.266
1	27.815	25.735	20.113	7.702	5.622
1	24.885	25.389	19.790	5.095	5.599
2	25.329	23.663	18.070	7.259	5.593
1	28.109	25.272	19.206	8.902	6.066
1	25.376	25.309	19.252	6.124	6.056
2	23.272	22.398	18.823	4.449	3.575
1	26.301	22.941	18.450	7.850	4.491
2	27.286	25.521	19.508	7.778	6.012
1	25.435	23.973	17.712	7.724	6.261
1	27.451	24.331	19.795	7.656	4.536
3	27.321	22.415	19.546	7.775	2.869
3	24.890	24.384	18.730	6.160	5.655
2	27.851	26.098	18.392	9.460	7.707
3	23.849	22.822	18.601	5.248	4.221
2	25.035	23.885	18.565	6.469	5.319

Table 29 – Mean C_T values (and differences between them) for the second test of the FSTL3, TAP1, and LIMCH1 qPCR panel in three normotensive SGA placentas from Chapter 5.

Microarray cluster	FSTL3	TAP1	LIMCH1	FSTL3-LIMCH1	TAP1-LIMCH1
1	26.996	24.565	19.183	7.813	5.382
2	26.146	25.751	20.825	5.321	4.926
3	25.303	22.548	20.199	5.104	2.349

6.3.5 Development of a second qPCR panel, using the PE cohort

The next goal was to replace FSTL3 in the qPCR panel for the separation of clusters 1-4. FLT1, ENG, TPBG, and MAN1C1 expression were all measured by qPCR in the original PE cohort and had the potential capacity to distinguish the PE-enriched clusters 2 and 3 from the control-enriched clusters 1 and 4 (the role of FSTL3 in the original panel) (**Table 23**). Raw differences in the C_T values between these genes and LIMCH1 were once again subjected to machine learning classification methods, and a second qPCR panel using FLT1 instead of FSTL3 was established (**Figure 37**). This decision tree was capable of correct cluster assignment in ~82% of the cluster 1-4 training PE cohort placentas (**Table 30**).

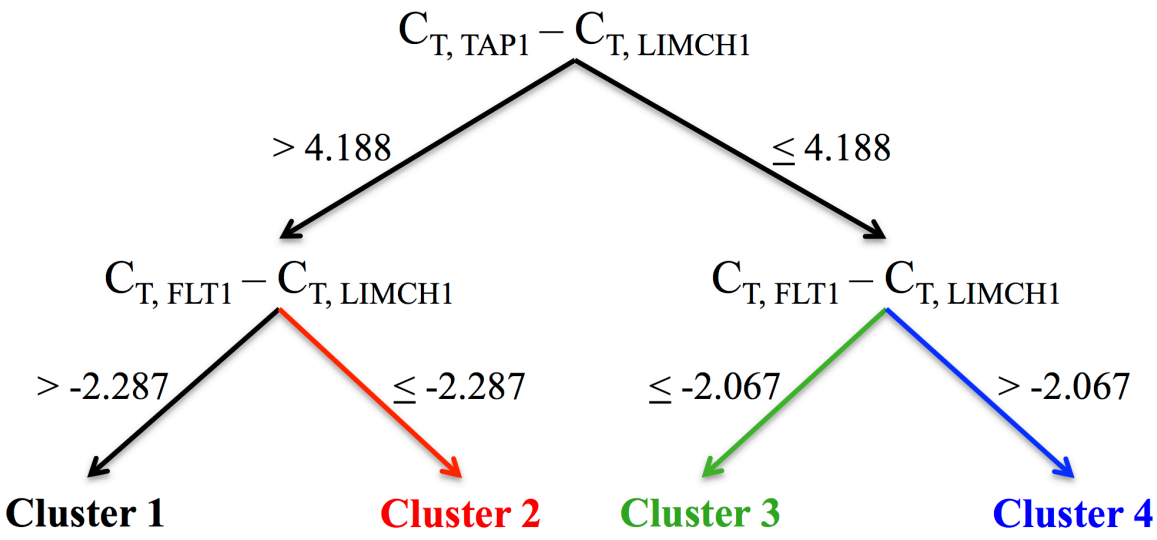

Figure 37 – The second qPCR panel. qPCR differences in the mean C_T values representing FLT1, LIMCH1, and TAP1 gene expression were developed into a second qPCR panel for distinguishing between clusters 1 (black), 2 (red), 3 (green), and 4 (blue) (accuracy: 82%). The immune-associated clusters 3 and 4 demonstrated more similar expression of TAP1 and LIMCH1 than the non-immune clusters 1 and 2, whereas the PE-enriched clusters 2 and 3 revealed elevated FLT1 expression compared with LIMCH1.

Table 30 – Confusion matrix for the classification of cluster 1-4 PE cohort samples using the second three-gene (FLT1, LIMCH1, and TAP1) qPCR panel (**Figure 37**).

Classified as → Microarray cluster ↓	**Cluster 1**	**Cluster 2**	**Cluster 3**	**Cluster 4**
Cluster 1	8	2	0	0
Cluster 2	1	7	0	0
Cluster 3	0	0	4	1
Cluster 4	1	0	0	4

6.3.6 Validation of the second qPCR panel, using the SGA cohort

The 17 (out of the 20) N-SGA placentas that were only tested once with the first panel (and, therefore, still had available tissue) were validated for cluster inclusion using the second qPCR decision tree (**Table 31**). Of these, 11 (65%) showed complete agreement between the microarray and qPCR cluster assignment, while two samples (12%) were on the border of the correct and an incorrect cluster by qPCR, and four samples (24%) were falsely classified (**Figure 38**). Interestingly, samples with cluster disagreement between the two molecular analyses (microarray and qPCR) plotted near the border of the two possible clusters by PCA of the microarray expression data from Chapter 5 (**Figure 38**). As such, this second qPCR panel appears to fairly accurately reflect the global transcriptional profiles of the PE and SGA cohort samples belonging to clusters 1-4 (Chapters 3 and 5).

Table 31 – Mean C_T values (and differences between them) for the validation of the FLT1, TAP1, and LIMCH1 qPCR panel in the remaining 17 normotensive SGA placentas from Chapter 5 with available tissue.

Microarray cluster	FLT1	TAP1	LIMCH1	FLT1-LIMCH1	TAP1-LIMCH1	qPCR cluster
1	19.828	26.467	20.626	-0.798	5.841	1
1	18.732	24.870	19.633	-0.901	5.237	1
2	18.110	25.002	19.952	-1.842	5.051	1
3	17.357	23.636	19.546	-2.189	4.090	3
1	17.531	24.164	19.255	-1.724	4.909	1
1	18.956	25.580	20.695	-1.739	4.885	1
1	18.797	25.239	20.041	-1.244	5.197	1
1	17.106	23.769	18.444	-1.338	5.325	1
2	16.986	25.208	19.267	-2.281	5.941	1/2
1	18.106	25.378	20.372	-2.266	5.006	1
2	16.059	22.545	19.129	-3.070	3.416	3
1	18.976	24.432	20.297	-1.321	4.135	1/4
3	15.944	22.885	19.435	-3.490	3.450	3
2	17.074	24.790	20.073	-2.999	4.717	2
2	17.213	23.926	18.912	-1.699	5.014	1
1	17.597	22.981	19.309	-1.712	3.672	4
2	16.488	23.588	19.245	-2.757	4.343	2

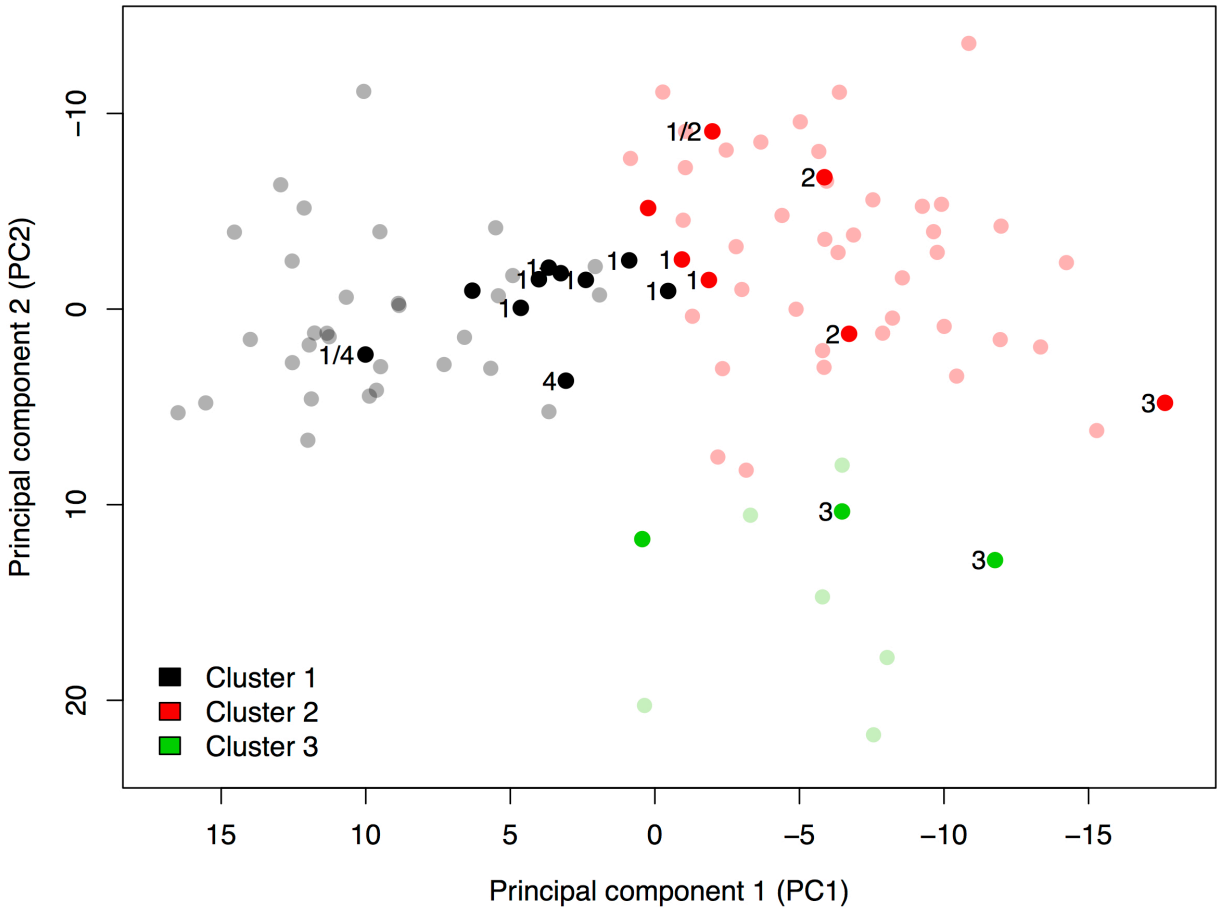

Figure 38 – Principal component analysis (PCA) plot of the microarray data from Chapter 5. Of the 20 normotensive, small-for-gestational-age (N-SGA) placentas presented in Chapter 5 (fully colored), 17 were validated for cluster inclusion using the second FLT1, LIMCH1, and TAP1 qPCR panel. Of these, 11 (65%) showed complete agreement between the microarray (colors black, red, and green representing clusters 1-3) and qPCR (numbers 1-4 representing clusters 1-4) cluster assignment, while two samples (12%) were on the border of the correct and an incorrect cluster by qPCR (shown with a "/"), and four samples (24%) were falsely classified. Samples with cluster disagreement between the two molecular analyses (colors and numbers) plotted on the border of the two possible clusters by PCA, indicating transcriptional contributions from both groups. The 77 samples from the PE cohort utilized in Chapter 5 are shown in semi-transparent colors.

6.3.7 Application of the second qPCR panel to two new pathological placentas

Lastly, this second qPCR panel (with TAP1, LIMCH1, and FLT1) was applied to two placentas from the same women four years apart (2012 and 2016) as part of a case study collaboration with Dr. David Grynspan. Clinically, her first pregnancy was diagnosed as HELLP with a borderline small-for-gestational-age male infant (~10^{th} percentile for birth weight at 34 weeks) delivered by emergency cesarean section. Histopathological assessment by Dr. Grynspan revealed significant syncytial knots and advanced villous maturity, along with focal perivillous fibrin deposition, which are considered signs of maternal vascular malperfusion (Chapters 4 and 5). Molecularly, this 2012 placenta revealed high FLT1 expression, but also higher TAP1 expression, and was, thus, classified as cluster 3 (**Table 32**).

The woman's second pregnancy, in 2016, was normotensive with a female SGA infant born at 36 weeks and 5 days with signs of pathological growth restriction (slowed growth, high umbilical artery PI, uterine artery notching, and birth weight <3^{rd} percentile). Histologically, this placenta showed evidence of massive perivillous fibrin deposition (MPFD) and villitis of unknown etiology (VUE), which are immunological-based indications of a maternal-fetal interface disturbance and chronic inflammation. The qPCR panel revealed highly elevated TAP1 expression, as well as upregulated FLT1, also classifying this placenta as cluster 3 (**Table 32**).

Table 32 – Mean C_T values (and differences between them) for the classification of two new case study placentas using the FLT1, TAP1, and LIMCH1 qPCR panel.

Pregnancy year	FLT1	TAP1	LIMCH1	FLT1-LIMCH1	TAP1-LIMCH1	Classification
2012	25.855	32.331	30.231	-4.376	2.100	Cluster 3
2016	27.741	32.508	31.954	-4.213	0.554	Cluster 3

6.4 Discussion

The first goal of this chapter was to investigate if the gene expression differences observed by microarray could be recapitulated in a qPCR analysis. Using 33 placentas from the PE-focused cohort (Chapters 3 and 4), 79% (11/14) of the tested genes exhibited significant correlations between the microarray and qPCR values. Interestingly, the three genes that did not correlate had previously demonstrated mean expression levels in the bottom quartile of all genes by microarray (Chapter 3). As a main limitation of microarray analysis is the difficulty in discerning true expression differences from background noise [703], we believe that this may have been the issue for these three potential markers, despite the application of background-correction techniques. As such, we propose that this bottom expression quartile of genes is unreliable and should be filtered out, a suggestion that has already been applied to the SGA cohort microarray analysis in Chapter 5.

The second goal of this chapter was to determine if a smaller group of genes was capable of separating placentas into clusters 1-5. Using the qPCR values for targets with correlating microarray and qPCR results, the PE cohort samples in clusters 1-4 could be fairly accurately discerned, but cluster 5, once again, could not be identified. Instead, these placentas were classified into clusters 1, 2, or 3, depending on their clinical and histopathological characteristics (Chapters 3 and 4). This indicates that the chromosomal abnormality-associated changes in gene expression responsible for the formation of cluster 5 are likely in addition to changes in gene expression caused by disease. As such, classification of cluster 5 samples using targeted qPCR (and/or histology) presumably results in more biologically meaningful cluster assignments for these placentas.

An additional finding of interest in this chapter was that cluster 2 members were again accurately identified using the known PE markers FLT1 and ENG, consistent with the results in Chapter 2. This was, of course, expected given that these placentas exhibit other “canonical” molecular, histological, and clinical features of preeclampsia. What was unexpected, however, was that the expression of the gene FSTL3 was more specifically enriched in the PE placentas than FLT1 or ENG. This protein-coding gene is an inhibitor of activin A, and, similar to FLT1 and ENG, has been previously found to be elevated in response to hypoxia [704]. Unfortunately, attempts to utilize FSTL3 in a small three-gene qPCR panel for the discrimination of clusters 1-4 could not

be validated, despite initial success in the PE cohort placentas. Currently, two potential explanations exist for the elevated C_T values observed in the SGA testing cohort for FSTL3. First, since FSTL3 is generally a shorter mRNA with only one targeted splice variant, compared to LIMCH1, TAP1, and FLT1 (2525bp versus 5852-6187bp, 2234-2974bp, and 1911-7123bp, respectively) [705], it is possible that the RNA could have preferentially degraded at this site [610]. The second potential explanation is that FSTL3 was inefficiently converted from RNA to cDNA in the SGA cohort samples due to a difference in the method used: in the PE cohort, a complex multi-step protocol involving a number of reagents from different companies was employed to convert the RNA to cDNA (**Appendix A**), whereas in the SGA cohort, the ThermoFisher High-Capacity RNA-to-cDNA™ Kit was utilized as a two-step streamlined approach. Specific differences include the random hexamers and the SuperScript™ II Reverse Transcriptase (ThermoFisher), a genetically engineered murine leukemia virus reverse transcriptase (RT), used in the individual reagent method in contrast to the random octamers and the wild-type RT, which can have less thermal stability [706], contained in the kit. Furthermore, the two methods may be differentially affected by the higher order RNA structure of FSTL3, which would influence its reverse transcription. Unfortunately, additional placental tissue from the SGA patients was not available for re-extraction and re-assessment to test any of these theories. Regardless, FSTL3 was considered to be an inconsistent marker and was, therefore, replaced.

Ultimately, the main finding of this chapter was that expression differences between LIMCH1, TAP1, and FLT1 genes were generally sufficient for discerning between both PE and SGA placentas belonging to clusters 1, 2, 3, and 4 by qPCR. LIMCH1 is involved in the organization of the actin cytoskeleton, gene transcription, and RNA processing [707], while TAP1, specifically upregulated in the immune-associated clusters, is implicated in antigen presentation and HLA expression on the cell surface [708]. As such, this small qPCR panel is a simple and convenient research tool for the subclassification of PE and suspected FGR placentas into "mild", "canonical", and "immunological" pathology groups. This may be useful for subtyping samples into clusters prior to performing other large-scale studies (ex. metabolomics or maternal blood arrays) or for interrogating subtype-specific responses to treatment.

Additionally, this second validated three-gene qPCR panel was discovered to have possible clinical utility as well. When applied to two case study placentas, the panel revealed molecular

similarity between the samples that was not evident histologically or clinically. In particular, the placenta from the woman's first pregnancy demonstrated an immunological signature that may have been an early sign of the maternal anti-fetal rejection response that took place in the second pregnancy [406]. Further, the original 2012 placenta contained evidence of focal perivillous fibrin deposition. While currently classified as a maternal vascular malperfusion lesion [385], a strong relationship between this histological feature and other immune-associated lesions has been observed (Chapter 4). Therefore, by subjecting a delivered placenta to the LIMCH1, TAP1, and FLT1 qPCR panel, and considering a re-classification or dual classification of the focal perivillous fibrin lesion, this may have significant predictive value for a woman's next pregnancy.

7 Chapter 7 – Overall Discussion

7.1 Summary of Findings and Interpretation

Preeclampsia and fetal growth restriction are two of the most common pathologies of pregnancy. Despite decades of research into the underlying etiologies of these disorders, as well as attempts to identify robust predictive markers and effective therapeutic interventions, no one single marker, treatment, or cause has been found to apply to the entire clinical spectrum of observed disease. Given the complexity of a healthy pregnancy, involving considerable maternal, fetal, and placental contributions, it is not surprising that substantial heterogeneity is observed in cases of pathology, with a wide range of potential etiologies or combinations of etiologies that may result in maternal and/or fetal symptoms. As such, a diagnosis of PE and/or FGR is associated with a number of clinical presentations and placental transcriptional and histological observations, likely due to the existence of multiple underlying disease subtypes [152, 153, 212, 556, 640, 688]. The primary goal of this thesis, therefore, was to test the hypothesis that these subtypes of PE and FGR could be elucidated using unsupervised molecular clustering techniques, and would demonstrate increased homogeneity for both clinical and histopathological characteristics.

Unsupervised clustering of placental gene expression in three overlapping large cohort microarray datasets revealed 3-5 clusters, depending on the study. Three clinically relevant subtypes of PE placentas were consistently identified within clusters 1-3, and were eventually found to each co-cluster with a group of placentas from normotensive pregnancies with confirmed SGA and suspected FGR (**Table 33**). Within cluster 1, PE and suspected FGR samples were associated with less severe clinical outcomes, molecular similarity to healthy term controls, and either no placental pathology or mild maternal vascular malperfusion lesions. This cluster, therefore, may contain a number of possible underlying groups: “mild” PE or FGR due to mild placental dysfunction, “maternal” PE caused predominately by subclinical maternal cardiovascular disease, “fetal” FGR due to an unknown fetal cause of pathology, and constitutionally small SGA infants, which would all be expected to be associated with relatively healthy placentas and cannot be properly distinguished with the currently available data. Cluster 2 PE and FGR placentas revealed overwhelming evidence of “canonical” maternal vascular

malperfusion pathology, lesions thought to develop as a consequence of reduced trophoblast invasion of the maternal decidua, poor spiral artery remodeling, and hypoxic damage, and linked to increased placental expression of the anti-angiogenic markers FLT1 and ENG, as well as other genes involved in hypoxia, hormone secretion, and metabolism. Cluster 3 PE and FGR samples displayed signs of an "immunological" pathology, with considerable differential expression of genes related to immune response, inflammatory response, apoptosis, and cytokine activity, and histological lesions with proposed affiliations to allograft rejection, such as MPFD, MFI, and VUE [222, 406]. In the largest investigated transcriptional dataset (Chapter 3, N=330), an additional two clusters were identified. Cluster 4 samples were preterm controls with clinical and histological chorioamnionitis (**Table 33**), while cluster 5 was associated with confined placental mosaicism, and contained some PE patients, but demonstrated no clinical, epigenetic [683], or histological cohesion. Furthermore, some patients displayed an intermediate phenotype between two of these clusters and were found to plot on the border of the two possible core groups by principal component analysis (PCA). As such, while the discovery of placental subtypes of PE and FGR using unsupervised clustering methods was successful, the heterogeneity within these pathologies may be even more extensive than anticipated.

Cluster 1 appears to contain PE and suspected FGR patients with both healthy and mild pathology placentas. However, our ability to separate these two groups is limited. It is also feasible that they are not truly distinct groups, but are instead the result of sampling differences. In cases where pathology is minimal, and not widespread across the placenta, the fact that biopsies were only taken from four locations across the tissue, and that the snap-frozen samples for microarray and the FFPE samples for histology were not the exact same biopsies, may have a greater impact. Simply by chance, regions without placental alterations could be sampled, resulting in the impression of a completely healthy tissue in a mild pathology placenta, or vice versa. These cluster 1 placentas may, therefore, be those that would benefit the most from a higher sampling rate. Furthermore, given the considerable clinical outcome heterogeneity still observed within this cluster, this is also the group that may greatly benefit from an increase in sample size, as well as the addition of a non-placental source of information (ex. maternal tissue).

Within these cohorts, the "canonical" maternal vascular malperfusion pathology characteristic of cluster 2 PE and FGR placentas appears to exist in a gradient of severity that is linked to the

severity of clinical outcomes (maternal hypertension levels, degree of fetal growth restriction, and gestational age), as well as the severity of placental FLT1 and ENG expression. Mild canonical pathology is associated with insufficient transcriptional changes for cluster 2 membership, and these patients generally fall into clusters 1 or 3, depending on the presence or absence of a co-occurring immune signature. This gradient of MVM pathology also exhibits a significant correlation with uterine and umbilical artery pulsatility indices during pregnancy. Therefore, while not all PE patients demonstrate significantly elevated Doppler ultrasound parameters or anti-angiogenic marker expression, those that do are likely robustly affiliated with MVM placental lesions. These findings support the notion that Doppler metrics and FLT1/ENG expression are predictive of "canonical" pathology, not necessarily PE or FGR themselves [359, 400-402, 451].

Possibly the most useful finding of this project was the separation of severe PE and pathological FGR patients into two distinct populations: cluster 2 and cluster 3. Both of these clusters demonstrate clinical, transcriptional, and histopathological features previously described in PE/FGR [2, 6, 150, 387-390, 392, 652], but this is the first time these two placenta-based pathology groups have been identified and distinguished, not just described. Additionally, a small qPCR panel of genes has been developed with the capacity to separate these two subtypes of pathological placentas. This panel may have considerable utility for classifying samples before performing any mechanistic experiments, which would likely only be applicable for one of the subtypes, as well as after delivery for any biomarker or therapeutic intervention investigation to determine if the marker or treatment in question was successful for a particular group. In this way, the true value of many prior PE/FGR findings that were, in actuality, driven by one specific subtype may be "unmasked". The qPCR panel may also have clinical utility as the cluster 3-associated maternal-fetal interface disturbance and chronic inflammation pathologies are associated with extremely high rates of recurrence in subsequent pregnancies [150, 405, 407, 408, 417, 419, 420].

Compared to the "canonical" cluster 2, the cluster 3 immunological pathology has not been as thoroughly assessed and is still poorly understood. The frequent identification of upregulated TNF expression in these placentas could indicate considerable villous damage [292], which may be triggering the widespread deposition of fibrin in the intervillous space, consistent with a massive perivillous fibrin deposition diagnosis. The initial source of the villous damage is not

fully elucidated, but an allograft rejection would be expected to result in an influx of maternal immune cells into the placenta, which could be responsible for this trophoblast injury [669, 672]. Interestingly, within the three histology studies included in the current thesis (PE cohort, SGA cohort, and case study samples), eight placentas were scored with MPFD, six of which were female. Therefore, within these datasets, female placentas (N=80) were 3.3 times more likely to be diagnosed with MPFD than male placentas (N=84) (p=0.16 by Fisher's exact test). However, this is likely not because females more commonly trigger an immune rejection response from the mother, quite the opposite. Although not well investigated, male infants associated with MPFD pathology are thought to result in worse clinical outcomes, such as miscarriage and stillbirth. This is not surprising given that male infants have been shown to be particularly affected by maternal alloimmunization [709], have been linked to increased rates of spontaneous abortions among anatomically normal fetuses [710], and their placentas have less reserve capacity to compensate for damage if pathology occurs [711]. Since we only collected placentas affiliated with live births, these more severe MPFD (more commonly male) samples would not have been included.

Additionally, within cluster 3, a group of BioBank placentas was initially identified associated with preterm deliveries, PE, and suspected FGR, but demonstrated transcriptional-histological discordance and severe maternal vascular malperfusion lesions. These samples are likely predominately responsible for the low cluster 3 stability discovered in Chapter 3 by bootstrapping (55%), as these placentas switch to cluster 2 when assessed again in Chapter 5 (although they still border cluster 3 by PCA). These patients demonstrate an interesting intermediate phenotype, where the dominant pathology appears to be canonical, but an immunological transcriptional signature is present. The first case study placenta from 2012 (Chapter 6) likely also belongs to this group. It is possible that placental biopsy differences, including cell composition differences, between the snap-frozen (microarray) and FFPE (histology) samples could be responsible for the existence of this intermediate subtype, although this would not explain the case study sample where qPCR was performed on RNA extracted from the FFPE tissue. It is also feasible that a mild increase in the number of invading maternal immune cells could induce some placental gene expression changes, but be insufficient to result in the observation of immune-related histopathology lesions. Furthermore, as observed in Chapter 6, this could be indicative of a future allograft rejection response, and, therefore, the

discovery of placentas belonging to this intermediate subtype after delivery may provide important information for a woman's next pregnancy.

Cluster 5 was by far the least stable group identified in these analyses. In Chapter 3, this distinct cluster was uncovered based on its global pattern of gene expression, but exhibited no clear pathway enrichments or unique clinical associations, and was eventually found to be driven by confined placental mosaicism in a maximum of 10-20% of biopsied placental cells. In the remaining chapters, cluster 5 showed no distinct histological lesions, and could not be discovered using targeted qPCR methods, but instead, samples fell into clusters 1-3 with improved clinical significance. Moreover, when some of these placentas that were linked to a co-occurring diagnosis of maternal hypertension and FGR were re-clustered again in Chapter 5 in a smaller dataset, they were not sufficiently powered to form their own cluster, although they were visibly different by PCA. Therefore, we conclude that cluster 5 is not a pathologically or clinically significant group, and its formation was likely only due to chance biopsying of more regions of CPM in these placentas [336]. As such, while caution is necessary for large-scale gene expression studies, samples with CPM will simply merge into more clinical relevant groups by histology and qPCR. The same conclusion concerning cluster 5 was also established in our recent DNA methylation study of cluster 1, 2, 3, and 5 placentas [683].

Table 33 – Dominant clinical, transcriptional, and histological characteristics of the core clusters 1-4 and the intermediate phenotypes.

	Clinical features[a]	**Transcriptional changes**	**Histopathological observations**
Core cluster 4	Very preterm deliveries (<30 weeks) Normotensive mothers AGA infants	Cell cycle, cell proliferation, DNA damage, inflammation	Chorioamnionitis
Cluster 1/4 intermediate group	Healthier placental gene expression with chorioamnionitis and placentas with elevated cell cycle and inflammation genes but no chorioamnionitis		
Core cluster 1	Normotensive, AGA delivered term or late preterm (30-34 weeks) "Maternal" PE Constitutionally small infants	Healthy	Minimal pathology
Cluster 1/2 intermediate group	PE or FGR with "mild" canonical pathology Relatively healthy clinical outcomes and insufficient transcriptional changes to belong to cluster 2		
Core cluster 2	Generally at least two of PE, FGR, and preterm delivery High uterine and umbilical artery PIs Severe PE symptoms High maternal BMI	Hormone secretion and activity, hypoxia, glycolysis, metabolism	Maternal vascular malperfusion (MVM) lesions
Cluster 2/3 intermediate group	PE and FGR with MVM lesions but immune-related gene expression		
Core cluster 3	Later preterm deliveries (30-37 weeks) FGR +/- PE Poor umbilical artery blood flow and narrow umbilical cords	Immune response, inflammatory response, hypoxia, apoptosis, allograft rejection, cytokine activity	Maternal-fetal interface disturbance and chronic inflammation lesions

[a]AGA= average-for-gestational-age, PE = preeclampsia, FGR = fetal growth restriction, BMI = body mass index, PI = pulsatility index

7.2 Limitations

The primary limitation of this project is the use of end-stage placental tissue for understanding underlying pathological etiologies (**Figure 39**). Although we believe that the considerable molecular, histological, and clinical distinctions observed across the clusters strongly implies that different originating insults are responsible for the presentation of PE/FGR in the different subtypes, this cannot be confirmed with the current data. Future work involving *in vitro* [712] and *in vivo* models will determine if the observation of multiple outcomes (clusters) is really due to multiple initial causative insults or one insult that is modified by maternal and environmental agents to different end stages. Certain animal models of PE and FGR are likely more suitable for the investigation of particular subtypes: maternal and genetic modifications for cluster 1 [584, 585, 588-590, 596], restriction of uterine blood flow, hypoxia, and angiogenic profile alterations for cluster 2 [321, 323, 581-583, 586, 594, 595], and immune system modulation for cluster 3 [587], and will, therefore, be essential for resolving this limitation.

Another potential concern is the effect of gestational age on the formation of the clusters. In all analyses, GA was significantly different across the clusters, with older placentas in cluster 1, and the early-onset PE and chorioamnionitis-affiliated preterm controls in clusters 2 and 4, respectively, driving early mean gestational ages in these groups. Since GA is so tightly correlated to clinical outcome and pathology, it was not controlled for in the clustering or direct assessments of differential expression, although it may significantly impact the measured expression values of various genes. PlGF is a good example of this problem. In healthy control pregnancies, levels of PlGF are expected to increase until 29-32 weeks of gestation, before dropping in the last two months of pregnancy [65]. As such, early-onset PE placentas delivered before or around 30 weeks could show higher or similar levels of placental PlGF to term controls simply due to differences in gestational age, even if these delivered PE samples have reduced PlGF expression for that particular GA. Therefore, correcting for GA may improve or alter our analysis, but will first require establishing the normal trajectory of expression for all individual genes on a week-by-week basis (currently available datasets group an entire trimester together [256]), which will be difficult to accomplish without confounding with preterm pathology. Measurements of placental RNA in maternal serum may be able to help with this issue, although perhaps only for genes expressed by placental cell types in contact with maternal blood [383].

In contrast, gestational age is considered in the histopathology analysis, where the expected villous maturity and quantity of syncytial knots is well established for any given GA [255]. As such, this could be at least partially responsible for some of the observed discrepancies between the transcriptional and histological results in this project. For example, a similar amount of placental infarctions and syncytial knots could be theoretically observed in a younger PE placenta and a term control placenta, associated with similar transcriptional changes. However, in the control, this would likely be given a histology score of zero because these lesions are expected to accumulate throughout pregnancy, but in the PE sample, a score of 1 or 2 would be noted. In this way, a histological difference could be discovered without a corresponding gene expression difference.

Otherwise, the integration of the transcriptional and histological data types provides complementary information and both compensate well for the other's limitations. The microarray assessment is more unbiased but can be subject to a number of computational issues that can affect the results [703], including the observed problem with background noise interfering with the accurate identification of differential expression in lowly expressed genes. On the other hand, histology has more immediate clinical applicability but is linked to known issues of observer bias [384], although we have minimized this concern by performing a blinded assessment with a standardized scoring rubric. Additionally, since these two analyses were not performed on the exact same tissue biopsies, and the placenta is such a heterogeneous organ [261-264], cell composition could be a significant contributing factor to any observed intra-sample difference. This sampling variably, and the resulting discrepancies in cell composition, could also contribute to inter-sample differences, which is a major criticism of both the current project and most prior placental studies. Very recent single-cell and cell-type specific investigations should start to rectify this issue [382, 383].

Finally, an important limitation of this thesis revolves around sample selection and pathology diagnosis. A number of essential clinical outcome groups were excluded or under-represented in these studies, including chronic hypertension, gestational hypertension, diabetes, maternal obesity with PE, normotensive preterm delivery with suspected FGR, stillbirth, SGA with no suspected FGR, etc. As such, additional placental subtypes of these pathologies may exist that were not discoverable in the current cohorts. These samples were also collected as a retrospective case-control study, and, therefore, the frequency of the observed lesions and pathology groups

are not representative of a true clinical population. Furthermore, PE diagnoses in the assessed patients were established based on the original Canadian criteria that required maternal proteinuria [71]. As such, some of the CH women may warrant a diagnosis of PE under the new (2014) requirements [1]. However, the samples that are more likely to merit a re-classification are those that fell into clusters 2 and 3, and the unsupervised analysis has identified them as pathological regardless.

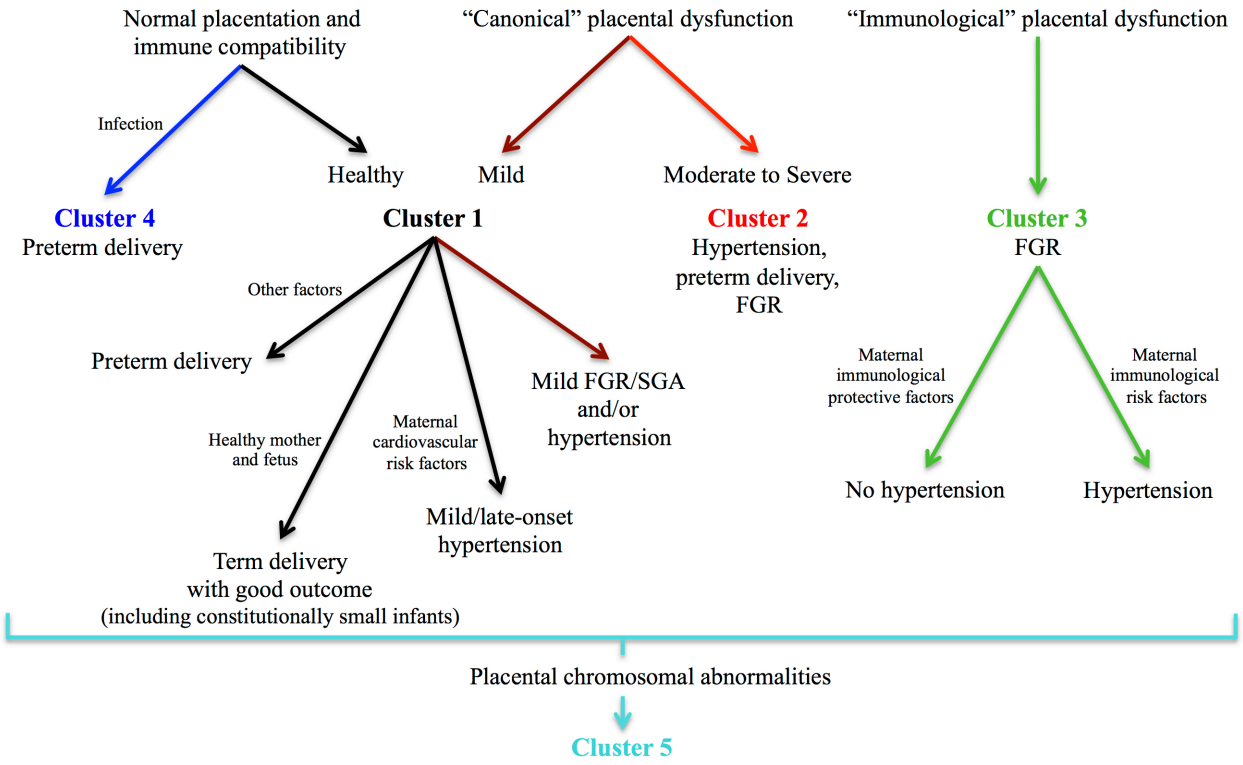

Figure 39 – Possible underlying etiologies resulting in placentas belonging to clusters 1-5. These will require additional investigations using *in vitro* and *in vivo* models.

7.3 Future Directions

One of the main future directions for this project is the expansion of the analyzed cohort to include a wider range of potential pregnancy complications. While we have assessed 350 placentas by microarray, a number of co-occurring pathologies (ex. preterm delivery and FGR) and healthier clinical presentations (ex. gestational hypertension and definitive non-FGR SGA) were not selected. Therefore, although our investigation has considerably improved upon prior studies by simultaneously assessing many different outcome groups, it is still possible that additional subtypes of PE and FGR exist and could be identified with a further increase in sample size. Furthermore, the addition of samples associated with other frequently co-occurring pathologies of pregnancy, such as stillbirth or diabetes, preferably as part of a prospectively collected cohort, would also be of interest in order to assess potential similarities and differences between these disease states at the placental level and improve the clinical applicability of the findings.

Also, as mentioned above, previously attempted therapeutics for PE and FGR should be re-evaluated with the knowledge of placental subtypes, as certain groups would be expected to respond more favorably than others. This is also true for previously discovered potential biomarkers. For example, sFLT1 and sENG may have considerable predictive value for cluster 2, while promising markers and treatments in transplantation medicine should be tested for application in cluster 3. Additionally, different subtypes likely carry varying degrees of risk for particular maternal and neonatal/infant/child post-pregnancy health outcomes (ex. maternal cardiovascular disease [93], infant allergy development [713], etc.), which should be investigated. As such, a future direction would involve the prediction of these possible long-term consequences from the transcriptional and histological information available in the placenta at delivery. The established qPCR panel may be helpful for this goal.

While some progress has been made towards understanding the formation of cluster 3, further assessment is necessary. In Chapter 3, relationships between immunological PE development and maternal blood type and pregnancy history were discovered. With the addition of the normotensive FGR cluster 3 patients in Chapter 5, the blood type association no longer held, but a potential link between having experienced a prior miscarriage and avoiding the development of this specific subtype of PE was still observed. This could be an interesting correlation, and is

another example of a previous PE-related finding [22] that was likely driven by a particular subset of PE patients. However, without extensive clinical information, specifically related to partner changes between pregnancies, this relationship cannot be fully comprehended and is, therefore, a future direction. Moreover, there is evidence of possible increased maternal immune cell infiltration into the cluster 3 placentas, based on the identification of intermediate cluster 2/3 transcriptional-histological discordant samples, the unexpected HLA gene enrichments, and the histological discovery of lesions affiliated with maternal immune cells in the intervillous space (ex. chronic intervillositis) [420]. As such, the quantification of T cells, B cells, natural killer cells, monocytes, and granulocytes by immunohistochemistry in cluster 3 slides, compared to the other clusters, is currently ongoing.

Another essential future direction is the improvement of placental sampling methods and tissue-specific tools for analysis. The lack of biological cohesion observed in cluster 5 indicates that it was likely by chance that more regions of CPM were biopsied. As such, four biopsies per placenta is still probably too few. Exactly how many are necessary is unknown, but ten sites per placenta has been proposed [264]. It is also important that these multiple biopsies from a given placenta are assessed separately, as well as decomposed into distinct cell types [382, 383, 714]. In this way, the contributions of individual placental regions and placental trophoblast, endothelial, stromal, and immune cell populations to pathology can be elucidated, and the frequency of mosaicism can be ascertained. Furthermore, in the pathway enrichment analyses, fewer significant gene sets are consistently discovered in cluster 2 samples, compared to cluster 1, than in cluster 3 samples. Since cluster 2 is a fairly homogeneous group, this is most likely occurring because these patients have a placenta-specific pathology, and human placenta-focused gene sets have not been well established. Cluster 3, with its immune-based pathology, can be more easily described with the currently available resources [715]. Therefore, the development of placenta-specific human gene sets is a future goal.

Lastly, the most critical future direction is the investigation of placentas with available matched maternal samples, such as maternal serum and/or endothelial cells. Our studies have revealed a considerable number of distinct clinical outcomes that cannot be explained by placental differences (ex. PE versus CH pregnancies and hypertensive versus normotensive FGR pregnancies), and are thus likely the result of maternal (mal)adaptations to pregnancy. Additionally, placentas with mild canonical pathology appear to be associated with either PE or

FGR, but not both, and this split must involve placenta-extrinsic factors (although they could also be fetal or environmental, not necessary just maternal). Furthermore, the identification of biomarkers for these individual clusters, which are measurable sufficiently early in pregnancy such that appropriate interventions can be initiated, will also require the assessment of maternal serum/blood. As such, a combined investigation of placental and maternal samples to discover any maternal differences between the placental subtypes is currently ongoing.

7.4 Conclusions

Overall, this thesis provides new insight into the placental heterogeneity observed in preeclampsia and fetal growth restriction. Multiple placental subtypes of both pathologies have been identified, which can be separated after delivery using the developed three-gene qPCR panel, and may reveal important information for a woman's next pregnancy. It is also essential that robust biomarkers for predicting these different PE/FGR subtypes are established, as these patients would likely benefit from different therapeutic interventions early in gestation. Additionally, we have demonstrated that late-onset PE may potentially be both a mild version of early-onset PE (in cluster 1) and a different pathology altogether (in cluster 3), and that the discovery of maternal serum markers for clusters 2 and 3 would be helpful towards the goal of distinguishing between constitutionally small and pathologically growth restricted SGA patients during pregnancy. However, somewhat surprisingly, samples associated with similar clinical outcomes do not necessarily demonstrate similar placental profiles. Conversely, although each of clusters 1-4 were linked to certain characteristic phenotypes (ex. the odds of PE in cluster 2 is much higher than in cluster 1), co-clustering placentas can demonstrate a variety of clinical features. While it is feasible that critical placental layers of information are still missing, a possibility that is supported by the considerable improvement observed with the addition of the histological scoring to the transcriptional data, it is likely that unmeasured maternal (and fetal) factors are involved in the development and severity of symptoms and pathology. As such, a larger study with a wider range of clinical groups and matched maternal and placental samples is required to enhance our understanding of these currently identified subtypes, discover additional subtypes, and reveal biomarkers and potential therapeutic targets for each individual pathology group. This personalized medicine approach to PE and FGR will no doubt improve short- and long-term health outcomes for both the mother and the child.

8 Chapter 8 – References

1. Magee LA, Pels A, Helewa M, Rey E, von Dadelszen P, Audibert F, Bujold E, Côté AM, Douglas MJ, Eastabrook G, Firoz T. Diagnosis, evaluation, and management of the hypertensive disorders of pregnancy: executive summary. Journal of Obstetrics and Gynaecology Canada. 2014 May 1;36(5):416-38.
2. Wang A, Rana S, Karumanchi SA. Preeclampsia: the role of angiogenic factors in its pathogenesis. Physiology. 2009 Jun;24(3):147-58.
3. Ghulmiyyah L, Sibai B. Maternal mortality from preeclampsia/eclampsia. In Seminars in perinatology 2012 Feb 1 (Vol. 36, No. 1, pp. 56-59). Elsevier.
4. Steegers EA, von Dadelszen P, Duvekot JJ, Pijnenborg R. Pre-eclampsia. The Lancet. 2010 Aug 21;376(9741):631-44.
5. Walker JJ. Pre-eclampsia. The Lancet. 2000 Oct 7;356(9237):1260-5.
6. Myatt L. Role of placenta in preeclampsia. Endocrine. 2002 Oct 1;19(1):103-11.
7. Kramer MS, Demissie K, Yang H, Platt RW, Sauvé R, Liston R, Fetal and Infant Health Study Group of the Canadian Perinatal Surveillance System. The contribution of mild and moderate preterm birth to infant mortality. JAMA. 2000 Aug 16;284(7):843-9.
8. van Esch JJ, van Heijst AF, de Haan AF, van der Heijden OW. Early-onset preeclampsia is associated with perinatal mortality and severe neonatal morbidity. The Journal of Maternal-Fetal & Neonatal Medicine. 2017 Dec 2;30(23):2789-94.
9. Altman D, Carroli G, Duley L, Farrell B, Moodley J, Neilson J, Smith D. Do women with pre-eclampsia, and their babies, benefit from magnesium sulphate? The Magpie Trial: a randomised placebo-controlled trial. The Lancet. 2002 Jun;359(9321):1877-90.
10. Wallis AB, Saftlas AF, Hsia J, Atrash HK. Secular trends in the rates of preeclampsia, eclampsia, and gestational hypertension, United States, 1987–2004. American journal of hypertension. 2008 May 1;21(5):521-6.
11. Hutcheon JA, Lisonkova S, Joseph KS. Epidemiology of pre-eclampsia and the other hypertensive disorders of pregnancy. Best practice & research: Clinical obstetrics & gynaecology. 2011 Aug 1;25(4):391-403.
12. Jeyabalan A. Epidemiology of preeclampsia: impact of obesity. Nutrition reviews. 2013 Oct 1;71(suppl_1):S18-25.
13. Janssen I. The public health burden of obesity in Canada. Canadian journal of diabetes. 2013 Apr 1;37(2):90-6.
14. Bartsch E, Medcalf KE, Park AL, Ray JG. Clinical risk factors for pre-eclampsia determined in early pregnancy: systematic review and meta-analysis of large cohort studies. BMJ. 2016 Apr 19;353:i1753.
15. Weissgerber TL, Mudd LM. Preeclampsia and diabetes. Current diabetes reports. 2015 Mar 1;15(3):9.
16. Bregar AT, Tul N, Vodušek VF, Verdenik I, Lucovnik M, Janša V, Blickstein I. A dose–response relation exists between different classes of pre-gravid obesity and selected perinatal outcomes. Archives of gynecology and obstetrics. 2017 Sep 1;296(3):465-8.

17. Challier JC, Basu S, Bintein T, Minium J, Hotmire K, Catalano PM, Hauguel-de Mouzon S. Obesity in pregnancy stimulates macrophage accumulation and inflammation in the placenta. Placenta. 2008 Mar 1;29(3):274-81.

18. Myatt L, Maloyan A. Obesity and placental function. Semin Reprod Med. 2016;34:42-9.

19. Zera CA, Seely EW, Wilkins-Haug LE, Lim KH, Parry SI, McElrath TF. The association of body mass index with serum angiogenic markers in normal and abnormal pregnancies. American Journal of Obstetrics & Gynecology. 2014 Sep 1;211(3):247-e1.

20. Lecarpentier E, Tsatsaris V, Goffinet F, Cabrol D, Sibai B, Haddad B. Risk factors of superimposed preeclampsia in women with essential chronic hypertension treated before pregnancy. PloS one. 2013 May 6;8(5):e62140.

21. Sibai BM, Koch MA, Freire S, e Silva JL, Rudge MV, Martins-Costa S, Moore J, de Barros Santos C, Cecatti JG, Costa R, Ramos JG. The impact of prior preeclampsia on the risk of superimposed preeclampsia and other adverse pregnancy outcomes in patients with chronic hypertension. American Journal of Obstetrics & Gynecology. 2011 Apr 1;204(4):345-e1.

22. Mol BW, Roberts CT, Thangaratinam S, Magee LA, De Groot CJ, Hofmeyr GJ. Pre-eclampsia. The Lancet. 2016 Mar 5;387(10022):999-1011.

23. Chappell LC, Enye S, Seed P, Briley AL, Poston L, Shennan AH. Adverse perinatal outcomes and risk factors for preeclampsia in women with chronic hypertension: a prospective study. Hypertension. 2008 Apr 1;51(4):1002-9.

24. Platt R. The nature of essential hypertension. In Essential Hypertension 1960 (pp. 39-52). Springer, Berlin, Heidelberg.

25. Dharmashankar K, Widlansky ME. Vascular endothelial function and hypertension: insights and directions. Current hypertension reports. 2010 Dec 1;12(6):448-55.

26. Brennan LJ, Morton JS, Davidge ST. Vascular dysfunction in preeclampsia. Microcirculation. 2014 Jan 1;21(1):4-14.

27. Lisonkova S, Joseph KS. Incidence of preeclampsia: risk factors and outcomes associated with early-versus late-onset disease. American Journal of Obstetrics & Gynecology. 2013 Dec 1;209(6):544-e1.

28. Ghosh G, Grewal J, Männistö T, Mendola P, Chen Z, Xie Y, Laughon SK. Racial/ethnic differences in pregnancy-related hypertensive disease in nulliparous women. Ethnicity & disease. 2014;24(3):283.

29. Surapaneni T, Bada VP, Nirmalan CP. Risk for recurrence of pre-eclampsia in the subsequent pregnancy. Journal of clinical and diagnostic research: JCDR. 2013 Dec;7(12):2889.

30. Ødegård RA, Vatten LJ, Nilsen ST, Salvesen KÅ, Austgulen R. Risk factors and clinical manifestations of pre-eclampsia. BJOG: An International Journal of Obstetrics & Gynaecology. 2000 Nov 1;107(11):1410-6.

31. Phadungkiatwattana P, Rujivejpongsathron J, Tunsatit T, Yanase Y. Analyzing pregnancy outcomes in women of extremely advanced maternal age (>or=45 years). J Med Assoc Thai. 2014 Jan 1;97(1):1-6.

32. Statistics Canada. Table 102-4508 - Live births, by age and parity of mother, Canada, annual, CANSIM (database) [accessed: April 5th, 2018].

33. Lamminpää R, Vehviläinen-Julkunen K, Gissler M, Heinonen S. Preeclampsia complicated by advanced maternal age: a registry-based study on primiparous women in Finland 1997–2008. BMC pregnancy and childbirth. 2012 Dec;12(1):47.

34. Klatsky PC, Delaney SS, Caughey AB, Tran ND, Schattman GL, Rosenwaks Z. The role of embryonic origin in preeclampsia: a comparison of autologous in vitro fertilization and ovum donor pregnancies. Obstetrics & Gynecology. 2010 Dec 1;116(6):1387-92.

35. Levron Y, Dviri M, Segol I, Yerushalmi GM, Hourvitz A, Orvieto R, Mazaki-Tovi S, Yinon Y. The 'immunologic theory' of preeclampsia revisited: a lesson from donor oocyte gestations. American Journal of Obstetrics & Gynecology. 2014 Oct 1;211(4):383-e1.

36. Masoudian P, Nasr A, de Nanassy J, Fung-Kee-Fung K, Bainbridge SA, El Demellawy D. Oocyte donation pregnancies and the risk of preeclampsia or gestational hypertension: a systematic review and metaanalysis. American Journal of Obstetrics & Gynecology. 2016 Mar 1;214(3):328-39.

37. Einarsson JI, Sangi-Haghpeykar H, Gardner MO. Sperm exposure and development of preeclampsia. American Journal of Obstetrics & Gynecology. 2003 May 1;188(5):1241-3.

38. Wang JX, Knottnerus AM, Schuit G, Norman RJ, Chan A, Dekker GA. Surgically obtained sperm, and risk of gestational hypertension and pre-eclampsia. The Lancet. 2002 Feb 23;359(9307):673-4.

39. Ota E, Ganchimeg T, Mori R, Souza JP. Risk factors of pre-eclampsia/eclampsia and its adverse outcomes in low-and middle-income countries: a WHO secondary analysis. PloS one. 2014 Mar 21;9(3):e91198.

40. Xie F, Hu Y, Magee LA, Money DM, Patrick DM, Krajden M, Thomas E, von Dadelszen P. An association between cytomegalovirus infection and pre-eclampsia: a case–control study and data synthesis. Acta obstetricia et gynecologica Scandinavica. 2010 Sep 1;89(9):1162-7.

41. von Dadelszen P, Magee LA, Krajden M, Alasaly K, Popovska V, Devarakonda RM, Money DM, Patrick DM, Brunham RC. Levels of antibodies against cytomegalovirus and Chlamydophila pneumoniae are increased in early onset pre-eclampsia. BJOG: an International Journal of Obstetrics & Gynaecology. 2003 Aug 1;110(8):725-30.

42. Arechavaleta-Velasco F, Ma Y, Zhang J, McGrath CM, Parry S. Adeno-associated virus-2 (AAV-2) causes trophoblast dysfunction, and placental AAV-2 infection is associated with preeclampsia. The American journal of pathology. 2006 Jun 1;168(6):1951-9.

43. Slatter TL, Hung NG, Clow WM, Royds JA, Devenish CJ, Hung NA. A clinicopathological study of episomal papillomavirus infection of the human placenta and pregnancy complications. Modern Pathology. 2015 Oct;28(10):1369.

44. McDonnold M, Dunn H, Hester A, Pacheco LD, Hankins GD, Saade GR, Costantine MM. High risk human papillomavirus at entry to prenatal care and risk of preeclampsia. American Journal of Obstetrics & Gynecology. 2014 Feb 1;210(2):138-e1.

45. Trogstad LI, Eskild A, Bruu AL, Jeansson S, Jenum PA. Is preeclampsia an infectious disease? Acta obstetricia et gynecologica Scandinavica. 2001 Nov 1;80(11):1036-8.

46. Sansone M, Sarno L, Saccone G, Berghella V, Maruotti GM, Migliucci A, Capone A, Martinelli P. Risk of Preeclampsia in Human Immunodeficiency Virus–Infected Pregnant Women. Obstetrics & Gynecology. 2016 Jun 1;127(6):1027-32.

47. Kwon JY, Romero R, Mor G. New insights into the relationship between viral infection and pregnancy complications. American Journal of Reproductive Immunology. 2014 May 1;71(5):387-90.

48. Salonen Ros H, Lichtenstein P, Lipworth L, Cnattingius S. Genetic effects on the liability of developing pre-eclampsia and gestational hypertension. American Journal of Medical Genetics Part A. 2000 Apr 10;91(4):256-60.

49. Nilsson E, Salonen Ros H, Cnattingius S, Lichtenstein P. The importance of genetic and environmental effects for pre-eclampsia and gestational hypertension: a family study. BJOG: An International Journal of Obstetrics & Gynaecology. 2004 Mar 1;111(3):200-6.

50. Thornton JG, Macdonald AM. Twin mothers, pregnancy hypertension and pre-eclampsia. BJOG: An International Journal of Obstetrics & Gynaecology. 1999 Jun 1;106(6):570-5.

51. Rijhsinghani A, Yankowitz J, Strauss RA, Kuller JA, Patil S, Williamson RA. Risk of preeclampsia in second-trimester triploid pregnancies. Obstetrics & Gynecology. 1997 Dec 1;90(6):884-8.

52. Jebbink J, Wolters A, Fernando F, Afink G, van der Post J, Ris-Stalpers C. Molecular genetics of preeclampsia and HELLP syndrome—a review. Biochimica et Biophysica Acta (BBA)-Molecular Basis of Disease. 2012 Dec 1;1822(12):1960-9.

53. Zhao L, Triche EW, Walsh KM, Bracken MB, Saftlas AF, Hoh J, Dewan AT. Genome-wide association study identifies a maternal copy-number deletion in PSG11 enriched among preeclampsia patients. BMC pregnancy and childbirth. 2012 Dec;12(1):61.

54. Johnson MP, Brennecke SP, East CE, Göring HH, Kent Jr JW, Dyer TD, Said JM, Roten LT, Iversen AC, Abraham LJ, Heinonen S. Genome-wide association scan identifies a risk locus for preeclampsia on 2q14, near the inhibin, beta B gene. PloS one. 2012 Mar 14;7(3):e33666.

55. Srinivas SK, Morrison AC, Andrela CM, Elovitz MA. Allelic variations in angiogenic pathway genes are associated with preeclampsia. American Journal of Obstetrics & Gynecology. 2010 May 1;202(5):445-e1.

56. Bell MJ, Roberts JM, Founds SA, Jeyabalan A, Terhorst L, Conley YP. Variation in endoglin pathway genes is associated with preeclampsia: a case–control candidate gene association study. BMC pregnancy and childbirth. 2013 Dec;13(1):82.

57. Lokki AI, Daly E, Triebwasser M, Kurki MI, Roberson ED, Häppölä P, Auro K, Perola M, Heinonen S, Kajantie E, Kere J. Protective Low-Frequency Variants for Preeclampsia in the Fms Related Tyrosine Kinase 1 Gene in the Finnish Population: Novelty and Significance. Hypertension. 2017 Aug 1;70(2):365-71.

58. Morrison AC, Srinivas SK, Elovitz MA, Puschett JB. Genetic variation in solute carrier genes is associated with preeclampsia. American Journal of Obstetrics & Gynecology. 2010 Nov 1;203(5):491-e1.

59. Haggerty CL, Ferrell RE, Hubel CA, Markovic N, Harger G, Ness RB. Association between allelic variants in cytokine genes and preeclampsia. American Journal of Obstetrics & Gynecology. 2005 Jul 1;193(1):209-15.

60. Carreiras M, Montagnani S, Layrisse Z. Preeclampsia: A Multifactorial Disease Resulting from the Interaction of the Feto-maternal HLA Genotype and HCMV Infection. American Journal of Reproductive Immunology. 2002 Sep 1;48(3):176-83.

61. Quach K, Grover SA, Kenigsberg S, Librach CL. A combination of single nucleotide polymorphisms in the 3′ untranslated region of HLA-G is associated with preeclampsia. Human immunology. 2014 Dec 1;75(12):1163-70.

62. Buurma AJ, Turner RJ, Driessen JH, Mooyaart AL, Schoones JW, Bruijn JA, Bloemenkamp KW, Dekkers OM, Baelde HJ. Genetic variants in pre-eclampsia: a meta-analysis. Human reproduction update. 2013 Jan 8;19(3):289-303.

63. Sakowicz A, Pietrucha T, Rybak-Krzyszkowska M, Huras H, Gach A, Sakowicz B, Banaszczyk M, Grzesiak M, Biesiada L. Double hit of NEMO gene in preeclampsia. PloS one. 2017 Jun 27;12(6):e0180065.

64. McGinnis R, Steinthorsdottir V, Williams NO, Thorleifsson G, Shooter S, Hjartardottir S, Bumpstead S, Stefansdottir L, Hildyard L, Sigurdsson JK, Kemp JP. Variants in the fetal genome near FLT1 are associated with risk of preeclampsia. Nature genetics. 2017 Aug;49(8):1255.

65. Levine RJ, Maynard SE, Qian C, Lim KH, England LJ, Yu KF, Schisterman EF, Thadhani R, Sachs BP, Epstein FH, Sibai BM. Circulating angiogenic factors and the risk of preeclampsia. New England journal of medicine. 2004 Feb 12;350(7):672-83.

66. Leclerc F, Dubois MF, Aris A. Maternal, placental and fetal exposure to bisphenol A in women with and without preeclampsia. Hypertension in pregnancy. 2014 Aug 1;33(3):341-8.

67. Dadvand P, Ostro B, Amato F, Figueras F, Minguillón MC, Martinez D, Basagaña X, Querol X, Nieuwenhuijsen M. Particulate air pollution and preeclampsia: a source-based analysis. Occup Environ Med. 2014 Mar 28:oemed-2013.

68. England L, Zhang J. Smoking and risk of preeclampsia: a systematic review. Front Biosci. 2007 Jan 1;12:2471-83.

69. Bainbridge SA, Sidle EH, Smith GN. Direct placental effects of cigarette smoke protect women from pre-eclampsia: the specific roles of carbon monoxide and antioxidant systems in the placenta. Medical hypotheses. 2005 Jan 1;64(1):17-27.

70. Jaskolka D, Retnakaran R, Zinman B, Kramer CK. Fetal sex and maternal risk of pre-eclampsia/eclampsia: a systematic review and meta-analysis. BJOG: An International Journal of Obstetrics & Gynaecology. 2017 Mar 1;124(4):553-60.

71. Magee LA, Helewa M, Moutquin JM, von Dadelszen P, Hypertension Guideline Committee. Diagnosis, evaluation, and management of the hypertensive disorders of pregnancy. Journal of Obstetrics and Gynaecology Canada. 2008 Mar 1;30(3 Supplement 1):S1-48.

72. American College of Obstetricians and Gynecologists. Hypertension in pregnancy. Report of the American College of Obstetricians and Gynecologists' task force on hypertension in pregnancy. Obstetrics and gynecology. 2013 Nov;122(5):1122.

73. Lowe SA, Brown MA, Dekker GA, Gatt S, McLintock CK, McMahon LP, Mangos G, Moore MP, Muller P, Paech M, Walters B; Society of Obstetric Medicine of Australia and New Zealand. Guidelines for the management of hypertensive disorders of pregnancy 2008. Australian and New Zealand Journal of Obstetrics and Gynaecology. 2009 Jun 1;49(3):242-6.

74. Tranquilli AL, Dekker G, Magee L, Roberts J, Sibai BM, Steyn W, Zeeman GG, Brown MA. The classification, diagnosis and management of the hypertensive disorders of pregnancy: a revised statement from the ISSHP. Pregnancy hypertension. 2014 Apr;4(2):97.

75. Baumwell S, Karumanchi SA. Pre-eclampsia: clinical manifestations and molecular mechanisms. Nephron Clinical practice. 2007;106(2):c72-81.

76. Craici IM, Wagner SJ, Weissgerber TL, Grande JP, Garovic VD. Advances in the pathophysiology of pre-eclampsia and related podocyte injury. Kidney international. 2014 Aug 1;86(2):275-85.

77. Tranquilli AL, Brown MA, Zeeman GG, Dekker G, Sibai BM. The definition of severe and early-onset preeclampsia. Statements from the International Society for the Study of Hypertension in Pregnancy (ISSHP). Pregnancy Hypertension: An International Journal of Women's Cardiovascular Health. 2013 Jan 1;3(1):44-7.

78. von Dadelszen P, Payne B, Li J, et al. Prediction of adverse maternal outcomes in pre-eclampsia: development and validation of the fullPIERS model. The Lancet. 2011 Jan 15;377(9761):219-27.

79. Magee LA, von Dadelszen P, Rey E, Ross S, Asztalos E, Murphy KE, Menzies J, Sanchez J, Singer J, Gafni A, Gruslin A. Less-tight versus tight control of hypertension in pregnancy. New England Journal of Medicine. 2015 Jan 29;372(5):407-17.

80. von Dadelszen P, Ornstein MP, Bull SB, Logan AG, Koren G, Magee LA. Fall in mean arterial pressure and fetal growth restriction in pregnancy hypertension: a meta-analysis. The Lancet. 2000 Jan 8;355(9198):87-92.

81. Amorim MM, Santosa LC, Faúndes A. Corticosteroid therapy for prevention of respiratory distress syndrome in severe preeclampsia. American Journal of Obstetrics & Gynecology. 1999 May 1;180(5):1283-8.

82. Murphy KE, Willan AR, Hannah ME, Ohlsson A, Kelly EN, Matthews SG, Saigal S, Asztalos E, Ross S, Delisle MF, Amankwah K. Effect of antenatal corticosteroids on fetal growth and gestational age at birth. Obstetrics & Gynecology. 2012 May 1;119(5):917-23.

83. Moisiadis VG, Constantinof A, Kostaki A, Szyf M, Matthews SG. Prenatal glucocorticoid exposure modifies endocrine function and behaviour for 3 generations following maternal and paternal transmission. Scientific reports. 2017 Sep 18;7(1):11814.

84. Mashiloane CD, Moodley J. Induction or caesarean section for preterm pre-eclampsia? Journal of Obstetrics and Gynaecology. 2002 Jan 1;22(4):353-6.

85. Williams D. Pregnancy: a stress test for life. Current Opinion in Obstetrics & Gynecology. 2003 Dec;15(6):465-71.

86. McDonald SD, Han Z, Walsh MW, Gerstein HC, Devereaux PJ. Kidney disease after preeclampsia: a systematic review and meta-analysis. American Journal of Kidney Diseases. 2010 Jun 1;55(6):1026-39.

87. Libby G, Murphy DJ, McEwan NF, Greene SA, Forsyth JS, Chien PW, Morris AD, DARTS/MEMO Collaboration. Pre-eclampsia and the later development of type 2 diabetes in mothers and their children: an intergenerational study from the Walker cohort. Diabetologia. 2007 Mar 1;50(3):523-30.

88. Levine RJ, Vatten LJ, Horowitz GL, Qian C, Romundstad PR, Kai FY, Hollenberg AN, Hellevik AI, Asvold BO, Karumanchi SA. Pre-eclampsia, soluble fms-like tyrosine kinase 1, and the risk of reduced thyroid function: nested case-control and population based study. BMJ. 2009 Nov 18;339:b4336.

89. Brussé I, Duvekot J, Jongerling J, Steegers E, De Koning I. Impaired maternal cognitive functioning after pregnancies complicated by severe pre-eclampsia: a pilot case-control study. Acta obstetricia et gynecologica Scandinavica. 2008 Apr 1;87(4):408-12.

90. Beharier O, Davidson E, Sergienko R, Szaingurten-Solodkin I, Kessous R, Charach R, Belfair NJ, Sheiner E. Preeclampsia and future risk for maternal ophthalmic complications. American journal of perinatology. 2016 Jun;33(07):703-7.

91. Mongraw-Chaffin ML, Cirillo PM, Cohn BA. Preeclampsia and cardiovascular disease death: prospective evidence from the child health and development studies cohort. Hypertension. 2010 Jul 1;56(1):166-71.

92. McDonald SD, Malinowski A, Zhou Q, Yusuf S, Devereaux PJ. Cardiovascular sequelae of preeclampsia/eclampsia: a systematic review and meta-analyses. American heart journal. 2008 Nov 1;156(5):918-30.

93. Bellamy L, Casas JP, Hingorani AD, Williams DJ. Pre-eclampsia and risk of cardiovascular disease and cancer in later life: systematic review and meta-analysis. BMJ. 2007 Nov 8;335(7627):974.

94. Cain MA, Salemi JL, Tanner JP, Kirby RS, Salihu HM, Louis JM. Pregnancy as a window to future health: maternal placental syndromes and short-term cardiovascular outcomes. American Journal of Obstetrics & Gynecology. 2016 Oct 1;215(4):484-e1.

95. Wilson BJ, Watson MS, Prescott GJ, Sunderland S, Campbell DM, Hannaford P, Smith WC. Hypertensive diseases of pregnancy and risk of hypertension and stroke in later life: results from cohort study. BMJ. 2003 Apr 19;326(7394):845.

96. Ray JG, Vermeulen MJ, Schull MJ, Redelmeier DA. Cardiovascular health after maternal placental syndromes (CHAMPS): population-based retrospective cohort study. The Lancet. 2005 Nov 19;366(9499):1797-803.

97. Lykke JA, Langhoff-Roos J, Sibai BM, Funai EF, Triche EW, Paidas MJ. Hypertensive pregnancy disorders and subsequent cardiovascular morbidity and type 2 diabetes mellitus in the mother. Hypertension. 2009 Jun 1;53(6):944-51.

98. Smith GN, Pudwell J, Walker M, Wen SW. Risk estimation of metabolic syndrome at one and three years after a pregnancy complicated by preeclampsia. Journal of Obstetrics and Gynaecology Canada. 2012 Sep 1;34(9):836-41.

99. Murphy MS, Vignarajah M, Smith GN. Increased microvascular vasodilation and cardiovascular risk following a pre-eclamptic pregnancy. Physiological reports. 2014 Nov 1;2(11).

100. Chambers JC, Fusi L, Malik IS, Haskard DO, De Swiet M, Kooner JS. Association of maternal endothelial dysfunction with preeclampsia. JAMA. 2001 Mar 28;285(12):1607-12.

101. Romundstad PR, Magnussen EB, Smith GD, Vatten LJ. Hypertension in pregnancy and later cardiovascular risk: common antecedents? Circulation. 2010 Aug 10;122(6):579-84.

102. Sharma D, Shastri S, Farahbakhsh N, Sharma P. Intrauterine growth restriction–part 1. The Journal of Maternal-Fetal & Neonatal Medicine. 2016 Dec 16;29(24):3977-87.

103. Sharma D, Farahbakhsh N, Shastri S, Sharma P. Intrauterine growth restriction–part 2. The Journal of Maternal-Fetal & Neonatal Medicine. 2016 Dec 16;29(24):4037-48.

104. Chisholm KM, Folkins AK. Placental and clinical characteristics of term small-for-gestational-age neonates: A case-control study. Pediatric and Developmental Pathology. 2016 Jan;19(1):37-46.

105. Lee AC, Katz J, Blencowe H, Cousens S, Kozuki N, Vogel JP, Adair L, Baqui AH, Bhutta ZA, Caulfield LE, Christian P. National and regional estimates of term and preterm babies born small for gestational age in 138 low-income and middle-income countries in 2010. The Lancet Global Health. 2013 Jul 1;1(1):e26-36.

106. Story L, Sankaran S, Mullins E, Tan S, Russell G, Kumar S, Kyle P. Survival of pregnancies with small for gestational age detected before 24 weeks gestation. European Journal of Obstetrics and Gynecology and Reproductive Biology. 2015 May 1;188:100-3.

107. Hoellen F, Beckmann A, Banz-Jansen C, Weichert J, Rody A, Bohlmann MK. Management of Very Early-onset Fetal Growth Restriction: Results from 92 Consecutive Cases. In Vivo. 2016 Mar 1;30(2):123-31.

108. Bellido-González M, Díaz-López MÁ, López-Criado S, Maldonado-Lozano J. Cognitive functioning and academic achievement in children aged 6–8 years, born at term after intrauterine growth restriction and fetal cerebral redistribution. Journal of pediatric psychology. 2016 Jun 21;42(3):345-54.

109. Cohen E, Wong FY, Horne RS, Yiallourou SR. Intrauterine growth restriction: impact on cardiovascular development and function throughout infancy. Pediatric research. 2016 Jun;79(6):821.

110. Ronkainen E, Dunder T, Kaukola T, Marttila R, Hallman M. Intrauterine growth restriction predicts lower lung function at school age in children born very preterm. Archives of Disease in Childhood-Fetal and Neonatal Edition. 2016 Sep 1;101(5):F412-7.

111. Trudell AS, Cahill AG, Tuuli MG, Macones GA, Odibo AO. Risk of stillbirth after 37 weeks in pregnancies complicated by small-for-gestational-age fetuses. American Journal of Obstetrics & Gynecology. 2013 May 1;208(5):376-e1.

112. American College of Obstetricians and Gynecologists. ACOG Practice bulletin no. 134: fetal growth restriction. Obstetrics and gynecology. 2013 May;121(5):1122.

113. Guellec I, Marret S, Baud O, Cambonie G, Lapillonne A, Roze JC, Fresson J, Flamant C, Charkaluk ML, Arnaud C, Ancel PY. Intrauterine growth restriction, head size at birth, and outcome in very preterm infants. The Journal of pediatrics. 2015 Nov 1;167(5):975-81.

114. Rosenberg A. The IUGR newborn. In Seminars in perinatology 2008 Jun 1 (Vol. 32, No. 3, pp. 219-224). Elsevier.

115. Sharma D, Shastri S, Sharma P. Intrauterine growth restriction: antenatal and postnatal aspects. Clinical Medicine Insights: Pediatrics. 2016 Jan;10:CMPed-S40070.

116. Khoury MJ, Erickson JD, Cordero JF, McCarthy BJ. Congenital malformations and intrauterine growth retardation: a population study. Pediatrics. 1988 Jul 1;82(1):83-90.

117. Baumeister FA, Engelsberger I, Schulze A. Pancreatic agenesis as cause for neonatal diabetes mellitus. Klinische Pädiatrie. 2005 Mar;217(02):76-81.

118. López M, Palacio M, Goncé A, Hernàndez S, Barranco FJ, García L, Loncà M, Coll JO, Gratacós E, Figueras F. Risk of intrauterine growth restriction among HIV-infected pregnant women: a cohort study. European Journal of Clinical Microbiology & Infectious Diseases. 2015 Feb 1;34(2):223-30.

119. Rijken MJ, Papageorghiou AT, Thiptharakun S, Kiricharoen S, Dwell SL, Wiladphaingern J, Pimanpanarak M, Kennedy SH, Nosten F, McGready R. Ultrasound evidence of early fetal growth restriction after maternal malaria infection. PloS one. 2012 Feb 9;7(2):e31411.

120. Naing ZW, Scott GM, Shand A, Hamilton ST, Zuylen WJ, Basha J, Hall B, Craig ME, Rawlinson WD. Congenital cytomegalovirus infection in pregnancy: a review of prevalence, clinical features, diagnosis and prevention. Australian and New Zealand Journal of Obstetrics and Gynaecology. 2016 Feb 1;56(1):9-18.

121. Al-Saleh I, Shinwari N, Mashhour A, Rabah A. Birth outcome measures and maternal exposure to heavy metals (lead, cadmium and mercury) in Saudi Arabian population. International journal of hygiene and environmental health. 2014 Mar 1;217(2-3):205-18.

122. Jaddoe VW, Bakker R, Hofman A, Mackenbach JP, Moll HA, Steegers EA, Witteman JC. Moderate alcohol consumption during pregnancy and the risk of low birth weight and preterm birth. The generation R study. Annals of epidemiology. 2007 Oct 1;17(10):834-40.

123. Gouin K, Murphy K, Shah PS. Effects of cocaine use during pregnancy on low birthweight and preterm birth: systematic review and metaanalyses. American Journal of Obstetrics & Gynecology. 2011 Apr 1;204(4):340-e1.

124. CARE Study Group. Maternal caffeine intake during pregnancy and risk of fetal growth restriction: a large prospective observational study. BMJ. 2008;337.

125. Halldorsson TI, Thorsdottir I, Meltzer HM, Nielsen F, Olsen SF. Linking exposure to polychlorinated biphenyls with fatty fish consumption and reduced fetal growth among Danish pregnant women: a cause for concern? American journal of epidemiology. 2008 Aug 21;168(8):958-65.

126. Veiga-Lopez A, Kannan K, Liao C, Ye W, Domino SE, Padmanabhan V. Gender-specific effects on gestational length and birth weight by early pregnancy BPA exposure. The Journal of Clinical Endocrinology & Metabolism. 2015 Nov 1;100(11):E1394-403.

127. Bullo M, Tschumi S, Bucher BS, Bianchetti MG, Simonetti GD. Pregnancy Outcome Following Exposure to Angiotensin-Converting Enzyme Inhibitors or Angiotensin Receptor Antagonists Novelty and Significance: A Systematic Review. Hypertension. 2012 Aug 1;60(2):444-50.

128. Ødegård RA, Vatten LJ, Nilsen ST, Salvesen KÅ, Austgulen R. Preeclampsia and fetal growth. Obstetrics & Gynecology. 2000 Dec 1;96(6):950-5.

129. Cavazos-Rehg PA, Krauss MJ, Spitznagel EL, Bommarito K, Madden T, Olsen MA, Subramaniam H, Peipert JF, Bierut LJ. Maternal age and risk of labor and delivery complications. Maternal and child health journal. 2015 Jun 1;19(6):1202-11.

130. Declercq E, Luke B, Belanoff C, Cabral H, Diop H, Gopal D, Hoang L, Kotelchuck M, Stern JE, Hornstein MD. Perinatal outcomes associated with assisted reproductive technology: the Massachusetts Outcomes Study of Assisted Reproductive Technologies (MOSART). Fertility and sterility. 2015 Apr 1;103(4):888-95.

131. Gutaj P, Wender-Ozegowska E. Diagnosis and management of IUGR in pregnancy complicated by type 1 diabetes mellitus. Current diabetes reports. 2016 May 1;16(5):39.

132. Dadhwal V, Sharma AK, Deka D, Gupta B, Mittal S. The obstetric outcome following treatment in a cohort of patients with antiphospholipid antibody syndrome in a tertiary care center. Journal of postgraduate medicine. 2011 Jan 1;57(1):16.

133. Moore LG. Fetal growth restriction and maternal oxygen transport during high altitude pregnancy. High Altitude Medicine & Biology. 2003 May 1;4(2):141-56.

134. Postigo L, Heredia G, Illsley NP, Torricos T, Dolan C, Echalar L, Tellez W, Maldonado I, Brimacombe M, Balanza E, Vargas E. Where the O2 goes to: preservation of human fetal oxygen delivery and consumption at high altitude. The Journal of physiology. 2009 Feb 1;587(3):693-708.

135. Delpisheh A, Brabin L, Drummond S, Brabin BJ. Prenatal smoking exposure and asymmetric fetal growth restriction. Annals of human biology. 2008 Jan 1;35(6):573-83.

136. McCowan LM, Dekker GA, Chan E, Stewart A, Chappell LC, Hunter M, Moss-Morris R, North RA. Spontaneous preterm birth and small for gestational age infants in women who stop smoking early in pregnancy: prospective cohort study. BMJ. 2009 Mar 27;338:b1081.

137. Wang A, Zsengellér ZK, Hecht JL, Buccafusca R, Burke SD, Rajakumar A, Weingart E, Paul BY, Salahuddin S, Karumanchi SA. Excess placental secreted frizzled-related protein 1 in maternal smokers impairs fetal growth. The Journal of clinical investigation. 2015 Nov 2;125(11):4021-5.

138. Triunfo S, Lanzone A. Impact of maternal under nutrition on obstetric outcomes. Journal of endocrinological investigation. 2015 Jan 1;38(1):31-8.

139. Wang H, Hu YF, Hao JH, Chen YH, Su PY, Wang Y, Yu Z, Fu L, Xu YY, Zhang C, Tao FB. Maternal zinc deficiency during pregnancy elevates the risks of fetal growth restriction: a population-based birth cohort study. Scientific Reports. 2015 Jun 8;5:11262.

140. Clark DC. Dairy and Growth, Latest Findings, and Lessons Learned. Food and nutrition bulletin. 2016 Mar;37(1_suppl):S22-8.

141. Sakuyama H, Katoh M, Wakabayashi H, Zulli A, Kruzliak P, Uehara Y. Influence of gestational salt restriction in fetal growth and in development of diseases in adulthood. Journal of biomedical science. 2016 Dec;23(1):12.

142. Daya S. Accuracy of gestational age estimation by means of fetal crown-rump length measurement. American journal of obstetrics and gynecology. 1993 Mar 1;168(3):903-8.

143. Papageorghiou AT, Kennedy SH, Salomon LJ, Ohuma EO, Cheikh Ismail L, Barros FC, Lambert A, Carvalho M, Jaffer YA, Bertino E, Gravett MG. International standards for early fetal size and

pregnancy dating based on ultrasound measurement of crown–rump length in the first trimester of pregnancy. Ultrasound in Obstetrics & Gynecology. 2014 Dec 1;44(6):641-8.

144. Butt K, Lim K, Bly S, Cargill Y, Davies G, Denis N, Hazlitt G, Morin L, Ouellet A, Salem S. Determination of gestational age by ultrasound. Journal of Obstetrics and gynaecology Canada. 2014 Feb 1;36(2):171-81.

145. Chavez MR, Ananth CV, Smulian JC, Vintzileos AM. Fetal transcerebellar diameter measurement for prediction of gestational age at the extremes of fetal growth. Journal of Ultrasound in Medicine. 2007 Sep 1;26(9):1167-71.

146. Melamed N, Ryan G, Windrim R, Toi A, Kingdom J. Choice of Formula and Accuracy of Fetal Weight Estimation in Small-for-Gestational-Age Fetuses. Journal of Ultrasound in Medicine. 2016 Jan 1;35(1):71-82.

147. Proctor LK, Rushworth V, Shah PS, Keunen J, Windrim R, Ryan G, Kingdom J. Incorporation of femur length leads to underestimation of fetal weight in asymmetric preterm growth restriction. Ultrasound in Obstetrics & Gynecology. 2010 Apr 1;35(4):442-8.

148. Hadlock FP, Harrist RB, Martinez-Poyer J. In utero analysis of fetal growth: a sonographic weight standard. Radiology. 1991 Oct;181(1):129-33.

149. Hiersch L, Melamed N. Fetal growth velocity and body proportion in the assessment of growth. American Journal of Obstetrics & Gynecology. 2018 Feb 1;218(2):S700-11.

150. Kingdom JC, Audette MC, Hobson SR, Windrim RC, Morgen E. A placenta clinic approach to the diagnosis and management of fetal growth restriction. American Journal of Obstetrics & Gynecology. 2018 Feb 1;218(2):S803-17.

151. Gardosi J, Madurasinghe V, Williams M, Malik A, Francis A. Maternal and fetal risk factors for stillbirth: population based study. BMJ. 2013 Jan 24;346:f108.

152. Figueras F, Gratacos E. An integrated approach to fetal growth restriction. Best Practice & Research: Clinical Obstetrics & Gynaecology. 2017 Jan 1;38:48-58.

153. Audette MC, Kingdom JC. Screening for fetal growth restriction and placental insufficiency. In Seminars in Fetal and Neonatal Medicine 2017 Dec 6. WB Saunders.

154. Gardosi J, Chang A, Kalyan B, Sahota D, Symonds EM. Customised antenatal growth charts. The Lancet. 1992 Feb 1;339(8788):283-7.

155. Parikh LI, Nolan III J, Tefera E, Driggers R. Fetal biometry: does patient ethnicity matter? The Journal of Maternal-Fetal & Neonatal Medicine. 2014 Mar 1;27(5):500-4.

156. Maso G, Jayawardane MA, Alberico S, Piccoli M, Senanayake HM. The implications of diagnosis of small for gestational age fetuses using European and South Asian growth charts: an outcome-based comparative study. The Scientific World Journal. 2014;2014.

157. Hinkle SN, Albert PS, Mendola P, Sjaarda LA, Yeung E, Boghossian NS, Laughon SK. The association between parity and birthweight in a longitudinal consecutive pregnancy cohort. Paediatric and perinatal epidemiology. 2014 Mar 1;28(2):106-15.

158. Voigt M, Rochow N, Jährig K, Straube S, Hufnagel S, Jorch G. Dependence of neonatal small and large for gestational age rates on maternal height and weight–an analysis of the German Perinatal Survey. Journal of perinatal medicine. 2010 Jul 1;38(4):425-30.

159. Kozuki N, Katz J, Lee AC, Vogel JP, Silveira MF, Sania A, Stevens GA, Cousens S, Caulfield LE, Christian P, Huybregts L. Short maternal stature increases risk of small-for-gestational-age and preterm births in low-and middle-income countries: individual participant data meta-analysis and population attributable fraction. The Journal of nutrition. 2015 Nov 1;145(11):2542-50.

160. Gardosi J. Customized fetal growth standards: rationale and clinical application. In Seminars in perinatology 2004 Feb 1 (Vol. 28, No. 1, pp. 33-40). Elsevier.

161. Gardosi J. Customized charts and their role in identifying pregnancies at risk because of fetal growth restriction. Journal of Obstetrics and Gynaecology Canada. 2014 May 1;36(5):408-15.

162. MacDonald TM, Hui L, Tong S, Robinson AJ, Dane KM, Middleton AL, Walker SP. Reduced growth velocity across the third trimester is associated with placental insufficiency in fetuses born at a normal birthweight: a prospective cohort study. BMC medicine. 2017 Dec;15(1):164.

163. Villar J, Altman DG, Purwar M, Noble JA, Knight HE, Ruyan P, Cheikh Ismail L, Barros FC, Lambert A, Papageorghiou AT, Carvalho M. The objectives, design and implementation of the INTERGROWTH-21st Project. BJOG: An International Journal of Obstetrics & Gynaecology. 2013 Sep 1;120(s2):9-26.

164. Anderson NH, Sadler LC, McKinlay CJ, McCowan LM. INTERGROWTH-21st vs customized birthweight standards for identification of perinatal mortality and morbidity. American Journal of Obstetrics & Gynecology. 2016 Apr 1;214(4):509-e1.

165. Mongelli M, Figueras F, Francis A, Gardosi J. A customised birthweight centile calculator developed for an Australian population. Australian and New Zealand journal of obstetrics and gynaecology. 2007 Apr 1;47(2):128-31.

166. Figueras F, Meler E, Iraola A, Eixarch E, Coll O, Figueras J, Francis A, Gratacos E, Gardosi J. Customized birthweight standards for a Spanish population. European Journal of Obstetrics and Gynecology and Reproductive Biology. 2008 Jan 1;136(1):20-4.

167. Gardosi J, Francis A. A customized standard to assess fetal growth in a US population. American Journal of Obstetrics & Gynecology. 2009 Jul 1;201(1):25-e1.

168. Unterscheider J, Geary MP, Daly S, McAuliffe FM, Kennelly MM, Dornan J, Morrison JJ, Burke G, Francis A, Gardosi J, Malone FD. The customized fetal growth potential: a standard for Ireland. European Journal of Obstetrics and Gynecology and Reproductive Biology. 2013 Jan 1;166(1):14-7.

169. Kramer MS, Platt RW, Wen SW, Joseph KS, Allen A, Abrahamowicz M, Blondel B, Bréart G, Fetal/Infant Health Study Group of the Canadian Perinatal Surveillance System. A new and improved population-based Canadian reference for birth weight for gestational age. Pediatrics. 2001 Aug 1;108(2):e35-.

170. Melamed N, Ray JG, Shah PS, Berger H, Kingdom JC. Should we use customized fetal growth percentiles in urban Canada? Journal of Obstetrics and Gynaecology Canada. 2014 Feb 1;36(2):164-70.

171. Seravalli V, Baschat AA. A uniform management approach to optimize outcome in fetal growth restriction. Obstetrics and Gynecology Clinics. 2015 Jun 1;42(2):275-88.

172. Gould JB, Gluck L, Kulovich MV. The relationship between accelerated pulmonary maturity and accelerated neurological maturity in certain chronically stressed pregnancies. American Journal of Obstetrics & Gynecology. 1977 Jan 15;127(2):181-6.

173. Pardi G, Buscaglia M, Ferrazzi E, Bozzetti P, Marconi AM, Cetin I, Battaglia FC, Makowski EL. Cord sampling for the evaluation of oxygenation and acid-base balance in growth-retarded human fetuses. American Journal of Obstetrics & Gynecology. 1987 Nov 1;157(5):1221-8.

174. Simchen MJ, Alkazaleh F, Adamson SL, Windrim R, Telford J, Beyene J, Kingdom J. The fetal cardiovascular response to antenatal steroids in severe early-onset intrauterine growth restriction. American Journal of Obstetrics & Gynecology. 2004 Feb 1;190(2):296-304.

175. Ting JY, Kingdom JC, Shah PS. Antenatal glucocorticoids, magnesium sulfate, and mode of birth in preterm fetal small for gestational age. American Journal of Obstetrics & Gynecology. 2018 Feb 1;218(2):S818-28.

176. Figueras F, Gratacós E. Update on the diagnosis and classification of fetal growth restriction and proposal of a stage-based management protocol. Fetal diagnosis and therapy. 2014;36(2):86-98.

177. Boers KE, Vijgen SM, Bijlenga D, van der Post JA, Bekedam DJ, Kwee A, van der Salm PC, van Pampus MG, Spaanderman ME, de Boer K, Duvekot JJ. Induction versus expectant monitoring for intrauterine growth restriction at term: randomised equivalence trial (DIGITAT). BMJ. 2010 Dec 21;341:c7087.

178. Mendez-Figueroa H, Pedroza C, Khan AM, Chauhan SP. Small-for-gestational-age infants among uncomplicated pregnancies at term: a secondary analysis of 9 Maternal-Fetal Medicine Units Network studies. American Journal of Obstetrics & Gynecology. 2016 Nov 1;215(5):628-e1.

179. Barbati A, Cappuccini B, Aisa MC, Grasselli C, Zamarra M, Bini V, Bellomo G, Orlacchio A, Di Renzo GC. Increased urinary cystatin-C levels correlate with reduced renal volumes in neonates with intrauterine growth restriction. Neonatology. 2016;109(2):154-60.

180. Ferguson AC. Prolonged impairment of cellular immunity in children with intrauterine growth retardation. The Journal of pediatrics. 1978 Jul 1;93(1):52-6.

181. Liu J, Chen XX, Li XW, Fu W, Zhang WQ. Metabolomic research on newborn infants with intrauterine growth restriction. Medicine. 2016 Apr;95(17).

182. Sehgal A, Allison BJ, Gwini SM, Miller SL, Polglase GR. Cardiac morphology and function in preterm growth restricted infants: relevance for clinical sequelae. The Journal of pediatrics. 2017 Sep 1;188:128-34.

183. Crispi F, Miranda J, Gratacós E. Long-term cardiovascular consequences of fetal growth restriction: biology, clinical implications, and opportunities for prevention of adult disease. American Journal of Obstetrics & Gynecology. 2018 Feb 1;218(2):S869-79.

184. Crispi F, Bijnens B, Figueras F, Bartrons J, Eixarch E, Le Noble F, Ahmed A, Gratacós E. Fetal growth restriction results in remodeled and less efficient hearts in children. Circulation. 2010 Jun 8;121(22):2427-36.

185. Chen J, Chen P, Bo T, Luo K. Cognitive and behavioral outcomes of intrauterine growth restriction school-age children. Pediatrics. 2016 Mar 16:peds-2015.

186. Beukers F, Aarnoudse-Moens CS, van Weissenbruch MM, Ganzevoort W, van Goudoever JB, van Wassenaer-Leemhuis AG. Fetal Growth Restriction with Brain Sparing: Neurocognitive and Behavioral Outcomes at 12 Years of Age. The Journal of pediatrics. 2017 Sep 1;188:103-9.

187. Østgård HF, Løhaugen GC, Bjuland KJ, Rimol LM, Brubakk AM, Martinussen M, Vik T, Håberg AK, Skranes J. Brain morphometry and cognition in young adults born small for gestational age at term. The Journal of pediatrics. 2014 Nov 1;165(5):921-7.

188. Brown LD, Hay Jr WW. Impact of placental insufficiency on fetal skeletal muscle growth. Molecular and cellular endocrinology. 2016 Nov 5;435:69-77.

189. Barker DJ. Fetal origins of coronary heart disease. BMJ. 1995 Jul 15;311(6998):171.

190. Hales CN, Barker DJ, Clark PM, Cox LJ, Fall C, Osmond C, Winter PD. Fetal and infant growth and impaired glucose tolerance at age 64. BMJ. 1991 Oct 26;303(6809):1019-22.

191. Barker DJ. The fetal and infant origins of adult disease. BMJ. 1990 Nov 17;301(6761):1111.

192. Rich-Edwards JW, Stampfer MJ, Manson JE, Rosner B, Hankinson SE, Colditz GA, Hennekens CH, Willet WC. Birth weight and risk of cardiovascular disease in a cohort of women followed up since 1976. BMJ. 1997 Aug 16;315(7105):396-400.

193. Lawlor DA, Ronalds G, Clark H, Smith GD, Leon DA. Birth weight is inversely associated with incident coronary heart disease and stroke among individuals born in the 1950s: findings from the Aberdeen Children of the 1950s prospective cohort study. Circulation. 2005 Sep 6;112(10):1414-8.

194. Osmond C, Barker DJ, Winter PD, Fall CH, Simmonds SJ. Early growth and death from cardiovascular disease in women. BMJ. 1993 Dec 11;307(6918):1519-24.

195. Taveras EM, Rifas-Shiman SL, Belfort MB, Kleinman KP, Oken E, Gillman MW. Weight status in the first 6 months of life and obesity at 3 years of age. Pediatrics. 2009 Apr 1;123(4):1177-83.

196. Perng W, Hajj H, Belfort MB, Rifas-Shiman SL, Kramer MS, Gillman MW, Oken E. Birth size, early life weight gain, and midchildhood cardiometabolic health. The Journal of pediatrics. 2016 Jun 1;173:122-30.

197. Heindel JJ, Balbus J, Birnbaum L, Brune-Drisse MN, Grandjean P, Gray K, Landrigan PJ, Sly PD, Suk W, Slechta DC, Thompson C. Developmental origins of health and disease: integrating environmental influences. Endocrinology. 2016 Jan 1;2016(1):17-22.

198. Thornburg KL, O'Tierney PF, Louey S. Review: the placenta is a programming agent for cardiovascular disease. Placenta 31 (Suppl.), S54–S59. doi: 10.1016. J. PLACENTA. 2010;2.

199. Cheong JN, Wlodek ME, Moritz KM, Cuffe JS. Programming of maternal and offspring disease: impact of growth restriction, fetal sex and transmission across generations. The Journal of physiology. 2016 Sep 1;594(17):4727-40.

200. Soto-Wright V, Bernstein M, Goldstein DP, Berkowitz RS. The changing clinical presentation of complete molar pregnancy. Obstetrics & Gynecology. 1995 Nov 1;86(5):775-9.

201. Kanter D, Lindheimer MD, Wang E, Borromeo RG, Bousfield E, Karumanchi SA, Stillman IE. Angiogenic dysfunction in molar pregnancy. American Journal of Obstetrics & Gynecology. 2010 Feb 1;202(2):184-e1.

202. Bdolah Y, Lam C, Rajakumar A, Shivalingappa V, Mutter W, Sachs BP, Lim KH, Bdolah-Abram T, Epstein FH, Karumanchi SA. Twin pregnancy and the risk of preeclampsia: bigger placenta or relative ischemia? American Journal of Obstetrics & Gynecology. 2008 Apr 1;198(4):428-e1.

203. Long PA, Oats JN. Preeclampsia in Twin Pregnancy-Severity and Pathogenesis. Australian and New Zealand Journal of Obstetrics and Gynaecology. 1987 Feb 1;27(1):1-5.

204. Gagnon R. Placental insufficiency and its consequences. European Journal of Obstetrics and Gynecology and Reproductive Biology. 2003 Sep 22;110:S99-107.

205. Gellersen B, Brosens IA, Brosens JJ. Decidualization of the human endometrium: mechanisms, functions, and clinical perspectives. In Seminars in reproductive medicine 2007 Nov (Vol. 25, No. 06, pp. 445-453). © Thieme Medical Publishers.

206. Staun-Ram E, Shalev E. Human trophoblast function during the implantation process. Reproductive Biology and Endocrinology. 2005 Dec;3(1):56.

207. Gellersen B, Brosens JJ. Cyclic decidualization of the human endometrium in reproductive health and failure. Endocrine reviews. 2014 Aug 20;35(6):851-905.

208. Dunn CL, Kelly RW, Critchley HO. Decidualization of the human endometrial stromal cell: an enigmatic transformation. Reproductive biomedicine online. 2003 Jan 1;7(2):151-61.

209. Faas MM, de Vos P. Uterine NK cells and macrophages in pregnancy. Placenta. 2017 Aug 1;56:44-52.

210. Cross JC, Werb Z, Fisher SJ. Implantation and the placenta: key pieces of the development puzzle. Science. 1994 Dec 2;266(5190):1508-18.

211. Bentin-Ley U, Horn T, Sjogren A, Sorensen S, Larsen JF, Hamberger L. Ultrastructure of human blastocyst-endometrial interactions in vitro. Journal of reproduction and fertility. 2000 Nov 1;120(2):337-50.

212. Huppertz B. Placental origins of preeclampsia: challenging the current hypothesis. Hypertension. 2008 Apr 1;51(4):970-5.

213. Tang Z, Abrahams VM, Mor G, Guller S. Placental Hofbauer cells and complications of pregnancy. Annals of the New York Academy of Sciences. 2011 Mar 1;1221(1):103-8.

214. Knöfler M, Pollheimer J. Human placental trophoblast invasion and differentiation: a particular focus on Wnt signaling. Frontiers in genetics. 2013 Sep 26;4:190.

215. Osol G, Mandala M. Maternal uterine vascular remodeling during pregnancy. Physiology. 2009 Feb;24(1):58-71.

216. Soares MJ, Chakraborty D, Kubota K, Renaud SJ, Rumi MK. Adaptive mechanisms controlling uterine spiral artery remodeling during the establishment of pregnancy. The International journal of developmental biology. 2014;58:247.

217. Gude NM, Roberts CT, Kalionis B, King RG. Growth and function of the normal human placenta. Thrombosis research. 2004 Jan 1;114(5):397-407.

218. Harris LK. Trophoblast-vascular cell interactions in early pregnancy: how to remodel a vessel. Placenta. 2010 Mar 1;31:S93-8.

219. Smith SD, Dunk CE, Aplin JD, Harris LK, Jones RL. Evidence for immune cell involvement in decidual spiral arteriole remodeling in early human pregnancy. The American journal of pathology. 2009 May 1;174(5):1959-71.

220. Fraser R, Whitley GS, Thilaganathan B, Cartwright JE. Decidual natural killer cells regulate vessel stability: implications for impaired spiral artery remodelling. Journal of reproductive immunology. 2015 Aug 1;110:54-60.

221. Hanna J, Goldman-Wohl D, Hamani Y, Avraham I, Greenfield C, Natanson-Yaron S, Prus D, Cohen-Daniel L, Arnon TI, Manaster I, Gazit R. Decidual NK cells regulate key developmental processes at the human fetal-maternal interface. Nature medicine. 2006 Sep;12(9):1065.

222. Kim CJ, Romero R, Chaemsaithong P, Kim JS. Chronic inflammation of the placenta: definition, classification, pathogenesis, and clinical significance. American Journal of Obstetrics & Gynecology. 2015 Oct 1;213(4):S53-69.

223. Rapacz-Leonard A, Dąbrowska M, Janowski T. Major histocompatibility complex I mediates immunological tolerance of the trophoblast during pregnancy and may mediate rejection during parturition. Mediators of inflammation. 2014;2014.

224. Rajagopalan S, Long EO. A human histocompatibility leukocyte antigen (HLA)-G–specific receptor expressed on all natural killer cells. Journal of Experimental Medicine. 1999 Apr 5;189(7):1093-100.

225. Hviid TV. HLA-G in human reproduction: aspects of genetics, function and pregnancy complications. Human reproduction update. 2005 Nov 9;12(3):209-32.

226. Hunt JS, Petroff MG, McIntire RH, Ober C. HLA-G and immune tolerance in pregnancy. The FASEB Journal. 2005 May 1;19(7):681-93.

227. King A, Allan DS, Bowen M, Powis SJ, Joseph S, Verma S, Hiby SE, McMichael AJ, Wai Loke Y, Braud VM. HLA-E is expressed on trophoblast and interacts with CD94/NKG2 receptors on decidual NK cells. European journal of immunology. 2000 Jun 1;30(6):1623-31.

228. Moffett A, Hiby SE, Sharkey AM. The role of the maternal immune system in the regulation of human birthweight. Phil. Trans. R. Soc. B. 2015 Mar 5;370(1663):20140071.

229. Murphy SP, Tomasi TB. Absence of MHC class II antigen expression in trophoblast cells results from a lack of class II transactivator (CIITA) gene expression. Molecular reproduction and development. 1998 Sep 1;51(1):1-2.

230. Weiss G, Sundl M, Glasner A, Huppertz B, Moser G. The trophoblast plug during early pregnancy: a deeper insight. Histochemistry and cell biology. 2016 Dec 1;146(6):749-56.

231. Jauniaux E, Watson AL, Hempstock J, Bao YP, Skepper JN, Burton GJ. Onset of maternal arterial blood flow and placental oxidative stress: a possible factor in human early pregnancy failure. The American journal of pathology. 2000 Dec 1;157(6):2111-22.

232. Burton GJ, Hempstock J, Jauniaux E. Oxygen, early embryonic metabolism and free radical-mediated embryopathies. Reproductive biomedicine online. 2003 Jan 1;6(1):84-96.

233. Watson AL, Skepper JN, Jauniaux E, Burton GJ. Susceptibility of human placental syncytiotrophoblastic mitochondria to oxygen-mediated damage in relation to gestational age. The Journal of Clinical Endocrinology & Metabolism. 1998 May 1;83(5):1697-705.

234. Genbacev O, Zhou Y, Ludlow JW, Fisher SJ. Regulation of human placental development by oxygen tension. Science. 1997 Sep 12;277(5332):1669-72.

235. Caniggia I, Mostachfi H, Winter J, Gassmann M, Lye SJ, Kuliszewski M, Post M. Hypoxia-inducible factor-1 mediates the biological effects of oxygen on human trophoblast differentiation through TGFβ 3. The Journal of clinical investigation. 2000 Mar 1;105(5):577-87.

236. Burton GJ, Watson AL, Hempstock J, Skepper JN, Jauniaux E. Uterine glands provide histiotrophic nutrition for the human fetus during the first trimester of pregnancy. The Journal of Clinical Endocrinology & Metabolism. 2002 Jun 1;87(6):2954-9.

237. Burton GJ, Hempstock J, Jauniaux E. Nutrition of the human fetus during the first trimester—a review. Placenta. 2001 Apr 1;22:S70-7.

238. Hempstock J, Cindrova-Davies T, Jauniaux E, Burton GJ. Endometrial glands as a source of nutrients, growth factors and cytokines during the first trimester of human pregnancy: a morphological and immunohistochemical study. Reproductive Biology and Endocrinology. 2004 Dec;2(1):58.

239. Rodesch F, Simon PH, Donner C, Jauniaux ER. Oxygen measurements in endometrial and trophoblastic tissues during early pregnancy. Obstetrics and gynecology. 1992 Aug;80(2):283-5.

240. Burton GJ, Woods AW, Jauniaux E, Kingdom JC. Rheological and physiological consequences of conversion of the maternal spiral arteries for uteroplacental blood flow during human pregnancy. Placenta. 2009 Jun 1;30(6):473-82.

241. Díaz P, Powell TL, Jansson T. The role of placental nutrient sensing in maternal-fetal resource allocation. Biology of reproduction. 2014 Oct 1;91(4).

242. Kingdom J, Huppertz B, Seaward G, Kaufmann P. Development of the placental villous tree and its consequences for fetal growth. European Journal of Obstetrics and Gynecology and Reproductive Biology. 2000 Sep 1;92(1):35-43.

243. Wheeler T, Elcock CL, Anthony FW. Angiogenesis and the placental environment. Placenta. 1995 Apr 1;16(3):289-96.

244. Baczyk D, Drewlo S, Proctor L, Dunk C, Lye S. Glial cell missing-1 transcription factor is required for the differentiation of the human trophoblast. Cell death and differentiation. 2009 May;16(5):719.

245. Mi S, Lee X, Li XP, Veldman GM, Finnerty H, Racie L, Lavallie E, Tang XY, Edouard P, Howes S, Keith Jr JC. Syncytin is a captive retroviral envelope protein involved in human placental morphogenesis. Nature. 2000 Feb;403(6771):785.

246. Fox H. Aging of the placenta. Archives of Disease in Childhood-Fetal and Neonatal Edition. 1997 Nov 1;77(3):F171-5.

247. Jauniaux E, Burton GJ, Hustin J, Moscoso GJ. Development of the early human placenta: a morphometric study. Placenta. 1991 May 1;12(3):269-76.

248. Burton GJ, Tham SW. Formation of vasculo-syncytial membranes in the human placenta. Journal of developmental physiology. 1992 Jul 1;18:43-.

249. Syme MR, Paxton JW, Keelan JA. Drug transfer and metabolism by the human placenta. Clinical pharmacokinetics. 2004 Jul 1;43(8):487-514.

250. Huppertz B, Kingdom JC. Apoptosis in the trophoblast—role of apoptosis in placental morphogenesis. Journal of the Society for Gynecologic Investigation. 2004 Sep;11(6):353-62.

251. Mayhew TM. Turnover of human villous trophoblast in normal pregnancy: what do we know and what do we need to know? Placenta. 2014 Apr 1;35(4):229-40.

252. Göhner C, Plösch T, Faas MM. Immune-modulatory effects of syncytiotrophoblast extracellular vesicles in pregnancy and preeclampsia. Placenta. 2017 Dec 1;60:S41-51.

253. Tannetta D, Masliukaite I, Vatish M, Redman C, Sargent I. Update of syncytiotrophoblast derived extracellular vesicles in normal pregnancy and preeclampsia. Journal of reproductive immunology. 2017 Feb 1;119:98-106.

254. Delorme-Axford E, Donker RB, Mouillet JF, Chu T, Bayer A, Ouyang Y, Wang T, Stolz DB, Sarkar SN, Morelli AE, Sadovsky Y. Human placental trophoblasts confer viral resistance to recipient cells. PNAS. 2013 Jul 16;110(29):12048-53.

255. Loukeris K, Sela R, Baergen RN. Syncytial knots as a reflection of placental maturity: reference values for 20 to 40 weeks' gestational age. Pediatric and Developmental Pathology. 2010 Jul;13(4):305-9.

256. Mikheev AM, Nabekura T, Kaddoumi A, Bammler TK, Govindarajan R, Hebert MF, Unadkat JD. Profiling gene expression in human placentae of different gestational ages: an OPRU* Network and UW SCOR Study. Reproductive sciences. 2008 Nov;15(9):866-77.

257. Lam C, Lim KH, Karumanchi SA. Circulating angiogenic factors in the pathogenesis and prediction of preeclampsia. Hypertension. 2005 Nov 1;46(5):1077-85.

258. Wang Y. Vascular biology of the placenta. In Colloquium Series on Integrated Systems Physiology: from Molecule to Function 2010 Aug 27 (Vol. 2, No. 1, pp. 1-98). Morgan & Claypool Life Sciences.

259. Pijnenborg R, Bland JM, Robertson WB, Dixon G, Brosens I. The pattern of interstitial trophoblasticinvasion of the myometrium in early human pregnancy. Placenta. 1981 Oct 1;2(4):303-15.

260. Jauniaux E, Hempstock J, Greenwold N, Burton GJ. Trophoblastic oxidative stress in relation to temporal and regional differences in maternal placental blood flow in normal and abnormal early pregnancies. The American journal of pathology. 2003 Jan 1;162(1):115-25.

261. Hughes DA, Kircher M, He Z, Guo S, Fairbrother GL, Moreno CS, Khaitovich P, Stoneking M. Evaluating intra-and inter-individual variation in the human placental transcriptome. Genome biology. 2015 Dec;16(1):54.

262. Sood R, Zehnder JL, Druzin ML, Brown PO. Gene expression patterns in human placenta. PNAS. 2006 Apr 4;103(14):5478-83.

263. Avila L, Yuen RK, Diego-Alvarez D, Penaherrera MS, Jiang R, Robinson WP. Evaluating DNA methylation and gene expression variability in the human term placenta. Placenta. 2010 Dec 1;31(12):1070-7.

264. Surmon L, Bobek G, Makris A, Chiu CL, Lind CA, Lind JM, Hennessy A. Variability in mRNA expression of fms-like tyrosine kinase-1 variants in normal and preeclamptic placenta. BMC research notes. 2014 Dec;7(1):154.

265. Gonzalez TL, Sun T, Koeppel AF, Lee B, Wang ET, Farber CR, Rich SS, Sundheimer LW, Buttle RA, Chen YD, Rotter JI. Sex differences in the late first trimester human placenta transcriptome. Biology of sex differences. 2018 Dec;9(1):4.

266. Buckberry S, Bianco-Miotto T, Bent SJ, Dekker GA, Roberts CT. Integrative transcriptome meta-analysis reveals widespread sex-biased gene expression at the human fetal–maternal interface. Molecular human reproduction. 2014 May 27;20(8):810-9.

267. Murji A, Proctor LK, Paterson AD, Chitayat D, Weksberg R, Kingdom J. Male sex bias in placental dysfunction. American Journal of Medical Genetics Part A. 2012 Apr 1;158(4):779-83.

268. Brar HS, Platt LD, DeVore GR, Horenstein J, Medearis AL. Qualitative assessment of maternal uterine and fetal umbilical artery blood flow and resistance in laboring patients by Doppler velocimetry. American journal of obstetrics and gynecology. 1988 Apr 1;158(4):952-6.

269. Fleischer A, Anyaegbunam AA, Schulman H, Farmakides G, Randolph G. Uterine and umbilical artery velocimetry during normal labor. American Journal of Obstetrics & Gynecology. 1987 Jul 1;157(1):40-3.

270. Cindrova-Davies T, Yung HW, Johns J, Spasic-Boskovic O, Korolchuk S, Jauniaux E, Burton GJ, Charnock-Jones DS. Oxidative stress, gene expression, and protein changes induced in the human placenta during labor. The American journal of pathology. 2007 Oct 1;171(4):1168-79.

271. Tan EK, Tan EL. Alterations in physiology and anatomy during pregnancy. Best practice & research Clinical obstetrics & gynaecology. 2013 Dec 1;27(6):791-802.

272. Hytten F. Blood volume changes in normal pregnancy. Clinics in haematology. 1985 Oct;14(3):601-12.

273. Sanghavi M, Rutherford JD. Cardiovascular physiology of pregnancy. Circulation. 2014 Sep 16;130(12):1003-8.

274. Carbillon L, Uzan M, Uzan S. Pregnancy, vascular tone, and maternal hemodynamics: a crucial adaptation. Obstetrical & gynecological survey. 2000 Sep 1;55(9):574-81.

275. Fujita K, Tatsumi K, Kondoh E, Chigusa Y, Mogami H, Fujita M, Konishi I. Endothelial function progressively deteriorates during normal pregnancy. Hypertension in pregnancy. 2013 May 1;32(2):129-38.

276. Khong TY, Wolf FD, Robertson WB, Brosens I. Inadequate maternal vascular response to placentation in pregnancies complicated by pre-eclampsia and by small-for-gestational age infants. BJOG: An International Journal of Obstetrics & Gynaecology. 1986 Oct 1;93(10):1049-59.

277. Roberts JM, Hubel CA. The two stage model of preeclampsia: variations on the theme. Placenta. 2009 Mar 1;30:32-7.

278. Roberts JM, Bell MJ. If we know so much about preeclampsia, why haven't we cured the disease? Journal of reproductive immunology. 2013 Sep 1;99(1-2):1-9.

279. Brosens I. The role of the spiral arteries in the pathogenesis of pre-eclampsia. Obstet Gynecol Ann. 1972;1:177-91.

280. Brosens I, Dixon HG, Robertson WB. Fetal growth retardation and the arteries of the placental bed. BJOG: An International Journal of Obstetrics & Gynaecology. 1977 Sep 1;84(9):656-63.

281. Zhou Y, Damsky CH, Fisher SJ. Preeclampsia is associated with failure of human cytotrophoblasts to mimic a vascular adhesion phenotype. One cause of defective endovascular invasion in this syndrome? The Journal of clinical investigation. 1997 May 1;99(9):2152-64.

282. Floridon C, Nielsen O, Hølund B, Sunde L, Westergaard JG, Thomsen SG, Teisner B. Localization of E-cadherin in villous, extravillous and vascular trophoblasts during intrauterine, ectopic and molar pregnancy. MHR: Basic science of reproductive medicine. 2000 Oct;6(10):943-50.

283. Lyall F, Bulmer JN, Duffie E, Cousins F, Theriault A, Robson SC. Human trophoblast invasion and spiral artery transformation: the role of PECAM-1 in normal pregnancy, preeclampsia, and fetal growth restriction. The American journal of pathology. 2001 May 1;158(5):1713-21.

284. Martin D, Conrad KP. Expression of endothelial nitric oxide synthase by extravillous trophoblast cells in the human placenta. Placenta. 2000 Jan 1;21(1):23-31.

285. Corthorn J, Germain AA, Chacón C, Rey S, Soto GX, Figueroa CD, Müller-Esterl W, Duarte I, Valdés G. Expression of kallikrein, bradykinin b2 receptor, and endothelial nitric oxide synthase in placenta in normal gestation, preeclampsia, and placenta accreta. Endocrine. 2006 Jun 1;29(3):491-9.

286. Orange SJ, Painter D, Horvath J, Yu B, Trent R, Hennessy A. Placental endothelial nitric oxide synthase localization and expression in normal human pregnancy and pre-eclampsia. Clinical and experimental pharmacology and physiology. 2003 May 1;30(5-6):376-81.

287. Caniggia I, Winter J, Lye SJ, Post M. Oxygen and placental development during the first trimester: implications for the pathophysiology of pre-eclampsia. Placenta. 2000 Mar 1;21:S25-30.

288. Hoffmann P, Saoudi Y, Benharouga M, Graham CH, Schaal JP, Mazouni C, Feige JJ, Alfaidy N. Role of EG-VEGF in human placentation: Physiological and pathological implications. Journal of cellular and molecular medicine. 2009 Aug 2;13(8b):2224-35.

289. Garrido-Gomez T, Dominguez F, Quiñonero A, Diaz-Gimeno P, Kapidzic M, Gormley M, Ona K, Padilla-Iserte P, McMaster M, Genbacev O, Perales A. Defective decidualization during and after severe preeclampsia reveals a possible maternal contribution to the etiology. PNAS. 2017 Oct 3;114(40):E8468-77.

290. DiFederico E, Genbacev O, Fisher SJ. Preeclampsia is associated with widespread apoptosis of placental cytotrophoblasts within the uterine wall. The American journal of pathology. 1999 Jul 1;155(1):293-301.

291. Reister F, Frank HG, Heyl W, Kosanke G, Huppertz B, Schröder W, Kaufmann P, Rath W. The distribution of macrophages in spiral arteries of the placental bed in pre-eclampsia differs from that in healthy patients. Placenta. 1999 Mar 1;20(2-3):229-33.

292. Yui J, Garcia-Lloret M, Wegmann TE, Guilbert LJ. Cytotoxicity of tumour necrosis factor-alpha and gamma-interferon against primary human placental trophoblasts. Placenta. 1994 Dec 1;15(8):819-35.

293. Kaufmann P, Black S, Huppertz B. Endovascular trophoblast invasion: implications for the pathogenesis of intrauterine growth retardation and preeclampsia. Biology of reproduction. 2003 Jul 1;69(1):1-7.

294. Kadyrov M, Kingdom JC, Huppertz B. Divergent trophoblast invasion and apoptosis in placental bed spiral arteries from pregnancies complicated by maternal anemia and early-onset preeclampsia/intrauterine growth restriction. American Journal of Obstetrics & Gynecology. 2006 Feb 1;194(2):557-63.

295. Burton GJ, Jauniaux E. Placental oxidative stress: from miscarriage to preeclampsia. Journal of the Society for Gynecologic Investigation. 2004 Sep;11(6):342-52.

296. Hung TH, Skepper JN, Charnock-Jones DS, Burton GJ. Hypoxia-reoxygenation: a potent inducer of apoptotic changes in the human placenta and possible etiological factor in preeclampsia. Circulation research. 2002 Jun 28;90(12):1274-81.

297. Soleymanlou N, Jurisica I, Nevo O, Ietta F, Zhang X, Zamudio S, Post M, Caniggia I. Molecular evidence of placental hypoxia in preeclampsia. The Journal of Clinical Endocrinology & Metabolism. 2005 Jul 1;90(7):4299-308.

298. Chiang MH, Liang FY, Chen CP, Chang CW, Cheong ML, Wang LJ, Liang CY, Lin FY, Chou CC, Chen H. Mechanism of hypoxia-induced GCM1 degradation implications for the pathogenesis of preeclampsia. Journal of Biological Chemistry. 2009 Jun 26;284(26):17411-9.

299. Nevo O, Soleymanlou N, Wu Y, Xu J, Kingdom J, Many A, Zamudio S, Caniggia I. Increased expression of sFlt-1 in in vivo and in vitro models of human placental hypoxia is mediated by HIF-1. American Journal of Physiology-Regulatory, Integrative and Comparative Physiology. 2006 Oct;291(4):R1085-93.

300. Ahmad S, Ahmed A. Elevated placental soluble vascular endothelial growth factor receptor-1 inhibits angiogenesis in preeclampsia. Circulation research. 2004 Oct 29;95(9):884-91.

301. Su EJ. Role of the fetoplacental endothelium in fetal growth restriction with abnormal umbilical artery Doppler velocimetry. American Journal of Obstetrics & Gynecology. 2015 Oct 1;213(4):S123-30.

302. Burton GJ, Jauniaux E. Pathophysiology of placental-derived fetal growth restriction. American Journal of Obstetrics & Gynecology. 2018 Feb 1;218(2):S745-61.

303. Jones S, Bischof H, Lang I, Desoye G, Greenwood SL, Johnstone ED, Wareing M, Sibley CP, Brownbill P. Dysregulated flow-mediated vasodilatation in the human placenta in fetal growth restriction. The Journal of physiology. 2015 Jul 15;593(14):3077-92.

304. Kingdom JC, Kaufmann P. Oxygen and placental villous development: origins of fetal hypoxia. Placenta. 1997 Nov 1;18(8):613-21.

305. Knerr I, Beinder E, Rascher W. Syncytin, a novel human endogenous retroviral gene in human placenta: evidence for its dysregulation in preeclampsia and HELLP syndrome. American Journal of Obstetrics & Gynecology. 2002 Feb 1;186(2):210-3.

306. Pardi G, Marconi AM, Cetin I. Placental-fetal interrelationship in IUGR fetuses—a review. Placenta. 2002 Apr 1;23:S136-41.

307. Langbein M, Strick R, Strissel PL, Vogt N, Parsch H, Beckmann MW, Schild RL. Impaired cytotrophoblast cell–cell fusion is associated with reduced Syncytin and increased apoptosis in patients with placental dysfunction. Molecular reproduction and development. 2008 Jan 1;75(1):175-83.

308. Sultana Z, Maiti K, Dedman L, Smith R. Is there a role for placental senescence in the genesis of obstetric complications and fetal growth restriction? American Journal of Obstetrics & Gynecology. 2018 Feb 1;218(2):S762-73.

309. Huppertz B, Kingdom J, Caniggia I, Desoye G, Black S, Korr H, Kaufmann P. Hypoxia favours necrotic versus apoptotic shedding of placental syncytiotrophoblast into the maternal circulation. Placenta. 2003 Feb 1;24(2):181-90.

310. Hartley JD, Ferguson BJ, Moffett A. The role of shed placental DNA in the systemic inflammatory syndrome of preeclampsia. American Journal of Obstetrics & Gynecology. 2015 Sep 1;213(3):268-77.

311. Ermini L, Ausman J, Melland-Smith M, Yeganeh B, Rolfo A, Litvack ML, Todros T, Letarte M, Post M, Caniggia I. A Single Sphingomyelin Species Promotes Exosomal Release of Endoglin into the Maternal Circulation in Preeclampsia. Scientific reports. 2017 Sep 22;7(1):12172.

312. Arkwright PD, Rademacher TW, Dwek RA, Redman CW. Pre-eclampsia is associated with an increase in trophoblast glycogen content and glycogen synthase activity, similar to that found in hydatidiform moles. The Journal of clinical investigation. 1993 Jun 1;91(6):2744-53.

313. de Resende Guimarães MF, Brandão AH, de Lima Rezende CA, Cabral AC, Brum AP, Leite HV, Capuruço CA. Assessment of endothelial function in pregnant women with preeclampsia and gestational diabetes mellitus by flow-mediated dilation of brachial artery. Archives of gynecology and obstetrics. 2014 Sep 1;290(3):441-7.

314. Roberts JM, Taylor RN, Musci TJ, Rodgers GM, Hubel CA, McLaughlin MK. Preeclampsia: an endothelial cell disorder. American journal of obstetrics and gynecology. 1989 Nov 1;161(5):1200-4.

315. Shen F, Wei J, Snowise S, DeSousa J, Stone P, Viall C, Chen Q, Chamley L. Trophoblast debris extruded from preeclamptic placentae activates endothelial cells: a mechanism by which the placenta communicates with the maternal endothelium. Placenta. 2014 Oct 1;35(10):839-47.

316. Xiao X, Xiao F, Zhao M, Tong M, Wise MR, Stone PR, Chamley LW, Chen Q. Treating normal early gestation placentae with preeclamptic sera produces extracellular micro and nano vesicles that activate endothelial cells. Journal of reproductive immunology. 2017 Apr 1;120:34-41.

317. Chen Q, Stone PR, McCowan LM, Chamley LW. Phagocytosis of necrotic but not apoptotic trophoblasts induces endothelial cell activation. Hypertension. 2006 Jan 1;47(1):116-21.

318. O'brien M, Baczyk D, Kingdom JC. Endothelial dysfunction in severe preeclampsia is mediated by soluble factors, rather than extracellular vesicles. Scientific Reports. 2017 Jul 19;7(1):5887.

319. Powe CE, Levine RJ, Karumanchi SA. Preeclampsia, a disease of the maternal endothelium: the role of antiangiogenic factors and implications for later cardiovascular disease. Circulation. 2011 Jun 21;123(24):2856-69.

320. Henao DE, Saleem MA, Cadavid ÁP. Glomerular disturbances in preeclampsia: disruption between glomerular endothelium and podocyte symbiosis. Hypertension in pregnancy. 2010 Feb 1;29(1):10-20.

321. Karumanchi SA, Stillman IE. In vivo rat model of preeclampsia. In Placenta and Trophoblast 2006 (pp. 393-399). Humana Press.

322. Amraoui F, Spijkers L, Lahsinoui HH, Vogt L, van der Post J, Peters S, Afink G, Ris-Stalpers C, van den Born BJ. SFlt-1 elevates blood pressure by augmenting endothelin-1-mediated vasoconstriction in mice. PloS one. 2014 Mar 14;9(3):e91897.

323. Venkatesha S, Toporsian M, Lam C, Hanai JI, Mammoto T, Kim YM, Bdolah Y, Lim KH, Yuan HT, Libermann TA, Stillman IE. Soluble endoglin contributes to the pathogenesis of preeclampsia. Nature medicine. 2006 Jun;12(6):642.

324. Stanhewicz AE, Jandu S, Santhanam L, Alexander LM. Increased Angiotensin II Sensitivity Contributes to Microvascular Dysfunction in Women Who Have Had Preeclampsia: Novelty and Significance. Hypertension. 2017 Aug 1;70(2):382-9.

325. Yampolsky M, Salafia CM, Shlakhter O, Haas D, Eucker B, Thorp J. Modeling the variability of shapes of a human placenta. Placenta. 2008 Sep 1;29(9):790-7.

326. Lau JS, Saw SN, Buist ML, Biswas A, Mattar CN, Yap CH. Mechanical testing and non-linear viscoelastic modelling of the human placenta in normal and growth restricted pregnancies. Journal of biomechanics. 2016 Jan 25;49(2):173-84.

327. Yampolsky M, Salafia CM, Shlakhter O, Haas D, Eucker B, Thorp J. Centrality of the umbilical cord insertion in a human placenta influences the placental efficiency. Placenta. 2009 Dec 1;30(12):1058-64.

328. Strid H, Bucht E, Jansson T, Wennergren M, Powell TL. ATP dependent Ca2+ transport across basal membrane of human syncytiotrophoblast in pregnancies complicated by intrauterine growth restriction or diabetes. Placenta. 2003 May 1;24(5):445-52.

329. Roos S, Powell TL, Jansson T. Human placental taurine transporter in uncomplicated and IUGR pregnancies: cellular localization, protein expression, and regulation. American Journal of Physiology-Regulatory, Integrative and Comparative Physiology. 2004 Oct;287(4):R886-93.

330. Gaccioli F, Lager S. Placental nutrient transport and intrauterine growth restriction. Frontiers in physiology. 2016 Feb 16;7:40.

331. Kalousek DK, Vekemans M. Confined placental mosaicism. Journal of medical genetics. 1996 Jul 1;33(7):529-33.

332. Robinson WP, Peñaherrera MS, Jiang R, Avila L, Sloan J, McFadden DE, Langlois S, von Dadelszen P. Assessing the role of placental trisomy in preeclampsia and intrauterine growth restriction. Prenatal diagnosis. 2010 Jan 1;30(1):1-8.

333. Yong PJ, Langlois S, von Dadelszen P, Robinson W. The association between preeclampsia and placental trisomy 16 mosaicism. Prenatal diagnosis. 2006 Oct 1;26(10):956-61.

334. Robinson WP, Barrett IJ, Bernard L, Telenius A, Bernasconi F, Wilson RD, Best RG, Howard-Peebles PN, Langlois S, Kalousek DK. Meiotic origin of trisomy in confined placental mosaicism is correlated with presence of fetal uniparental disomy, high levels of trisomy in trophoblast, and increased risk of fetal intrauterine growth restriction. American journal of human genetics. 1997 Apr;60(4):917.

335. Toutain J, Labeau-Gaüzere C, Barnetche T, Horovitz J, Saura R. Confined placental mosaicism and pregnancy outcome: a distinction needs to be made between types 2 and 3. Prenatal diagnosis. 2010 Dec 1;30(12-13):1155-64.

336. Yuen RK, Robinson WP. A high capacity of the human placenta for genetic and epigenetic variation: implications for assessing pregnancy outcome. Placenta. 2011 Mar 1;32:S136-41.

337. Eastabrook G, Brown M, Sargent I. The origins and end-organ consequence of pre-eclampsia. Best Practice & Research Clinical Obstetrics & Gynaecology. 2011 Aug 1;25(4):435-47.

338. Staff AC, Benton SJ, von Dadelszen P, Roberts JM, Taylor RN, Powers RW, Charnock-Jones DS, Redman CW. Redefining preeclampsia using placenta-derived biomarkers. Hypertension. 2013 May 1;61(5):932-42.

339. Borzychowski AM, Sargent IL, Redman CW. Inflammation and pre-eclampsia. In Seminars in fetal and neonatal medicine 2006 Oct 1 (Vol. 11, No. 5, pp. 309-316). Elsevier.

340. Redman CW, Sargent IL. Immunology of pre-eclampsia. American Journal of Reproductive Immunology. 2010 Jun 1;63(6):534-43.

341. Sibai B, Dekker G, Kupferminc M. Pre-eclampsia. The Lancet. 2005 Feb 26;365(9461):785-99.

342. Hiby SE, Walker JJ, O'Shaughnessy KM, Redman CW, Carrington M, Trowsdale J, Moffett A. Combinations of maternal KIR and fetal HLA-C genes influence the risk of preeclampsia and reproductive success. Journal of Experimental Medicine. 2004 Oct 18;200(8):957-65.

343. Hiby SE, Regan L, Lo W, Farrell L, Carrington M, Moffett A. Association of maternal killer-cell immunoglobulin-like receptors and parental HLA-C genotypes with recurrent miscarriage. Human reproduction. 2008 Feb 8;23(4):972-6.

344. Baban B, Chandler PR, Sharma MD, Pihkala J, Koni PA, Munn DH, Mellor AL. IDO activates regulatory T cells and blocks their conversion into Th17-like T cells. The Journal of Immunology. 2009 Aug 15;183(4):2475-83.

345. Von Rango U, Krusche CA, Beier HM, Classen-Linke I. Indoleamine-dioxygenase is expressed in human decidua at the time maternal tolerance is established. Journal of reproductive immunology. 2007 Jun 1;74(1-2):34-45.

346. Hönig A, Rieger L, Kapp M, Sütterlin M, Dietl J, Kämmerer U. Indoleamine 2, 3-dioxygenase (IDO) expression in invasive extravillous trophoblast supports role of the enzyme for materno-fetal tolerance. Journal of reproductive immunology. 2004 Apr 1;61(2):79-86.

347. Munn DH, Zhou M, Attwood JT, Bondarev I, Conway SJ, Marshall B, Brown C, Mellor AL. Prevention of allogeneic fetal rejection by tryptophan catabolism. Science. 1998 Aug 21;281(5380):1191-3.

348. Mellembakken JR, Aukrust P, Olafsen MK, Ueland T, Hestdal K, Videm V. Activation of leukocytes during the uteroplacental passage in preeclampsia. Hypertension. 2002 Jan 1;39(1):155-60.

349. Dechend R, Müller DN, Wallukat G, Homuth V, Krause M, Dudenhausen J, Luft FC. Activating auto-antibodies against the AT1 receptor in preeclampsia. Autoimmunity reviews. 2005 Jan 1;4(1):61-5.

350. Abrahams VM. Mechanisms of antiphospholipid antibody-associated pregnancy complications. Thrombosis research. 2009 Nov 1;124(5):521-5.

351. Struwe E, Berzl G, Schild R, Blessing H, Drexel L, Hauck B, Tzschoppe A, Weidinger M, Sachs M, Scheler C, Schleussner E. Microarray analysis of placental tissue in intrauterine growth restriction. Clinical endocrinology. 2010 Feb 1;72(2):241-7.

352. Sitras V, Paulssen R, Leirvik J, Vårtun Å, Acharya G. Placental gene expression profile in intrauterine growth restriction due to placental insufficiency. Reproductive Sciences. 2009 Jul;16(7):701-11.

353. Nishizawa H, Ota S, Suzuki M, Kato T, Sekiya T, Kurahashi H, Udagawa Y. Comparative gene expression profiling of placentas from patients with severe pre-eclampsia and unexplained fetal growth restriction. Reproductive Biology and Endocrinology. 2011 Dec;9(1):107.

354. McMinn J, Wei M, Schupf N, Cusmai J, Johnson EB, Smith AC, Weksberg R, Thaker HM, Tycko B. Unbalanced placental expression of imprinted genes in human intrauterine growth restriction. Placenta. 2006 Jun 1;27(6):540-9.

355. McCarthy C, Cotter FE, McElwaine S, Twomey A, Mooney EE, Ryan F, Vaughan J. Altered gene expression patterns in intrauterine growth restriction: potential role of hypoxia. American Journal of Obstetrics & Gynecology. 2007 Jan 1;196(1):70-e1.

356. Maulik D, De A, Ragolia L, Evans J, Grigoryev D, Lankachandra K, Mundy D, Muscat J, Gerkovich MM, Ye SQ. Down-regulation of placental neuropilin-1 in fetal growth restriction. American Journal of Obstetrics & Gynecology. 2016 Feb 1;214(2):279-e1.

357. Madeleneau D, Buffat C, Mondon F, Grimault H, Rigourd V, Tsatsaris V, Letourneur F, Vaiman D, Barbaux S, Gascoin G. Transcriptomic analysis of human placenta in intrauterine growth restriction. Pediatric research. 2015 Jun;77(6):799.

358. Thomson M. The physiological roles of placental corticotropin releasing hormone in pregnancy and childbirth. Journal of physiology and biochemistry. 2013 Sep 1;69(3):559-73.

359. Leavey K, Benton SJ, Grynspan D, Bainbridge SA, Morgen EK, Cox BJ. Gene markers of normal villous maturation and their expression in placentas with maturational pathology. Placenta. 2017 Oct 1;58:52-9.

360. Park MJ, Lee DH, Joo BS, Lee YJ, Joo JK, An BS, Kim SC, Lee KS. Leptin, leptin receptors and hypoxia-induced factor-1α expression in the placental bed of patients with and without preeclampsia during pregnancy. Molecular medicine reports. 2018 Apr 1;17(4):5292-9.

361. Schanton M, Maymó JL, Pérez-Pérez A, Sánchez-Margalet V, Varone CL. Involvement of leptin in the molecular physiology of the placenta. Reproduction. 2018 Jan 1;155(1):R1-2.

362. Nevo O, Many A, Xu J, Kingdom J, Piccoli E, Zamudio S, Post M, Bocking A, Todros T, Caniggia I. Placental expression of soluble fms-like tyrosine kinase 1 is increased in singletons and twin pregnancies with intrauterine growth restriction. The Journal of Clinical Endocrinology & Metabolism. 2008 Jan 1;93(1):285-92.

363. Tsai S, Hardison NE, James AH, Motsinger-Reif AA, Bischoff SR, Thames BH, Piedrahita JA. Transcriptional profiling of human placentas from pregnancies complicated by preeclampsia reveals disregulation of sialic acid acetylesterase and immune signalling pathways. Placenta. 2011 Feb 1;32(2):175-82.

364. Blair JD, Yuen RK, Lim BK, McFadden DE, von Dadelszen P, Robinson WP. Widespread DNA hypomethylation at gene enhancer regions in placentas associated with early-onset pre-eclampsia. Molecular human reproduction. 2013 Jun 13;19(10):697-708.

365. Meng T, Chen H, Sun M, Wang H, Zhao G, Wang X. Identification of differential gene expression profiles in placentas from preeclamptic pregnancies versus normal pregnancies by DNA microarrays. Omics: a journal of integrative biology. 2012 Jun 1;16(6):301-11.

366. Nishizawa H, Pryor-Koishi K, Kato T, Kowa H, Kurahashi H, Udagawa Y. Microarray analysis of differentially expressed fetal genes in placental tissue derived from early and late onset severe pre-eclampsia. Placenta. 2007 May 1;28(5):487-97.

367. Sitras V, Paulssen RH, Grønaas H, Leirvik J, Hanssen TA, Vårtun Å, Acharya G. Differential placental gene expression in severe preeclampsia. Placenta. 2009 May 1;30(5):424-33.

368. Xiang Y, Cheng Y, Li X, Li Q, Xu J, Zhang J, Liu Y, Xing Q, Wang L, He L, Zhao X. Up-regulated expression and aberrant DNA methylation of LEP and SH3PXD2A in pre-eclampsia. PloS one. 2013 Mar 27;8(3):e59753.

369. Song Y, Liu J, Huang S, Zhang L. Analysis of differentially expressed genes in placental tissues of preeclampsia patients using microarray combined with the Connectivity Map database. Placenta. 2013 Dec 1;34(12):1190-5.

370. Enquobahrie DA, Meller M, Rice K, Psaty BM, Siscovick DS, Williams MA. Differential placental gene expression in preeclampsia. American Journal of Obstetrics & Gynecology. 2008 Nov 1;199(5):566-e1.

371. Cox B, Leavey K, Nosi U, Wong F, Kingdom J. Placental transcriptome in development and pathology: expression, function, and methods of analysis. American Journal of Obstetrics & Gynecology. 2015 Oct 1;213(4):S138-51.

372. Ajayi F, Kongoasa N, Gaffey T, Asmann YW, Watson WJ, Baldi A, Lala P, Shridhar V, Brost B, Chien J. Elevated expression of serine protease HtrA1 in preeclampsia and its role in trophoblast cell migration and invasion. American Journal of Obstetrics & Gynecology. 2008 Nov 1;199(5):557-e1.

373. Muttukrishna S. Role of inhibin in normal and high-risk pregnancy. In Seminars in reproductive medicine 2004 Aug (Vol. 22, No. 03, pp. 227-234). Copyright© 2004 by Thieme Medical Publishers, Inc., 333 Seventh Avenue, New York, NY 10001, USA..

374. Varkonyi T, Nagy B, Füle T, Tarca AL, Karaszi K, Schönléber J, Hupuczi P, Mihalik N, Kovalszky I, Rigo J, Meiri H. Microarray profiling reveals that placental transcriptomes of early-onset HELLP syndrome and preeclampsia are similar. Placenta. 2011 Feb 1;32:S21-9.

375. Vaiman D, Calicchio R, Miralles F. Landscape of transcriptional deregulations in the preeclamptic placenta. PloS one. 2013 Jun 13;8(6):e65498.

376. Kleinrouweler CE, van Uitert M, Moerland PD, Ris-Stalpers C, van der Post JA, Afink GB. Differentially expressed genes in the pre-eclamptic placenta: a systematic review and meta-analysis. PloS one. 2013 Jul 12;8(7):e68991.

377. Moslehi R, Mills JL, Signore C, Kumar A, Ambroggio X, Dzutsev A. Integrative transcriptome analysis reveals dysregulation of canonical cancer molecular pathways in placenta leading to preeclampsia. Scientific reports. 2013 Aug 30;3:2407.

378. Van Uitert M, Moerland PD, Enquobahrie DA, Laivuori H, Van Der Post JA, Ris-Stalpers C, Afink GB. Meta-analysis of placental transcriptome data identifies a novel molecular pathway related to preeclampsia. PloS one. 2015 Jul 14;10(7):e0132468.

379. Brew O, Sullivan MH, Woodman A. Comparison of normal and pre-eclamptic placental gene expression: a systematic review with meta-analysis. PloS one. 2016 Aug 25;11(8):e0161504.

380. Winn VD, Gormley M, Paquet AC, Kjaer-Sorensen K, Kramer A, Rumer KK, Haimov-Kochman R, Yeh RF, Overgaard MT, Varki A, Oxvig C. Severe preeclampsia-related changes in gene expression at the maternal-fetal interface include sialic acid-binding immunoglobulin-like lectin-6 and pappalysin-2. endocrinology. 2008 Sep 25;150(1):452-62.

381. Dunk CE, Roggensack AM, Cox B, Perkins JE, Åsenius F, Keating S, Weksberg R, Adamson SL. A distinct microvascular endothelial gene expression profile in severe IUGR placentas. Placenta. 2012 Apr 1;33(4):285-93.

382. Gormley M, Ona K, Kapidzic M, Garrido-Gomez T, Zdravkovic T, Fisher SJ. Preeclampsia: Novel insights from global RNA profiling of trophoblast subpopulations. American Journal of Obstetrics & Gynecology. 2017 Aug 1;217(2):200-e1.

383. Tsang JC, Vong JS, Ji L, Poon LC, Jiang P, Lui KO, Ni YB, To KF, Cheng YK, Chiu RW, Lo YM. Integrative single-cell and cell-free plasma RNA transcriptomics elucidates placental cellular dynamics. PNAS. 2017 Sep 12;114(37):E7786-95.

384. Khong TY, Staples A, Bendon RW, Chambers HM, Gould SJ, Knowles S, Shen-Schwarz S. Observer reliability in assessing placental maturity by histology. Journal of clinical pathology. 1995 May 1;48(5):420-3.

385. Khong TY, Mooney EE, Ariel I, Balmus NC, Boyd TK, Brundler MA, Derricott H, Evans MJ, Faye-Petersen OM, Gillan JE, Heazell AE. Sampling and definitions of placental lesions: Amsterdam placental workshop group consensus statement. Archives of pathology & laboratory medicine. 2016 May 25;140(7):698-713.

386. Redline RW. Classification of placental lesions. American Journal of Obstetrics & Gynecology. 2015 Oct 1;213(4):S21-8.

387. Kovo M, Schreiber L, Ben-Haroush A, Cohen G, Weiner E, Golan A, Bar J. The placental factor in early-and late-onset normotensive fetal growth restriction. Placenta. 2013 Apr 1;34(4):320-4.

388. Wright E, Audette MC, Xiang YY, Keating S, Hoffman B, Lye SJ, Shah PS, Kingdom JC. Maternal vascular malperfusion and adverse perinatal outcomes in low-risk nulliparous women. Obstetrics & Gynecology. 2017 Nov 1;130(5):1112-20.

389. Helfrich BB, Chilukuri N, He H, Cerda SR, Hong X, Wang G, Pearson C, Burd I, Wang X. Maternal vascular malperfusion of the placental bed associated with hypertensive disorders in the Boston Birth Cohort. Placenta. 2017 Apr 1;52:106-13.

390. Mandsager NT, Bendon R, Mostello D, Rosenn B, Miodovnik M, Siddiqi TA. Maternal floor infarction of the placenta: prenatal diagnosis and clinical significance. Obstetrics and gynecology. 1994 May;83(5 Pt 1):750-4.

391. Devisme L, Chauvière C, Franquet-Ansart H, Chudzinski A, Stichelbout M, Houfflin-Debarge V, Subtil D. Perinatal outcome of placental massive perivillous fibrin deposition: a case–control study. Prenatal diagnosis. 2017 Apr 1;37(4):323-8.

392. Chen A, Roberts DJ. Placental pathologic lesions with a significant recurrence risk–what not to miss!. APMIS. 2017 Dec 22.

393. Redline RW. Villitis of unknown etiology: noninfectious chronic villitis in the placenta. Human pathology. 2007 Oct 1;38(10):1439-46.

394. Redline RW, Boyd T, Campbell V, Hyde S, Kaplan C, Khong TY, Prashner HR, Waters BL. Maternal vascular underperfusion: nosology and reproducibility of placental reaction patterns. Pediatric and Developmental Pathology. 2004 Jun 1;7(3):237-49.

395. Fogarty NM, Ferguson-Smith AC, Burton GJ. Syncytial knots (Tenney-Parker changes) in the human placenta: evidence of loss of transcriptional activity and oxidative damage. The American journal of pathology. 2013 Jul 1;183(1):144-52.

396. Fitzgerald B, Kingdom J, Keating S. Distal villous hypoplasia. Diagnostic Histopathology. 2012 May 1;18(5):195-200.

397. Kaufmann P, Huppertz B, Frank HG. The fibrinoids of the human placenta: origin, composition and functional relevance. Annals of Anatomy-Anatomischer Anzeiger. 1996 Dec 1;178(6):485-501.

398. Huppertz B. Maternal–fetal interactions, predictive markers for preeclampsia, and programming. Journal of reproductive immunology. 2015 Apr 1;108:26-32.

399. Nelson DM. Apoptotic changes occur in syncytiotrophoblast of human placental villi where fibrin type fibrinoid is deposited at discontinuities in the villous trophoblast. Placenta. 1996 Sep 1;17(7):387-91.

400. Vinnars MT, Nasiell J, Ghazi SA, Westgren M, Papadogiannakis N. The severity of clinical manifestations in preeclampsia correlates with the amount of placental infarction. Acta obstetricia et gynecologica Scandinavica. 2011 Jan 1;90(1):19-25.

401. Moldenhauer JS, Stanek J, Warshak C, Khoury J, Sibai B. The frequency and severity of placental findings in women with preeclampsia are gestational age dependent. American Journal of Obstetrics & Gynecology. 2003 Oct 1;189(4):1173-7.

402. Salafia CM, Pezzullo JC, Ghidini A, Lopez-Zeno JA, Whittington SS. Clinical correlations of patterns of placental pathology in preterm pre-eclampsia. Placenta. 1998 Jan 1;19(1):67-72.

403. Ogge G, Chaiworapongsa T, Romero R, Hussein Y, Kusanovic JP, Yeo L, Kim CJ, Hassan SS. Placental lesions associated with maternal underperfusion are more frequent in early-onset than in late-onset preeclampsia. Journal of perinatal medicine. 2011 Nov 1;39(6):641-52.

404. Redline RW, Ariel I, Baergen RN, Derek J, Kraus FT, Roberts DJ, Sander CM. Fetal vascular obstructive lesions: nosology and reproducibility of placental reaction patterns. Pediatric and Developmental Pathology. 2004 Nov 1;7(5):443-52.

405. Katzman PJ, Genest DR. Maternal floor infarction and massive perivillous fibrin deposition: histological definitions, association with intrauterine fetal growth restriction, and risk of recurrence. Pediatric and developmental pathology. 2002 Mar 1;5(2):159-64.

406. Romero R, Whitten A, Korzeniewski SJ, Than NG, Chaemsaithong P, Miranda J, Dong Z, Hassan SS, Chaiworapongsa T. Maternal floor infarction/massive perivillous fibrin deposition: a manifestation of maternal antifetal rejection? American Journal of Reproductive Immunology. 2013 Oct 1;70(4):285-98.

407. Bane AL, Gillan JE. Massive perivillous fibrinoid causing recurrent placental failure. BJOG: An International Journal of Obstetrics & Gynaecology. 2003 Mar 1;110(3):292-5.

408. Andres RL, Kuyper W, Resnik R, Piacquadio KM, Benirschke K. The association of maternal floor infarction of the placenta with adverse perinatal outcome. American journal of obstetrics and gynecology. 1990 Sep 1;163(3):935-8.

409. Faye-Petersen OM, Ernst LM. Maternal floor infarction and massive perivillous fibrin deposition. Surgical pathology clinics. 2013 Mar 1;6(1):101-14.

410. Bendon RW, Hommel AB. Maternal floor infarction in autoimmune disease: two cases. Pediatric Pathology & Laboratory Medicine. 1996 Jan 1;16(2):293-8.

411. Whitten AE, Romero R, Korzeniewski SJ, Tarca AL, Schwartz AG, Yeo L, Dong Z, Hassan SS, Chaiworapongsa T. Evidence of an imbalance of angiogenic/antiangiogenic factors in massive perivillous fibrin deposition (maternal floor infarction): a placental lesion associated with recurrent miscarriage and fetal death. American Journal of Obstetrics & Gynecology. 2013 Apr 1;208(4):310-e1.

412. Wentworth P. The incidence and significance of intervillous thrombi in the human placenta. BJOG: An International Journal of Obstetrics & Gynaecology. 1964 Dec 1;71(6):894-8.

413. Benirschke K, Coen R, Patterson B, Key T. Villitis of known origin: varicella and toxoplasma. Placenta. 1999 Jul 1;20(5-6):395-9.

414. Kim MJ, Romero R, Kim CJ, Tarca AL, Chhauy S, LaJeunesse C, Lee DC, Draghici S, Gotsch F, Kusanovic JP, Hassan SS. Villitis of unknown etiology is associated with a distinct pattern of chemokine up-regulation in the feto-maternal and placental compartments: implications for conjoint maternal allograft rejection and maternal anti-fetal graft-versus-host disease. The Journal of Immunology. 2009 Mar 15;182(6):3919-27.

415. Tamblyn JA, Lissauer DM, Powell R, Cox P, Kilby MD. The immunological basis of villitis of unknown etiology–review. Placenta. 2013 Oct 1;34(10):846-55.

416. Styer AK, Parker HJ, Roberts DJ, Palmer-Toy D, Toth TL, Ecker JL. Placental villitis of unclear etiology during ovum donor in vitro fertilization pregnancy. American Journal of Obstetrics & Gynecology. 2003 Oct 1;189(4):1184-6.

417. Feeley L, Mooney EE. Villitis of unknown aetiology: correlation of recurrence with clinical outcome. Journal of Obstetrics and Gynaecology. 2010 Jul 1;30(5):476-9.

418. Jacques SM, Qureshi F. Chronic intervillositis of the placenta. Archives of pathology & laboratory medicine. 1993 Oct;117(10):1032-5.

419. Contro E, Bhide A. Chronic intervillositis of the placenta: a systematic review. Placenta. 2010 Dec 1;31(12):1106-10.

420. Boyd TK, Redline RW. Chronic histiocytic intervillositis: a placental lesion associated with recurrent reproductive loss. Human pathology. 2000 Nov 1;31(11):1389-96.

421. Labarrere CA, Bammerlin E, Hardin JW, DiCarlo HL. Intercellular adhesion molecule-1 expression in massive chronic intervillositis: implications for the invasion of maternal cells into fetal tissues. Placenta. 2014 May 1;35(5):311-7.

422. Feist H, Blöcker T, Hussein K. Massive perivillous fibrin deposition, chronic histiocytic intervillositis and villitis of unknown etiology: Lesions of the placenta at the fetomaternal interface with risk of recurrence. Der Pathologe. 2015 Jul;36(4):355-61.

423. Kaspar HG, Abu-Musa A, Hannoun A, Seoud M, Shammas M, Usta I, Khalil A. The placenta in meconium staining: lesions and early neonatal outcome. Clinical and experimental obstetrics & gynecology. 2000;27(1):63-6.

424. Lahra MM, Jeffery HE. A fetal response to chorioamnionitis is associated with early survival after preterm birth. American Journal of Obstetrics & Gynecology. 2004 Jan 1;190(1):147-51.

425. Martinelli P, Sarno L, Maruotti GM, Paludetto R. Chorioamnionitis and prematurity: a critical review. The Journal of Maternal-Fetal & Neonatal Medicine. 2012 Oct 1;25(sup4):21-3.

426. Cottrell EC, Sibley CP. From pre-clinical studies to clinical trials: generation of novel therapies for pregnancy complications. International journal of molecular sciences. 2015 Jun 8;16(6):12907-24.

427. Chitayat D, Langlois S, Wilson RD, Audibert F, Blight C, Brock JA, Cartier L, Carroll J, Désilets VA, Gagnon A, Johnson JA. Prenatal screening for fetal aneuploidy in singleton pregnancies. Journal of obstetrics and gynaecology Canada. 2011 Jul 1;33(7):736-50.

428. Dugoff L. First-and second-trimester maternal serum markers for aneuploidy and adverse obstetric outcomes. Obstetrics & Gynecology. 2010 May 1;115(5):1052-61.

429. Ong CY, Liao AW, Spencer K, Munim S, Nicolaides KH. First trimester maternal serum free β human chorionic gonadotrophin and pregnancy associated plasma protein A as predictors of pregnancy complications. BJOG: An International Journal of Obstetrics & Gynaecology. 2000 Oct 1;107(10):1265-70.

430. Bersinger NA, Smárason AK, Muttukrishna S, Groome NP, Redman CW. Women with preeclampsia have increased serum levels of pregnancy-associated plasma protein A (PAPP-A), inhibin A, activin A and soluble E-selectin. Hypertension in pregnancy. 2003 Jan 1;22(1):45-55.

431. Huang T, Hoffman B, Meschino W, Kingdom J, Okun N. Prediction of adverse pregnancy outcomes by combinations of first and second trimester biochemistry markers used in the routine prenatal screening of Down syndrome. Prenatal diagnosis. 2010 May 1;30(5):471-7.

432. Hui D, Okun N, Murphy K, Uleryk E, Shah PS. Combinations of maternal serum markers to predict preeclampsia, small for gestational age, and stillbirth: a systematic review. Journal of Obstetrics and Gynaecology Canada. 2012 Feb 1;34(2):142-53.

433. Fitzgerald B, Levytska K, Kingdom J, Walker M, Baczyk D, Keating S. Villous trophoblast abnormalities in extremely preterm deliveries with elevated second trimester maternal serum hCG or inhibin-A. Placenta. 2011 Apr 1;32(4):339-45.

434. Smith GC, Stenhouse EJ, Crossley JA, Aitken DA, Cameron AD, Connor JM. Early pregnancy levels of pregnancy-associated plasma protein a and the risk of intrauterine growth restriction, premature birth, preeclampsia, and stillbirth. The Journal of Clinical Endocrinology & Metabolism. 2002 Apr 1;87(4):1762-7.

435. Morris RK, Cnossen JS, Langejans M, Robson SC, Kleijnen J, ter Riet G, Mol BW, van der Post JA, Khan KS. Serum screening with Down's syndrome markers to predict pre-eclampsia and small for gestational age: systematic review and meta-analysis. BMC pregnancy and childbirth. 2008 Dec;8(1):33.

436. Redman CW, Sargent IL, Staff AC. IFPA Senior Award Lecture: making sense of pre-eclampsia–two placental causes of preeclampsia? Placenta. 2014 Feb 1;35:S20-5.

437. Saffer C, Olson G, Boggess KA, Beyerlein R, Eubank C, Sibai BM, NORMALS Study Group. Determination of placental growth factor (PlGF) levels in healthy pregnant women without signs or symptoms of preeclampsia. Pregnancy Hypertension: An International Journal of Women's Cardiovascular Health. 2013 Apr 1;3(2):124-32.

438. Levine RJ, Lam C, Qian C, Yu KF, Maynard SE, Sachs BP, Sibai BM, Epstein FH, Romero R, Thadhani R, Karumanchi SA. Soluble endoglin and other circulating antiangiogenic factors in preeclampsia. New England Journal of Medicine. 2006 Sep 7;355(10):992-1005.

439. Powers RW, Roberts JM, Cooper KM, Gallaher MJ, Frank MP, Harger GF, Ness RB. Maternal serum soluble fms-like tyrosine kinase 1 concentrations are not increased in early pregnancy and decrease more slowly postpartum in women who develop preeclampsia. American Journal of Obstetrics & Gynecology. 2005 Jul 1;193(1):185-91.

440. Kleinrouweler CE, Wiegerinck MM, Ris-Stalpers C, Bossuyt PM, van der Post JA, von Dadelszen P, Mol BW, Pajkrt E. Accuracy of circulating placental growth factor, vascular endothelial growth factor, soluble fms-like tyrosine kinase 1 and soluble endoglin in the prediction of pre-eclampsia: a systematic review and meta-analysis. BJOG: an International Journal of Obstetrics & Gynaecology. 2012 Jun 1;119(7):778-87.

441. Forest JC, Thériault S, Massé J, Bujold E, Giguère Y. Soluble Fms-like tyrosine kinase-1 to placental growth factor ratio in mid-pregnancy as a predictor of preterm preeclampsia in asymptomatic pregnant women. Clinical Chemistry and Laboratory Medicine (CCLM). 2014 Aug 1;52(8):1169-78.

442. Chappell LC, Duckworth S, Seed PT, Griffin M, Myers J, Mackillop L, Simpson N, Waugh J, Anumba D, Kenny LC, Redman CW. Diagnostic Accuracy of Placental Growth Factor in Women With Suspected PreeclampsiaClinical Perspective: A Prospective Multicenter Study. Circulation. 2013 Nov 5;128(19):2121-31.

443. Åsvold BO, Eskild A, Vatten LJ. Human chorionic gonadotropin, angiogenic factors, and preeclampsia risk: a nested case–control study. Acta obstetricia et gynecologica Scandinavica. 2014 May 1;93(5):454-62.

444. Audibert F, Boucoiran I, An N, Aleksandrov N, Delvin E, Bujold E, Rey E. Screening for preeclampsia using first-trimester serum markers and uterine artery Doppler in nulliparous women. American Journal of Obstetrics & Gynecology. 2010 Oct 1;203(4):383-e1.

445. Stubert J, Ullmann S, Bolz M, Külz T, Dieterich M, Richter DU, Reimer T. Prediction of preeclampsia and induced delivery at<34 weeks gestation by sFLT-1 and PlGF in patients with abnormal midtrimester uterine Doppler velocimetry: a prospective cohort analysis. BMC pregnancy and childbirth. 2014 Dec;14(1):292.

446. Herraiz I, Dröge LA, Gómez-Montes E, Henrich W, Galindo A, Verlohren S. Characterization of the soluble fms-like tyrosine kinase-1 to placental growth factor ratio in pregnancies complicated by fetal growth restriction. Obstetrics & Gynecology. 2014 Aug 1;124(2, PART 1):265-73.

447. Griffin M, Seed PT, Webster L, Myers J, MacKillop L, Simpson N, Anumba D, Khalil A, Denbow M, Sau A, Hinshaw K. Diagnostic accuracy of placental growth factor and ultrasound parameters to

predict the small-for-gestational-age infant in women presenting with reduced symphysis–fundus height. Ultrasound in Obstetrics & Gynecology. 2015 Aug 1;46(2):182-90.

448. Åsvold BO, Vatten LJ, Romundstad PR, Jenum PA, Karumanchi SA, Eskild A. Angiogenic factors in maternal circulation and the risk of severe fetal growth restriction. American journal of epidemiology. 2011 Feb 11;173(6):630-9.

449. Stepan H, Unversucht A, Wessel N, Faber R. Predictive value of maternal angiogenic factors in second trimester pregnancies with abnormal uterine perfusion. Hypertension. 2007 Apr 1;49(4):818-24.

450. Conde-Agudelo A, Papageorghiou AT, Kennedy SH, Villar J. Novel biomarkers for predicting intrauterine growth restriction: a systematic review and meta-analysis. BJOG: An International Journal of Obstetrics & Gynaecology. 2013 May 1;120(6):681-94.

451. Baltajian K, Hecht JL, Wenger JB, Salahuddin S, Verlohren S, Perschel FH, Zsengeller ZK, Thadhani R, Karumanchi SA, Rana S. Placental lesions of vascular insufficiency are associated with anti-angiogenic state in women with preeclampsia. Hypertension in pregnancy. 2014 Nov 1;33(4):427-39.

452. Korzeniewski SJ, Romero R, Chaiworapongsa T, Chaemsaithong P, Kim CJ, Kim YM, Kim JS, Yoon BH, Hassan SS, Yeo L. Maternal plasma angiogenic index-1 (placental growth factor/soluble vascular endothelial growth factor receptor-1) is a biomarker for the burden of placental lesions consistent with uteroplacental underperfusion: a longitudinal case-cohort study. American Journal of Obstetrics & Gynecology. 2016 May 1;214(5):629-e1.

453. Triunfo S, Lobmaier S, Parra-Saavedra M, Crovetto F, Peguero A, Nadal A, Gratacos E, Figueras F. Angiogenic factors at diagnosis of late-onset small-for-gestational age and histological placental underperfusion. Placenta. 2014 Jun 1;35(6):398-403.

454. Benton SJ, McCowan LM, Heazell AE, Grynspan D, Hutcheon JA, Senger C, Burke O, Chan Y, Harding JE, Yockell-Lelièvre J, Hu Y. Placental growth factor as a marker of fetal growth restriction caused by placental dysfunction. Placenta. 2016 Jun 1;42:1-8.

455. Walker MG, Bujold E, Kingdom JC. Is Canada Ready to Adopt Maternal Placental Growth Factor Testing to Improve Clinical Outcomes for Women with Suspected Preeclampsia? Journal of Obstetrics and Gynaecology Canada. 2017 Jul 1;39(7):580-3.

456. Cardaropoli S, Ietta F, Romagnoli R, Rolfo A, Paulesu L, Todros T. Lower macrophage migration inhibitory factor concentrations in maternal serum before pre-eclampsia onset. Journal of Interferon & Cytokine Research. 2014 Jul 1;34(7):537-42.

457. Sahay AS, Patil VV, Sundrani DP, Joshi AA, Wagh GN, Gupte SA, Joshi SR. A longitudinal study of circulating angiogenic and antiangiogenic factors and AT1-AA levels in preeclampsia. Hypertension Research. 2014 Aug;37(8):753.

458. Wölter M, Röwer C, Koy C, Rath W, Pecks U, Glocker MO. Proteoform profiling of peripheral blood serum proteins from pregnant women provides a molecular IUGR signature. Journal of proteomics. 2016 Oct 21;149:44-52.

459. Atiba AS, Abbiyesuku FM, Oparinde DP, Ajose OA. Free radical attack on membrane lipid and antioxidant vitamins in the course of pre-eclamptic pregnancy. Ethiopian journal of health sciences. 2014;24(1):35-42.

460. Levine RJ, Qian C, LeShane ES, Kai FY, England LJ, Schisterman EF, Wataganara T, Romero R, Bianchi DW. Two-stage elevation of cell-free fetal DNA in maternal sera before onset of preeclampsia. American Journal of Obstetrics & Gynecology. 2004 Mar 1;190(3):707-13.

461. Karampas G, Eleftheriades M, Panoulis K, Rizou M, Haliassos A, Hassiakos D, Vitoratos N, Rizos D. Maternal serum levels of neutrophil gelatinase-associated lipocalin (NGAL), matrix metalloproteinase-9 (MMP-9) and their complex MMP-9/NGAL in pregnancies with preeclampsia and those with a small for gestational age neonate: a longitudinal study. Prenatal diagnosis. 2014 Aug 1;34(8):726-33.

462. Sifakis S, Akolekar R, Kappou D, Mantas N, Nicolaides KH. Maternal serum placental growth hormone at 11–13 weeks' gestation in pregnancies delivering small for gestational age neonates. The Journal of Maternal-Fetal & Neonatal Medicine. 2012 Sep 1;25(9):1796-9.

463. Franco-Sena AB, Goldani MZ, Do Carmo MD, Velásquez-Melendez G, Kac G. Low leptin concentration in the first gestational trimester is associated with being born small for gestational age: prospective study in Rio de Janeiro, Brazil. Neonatology. 2010;97(4):291-8.

464. Potdar N, Singh R, Mistry V, Evans MD, Farmer PB, Konje JC, Cooke MS. First-trimester increase in oxidative stress and risk of small-for-gestational-age fetus. BJOG: An International Journal of Obstetrics & Gynaecology. 2009 Apr 1;116(5):637-42.

465. Than NG, Romero R, Meiri H, Erez O, Xu Y, Tarquini F, Barna L, Szilagyi A, Ackerman R, Sammar M, Fule T. PP13, maternal ABO blood groups and the risk assessment of pregnancy complications. PloS one. 2011 Jul 25;6(7):e21564.

466. Ernst GD, de Jonge LL, Hofman A, Lindemans J, Russcher H, Steegers EA, Jaddoe VW. C-reactive protein levels in early pregnancy, fetal growth patterns, and the risk for neonatal complications: the Generation R Study. American Journal of Obstetrics & Gynecology. 2011 Aug 1;205(2):132-e1.

467. Georgiou HM, Thio YS, Russell C, Permezel M, Heng YJ, Lee S, Tong S. Association between maternal serum cytokine profiles at 7-10 weeks' gestation and birthweight in small for gestational age infants. American Journal of Obstetrics & Gynecology. 2011 May 1;204(5):415-e1.

468. Chafetz I, Kuhnreich I, Sammar M, Tal Y, Gibor Y, Meiri H, Cuckle H, Wolf M. First-trimester placental protein 13 screening for preeclampsia and intrauterine growth restriction. American Journal of Obstetrics & Gynecology. 2007 Jul 1;197(1):35-e1.

469. Anton L, Olarerin-George AO, Schwartz N, Srinivas S, Bastek J, Hogenesch JB, Elovitz MA. miR-210 inhibits trophoblast invasion and is a serum biomarker for preeclampsia. The American journal of pathology. 2013 Nov 1;183(5):1437-45.

470. Whitehead CL, McNamara H, Walker SP, Alexiadis M, Fuller PJ, Vickers DK, Hannan NJ, Hastie R, Tuohey L, Tu'uhevaha J, Tong S. Identifying late-onset fetal growth restriction by measuring circulating placental RNA in the maternal blood at 28 weeks' gestation. American Journal of Obstetrics & Gynecology. 2016 Apr 1;214(4):521-e1.

471. Xu P, Zhao Y, Liu M, Wang Y, Wang H, Li YX, Zhu X, Yao Y, Wang H, Qiao J, Ji L. Variations of microRNAs in human placentas and plasma from preeclamptic pregnancy. Hypertension. 2014 Jun;63(6):1276-84.

472. Chen Q, Wang Y, Li Y, Zhao M, Nie G. Serum podocalyxin is significantly increased in early-onset preeclampsia and may represent a novel marker of maternal endothelial dysfunction. Placenta. 2017 Sep 1;57:322.

473. Akkurt MO, Akkurt I, Altay M, Coskun B, Erkaya S, Sezik M. Maternal serum ferritin as a clinical tool at 34–36 weeks' gestation for distinguishing subgroups of fetal growth restriction. The Journal of Maternal-Fetal & Neonatal Medicine. 2017 Feb 16;30(4):452-6.

474. Wu P, Van Den Berg C, Alfirevic Z, O'brien S, Röthlisberger M, Baker PN, Kenny LC, Kublickiene K, Duvekot JJ. Early pregnancy biomarkers in pre-eclampsia: a systematic review and meta-analysis. International journal of molecular sciences. 2015 Sep 23;16(9):23035-56.

475. Lesmes C, Gallo DM, Panaiotova J, Poon LC, Nicolaides KH. Prediction of small-for-gestational-age neonates: screening by fetal biometry at 19–24 weeks. Ultrasound in Obstetrics & Gynecology. 2015 Aug 1;46(2):198-207.

476. Bakalis S, Silva M, Akolekar R, Poon LC, Nicolaides KH. Prediction of small-for-gestational-age neonates: screening by fetal biometry at 30–34 weeks. Ultrasound in Obstetrics & Gynecology. 2015 May 1;45(5):551-8.

477. Fadigas C, Saiid Y, Gonzalez R, Poon LC, Nicolaides KH. Prediction of small-for-gestational-age neonates: screening by fetal biometry at 35–37 weeks. Ultrasound in Obstetrics & Gynecology. 2015 May 1;45(5):559-65.

478. Callec R, Lamy C, Perdriolle-Galet E, Patte C, Heude B, Morel O. Impact on obstetric outcome of third-trimester screening for small-for-gestational-age fetuses. Ultrasound in Obstetrics & Gynecology. 2015 Aug 1;46(2):216-20.

479. Vachon-Marceau C, Demers S, Markey S, Okun N, Girard M, Bujold E. First-trimester placental thickness and the risk of preeclampsia or SGA. Placenta. 2017 Sep 1;57:123-8.

480. Gómez O, Figueras F, Fernández S, Bennasar M, Martinez JM, Puerto B, Gratacós E. Reference ranges for uterine artery mean pulsatility index at 11–41 weeks of gestation. Ultrasound in Obstetrics & Gynecology. 2008 Aug 1;32(2):128-32.

481. Acharya G, Wilsgaard T, Berntsen GK, Maltau JM, Kiserud T. Reference ranges for serial measurements of umbilical artery Doppler indices in the second half of pregnancy. American Journal of Obstetrics & Gynecology. 2005 Mar 1;192(3):937-44.

482. Garcia B, Llurba E, Valle L, Gómez-Roig MD, Juan M, Pérez-Matos C, Fernández M, García-Hernández JA, Alijotas-Reig J, Higueras MT, Calero I. Do knowledge of uterine artery resistance in the second trimester and targeted surveillance improve maternal and perinatal outcome? UTOPIA study: a randomized controlled trial. Ultrasound in Obstetrics & Gynecology. 2016 Jun 1;47(6):680-9.

483. Velauthar L, Plana MN, Kalidindi M, Zamora J, Thilaganathan B, Illanes SE, Khan KS, Aquilina J, Thangaratinam S. First-trimester uterine artery Doppler and adverse pregnancy outcome: a meta-analysis involving 55 974 women. Ultrasound in Obstetrics & Gynecology. 2014 May 1;43(5):500-7.

484. Melchiorre K, Wormald B, Leslie K, Bhide A, Thilaganathan B. First-trimester uterine artery Doppler indices in term and preterm pre-eclampsia. Ultrasound in Obstetrics & Gynecology. 2008 Aug 1;32(2):133-7.

485. Myatt L, Clifton RG, Roberts JM, Spong CY, Hauth JC, Varner MW, Wapner RJ, Thorp Jr JM, Mercer BM, Grobman WA, Ramin SM. The utility of uterine artery Doppler velocimetry in prediction of preeclampsia in a low-risk population. Obstetrics and gynecology. 2012 Oct;120(4):815.

486. Vainio M, Kujansuu E, Koivisto AM, Mäenpää J. Bilateral notching of uterine arteries at 12–14 weeks of gestation for prediction of hypertensive disorders of pregnancy. Acta obstetricia et gynecologica Scandinavica. 2005 Nov 1;84(11):1062-7.

487. Cnossen JS, Morris RK, ter Riet G, Mol BW, van der Post JA, Coomarasamy A, Zwinderman AH, Robson SC, Bindels PJ, Kleijnen J, Khan KS. Use of uterine artery Doppler ultrasonography to predict pre-eclampsia and intrauterine growth restriction: a systematic review and bivariable meta-analysis. Canadian Medical Association Journal. 2008 Mar 11;178(6):701-11.

488. Levytska K, Higgins M, Keating S, Melamed N, Walker M, Sebire NJ, Kingdom JC. Placental pathology in relation to uterine artery doppler findings in pregnancies with severe intrauterine

growth restriction and abnormal umbilical artery doppler changes. American journal of perinatology. 2017;34(5):451-7.

489. Orabona R, Donzelli CM, Falchetti M, Santoro A, Valcamonico A, Frusca T. Placental histological patterns and uterine artery Doppler velocimetry in pregnancies complicated by early or late pre-eclampsia. Ultrasound in Obstetrics & Gynecology. 2016 May 1;47(5):580-5.

490. Turan OM, Turan S, Gungor S, Berg C, Moyano D, Gembruch U, Nicolaides KH, Harman CR, Baschat AA. Progression of Doppler abnormalities in intrauterine growth restriction. Ultrasound in Obstetrics & Gynecology. 2008 Aug 1;32(2):160-7.

491. De Paco C, Ventura W, Oliva R, Miguel M, Arteaga A, Nieto A, Delgado JL. Umbilical artery Doppler at 19 to 22 weeks of gestation in the prediction of adverse pregnancy outcomes. Prenatal diagnosis. 2014 Jul 1;34(7):711-5.

492. Vergani P, Andreotti C, Roncaglia N, Zani G, Pozzi E, Pezzullo JC, Ghidini A. Doppler predictors of adverse neonatal outcome in the growth restricted fetus at 34 weeks' gestation or beyond. American Journal of Obstetrics & Gynecology. 2003 Oct 1;189(4):1007-11.

493. Karsdorp VH, Van Vugt JM, Van Geijn HP, Kostense PJ, Arduim D, Montenegro N, Todros T. Clinical significance of absent or reversed end diastolic velocity waveforms in umbilical artery. The Lancet. 1994 Dec 17;344(8938):1664-8.

494. Nicolini U, Nicolaidis P, Fisk NM, Vaughan JI, Rodeck CH, Fusi L, Gleeson R. Limited role of fetal blood sampling in prediction of outcome in intrauterine growth retardation. The Lancet. 1990 Sep 29;336(8718):768-72.

495. Sun L, Macgowan CK, Portnoy S, Sled JG, Yoo SJ, Grosse-Wortmann L, Jaeggi E, Kingdom J, Seed M. New advances in fetal cardiovascular magnetic resonance imaging for quantifying the distribution of blood flow and oxygen transport: Potential applications in fetal cardiovascular disease diagnosis and therapy. Echocardiography. 2017 Dec 1;34(12):1799-803.

496. Zhu MY, Milligan N, Keating S, Windrim R, Keunen J, Thakur V, Ohman A, Portnoy S, Sled JG, Kelly E, Yoo SJ, Gross-Wortmann L, Jaeggi E, Macgowan CK, Kingdom JC, Seed M. The hemodynamics of late-onset intrauterine growth restriction by MRI. American Journal of Obstetrics & Gynecology. 2016 Mar 1;214(3):367-e1.

497. Khalil A, Garcia-Mandujano R, Maiz N, Elkhouli M, Nicolaides KH. Longitudinal changes in maternal hemodynamics in a population at risk for pre-eclampsia. Ultrasound in Obstetrics & Gynecology. 2014 Aug 1;44(2):197-204.

498. Doherty A, Carvalho JC, Drewlo S, Afif EK, Downey K, Dodds M, Kingdom J. Altered hemodynamics and hyperuricemia accompany an elevated sFlt-1/PlGF ratio before the onset of early severe preeclampsia. Journal of Obstetrics and Gynaecology Canada. 2014 Aug 1;36(8):692-700.

499. Brandão AH, Félix LR, do Carmo Patrício E, Leite HV, Cabral AC. Difference of endothelial function during pregnancies as a method to predict preeclampsia. Archives of gynecology and obstetrics. 2014 Sep 1;290(3):471-7.

500. Antonios TF, Nama V, Wang D, Manyonda IT. Microvascular remodelling in preeclampsia: quantifying capillary rarefaction accurately and independently predicts preeclampsia. American journal of hypertension. 2013 Jun 11;26(9):1162-9.

501. Gallo D, Poon LC, Fernandez M, Wright D, Nicolaides KH. Prediction of preeclampsia by mean arterial pressure at 11-13 and 20-24 weeks' gestation. Fetal diagnosis and therapy. 2014;36(1):28-37.

502. Monteith C, McSweeney L, Breatnach CR, Doherty A, Shirren L, Tully EC, Dicker P, Malone FD, Afif EK, Kent E. Non-invasive cardiac output monitoring (NICOM®) can predict the evolution of uteroplacental disease—Results of the prospective HANDLE study. European Journal of Obstetrics and Gynecology and Reproductive Biology. 2017 Sep 1;216:116-24.

503. North RA, McCowan LM, Dekker GA, Poston L, Chan EH, Stewart AW, Black MA, Taylor RS, Walker JJ, Baker PN, Kenny LC. Clinical risk prediction for pre-eclampsia in nulliparous women: development of model in international prospective cohort. BMJ. 2011 Apr 7;342:d1875.

504. Akolekar R, Syngelaki A, Sarquis R, Zvanca M, Nicolaides KH. Prediction of early, intermediate and late pre-eclampsia from maternal factors, biophysical and biochemical markers at 11–13 weeks. Prenatal diagnosis. 2011 Jan 1;31(1):66-74.

505. Myatt L, Clifton RG, Roberts JM, Spong CY, Hauth JC, Varner MW, Thorp Jr JM, Mercer BM, Peaceman AM, Ramin SM, Carpenter MW. First-trimester prediction of preeclampsia in low-risk nulliparous women. Obstetrics and gynecology. 2012 Jun;119(6):1234.

506. Myers JE, Kenny LC, McCowan LM, Chan EH, Dekker GA, Poston L, Simpson NA, North RA. Angiogenic factors combined with clinical risk factors to predict preterm pre-eclampsia in nulliparous women: a predictive test accuracy study. BJOG: An International Journal of Obstetrics & Gynaecology. 2013 Sep 1;120(10):1215-23.

507. Akolekar R, Syngelaki A, Poon L, Wright D, Nicolaides KH. Competing risks model in early screening for preeclampsia by biophysical and biochemical markers. Fetal diagnosis and therapy. 2013;33(1):8-15.

508. Crovetto F, Figueras F, Triunfo S, Crispi F, Rodriguez-Sureda V, Peguero A, Dominguez C, Gratacos E. Added value of angiogenic factors for the prediction of early and late preeclampsia in the first trimester of pregnancy. Fetal diagnosis and therapy. 2014;35(4):258-66.

509. Lesmes C, Gallo DM, Saiid Y, Poon LC, Nicolaides KH. Prediction of small-for-gestational-age neonates: screening by uterine artery Doppler and mean arterial pressure at 19–24 weeks. Ultrasound in Obstetrics & Gynecology. 2015 Sep 1;46(3):332-40.

510. Lassala A, Bazer FW, Cudd TA, Datta S, Keisler DH, Satterfield MC, Spencer TE, Wu G. Parenteral Administration of L-Arginine Prevents Fetal Growth Restriction in Undernourished Ewes, 2. The Journal of nutrition. 2010 May 26;140(7):1242-8.

511. Vosatka RJ, Hassoun PM, Harvey-Wilkes KB. Dietary L-arginine prevents fetal growth restriction in rats. American Journal of Obstetrics & Gynecology. 1998 Feb 1;178(2):242-6.

512. Rytlewski K, Olszanecki R, Korbut R, Zdebski Z. Effects of prolonged oral supplementation with l-arginine on blood pressure and nitric oxide synthesis in preeclampsia. European journal of clinical investigation. 2005 Jan 1;35(1):32-7.

513. Sieroszewski P, Suzin J, Karowicz-Bilińska A. Ultrasound evaluation of intrauterine growth restriction therapy by a nitric oxide donor (L-arginine). The Journal of Maternal-Fetal & Neonatal Medicine. 2004 Jun 1;15(6):363-6.

514. Cureton N, Korotkova I, Baker B, Greenwood S, Wareing M, Kotamraju VR, Teesalu T, Cellesi F, Tirelli N, Ruoslahti E, Aplin JD. Selective targeting of a novel vasodilator to the uterine vasculature to treat impaired uteroplacental perfusion in pregnancy. Theranostics. 2017;7(15):3715.

515. Wareing M, Myers JE, O'hara M, Baker PN. Sildenafil citrate (Viagra) enhances vasodilatation in fetal growth restriction. The Journal of Clinical Endocrinology & Metabolism. 2005 May 1;90(5):2550-5.

516. Ramesar SV, Mackraj I, Gathiram P, Moodley J. Sildenafil citrate decreases sFlt-1 and sEng in pregnant l-NAME treated Sprague–Dawley rats. European Journal of Obstetrics and Gynecology and Reproductive Biology. 2011 Aug 1;157(2):136-40.

517. Herraiz S, Pellicer B, Serra V, Cauli O, Cortijo J, Felipo V, Pellicer A. Sildenafil citrate improves perinatal outcome in fetuses from pre-eclamptic rats. BJOG: An International Journal of Obstetrics & Gynaecology. 2012 Oct 1;119(11):1394-402.

518. Sharp A, Cornforth C, Jackson R, Harrold J, Turner MA, Kenny LC, Baker PN, Johnstone ED, Khalil A, von Dadelszen P, Papageorghiou AT. Maternal sildenafil for severe fetal growth restriction (STRIDER): a multicentre, randomised, placebo-controlled, double-blind trial. The Lancet Child & Adolescent Health. 2018 Feb 1;2(2):93-102.

519. Crandon AJ, Isherwood DM. Effect of aspirin on incidence of pre-eclampsia. The Lancet. 1979 Jun 23;313(8130):1356.

520. Taubert D, Berkels R, Grosser N, Schröder H, Gründemann D, Schömig E. Aspirin induces nitric oxide release from vascular endothelium: a novel mechanism of action. British journal of pharmacology. 2004 Sep 1;143(1):159-65.

521. Roberge S, Villa P, Nicolaides K, Giguère Y, Vainio M, Bakthi A, Ebrashy A, Bujold E. Early administration of low-dose aspirin for the prevention of preterm and term preeclampsia: a systematic review and meta-analysis. Fetal diagnosis and therapy. 2012;31(3):141-6.

522. Bujold E, Roberge S, Lacasse Y, Bureau M, Audibert F, Marcoux S, Forest JC, Giguère Y. Prevention of preeclampsia and intrauterine growth restriction with aspirin started in early pregnancy: a meta-analysis. Obstetrics & Gynecology. 2010 Aug 1;116(2, Part 1):402-14.

523. Roberge S, Nicolaides K, Demers S, Hyett J, Chaillet N, Bujold E. The role of aspirin dose on the prevention of preeclampsia and fetal growth restriction: systematic review and meta-analysis. American Journal of Obstetrics & Gynecology. 2017 Feb 1;216(2):110-20.

524. Rolnik DL, Wright D, Poon LC, O'gorman N, Syngelaki A, de Paco Matallana C, Akolekar R, Cicero S, Janga D, Singh M, Molina FS. Aspirin versus placebo in pregnancies at high risk for preterm preeclampsia. New England Journal of Medicine. 2017 Aug 17;377(7):613-22.

525. Bartsch E, Park AL, Kingdom JC, Ray JG. Risk threshold for starting low dose aspirin in pregnancy to prevent preeclampsia: an opportunity at a low cost. PloS one. 2015 Mar 19;10(3):e0116296.

526. Buyse FG, Wormgoor BH, Bernard JT, Koudstaal J. Anticoagulant therapy of patients with repeated placental infarction. Obstetrics & Gynecology. 1974 Jun 1;43(6):844-8.

527. Mousavi S, Moradi M, Khorshidahmad T, Motamedi M. Anti-inflammatory effects of heparin and its derivatives: a systematic review. Advances in pharmacological sciences. 2015;2015.

528. Sobel ML, Kingdom JC, Drewlo S. Angiogenic response of placental villi to heparin. Obstetrics & Gynecology. 2011 Jun 1;117(6):1375-83.

529. Yinon Y, Meir EB, Margolis L, Lipitz S, Schiff E, Mazaki-Tovi S, Simchen MJ. Low molecular weight heparin therapy during pregnancy is associated with elevated circulatory levels of placental growth factor. Placenta. 2015 Feb 1;36(2):121-4.

530. McLaughlin K, Baczyk D, Potts A, Hladunewich M, Parker JD, Kingdom JC. Low molecular weight heparin improves endothelial function in pregnant women at high risk of preeclampsia. Hypertension. 2017 Jan;69(1):180-188.

531. Rey E, Garneau P, David M, Gauthier R, Leduc L, Michon N, Morin F, Demers C, Kahn SR, Magee LA, Rodger M. Dalteparin for the prevention of recurrence of placental-mediated complications of pregnancy in women without thrombophilia: a pilot randomized controlled trial. Journal of Thrombosis and Haemostasis. 2009 Jan 1;7(1):58-64.

532. de Vries JI, van Pampus MG, Hague WM, Bezemer PD, Joosten JH. Low-molecular-weight heparin added to aspirin in the prevention of recurrent early-onset pre-eclampsia in women with inheritable thrombophilia: the FRUIT-RCT. Journal of Thrombosis and Haemostasis. 2012 Jan 1;10(1):64-72.

533. Dodd JM, McLeod A, Windrim RC, Kingdom J. Antithrombotic therapy for improving maternal or infant health outcomes in women considered at risk of placental dysfunction. The Cochrane Library. 2013 Jan 1.

534. Kingdom JC, Drewlo S. Is heparin a placental anticoagulant in high-risk pregnancies? Blood. 2011 Nov 3;118(18):4780-8.

535. Dodd JM, Sahi K, Mcleod A, Windrim RC, Kingdom JC. Heparin therapy for complications of placental dysfunction: A systematic review of the literature. Acta obstetricia et gynecologica Scandinavica. 2008 Aug 1;87(8):804-11.

536. Kingdom JC, Walker M, Proctor LK, Keating S, Shah PS, Mcleod A, Keunen J, Windrim RC, Dodd JM. Unfractionated heparin for second trimester placental insufficiency: a pilot randomized trial. Journal of Thrombosis and Haemostasis. 2011 Aug 1;9(8):1483-92.

537. Groom KM, David AL. The role of aspirin, heparin, and other interventions in the prevention and treatment of fetal growth restriction. American Journal of Obstetrics & Gynecology. 2018 Feb 1;218(2):S829-40.

538. Chappell LC, Seed PT, Briley AL, Kelly FJ, Lee R, Hunt BJ, Parmar K, Bewley SJ, Shennan AH, Steer PJ, Poston L. Effect of antioxidants on the occurrence of pre-eclampsia in women at increased risk: a randomised trial. The Lancet. 1999 Sep 4;354(9181):810-6.

539. Poston L, Briley AL, Seed PT, Kelly FJ, Shennan AH, Vitamins in Pre-eclampsia (VIP) Trial Consortium. Vitamin C and vitamin E in pregnant women at risk for pre-eclampsia (VIP trial): randomised placebo-controlled trial. The Lancet. 2006 Apr 8;367(9517):1145-54.

540. Xu H, Perez-Cuevas R, Xiong X, Reyes H, Roy C, Julien P, Smith G, von Dadelszen P, Leduc L, Audibert F, Moutquin JM. An international trial of antioxidants in the prevention of preeclampsia (INTAPP). American Journal of Obstetrics & Gynecology. 2010 Mar 1;202(3):239-e1.

541. Hobson SR, Lim R, Gardiner EE, Alers NO, Wallace EM. Phase I pilot clinical trial of antenatal maternally administered melatonin to decrease the level of oxidative stress in human pregnancies affected by pre-eclampsia (PAMPR): study protocol. BMJ open. 2013 Sep 1;3(9):e003788.

542. Alers NO, Jenkin G, Miller SL, Wallace EM. Antenatal melatonin as an antioxidant in human pregnancies complicated by fetal growth restriction—a phase I pilot clinical trial: study protocol. BMJ open. 2013 Dec 1;3(12):e004141.

543. Montgomery RA, Lonze BE, King KE, Kraus ES, Kucirka LM, Locke JE, Warren DS, Simpkins CE, Dagher NN, Singer AL, Zachary AA. Desensitization in HLA-incompatible kidney recipients and survival. New England Journal of Medicine. 2011 Jul 28;365(4):318-26.

544. Hutton B, Sharma R, Fergusson D, Tinmouth A, Hebert P, Jamieson J, Walker M. Use of intravenous immunoglobulin for treatment of recurrent miscarriage: a systematic review. BJOG: An International Journal of Obstetrics & Gynaecology. 2007 Feb 1;114(2):134-42.

545. Stephenson MD, Kutteh WH, Purkiss S, Librach C, Schultz P, Houlihan E, Liao C. Intravenous immunoglobulin and idiopathic secondary recurrent miscarriage: a multicentered randomized placebo-controlled trial. Human reproduction. 2010 Jul 15;25(9):2203-9.

546. Coulam CB, Acacio B. Does immunotherapy for treatment of reproductive failure enhance live births? American Journal of Reproductive Immunology. 2012 Apr 1;67(4):296-304.

547. Chang P, Millar D, Tsang P, Lim K, Houlihan E, Stephenson M. Intravenous immunoglobulin in antiphospholipid syndrome and maternal floor infarction when standard treatment fails: a case report. American journal of perinatology. 2006 Feb;16(02):125-30.

548. Abdulghani S, Moretti F, Gruslin A, Grynspan D. Recurrent massive perivillous fibrin deposition and chronic intervillositis treated with heparin and intravenous immunoglobulin: a case report. Journal of Obstetrics and Gynaecology Canada. 2017 Aug 1;39(8):676-81.

549. Chaiworapongsa T, Romero R, Korzeniewski SJ, Chaemsaithong P, Hernandez-Andrade E, Segars JH, DeCherney AH, McCoy MC, Kim CJ, Yeo L, Hassan SS. Pravastatin to prevent recurrent fetal death in massive perivillous fibrin deposition of the placenta (MPFD). The Journal of Maternal-Fetal & Neonatal Medicine. 2016 Mar 18;29(6):855-62.

550. Saad AF, Kechichian T, Yin H, Sbrana E, Longo M, Wen M, Tamayo E, Hankins GD, Saade GR, Costantine MM. Effects of pravastatin on angiogenic and placental hypoxic imbalance in a mouse model of preeclampsia. Reproductive Sciences. 2014 Jan;21(1):138-45.

551. Kumasawa K, Ikawa M, Kidoya H, Hasuwa H, Saito-Fujita T, Morioka Y, Takakura N, Kimura T, Okabe M. Pravastatin induces placental growth factor (PGF) and ameliorates preeclampsia in a mouse model. PNAS. 2011 Jan 25;108(4):1451-5.

552. Lefkou E, Mamopoulos A, Fragakis N, Dagklis T, Vosnakis C, Nounopoulos E, Rousso D, Girardi G. Clinical improvement and successful pregnancy in a preeclamptic patient with antiphospholipid syndrome treated with pravastatin. Hypertension. 2014 May 1;63(5):e118-9.

553. Zarek J, DeGorter MK, Lubetsky A, Kim RB, Laskin CA, Berger H, Koren G. The transfer of pravastatin in the dually perfused human placenta. Placenta. 2013 Aug 1;34(8):719-21.

554. Spencer R, Ambler G, Brodszki J, Diemert A, Figueras F, Gratacós E, Hansson SR, Hecher K, Huertas-Ceballos A, Marlow N, Marsál K. EVERREST prospective study: a 6-year prospective study to define the clinical and biological characteristics of pregnancies affected by severe early onset fetal growth restriction. BMC pregnancy and childbirth. 2017 Dec;17(1):43.

555. Thadhani R, Kisner T, Hagmann H, Bossung V, Noack S, Schaarschmidt W, Jank A, Kribs A, Cornely OA, Kreyssig C, Hemphill L. Pilot Study of Extracorporeal Removal of Soluble Fms-Like Tyrosine Kinase 1 in PreeclampsiaClinical Perspective. Circulation. 2011 Aug 23;124(8):940-50.

556. Mifsud W, Sebire NJ. Placental pathology in early-onset and late-onset fetal growth restriction. Fetal diagnosis and therapy. 2014;36(2):117-28.

557. McKinney D, Boyd H, Langager A, Oswald M, Pfister A, Warshak CR. The impact of fetal growth restriction on latency in the setting of expectant management of preeclampsia. American Journal of Obstetrics & Gynecology. 2016 Mar 1;214(3):395-e1.

558. Kovo M, Schreiber L, Elyashiv O, Ben-Haroush A, Abraham G, Bar J. Pregnancy outcome and placental findings in pregnancies complicated by fetal growth restriction with and without preeclampsia. Reproductive Sciences. 2015 Mar;22(3):316-21.

559. Villar J, Carroli G, Wojdyla D, Abalos E, Giordano D, Ba'aqeel H, Farnot U, Bergsjø P, Bakketeig L, Lumbiganon P, Campodónico L. Preeclampsia, gestational hypertension and intrauterine growth restriction, related or independent conditions? American Journal of Obstetrics & Gynecology. 2006 Apr 1;194(4):921-31.

560. Hafner E, Metzenbauer M, Höfinger D, Munkel M, Gassner R, Schuchter K, Dillinger-Paller B, Philipp K. Placental growth from the first to the second trimester of pregnancy in SGA-foetuses and pre-eclamptic pregnancies compared to normal foetuses. Placenta. 2003 Apr 1;24(4):336-42.

561. Goswami D, Tannetta DS, Magee LA, Fuchisawa A, Redman CW, Sargent IL, von Dadelszen P. Excess syncytiotrophoblast microparticle shedding is a feature of early-onset pre-eclampsia, but not normotensive intrauterine growth restriction. Placenta. 2006 Jan 1;27(1):56-61.

562. Londero AP, Orsaria M, Marzinotto S, Grassi T, Fruscalzo A, Calcagno A, Bertozzi S, Nardini N, Stella E, Lellé RJ, Driul L. Placental aging and oxidation damage in a tissue micro-array model: an immunohistochemistry study. Histochemistry and cell biology. 2016 Aug 1;146(2):191-204.

563. Stergiotou I, Bijnens B, Cruz-Lemini M, Figueras F, Gratacos E, Crispi F. Maternal subclinical vascular changes in fetal growth restriction with and without pre-eclampsia. Ultrasound in Obstetrics & Gynecology. 2015 Dec 1;46(6):706-12.

564. Kovo M, Schreiber L, Ben-Haroush A, Gold E, Golan A, Bar J. The placental component in early-onset and late-onset preeclampsia in relation to fetal growth restriction. Prenatal diagnosis. 2012 Jul 1;32(7):632-7.

565. Powers RW, Roberts JM, Plymire DA, Pucci D, Datwyler SA, Laird DM, Sogin DC, Jeyabalan A, Hubel CA, Gandley RE. Low placental growth factor across pregnancy identifies a subset of women with preterm preeclampsia: type 1 versus type 2 preeclampsia? Hypertension. 2012 Jul;60(1):239-46.

566. Founds SA, Tsigas E, Ren D, Barmada MM. Associating Symptom Phenotype and Genotype in Preeclampsia. Biological research for nursing. 2018 Mar;20(2):126-36.

567. Abalos E, Cuesta C, Carroli G, Qureshi Z, Widmer M, Vogel JP, Souza JP. Pre-eclampsia, eclampsia and adverse maternal and perinatal outcomes: a secondary analysis of the World Health Organization Multicountry Survey on Maternal and Newborn Health. BJOG: An International Journal of Obstetrics & Gynaecology. 2014 Mar 1;121(s1):14-24.

568. Raymond D, Peterson E. A critical review of early-onset and late-onset preeclampsia. Obstetrical & gynecological survey. 2011 Aug 1;66(8):497-506.

569. Long PA, Abell DA, Beischer NA. Fetal growth retardation and pre-eclampsia. BJOG: An International Journal of Obstetrics & Gynaecology. 1980 Jan 1;87(1):13-8.

570. Stark MW, Clark L, Craver RD. Histologic differences in placentas of preeclamptic/eclamptic gestations by birthweight, placental weight, and time of onset. Pediatric and Developmental Pathology. 2014 May;17(3):181-9.

571. Yung HW, Atkinson D, Campion-Smith T, Olovsson M, Charnock-Jones DS, Burton GJ. Differential activation of placental unfolded protein response pathways implies heterogeneity in causation of early-and late-onset pre-eclampsia. The Journal of pathology. 2014 Oct 1;234(2):262-76.

572. Sohlberg S, Mulic-Lutvica A, Lindgren P, Ortiz-Nieto F, Wikström AK, Wikström J. Placental perfusion in normal pregnancy and early and late preeclampsia: a magnetic resonance imaging study. Placenta. 2014 Mar 1;35(3):202-6.

573. Chen Y, Huang Y, Jiang R, Teng Y. Syncytiotrophoblast-derived microparticle shedding in early-onset and late-onset severe pre-eclampsia. International Journal of Gynecology & Obstetrics. 2012 Dec 1;119(3):234-8.

574. Valensise H, Vasapollo B, Gagliardi G, Novelli GP. Early and late preeclampsia: two different maternal hemodynamic states in the latent phase of the disease. Hypertension. 2008 Nov 1;52(5):873-80.

575. Salimi S, Farajian-Mashhadi F, Naghavi A, Mokhtari M, Shahrakipour M, Saravani M, Yaghmaei M. Different profile of serum leptin between early onset and late onset preeclampsia. Disease markers. 2014;2014.

576. Ureyen I, Ozyuncu O, Sahin-Uysal N, Kara O, Basaran D, Turgal M, Deren O. Relationship of maternal mean platelet volume with fetal doppler parameters and neonatal complications in

pregnancies with and without intrauterine growth restriction. The Journal of Maternal-Fetal & Neonatal Medicine. 2017 Feb 16;30(4):471-4.

577. Yeter A, Topcu HO, Guzel AI, Ozgu E, Danisman N. Maternal plasma homocysteine levels in intrauterine growth retardation. The Journal of Maternal-Fetal & Neonatal Medicine. 2015 Apr 13;28(6):709-12.

578. Roje D, Zekic Tomas S, Capkun V, Marusic J, Resic J, Kuzmic Prusac I. Asymmetrical fetal growth is not associated with altered trophoblast apoptotic activity in idiopathic intrauterine growth retardation. Journal of obstetrics and gynaecology research. 2014 Feb 1;40(2):410-7.

579. Bansal S, Deka D, Dhadwal V, Mahendru R. Doppler changes as the earliest parameter in fetal surveillance to detect fetal compromise in intrauterine growth-restricted fetuses. Srpski arhiv za celokupno lekarstvo. 2016;144(1-2):69-73.

580. Derricott H, Jones RL, Heazell AE. Investigating the association of villitis of unknown etiology with stillbirth and fetal growth restriction–a systematic review. Placenta. 2013 Oct 1;34(10):856-62.

581. Losonczy G, Brown G, Venuto RC. Increased peripheral resistance during reduced uterine perfusion pressure hypertension in pregnant rabbits. The American journal of the medical sciences. 1992 Apr 1;303(4):233-40.

582. Cavanagh D, Rao PS, Knuppel RA, Desai U, Balis JU. Pregnancy-induced hypertension: development of a model in the pregnant primate (Papio anubis). American journal of obstetrics and gynecology. 1985 Apr 1;151(7):987-99.

583. Crews JK, Herrington JN, Granger JP, Khalil RA. Decreased endothelium-dependent vascular relaxation during reduction of uterine perfusion pressure in pregnant rat. Hypertension. 2000 Jan 1;35(1):367-72.

584. Ganaway JR, Allen AM. Obesity predisposes to pregnancy toxemia (ketosis) of guinea pigs. Laboratory animal science. 1971 Feb;21(1):40-4.

585. Belizán JM, Pineda O, Sainz E, Menendez LA, Villar J. Rise of blood pressure in calcium-deprived pregnant rats. American journal of obstetrics and gynecology. 1981 Sep 15;141(2):163-9.

586. Li Z, Zhang Y, Ma JY, Kapoun AM, Shao Q, Kerr I, Lam A, O'Young G, Sannajust F, Stathis P, Schreiner G, Karumanchi SA, Protter AA, Pollitt NS. Recombinant vascular endothelial growth factor 121 attenuates hypertension and improves kidney damage in a rat model of preeclampsia. Hypertension. 2007 Oct 1;50(4):686-92.

587. Faas MM, Schuiling GA, Baller JF, Visscher CA, Bakker WW. A new animal model for human preeclampsia: ultra-lowdose endotoxin infusion in pregnant rats. American journal of obstetrics and gynecology. 1994 Jul 1;171(1):158-64.

588. Beauséjour A, Auger K, St-Louis J, Brochu M. High-sodium intake prevents pregnancy-induced decrease of blood pressure in the rat. American Journal of Physiology-Heart and Circulatory Physiology. 2003 Jul;285(1):H375-83.

589. Ianosi-Irimie M, Vu HV, Whitbred JM, Pridjian CA, Nadig JD, Williams MY, Wrenn DC, Pridjian G, Puschett JB. A rat model of preeclampsia. Clinical and experimental hypertension. 2005 Jan 1;27(8):605-17.

590. Davisson RL, Hoffmann DS, Butz GM, Aldape G, Schlager G, Merrill DC, Sethi S, Weiss RM, Bates JN. Discovery of a spontaneous genetic mouse model of preeclampsia. Hypertension. 2002 Feb 1;39(2):337-42.

591. Kanayama N, Takahashi K, Matsuura T, Sugimura M, Kobayashi T, Moniwa N, Tomita M, Nakayama K. Deficiency in p57 Kip2 expression induces preeclampsia-like symptoms in mice. Molecular human reproduction. 2002 Dec 1;8(12):1129-35.

592. Carmeliet P, Ferreira V, Breier G, Pollefeyt S, Kieckens L, Gertsenstein M, Fahrig M, Vandenhoeck A, Harpal K, Eberhardt C, Declercq C. Abnormal blood vessel development and lethality in embryos lacking a single VEGF allele. Nature. 1996 Apr;380(6573):435.

593. Kusinski LC, Stanley JL, Dilworth MR, Hirt CJ, Andersson IJ, Renshall LJ, Baker BC, Baker PN, Sibley CP, Wareing M, Glazier JD. eNOS knockout mouse as a model of fetal growth restriction with an impaired uterine artery function and placental transport phenotype. American Journal of Physiology-Regulatory, Integrative and Comparative Physiology. 2012 May 2;303(1):R86-93.

594. Tanaka M, Natori M, Ishimoto H, Miyazaki T, Kobayashi T, Nozawa S. Experimental growth retardation produced by transient period of uteroplacental ischemia in pregnant Sprague-Dawley rats. American journal of obstetrics and gynecology. 1994 Nov 1;171(5):1231-4.

595. de Grauw TJ, Myers RE, Scott WJ. Fetal growth retardation in rats from different levels of hypoxia. Neonatology. 1986;49(2):85-9.

596. Roberts CT, Sohlstrom A, Kind KL, Earl RA, Khong TY, Robinson JS, Owens PC, Owens JA. Maternal food restriction reduces the exchange surface area and increases the barrier thickness of the placenta in the guinea-pig. Placenta. 2001 Feb 1;22(2-3):177-85.

597. Swanson AM, David AL. Animal models of fetal growth restriction: Considerations for translational medicine. Placenta. 2015 Jun 1;36(6):623-30.

598. Boutros PC, Okey AB. Unsupervised pattern recognition: an introduction to the whys and wherefores of clustering microarray data. Briefings in bioinformatics. 2005 Dec 1;6(4):331-43.

599. Van't Veer LJ, Dai H, Van De Vijver MJ, He YD, Hart AA, Mao M, Peterse HL, Van Der Kooy K, Marton MJ, Witteveen AT, Schreiber GJ. Gene expression profiling predicts clinical outcome of breast cancer. Nature. 2002 Jan;415(6871):530.

600. Cardoso F, Piccart-Gebhart M, Veer LV, Rutgers E. The MINDACT trial: the first prospective clinical validation of a genomic tool. Molecular oncology. 2007 Dec 1;1(3):246-51.

601. Lapointe J, Li C, Higgins JP, Van De Rijn M, Bair E, Montgomery K, Ferrari M, Egevad L, Rayford W, Bergerheim U, Ekman P. Gene expression profiling identifies clinically relevant subtypes of prostate cancer. PNAS. 2004 Jan 20;101(3):811-6.

602. Gomez-Raposo C, Mendiola M, Barriuso J, Hardisson D, Redondo A. Molecular characterization of ovarian cancer by gene-expression profiling. Gynecologic oncology. 2010 Jul 1;118(1):88-92.

603. Rohrbeck A, Neukirchen J, Rosskopf M, Pardillos GG, Geddert H, Schwalen A, Gabbert HE, von Haeseler A, Pitschke G, Schott M, Kronenwett R. Gene expression profiling for molecular distinction and characterization of laser captured primary lung cancers. Journal of translational medicine. 2008 Dec;6(1):69.

604. Alizadeh AA, Eisen MB, Davis RE, Ma C, Lossos IS, Rosenwald A, Boldrick JC, Sabet H, Tran T, Yu X, Powell JI. Distinct types of diffuse large B-cell lymphoma identified by gene expression profiling. Nature. 2000 Feb;403(6769):503.

605. Cox B, Sharma P, Evangelou AI, Whiteley K, Ignatchenko V, Ignatchenko A, Baczyk D, Czikk M, Kingdom J, Rossant J, Gramolini AO, Adamson SL. Translational analysis of mouse and human placental protein and mRNA reveals distinct molecular pathologies in human preeclampsia. Molecular & Cellular Proteomics. 2011 Dec 1;10(12):M111-012526.

606. Wolfe LM, Thiagarajan RD, Boscolo F, Tache V, Coleman RL, Kim J, Kwan WK, Loring JF, Parast M, Laurent LC. Banking placental tissue: an optimized collection procedure for genome-wide analysis of nucleic acids. Placenta. 2014 Aug 1;35(8):645-54.

607. Kolbert CP, Feddersen RM, Rakhshan F, Grill DE, Simon G, Middha S, Jang JS, Simon V, Schultz DA, Zschunke M, Lingle W. Multi-platform analysis of microRNA expression measurements in RNA from fresh frozen and FFPE tissues. PloS one. 2013 Jan 31;8(1):e52517.

608. Kocjan BJ, Hosnjak L, Poljak M. Commercially available kits for manual and automatic extraction of nucleic acids from formalin-fixed, paraffin-embedded (FFPE) tissues. Acta Dermatovenerol Alp Pannonica Adriat. 2015 Jan 1;24(3):47-53.

609. Schroeder A, Mueller O, Stocker S, Salowsky R, Leiber M, Gassmann M, Lightfoot S, Menzel W, Granzow M, Ragg T. The RIN: an RNA integrity number for assigning integrity values to RNA measurements. BMC molecular biology. 2006 Dec;7(1):3.

610. Opitz L, Salinas-Riester G, Grade M, Jung K, Jo P, Emons G, Ghadimi BM, Beißbarth T, Gaedcke J. Impact of RNA degradation on gene expression profiling. BMC medical genomics. 2010 Dec;3(1):36.

611. Malone JH, Oliver B. Microarrays, deep sequencing and the true measure of the transcriptome. BMC biology. 2011 Dec;9(1):34.

612. Schena M, Shalon D, Davis RW, Brown PO. Quantitative monitoring of gene expression patterns with a complementary DNA microarray. Science. 1995 Oct 20;270(5235):467-70.

613. van Hal NL, Vorst O, van Houwelingen AM, Kok EJ, Peijnenburg A, Aharoni A, van Tunen AJ, Keijer J. The application of DNA microarrays in gene expression analysis. Journal of Biotechnology. 2000 Mar 31;78(3):271-80.

614. Gautier L, Cope L, Bolstad BM, Irizarry RA. affy—analysis of Affymetrix GeneChip data at the probe level. Bioinformatics. 2004 Feb 12;20(3):307-15.

615. Irizarry RA, Hobbs B, Collin F, Beazer-Barclay YD, Antonellis KJ, Scherf U, Speed TP. Exploration, normalization, and summaries of high density oligonucleotide array probe level data. Biostatistics. 2003 Apr 1;4(2):249-64.

616. Quackenbush J. Microarray data normalization and transformation. Nature genetics. 2002 Dec 1;32:496.

617. Bolstad BM, Irizarry RA, Åstrand M, Speed TP. A comparison of normalization methods for high density oligonucleotide array data based on variance and bias. Bioinformatics. 2003 Jan 22;19(2):185-93.

618. Heider A, Alt R. virtualArray: a R/bioconductor package to merge raw data from different microarray platforms. BMC bioinformatics. 2013 Dec;14(1):75.

619. Johnson WE, Li C, Rabinovic A. Adjusting batch effects in microarray expression data using empirical Bayes methods. Biostatistics. 2007 Jan 1;8(1):118-27.

620. Leek JT, Johnson WE, Parker HS, Jaffe AE, Storey JD. The sva package for removing batch effects and other unwanted variation in high-throughput experiments. Bioinformatics. 2012 Jan 17;28(6):882-3.

621. Yeung KY, Fraley C, Murua A, Raftery AE, Ruzzo WL. Model-based clustering and data transformations for gene expression data. Bioinformatics. 2001 Oct 1;17(10):977-87.

622. Quackenbush J. Computational genetics: computational analysis of microarray data. Nature reviews genetics. 2001 Jun;2(6):418.

623. Suzuki R, Shimodaira H. Pvclust: an R package for assessing the uncertainty in hierarchical clustering. Bioinformatics. 2006 Apr 4;22(12):1540-2.

624. Culhane AC, Thioulouse J, Perrière G, Higgins DG. MADE4: an R package for multivariate analysis of gene expression data. Bioinformatics. 2005 Mar 29;21(11):2789-90.

625. Carey RN, Wold S, Westgard JO. Principal component analysis. Alternative to referee methods in method comparison studies. Analytical chemistry. 1975 Sep 1;47(11):1824-9.

626. Sitras V, Fenton C, Paulssen R, Vårtun Å, Acharya G. Differences in gene expression between first and third trimester human placenta: a microarray study. PloS one. 2012 Mar 19;7(3):e33294.

627. Mukherjee R. Morphometric evaluation of preeclamptic placenta using light microscopic images. BioMed research international. 2014;2014.

628. Maaten LV, Hinton G. Visualizing data using t-SNE. Journal of machine learning research. 2008;9(Nov):2579-605.

629. Khatri P, Sirota M, Butte AJ. Ten years of pathway analysis: current approaches and outstanding challenges. PLoS computational biology. 2012 Feb 23;8(2):e1002375.

630. Ashburner M, Ball CA, Blake JA, Botstein D, Butler H, Cherry JM, Davis AP, Dolinski K, Dwight SS, Eppig JT, Harris MA. Gene Ontology: tool for the unification of biology. Nature genetics. 2000 May 1;25(1):25.

631. Kanehisa M, Goto S. KEGG: kyoto encyclopedia of genes and genomes. Nucleic acids research. 2000 Jan 1;28(1):27-30.

632. Subramanian A, Tamayo P, Mootha VK, Mukherjee S, Ebert BL, Gillette MA, Paulovich A, Pomeroy SL, Golub TR, Lander ES, Mesirov JP. Gene set enrichment analysis: a knowledge-based approach for interpreting genome-wide expression profiles. PNAS. 2005 Oct 25;102(43):15545-50.

633. Tian L, Greenberg SA, Kong SW, Altschuler J, Kohane IS, Park PJ. Discovering statistically significant pathways in expression profiling studies. PNAS. 2005 Sep 20;102(38):13544-9.

634. Founds SA, Terhorst LA, Conrad KP, Hogge WA, Jeyabalan A, Conley YP. Gene expression in first trimester preeclampsia placenta. Biological research for nursing. 2011 Apr;13(2):134-9.

635. Bernard PS, Wittwer CT. Real-time PCR technology for cancer diagnostics. Clinical Chemistry. 2002 Aug 1;48(8):1178-85.

636. Wilkerson MD, Schallheim JM, Hayes DN, Roberts PJ, Bastien RR, Mullins M, Yin X, Miller CR, Thorne LB, Geiersbach KB, Muldrew KL. Prediction of lung cancer histological types by RT-qPCR gene expression in FFPE specimens. The Journal of Molecular Diagnostics. 2013 Jul 1;15(4):485-97.

637. Holland PM, Abramson RD, Watson R, Gelfand DH. Detection of specific polymerase chain reaction product by utilizing the 5'----3'exonuclease activity of Thermus aquaticus DNA polymerase. PNAS. 1991 Aug 15;88(16):7276-80.

638. Sanders R, Mason DJ, Foy CA, Huggett JF. Considerations for accurate gene expression measurement by reverse transcription quantitative PCR when analysing clinical samples. Analytical and bioanalytical chemistry. 2014 Oct 1;406(26):6471-83.

639. Leavey K, Bainbridge SA, Cox BJ. Large scale aggregate microarray analysis reveals three distinct molecular subclasses of human preeclampsia. PloS one. 2015 Feb 13;10(2):e0116508.

640. von Dadelszen P, Magee LA, Roberts JM. Subclassification of preeclampsia. Hypertension in pregnancy. 2003 Jan 1;22(2):143-8.

641. Barrett T, Wilhite SE, Ledoux P, Evangelista C, Kim IF, Tomashevsky M, Marshall KA, Phillippy KH, Sherman PM, Holko M, Yefanov A. NCBI GEO: archive for functional genomics datasets—update. Nucleic acids research. 2012 Nov 26;41(D1):D991-5.

642. Gifford RW. Report of the national high blood pressure education program working group on high blood pressure in pregnancy. American Journal of Obstetrics & Gynecology. 2000;183:S1-5.

643. Smyth GK. Limma: linear models for microarray data. In Bioinformatics and computational biology solutions using R and Bioconductor 2005 (pp. 397-420). Springer, New York, NY.

644. Bowman AW, Azzalini A. R package sm: nonparametric smoothing methods. R packege version. 2014:2-.

645. Gewehr JE, Szugat M, Zimmer R. BioWeka—extending the weka framework for bioinformatics. Bioinformatics. 2007 Jan 19;23(5):651-3.

646. Mayhew TM. Taking tissue samples from the placenta: an illustration of principles and strategies. Placenta. 2008 Jan 1;29(1):1-4.

647. Merico D, Isserlin R, Stueker O, Emili A, Bader GD. Enrichment map: a network-based method for gene-set enrichment visualization and interpretation. PloS one. 2010 Nov 15;5(11):e13984.

648. Uhlen M, Oksvold P, Fagerberg L, Lundberg E, Jonasson K, Forsberg M, Zwahlen M, Kampf C, Wester K, Hober S, Wernerus H. Towards a knowledge-based human protein atlas. Nature biotechnology. 2010 Dec 7;28(12):1248.

649. Maglott D, Ostell J, Pruitt KD, Tatusova T. Entrez Gene: gene-centered information at NCBI. Nucleic acids research. 2005 Jan 1;33(suppl_1):D54-8.

650. Lee KJ, Shim SH, Kang KM, Kang JH, Park DY, Kim SH, Farina A, Shim SS, Cha DH. Global gene expression changes induced in the human placenta during labor. Placenta. 2010 Aug 1;31(8):698-704.

651. Nait–Oumesmar B, Copperman AB, Lazzarini RA. Placental expression and chromosomal localization of the human Gcm 1 gene. Journal of Histochemistry & Cytochemistry. 2000 Jul;48(7):915-22.

652. Gleicher N. Why much of the pathophysiology of preeclampsia-eclampsia must be of an autoimmune nature. American Journal of Obstetrics & Gynecology. 2007 Jan 1;196(1):5-e1.

653. Dekker G. The partner's role in the etiology of preeclampsia. Journal of reproductive immunology. 2002 Oct 1;57(1-2):203-15.

654. Noori M, Donald AE, Angelakopoulou A, Hingorani AD, Williams DJ. Prospective study of placental angiogenic factors and maternal vascular function before and after preeclampsia and gestational hypertension. Circulation. 2010 Aug 3;122(5):478-87.

655. Szekeres-Bartho J. Immunological relationship between the mother and the fetus. International reviews of immunology. 2002 Jan 1;21(6):471-95.

656. Apps R, Murphy SP, Fernando R, Gardner L, Ahad T, Moffett A. Human leucocyte antigen (HLA) expression of primary trophoblast cells and placental cell lines, determined using single antigen beads to characterize allotype specificities of anti-HLA antibodies. Immunology. 2009 May 1;127(1):26-39.

657. Hunt JS, Fishback JL, Andrews GK, Wood GW. Expression of class I HLA genes by trophoblast cells. Analysis by in situ hybridization. The Journal of Immunology. 1988 Feb 15;140(4):1293-9.

658. Constantin CM, Masopust D, Gourley T, Grayson J, Strickland OL, Ahmed R, Bonney EA. Normal establishment of virus-specific memory CD8 T cell pool following primary infection during pregnancy. The Journal of Immunology. 2007 Oct 1;179(7):4383-9.

659. Jordan JA, Huff D, DeLoia JA. Placental cellular immune response in women infected with human parvovirus B19 during pregnancy. Clinical and diagnostic laboratory immunology. 2001 Mar 1;8(2):288-92.

660. Leavey K, Benton SJ, Grynspan D, Bainbridge SA, Cox BJ. Unsupervised placental gene expression profiling identifies clinically relevant subclasses of human preeclampsia. Hypertension. 2016 Jul;68(1):137-47.

661. Ness RB, Roberts JM. Heterogeneous causes constituting the single syndrome of preeclampsia: a hypothesis and its implications. American Journal of Obstetrics & Gynecology. 1996 Nov 1;175(5):1365-70.

662. Li DK, Wi S. Changing paternity and the risk of preeclampsia/eclampsia in the subsequent pregnancy. American journal of epidemiology. 2000 Jan 1;151(1):57-62.

663. Redman CW. Pre-eclampsia: a complex and variable disease. Pregnancy Hypertension: An International Journal of Women's Cardiovascular Health. 2014 Jul 1;4(3):241-2.

664. Page GP, Edwards JW, Gadbury GL, Yelisetti P, Wang J, Trivedi P, Allison DB. The PowerAtlas: a power and sample size atlas for microarray experimental design and research. BMC bioinformatics. 2006 Dec;7(1):84.

665. Burton GJ, Sebire NJ, Myatt L, Tannetta D, Wang YL, Sadovsky Y, Staff AC, Redman CW. Optimising sample collection for placental research. Placenta. 2014 Jan 1;35(1):9-22.

666. Hennig C. fpc: Flexible procedures for clustering. R package version. 2010;2(2):0-3.

667. Thompson JM, Irgens LM, Skjaerven R, Rasmussen S. Placenta weight percentile curves for singleton deliveries. BJOG: An International Journal of Obstetrics & Gynaecology. 2007 Jun 1;114(6):715-20.

668. de Ronde JJ, Klijn C, Velds A, Holstege H, Reinders MJ, Jonkers J, Wessels LF. KC-SMARTR: An R package for detection of statistically significant aberrations in multi-experiment aCGH data. BMC research notes. 2010 Dec;3(1):298.

669. Agostini C, Calabrese F, Rea F, Facco M, Tosoni A, Loy M, Binotto G, Valente M, Trentin L, Semenzato G. Cxcr3 and its ligand CXCL10 are expressed by inflammatory cells infiltrating lung allografts and mediate chemotaxis of T cells at sites of rejection. The American journal of pathology. 2001 May 1;158(5):1703-11.

670. Rekers NV, Bajema IM, Mallat MJ, Petersen B, Anholts JD, Swings GM, Miert PP, Kerkhoff C, Roth J, Popp D, Groningen MC. Beneficial Immune Effects of Myeloid-Related Proteins in Kidney Transplant Rejection. American Journal of Transplantation. 2016 May 1;16(5):1441-55.

671. Machado PG, Tedesco HS, Silva RG, Pacheco-Silva A, Medina JO. Use of reduced dose of OKT3 (2.5 mg) after renal transplantation. In Transplantation proceedings 2002 Feb 1 (Vol. 34, No. 1, p. 104). Elsevier.

672. Thaunat O, Patey N, Caligiuri G, Gautreau C, Mamani-Matsuda M, Mekki Y, Dieu-Nosjean MC, Eberl G, Ecochard R, Michel JB, Graff-Dubois S. Chronic rejection triggers the development of an aggressive intragraft immune response through recapitulation of lymphoid organogenesis. The Journal of Immunology. 2010 Jul 1;185(1):717-28.

673. Kamei H, Masuda S, Nakamura T, Oike F, Takada Y, Hamajima N. Association of transporter associated with antigen processing (TAP) gene polymorphisms in donors with acute cellular rejection in living donor liver transplantation. J Gastrointestin Liver Dis. 2013 Jun 1;22(2):167-71.

674. Giglio S, Broman KW, Matsumoto N, Calvari V, Gimelli G, Neumann T, Ohashi H, Voullaire L, Larizza D, Giorda R, Weber JL. Olfactory receptor–gene clusters, genomic-inversion polymorphisms, and common chromosome rearrangements. The American Journal of Human Genetics. 2001 Apr 1;68(4):874-83.

675. Freeman JL, Perry GH, Feuk L, Redon R, McCarroll SA, Altshuler DM, Aburatani H, Jones KW, Tyler-Smith C, Hurles ME, Carter NP. Copy number variation: new insights in genome diversity. Genome research. 2006 Aug 1;16(8):949-61.

676. Torres MI, López-Casado MA, Luque J, Peña J, Ríos A. New advances in coeliac disease: serum and intestinal expression of HLA-G. International immunology. 2006 Mar 28;18(5):713-8.

677. Lila N, Amrein C, Guillemain R, Chevalier P, Latremouille C, Fabiani JN, Dausset J, Carosella ED, Carpentier A. Human leukocyte antigen-G expression after heart transplantation is associated with a reduced incidence of rejection. Circulation. 2002 Apr 23;105(16):1949-54.

678. Phaloprakarn C, Tangjitgamol S. Maternal ABO blood group and adverse pregnancy outcomes. Journal of Perinatology. 2013 Feb;33(2):107.

679. Tanner MM, Karhu RA, Nupponen NN, Borg Å, Baldetorp B, Pejovic T, Fernö M, Killander D, Isola JJ. Genetic aberrations in hypodiploid breast cancer: frequent loss of chromosome 4 and amplification of cyclin D1 oncogene. The American journal of pathology. 1998 Jul 1;153(1):191-9.

680. Zielenska M, Bayani J, Pandita A, Toledo S, Marrano P, Andrade J, Petrilli A, Thorner P, Sorensen P, Squire JA. Comparative genomic hybridization analysis identifies gains of 1p35∼ p36 and chromosome 19 in osteosarcoma. Cancer genetics and cytogenetics. 2001 Oct 1;130(1):14-21.

681. Weier JF, Weier HU, Jung CJ, Gormley M, Zhou Y, Chu LW, Genbacev O, Wright AA, Fisher SJ. Human cytotrophoblasts acquire aneuploidies as they differentiate to an invasive phenotype. Developmental biology. 2005 Mar 15;279(2):420-32.

682. Ness RB, Roberts JM. Heterogeneous causes constituting the single syndrome of preeclampsia: a hypothesis and its implications. American Journal of Obstetrics & Gynecology. 1996 Nov 1;175(5):1365-70.

683. Leavey K, Wilson SL, Bainbridge SA, Robinson WP, Cox BJ. Epigenetic regulation of placental gene expression in transcriptional subtypes of preeclampsia. Clinical Epigenetics. 2018 Mar 2;10:28.

684. Warrander LK, Batra G, Bernatavicius G, Greenwood SL, Dutton P, Jones RL, Sibley CP, Heazell AE. Maternal perception of reduced fetal movements is associated with altered placental structure and function. PloS one. 2012 Apr 16;7(4):e34851.

685. Redline RW, Faye-Petersen O, Heller D, Qureshi F, Savell V, Vogler C. Amniotic infection syndrome: nosology and reproducibility of placental reaction patterns. Pediatric and Developmental Pathology. 2003 Oct 1;6(5):435-48.

686. Paradis E, Claude J, Strimmer K. APE: analyses of phylogenetics and evolution in R language. Bioinformatics. 2004 Jan 22;20(2):289-90.

687. Deter RL, Levytska K, Melamed N, Lee W, Kingdom JC. Classifying neonatal growth outcomes: use of birth weight, placental evaluation and individualized growth assessment. The Journal of Maternal-Fetal & Neonatal Medicine. 2016 Dec 16;29(24):3939-49.

688. Zimmer EZ, Divon MY. Sonographic diagnosis of IUGR-macrosomia. Clinical obstetrics and gynecology. 1992 Mar;35(1):172-84.

689. Babic I, Ferraro ZM, Garbedian K, Oulette A, Ball CG, Moretti F, Gruslin A. Intraplacental villous artery resistance indices and identification of placenta-mediated diseases. Journal of Perinatology. 2015 Oct;35(10):793.

690. Carvalho BS, Irizarry RA. A framework for oligonucleotide microarray preprocessing. Bioinformatics. 2010 Aug 5;26(19):2363-7.

691. Scrucca L, Fop M, Murphy TB, Raftery AE. mclust 5: Clustering, classification and density estimation using gaussian finite mixture models. The R journal. 2016 Aug;8(1):289.

692. Ackermann M, Strimmer K. A general modular framework for gene set enrichment analysis. BMC bioinformatics. 2009 Dec;10(1):47.

693. Maciejewski H. Gene set analysis methods: statistical models and methodological differences. Briefings in bioinformatics. 2013 Feb 9;15(4):504-18.

694. Liberzon A, Subramanian A, Pinchback R, Thorvaldsdóttir H, Tamayo P, Mesirov JP. Molecular signatures database (MSigDB) 3.0. Bioinformatics. 2011 May 5;27(12):1739-40.

695. Liberzon A, Birger C, Thorvaldsdottir H, Ghandi M, Mesirov JP, Tamayo P. The Molecular Signatures Database (MSigDB) hallmark gene set collection. Cell Syst. 2015; 1 (6): 417–25.

696. Wallenstein MB, Harper LM, Odibo AO, Roehl KA, Longman RE, Macones GA, Cahill AG. Fetal congenital heart disease and intrauterine growth restriction: a retrospective cohort study. The Journal of Maternal-Fetal & Neonatal Medicine. 2012 Jun 1;25(6):662-5.

697. Macdonald-Wallis C, Tilling K, Fraser A, Nelson SM, Lawlor DA. Associations of blood pressure change in pregnancy with fetal growth and gestational age at delivery: findings from a prospective cohort. Hypertension. 2014 Jul;64(1):36-44.

698. Chan JS. Villitis of unknown etiology and massive chronic intervillositis. Surgical pathology clinics. 2013 Mar 1;6(1):115-26.

699. Kaufmann P, Huppertz B. Tenney–Parker changes and apoptotic versus necrotic shedding of trophoblast in normal pregnancy. Pre-eclampsia: etiology and clinical practice. 2007 May 10:152.

700. Kingdom J, Keating S. Distal villous hypoplasia. Diagnostic Histopathology. 2012 May 31;18(5):195-200.

701. Schmittgen TD, Livak KJ. Analyzing real-time PCR data by the comparative C T method. Nature protocols. 2008 Jun;3(6):1101.

702. Hall MA. Correlation-based feature selection for machine learning. 1997.

703. Jaksik R, Iwanaszko M, Rzeszowska-Wolny J, Kimmel M. Microarray experiments and factors which affect their reliability. Biology direct. 2015 Dec;10(1):46.

704. Biron-Shental T, Schaiff WT, Rimon E, Shim TL, Nelson DM, Sadovsky Y. Hypoxia enhances the expression of follistatin-like 3 in term human trophoblasts. Placenta. 2008 Jan 1;29(1):51-7.

705. Nucleotide. Bethesda (MD): National Library of Medicine (US), National Center for Biotechnology Information [accessed: April 7th, 2018]. https://www.ncbi.nlm.nih.gov/nuccore

706. Konishi A, Ma X, Yasukawa K. Stabilization of Moloney murine leukemia virus reverse transcriptase by site-directed mutagenesis of surface residue Val433. Bioscience, biotechnology, and biochemistry. 2014 Jan 2;78(1):75-8.

707. Gettemans J, Van Impe K, Delanote V, Hubert T, Vandekerckhove J, De Corte V. Nuclear actin-binding proteins as modulators of gene transcription. Traffic. 2005 Oct 1;6(10):847-57.

708. Roby KF, Gershon D, Hunt JS. Expression of the transporter for antigen processing-1 (Tap-1) gene in subpopulations of human trophoblast cells. Placenta. 1996 Jan 1;17(1):27-32.

709. Ulm B, Svolba G, Ulm MR, Bernaschek G, Panzer S. Male fetuses are particularly affected by maternal alloimmunization to D antigen. Transfusion. 1999 Feb 1;39(2):169-73.

710. Byrne J, Warburton D, Opitz JM, Reynolds JF. Male excess among anatomically normal fetuses in spontaneous abortions. American Journal of Medical Genetics Part A. 1987 Mar 1;26(3):605-11.

711. Eriksson JG, Kajantie E, Osmond C, Thornburg K, Barker DJ. Boys live dangerously in the womb. American Journal of Human Biology. 2010 May 1;22(3):330-5.

712. Orendi K, Kivity V, Sammar M, Grimpel Y, Gonen R, Meiri H, Lubzens E, Huppertz B. Placental and trophoblastic in vitro models to study preventive and therapeutic agents for preeclampsia. Placenta. 2011 Feb 1;32:S49-54.

713. Gatford KL, Wooldridge AL, Kind KL, Bischof R, Clifton VL. Pre-birth origins of allergy and asthma. Journal of reproductive immunology. 2017 Jul 20.

714. Rouault C, Clément K, Guesnon M, Henegar C, Charles MA, Heude B, Evain-Brion D, Degrelle SA, Fournier T. Transcriptomic signatures of villous cytotrophoblast and syncytiotrophoblast in term human placenta. Placenta. 2016 Aug 1;44:83-90.

715. Godec J, Tan Y, Liberzon A, Tamayo P, Bhattacharya S, Butte AJ, Mesirov JP, Haining WN. Compendium of immune signatures identifies conserved and species-specific biology in response to inflammation. Immunity. 2016 Jan 19;44(1):194-206.

9 Chapter 9 – Appendices

9.1 Appendix A – RNA to cDNA protocol used for the PE cohort samples

Purchase:
Invitrogen™ catalog number 48190011: random primers (mostly hexamers)
Invitrogen™ catalog number 18064014: SuperScript™ II Reverse Transcriptase
Thermo Scientific™ catalog number R0192: dNTP mix containing dATP, dCTP, dGTP and dTTP
New England BioLabs product code M0297S: RNase H
New England BioLabs product code M0303S: DNase I and DNase I buffer

1. Get ice. Label PCR tubes (+, -, and water) and place in rack on ice
2. Take DNase 1 buffer and DNase 1 out of freezer to defrost
3. Turn on PCR machine
4. Get RNA from -70°C freezer and place in ice to defrost
5. In + tubes, add necessary volume of DEPC (DNase, RNase free) water to dilute RNA to 5ug in 16ul. Include a water control (16ul)
6. Add necessary volume of RNA to tubes for a concentration of 5ug/16ul
7. To both + tubes and water control, add:
   - 2ul of 10X DNase 1 buffer
   - 2ul of 1U/ul DNase 1
8. Take off ice and incubate at 25°C for 15 minutes
9. Set PCR to incubate at 65°C and make sure 25mM ethylenediaminetetraacetic acid (EDTA) is ready (2.5ul of 0.5M EDTA + 47.5ul water)
10. To both + tubes and water control, add:
    - 2ul of 25mM EDTA
11. Use larger pipette to mix thoroughly
12. Incubate at 65°C for 10 minutes
13. Make sure random primers and dNTPs are defrosted and random primers have been diluted to 125ng/ul (1ul of 3ug/ul random primers + 23ul water)
14. Place tubes back on ice
15. To both + tubes and water control, add:
    - 2ul of 125ng/ul random primers
    - 2ul of 10mM dNTPs
16. Incubate at 65°C for 5 minutes
17. Make sure 5X 1st strand reverse transcription (RT) buffer and dithiothreitol (DTT) are defrosted
18. Place tubes back on ice and cool completely
19. To both + tubes and water control, add:
    - 8ul of 5X 1st strand RT buffer
    - 4ul of 0.1M DTT
20. Use larger pipette to mix thoroughly
21. Transfer 8ul from + tubes to – tubes
22. Take off ice and incubate at 25°C for 5 minutes

23. Set the PCR machine to incubate at 25°C and make sure the superscript II is defrosted
24. To both + tubes and water control but NOT the – tubes, add:
    - 1.75ul superscript II reverse transcriptase
25. Mix gently
26. Place in PCR machine and run the "Superscript I" protocol (25°C for 10 minutes, 42°C for 50 minutes, 70°C for 15 minutes, 0°C for 5 minutes)
27. Make sure the RNase H is defrosted
28. Set the PCR machine to incubate at 37°C
29. To both + tubes and water control, add:
    - 0.64ul of 5U/ul RNase H
30. To the – tubes, add:
    - 0.1ul of 5U/ul RNase H
31. Place in PCR machine and run the "Superscript II" protocol (37°C for 20 minutes, 65°C for 10 minutes, cool to 0°C)
32. Store cDNA in fridge
33. Turn off PCR machine and return -20°C block with reagents to freezer

9.2 Appendix B – Rubric for histopathology scoring

Developed by Drs. Samantha Benton, David Grynspan, and Shannon Bainbridge at the University of Ottawa.

Macroscopic Lesions
Retroplacental hematoma/hemorrhage? Yes or no *Hemorrhage on the maternal surface of the disk, with congestion/compression of the overlying parenchyma* Number: _____ Estimated volume(s) as a percent of total disc volume: _____ % Location: _____
Maternal surface fibrin? Yes or no Greatest thickness: _____ mm Estimated volume(s) as a percent of total disc volume: _____ % Location: Plaques? Yes or no Diffuse fibrin occupying entire maternal surface? Yes or no
Impression of intervillous fibrin? Yes or no Estimate volume(s) as a percent of total disc volume: _____ % Location: _____

Presence of lesions resembling infarcts? Yes or no Number: _____ Size(s): _____ Estimate volume(s) as a percent of total disc volume: _____ % Location: _____
Presence of lesions resembling intervillous thrombi? Yes or no Number: _____ Size(s): _____ Estimate volume(s) as a percent of total disc volume: _____ % Location: _____ Recent, remote or mixed? _____
Indeterminate lesions? Yes or no Number: _____ Size(s): _____ Estimate volume(s) as a percent of total disc volume: _____ % Location: _____ Recent, remote or mixed? _____
Microscopic Lesions
Evidence of maternal vascular malperfusion

Placental infarct(s) • *Refer to gross description, exclude marginal infarctions in a term placenta* 0 = No infarcts present 1 = Focal infarctions (1 – 3 peripherally located, <3 cm in size) 2 = Multifocal and/or diffuse infarctions (>3 peripherally located) and/or any infarct ≥3cm in size; >10% of villous volume	Grade: _____ * Qualify infarct as recent, remote or mixed

Distal villous hypoplasia • *Reduction in size of intermediate villi with dispersed terminal villi and reduced number that appear thin and elongated, widening of intervillous space; adjusted for gestational age at delivery; involves at least 30% of full thickness slide* 0 = Not present 1 = Focal (1 slide only) *1+ = Mild to moderate pattern present in term placenta* 2 = Diffuse (≥2 slides) *2+ = Severe pattern present in term placenta*	Grade: _____
Advanced villous maturation • *Presence of term-appearing/hypermature villi for gestational age, not in areas adjacent to infarction* 0 = Villi structure and vessel pattern appropriate for gestational age 1 = Focal hypermature for gestational age 2 = Diffuse hypermature for gestational age	Grade: _____
Syncytial knots • *Aggregates of syncytiotrophoblast nuclei along stem and/or at terminal villi* 0 = Focal and infrequent presence of syncytial knots, expected for gestational age (<30% terminal villi with knots) 1 = Syncytial knots excessively increased for gestational age (≤30% parenchyma) 2 = Syncytial knots excessively increased for gestational age (>30% parenchyma)	Grade: _____

Focal perivillous fibrin deposition • *Increased amounts of fibrin coating proximal stem villi and/or terminal villi* 0 = Not present 1 = Present, seen on <2 slides; increased for gestational age Estimated % volume occupied:	Grade: _____
Villous agglutination • *Clusters of adherent terminal villi (>2, <20), enmeshed by fibrin and/or bridging syncytial knots* 0 = Not present 1 = Focal 2 = Patchy 3 = Diffused	Grade: _____
Maternal decidual vasculopathy • *Insufficient vessel remodelling* • *Fibrinoid change*	Yes or no
Implantation site abnormalities	
Microscopic accreta • *Bundles of myometrium adherent to the basal plate without intervening decidua* 0 = Not present 1 = Focal 2 = Multifocal or diffuse (more than one focus)	Grade: _____

Increased basement membrane fibrin 0 = Not present 1 = Patchy fibrin on the maternal surface (basal plate) 2 = Diffuse fibrin on the maternal surface (basal plate)	Grade: _____
Evidence of ascending intrauterine infection	
Maternal inflammatory response **Stage:** 0 = Not present 1 = Stage 1 – neutrophils in subchorionic fibrin and/or trophoblast layer of membrane 2 = Stage 2 – diffuse or patchy neutrophils in fibrous chorion or amnion 3 = Stage 3 – membrane or chorionic plate necrosis	Stage: _____
Grade 0 = Not present 1 = Mild or moderate – lacks criteria for Grade 2 2 = Severe – confluent neutrophils between chorion and decidua, greater than 10 x 20 cells in extent with greater than 3 foci or a large continuous band	Grade: _____
Fetal inflammatory response **Stage:** 0 = Not present 1 = Stage 1 – chorionic vessel vasculitis or umbilical venous vasculitis 2 = Stage 2 – umbilical vasculitis with umbilical arteritis 3 = Stage 3 – necrotizing funititis/concentric umbilical perivasculitis	Stage: _____
Grade 0 = Not present 1 = Mild to moderate – lacks criteria for Grade 2 2 = Severe – heavy inflammation of vessel within the umbilical cord or chorionic plate vessel with vessel wall damage	Grade: _____
Thrombosis of any of the umbilical or chorionic fetal vessels present	Yes or no
Specific patterns	
Candida spp • Gross punctate white nodules on umbilical cord (Yes or no); refer to gross findings • Subamniotic microabcesses on umbilical cord (Yes or no) ○ **Grocott stain:** □ not done □ negative □ positive Histochemical pseudohyphae and yeast forms (yes or no)	
Listeria • Gross intervillous abscesses (yes or no); refer to gross findings • Histological intervillous abscesses ○ **Gram stain:** □ not done □ negative □ positive Gram-negative rods within abscesses (yes or no)	

Evidence of placenta villous maldevelopment	
Chorangiosis • *Hypercapillarised terminal villi* 0 = Not present 1 = Present with >10 terminal villi with ≥10 capillaries, seen in ≥3 foci	Grade: _____
Chorangiomas 0 = Not present 1 = Present and <3 cm in size 2 = Present and ≥ 3cm in size or >5 total nodules	Grade: _____
Delayed villous maturation • *Monotonous villi (≥10) with centrally placed capillaries and decreased vasculosyncytial membranes resembling villi in early pregnancy, present in at least 30% of full thickness section* 0 = No villous immaturity 1 = Focal – lesion seen on one slide only 2 = Diffuse – seen on ≥2 slides	Grade: _____
Evidence of fetal vascular malperfusion	
Avascular fibrotic villi 0 = None present 1 = Small foci – 3 or more foci of 2-4 terminal villi showing complete loss of villous capillaries and bland hyaline fibrosis of the villous stroma 2 = Intermediate foci – 3 or more foci of 5-10 terminal villi 3 = Large foci – 3 or more foci of >10 villi	Grade: _____
Thrombosis 0 = Not present 1 = Present Location: Umbilical, chorionic plate, stem vessel Number: _____ □ Occlusive OR □ Non-occlusive	Grade: _____
Intramural fibrin deposition • *Subendothelial or intramuscular fibrin or fibrinoid deposition within the wall of large fetal vessel (recent), with calcifications (remote)* 0 = Not present 1 = Recent, isolated (only one seen per slide) 1+ = non-isolated (>1 seen per slide) 2 = Remote, isolated (only one seen per slide) 2+ = non-isolated (>1 seen per slide)	Grade: _____
Evidence of chronic utero-placental separation	
Chorionic hemosiderosis 0 = No 1 = Yes	Grade: _____
Presence of retroplacental adherent hematoma (blood clots) • *Refer to gross description, confirm histologically* 0 = No 1 = Yes	Grade: _____
Laminar necrosis of decidua capsularis	Grade:

0 = No 1 = Yes	_____
Evidence of maternal-fetal interface disturbance	
Massive perivillous fibrin deposition pattern 0 = Not present 1 = Diffusely present, 30-50% of intervillous volume, seen on at least 2 slides 2 = Diffusely present, >50% of intervillous volume, seen on all slides	Grade: _____
Maternal floor infarct pattern 0 = Not present 1 = Present in one to two slides 2 = Whole floor, present in all slides Thickness:_____	Grade: _____
Intervillous thrombi 0 = Not present 1 = Present Number: _____ Size(s): _____ Estimate volume(s) as a percent of total disc volume: _____ %	Grade: _____
Evidence of chronic inflammation	
Infectious villitis 0 = Not present 1 = Placental villous inflammation suggesting an infectious etiology: • Plasma cell villitis • Viral cytopathic effect/CMV • Viral cytopathic effect – HSV • Viral cytopathic effect – NOS • Toxoplasmosis Immunohistochemistry or ISH positive for an infectious agent, specify:	Grade: _____
Villitis of unknown etiology 0 = Not present 1 = Low-grade, inflammation affecting <10 contiguous villi in any one focus or >1 focus **Denote focal (1 slide only) OR multifocal (>1 slide)* 2 = High-grade VUE – inflammation affecting >10 contiguous villi, seen in multiple foci on >1 section **Denote patchy (multiple foci, 1 with >10 contiguous villi) OR diffuse (>30% of all terminal villi involved)* * With or without vascular damage	Grade: _____

Chronic intervillositis 0 = Not present 1 = Infiltration of the intervillous space by histocytes, <50% of the total placental intervillous volume 2 = Infiltration of the intervillous space by histocytes, >50% of the total placental intervillous volume	Grade: _____
Chronic deciduitis 0 = Not present 1 = Present 1+ = Plasma cells present	Grade: _____
Additional findings	
Meconium histiocytes/macrophages within membranes 0 = Not present 1 = Present	Grade: _____
Meconium-induced myonecrosis 0 = Not present 1 = Present	Grade: _____
Note any significant lesions observed that are not listed above	

9.3 Appendix C – Supplementary tables for Chapter 5

Supplementary Table 1. Significant (q<0.05) GO pathways for the cluster 1 normotensive SGA samples compared to the cluster 1 controls.

Pathway	Set Size	NTk Stat	NTk q-value	NTk Rank	NEk Stat	NEk q-value	NEk Rank
GO POSITIVE REGULATION OF DEFENSE RESPONSE	275	-7.21	0.00	4	-4.06	0.00	4
GO MYELOID CELL ACTIVATION INVOLVED IN IMMUNE RESPONSE	35	-6.41	0.00	9	-4.94	0.00	1
GO REGULATION OF DEFENSE RESPONSE	552	-7.14	0.00	6	-3.79	0.00	14
GO POSITIVE REGULATION OF INNATE IMMUNE RESPONSE	194	-6.58	0.00	7	-3.72	0.00	17
GO ACTIVATION OF IMMUNE RESPONSE	308	-7.68	0.00	3	-3.69	0.00	23
GO POSITIVE REGULATION OF IMMUNE RESPONSE	397	-7.79	0.00	2	-3.58	0.00	26
GO IMMUNE RESPONSE REGULATING CELL SURFACE RECEPTOR SIGNALING PATHWAY	231	-6.30	0.00	10	-3.72	0.00	18
GO GRANULOCYTE MIGRATION	50	-5.59	0.00	24	-4.04	0.00	5
GO ADP METABOLIC PROCESS	33	5.68	0.00	21	3.83	0.00	10
GO MACROPHAGE ACTIVATION INVOLVED IN IMMUNE RESPONSE	10	-5.20	0.00	30	-4.48	0.00	2
GO CELL ACTIVATION INVOLVED IN IMMUNE RESPONSE	96	-6.27	0.00	11	-3.69	0.00	24
GO CARBOHYDRATE KINASE ACTIVITY	15	5.14	0.00	32	3.98	0.00	6
GO REGULATION OF INNATE IMMUNE RESPONSE	272	-6.17	0.00	12	-3.51	0.00	27
GO MYELOID LEUKOCYTE ACTIVATION	80	-6.10	0.00	14	-3.66	0.00	25
GO MACROPHAGE ACTIVATION	27	-5.51	0.00	26	-3.75	0.00	16
GO ANTIGEN RECEPTOR MEDIATED SIGNALING PATHWAY	142	-5.10	0.00	33	-3.81	0.00	12
GO RESPIRATORY BURST	10	-4.92	0.00	40	-3.78	0.00	15
GO LEUKOCYTE CHEMOTAXIS	76	-5.60	0.00	23	-3.32	0.00	36
GO NEUTROPHIL ACTIVATION INVOLVED IN IMMUNE RESPONSE	11	-4.62	0.00	53	-3.91	0.00	8
GO RELAXATION OF MUSCLE	17	-4.49	0.00	59	-3.89	0.00	9
GO MYELOID LEUKOCYTE MIGRATION	68	-4.76	0.00	45	-3.43	0.00	32
GO ATP GENERATION FROM ADP	27	4.97	0.00	37	3.26	0.00	42
GO GRANULOCYTE ACTIVATION	18	-4.35	0.00	69	-3.72	0.00	19
GO HEXOSE CATABOLIC PROCESS	37	5.02	0.00	35	3.13	0.00	55
GO MONOSACCHARIDE CATABOLIC PROCESS	45	4.91	0.00	41	3.17	0.00	51
GO NUCLEOTIDE PHOSPHORYLATION	42	4.59	0.00	55	3.29	0.00	39
GO REGULATION OF INTERLEUKIN 6 PRODUCTION	74	-4.35	0.00	70	-3.43	0.00	31
GO POSITIVE REGULATION OF MACROPHAGE CHEMOTAXIS	10	-4.46	0.00	62	-3.24	0.00	44
GO RELAXATION OF CARDIAC MUSCLE	10	-3.98	0.00	107	-3.94	0.00	7
GO POSITIVE REGULATION OF TUMOR NECROSIS FACTOR SUPERFAMILY CYTOKINE PRODUCTION	46	-4.23	0.00	81	-3.39	0.00	35
GO CARBOHYDRATE PHOSPHORYLATION	17	4.28	0.00	77	3.29	0.00	40
GO DEFENSE RESPONSE TO GRAM POSITIVE BACTERIUM	41	-3.90	0.00	114	-3.83	0.00	11
GO NEGATIVE REGULATION OF INTERLEUKIN 6 PRODUCTION	23	-3.99	0.00	106	-3.71	0.00	21
GO MICROGLIAL CELL ACTIVATION	10	-3.76	0.00	125	-3.49	0.00	28
GO POSITIVE REGULATION OF PROTEIN COMPLEX ASSEMBLY	155	-3.72	0.00	132	-3.70	0.00	22
GO REGULATION OF TYPE I INTERFERON PRODUCTION	99	-3.67	0.00	139	-3.25	0.00	43
GO PRODUCTION OF MOLECULAR MEDIATOR INVOLVED IN INFLAMMATORY RESPONSE	11	-3.39	0.00	170	-3.80	0.00	13
GO ENDOLYSOSOME	14	-3.56	0.00	150	-3.41	0.00	34
GO IMMUNOLOGICAL SYNAPSE	26	-3.65	0.00	140	-3.20	0.00	47
GO RESPONSE TO ANGIOTENSIN	10	-3.32	0.00	184	-3.72	0.00	20
GO LEUKOCYTE DEGRANULATION	26	-3.09	0.03	242	-4.08	0.00	3
GO POSITIVE REGULATION OF MAST CELL ACTIVATION INVOLVED IN IMMUNE RESPONSE	10	-3.09	0.03	242	-3.28	0.00	41
GO POSITIVE REGULATION OF CD4 POSITIVE ALPHA BETA T CELL ACTIVATION	16	-3.09	0.03	242	-3.24	0.00	45
GO MHC PROTEIN COMPLEX BINDING	10	-3.09	0.03	242	-3.18	0.00	49
GO POSITIVE REGULATION OF ALPHA BETA T CELL ACTIVATION	33	-3.09	0.03	242	-3.18	0.00	50
GO REGULATION OF MAST CELL ACTIVATION INVOLVED IN IMMUNE RESPONSE	26	-3.09	0.03	242	-3.17	0.00	52
GO CARDIAC MUSCLE CELL ACTION POTENTIAL	26	-2.97	0.03	283	-3.24	0.00	46

GO POSITIVE REGULATION OF LEUKOCYTE DEGRANULATION	15	-2.94	0.03	285	-3.19	0.00	48
GO ENDOLYSOSOME MEMBRANE	11	-2.88	0.05	319.5	-3.30	0.00	37
GO REGULATION OF INTERLEUKIN 17 PRODUCTION	11	-2.88	0.05	319.5	-3.29	0.00	38
GO POSITIVE REGULATION OF PROTEIN IMPORT INTO NUCLEUS TRANSLOCATION	10	-2.88	0.05	319.5	-3.16	0.00	53

Supplementary Table 2. Significant (q<0.05) GO pathways for the cluster 2 normotensive SGA samples compared to the cluster 1 controls.

Pathway	Set Size	NTk Stat	NTk q-value	NTk Rank	NEk Stat	NEk q-value	NEk Rank
GO GLUCOSE CATABOLIC PROCESS	21	5.87	0.00	10	3.95	0.00	26
GO ATP GENERATION FROM ADP	27	5.31	0.00	18	4.10	0.00	18
GO ADP METABOLIC PROCESS	33	4.93	0.00	30	4.12	0.00	15
GO HEXOSE CATABOLIC PROCESS	37	5.45	0.00	15	3.85	0.00	34
GO NEGATIVE REGULATION OF HORMONE SECRETION	58	4.57	0.00	46	4.24	0.00	8
GO MYD88 DEPENDENT TOLL LIKE RECEPTOR SIGNALING PATHWAY	26	-4.54	0.00	50	-4.38	0.00	7
GO MACROPHAGE ACTIVATION	27	-4.32	0.00	66	-4.62	0.00	5
GO MONOSACCHARIDE CATABOLIC PROCESS	45	4.74	0.00	36	3.76	0.00	43
GO PYRUVATE METABOLIC PROCESS	46	4.46	0.00	56	4.01	0.00	24
GO NUCLEOTIDE PHOSPHORYLATION	42	4.63	0.00	43	3.71	0.00	49
GO MICROGLIAL CELL ACTIVATION	10	-4.00	0.00	94	-5.53	0.00	1
GO CELL PROJECTION ASSEMBLY	189	-4.39	0.00	57	-3.80	0.00	40
GO REGULATION OF ENDOCRINE PROCESS	39	4.07	0.00	83	4.10	0.00	17
GO REGULATION OF GONADOTROPIN SECRETION	11	3.97	0.00	101	4.71	0.00	3
GO SULFUR COMPOUND TRANSMEMBRANE TRANSPORTER ACTIVITY	15	-3.94	0.00	105	-4.67	0.00	4
GO RELAXATION OF MUSCLE	17	-4.05	0.00	85	-3.89	0.00	28
GO NAD METABOLIC PROCESS	42	4.37	0.00	60	3.65	0.00	56
GO NADH METABOLIC PROCESS	28	4.59	0.00	44	3.45	0.00	83
GO REGULATION OF DEFENSE RESPONSE TO VIRUS BY VIRUS	24	-4.15	0.00	78	-3.59	0.00	62
GO HORMONE ACTIVITY	70	5.94	0.00	9	3.19	0.00	135
GO EPIDERMIS DEVELOPMENT	199	5.85	0.00	11	3.11	0.00	154
GO MONOSACCHARIDE BINDING	56	3.90	0.00	114	3.53	0.00	71
GO MYELOID CELL ACTIVATION INVOLVED IN IMMUNE RESPONSE	35	-3.38	0.00	182	-4.19	0.00	10
GO GABAERGIC NEURON DIFFERENTIATION	13	3.90	0.00	115	3.50	0.00	80
GO RIBONUCLEOSIDE DIPHOSPHATE METABOLIC PROCESS	48	3.65	0.00	144	3.69	0.00	51
GO NEGATIVE REGULATION OF CYTOKINE BIOSYNTHETIC PROCESS	24	3.68	0.00	140	3.64	0.00	58
GO NEUROPEPTIDE RECEPTOR BINDING	20	4.00	0.00	96	3.36	0.00	103
GO NUCLEOSIDE DIPHOSPHATE METABOLIC PROCESS	60	3.71	0.00	136	3.58	0.00	65
GO CERAMIDE CATABOLIC PROCESS	11	3.29	0.00	190	4.17	0.00	14
GO ENDOLYSOSOME	14	-3.29	0.00	189	-4.08	0.00	19
GO KERATIN FILAMENT	58	6.61	0.00	3	3.09	0.02	210
GO REGULATION OF DEFENSE RESPONSE TO VIRUS	139	-3.66	0.00	141	-3.53	0.00	73
GO POSITIVE REGULATION OF SYNAPSE ASSEMBLY	35	3.64	0.00	145	3.51	0.00	77
GO REGULATION OF NITRIC OXIDE SYNTHASE BIOSYNTHETIC PROCESS	12	-3.31	0.00	188	-3.83	0.00	36
GO CARBOHYDRATE CATABOLIC	80	3.71	0.00	134	3.41	0.00	91

PROCESS							
GO INTRACELLULAR PROTEIN TRANSPORT	627	-5.45	0.00	16	-3.09	0.02	210
GO CENTROSOME	387	-5.27	0.00	19	-3.09	0.02	210
GO ACETYLCHOLINE RECEPTOR ACTIVITY	13	3.93	0.00	107	3.23	0.00	124
GO PHOSPHATIDYLINOSITOL BINDING	160	-3.63	0.00	148	-3.41	0.00	92
GO NEUROTRANSMITTER BINDING	13	3.59	0.00	158	3.42	0.00	86
GO ANTIGEN PROCESSING AND PRESENTATION OF EXOGENOUS PEPTIDE ANTIGEN VIA MHC CLASS I	49	-4.68	0.00	40	-3.09	0.02	210
GO LIPID TRANSLOCATION	16	-3.09	0.00	213	-3.75	0.00	44
GO MYELIN ASSEMBLY	13	-3.09	0.02	262	-5.24	0.00	2
GO POSITIVE REGULATION OF HORMONE SECRETION	90	3.80	0.00	124	3.16	0.00	143
GO ACTIVATION OF INNATE IMMUNE RESPONSE	165	-4.39	0.00	58	-3.09	0.02	210
GO REGULATION OF PSEUDOPODIUM ASSEMBLY	12	3.09	0.02	262	4.22	0.00	9
GO SYNAPTIC TRANSMISSION CHOLINERGIC	16	3.78	0.00	126	3.14	0.00	149
GO IRON ION BINDING	97	3.09	0.02	262	4.17	0.00	13
GO M BAND	11	3.09	0.02	262	4.12	0.00	16
GO MYELOID LEUKOCYTE ACTIVATION	80	-3.52	0.00	166	-3.29	0.00	115
GO DIOL METABOLIC PROCESS	10	3.09	0.02	262	4.05	0.00	20
GO NEGATIVE REGULATION OF PEPTIDE SECRETION	37	3.09	0.02	262	4.04	0.00	21
GO REGULATION OF IMMUNE EFFECTOR PROCESS	301	-3.75	0.00	130	-3.10	0.00	157
GO GLYCOLIPID CATABOLIC PROCESS	11	3.09	0.02	262	3.97	0.00	25
GO PHOSPHOLIPID TRANSLOCATING ATPASE ACTIVITY	11	-3.09	0.02	262	-3.89	0.00	29
GO SULFUR COMPOUND TRANSPORT	21	-3.09	0.02	262	-3.89	0.00	30
GO MEMBRANE TUBULATION	10	3.09	0.02	262	3.88	0.00	31
GO POSITIVE REGULATION OF INTERLEUKIN 10 PRODUCTION	20	-3.09	0.02	262	-3.85	0.00	33
GO ENDOSOMAL PART	345	-4.03	0.00	89	-3.09	0.02	210
GO SECRETORY GRANULE	236	3.65	0.00	143	3.10	0.00	156
GO REGULATION OF MRNA 3 END PROCESSING	25	-3.09	0.02	262	-3.82	0.00	37
GO SPHINGOID METABOLIC PROCESS	12	3.09	0.02	262	3.82	0.00	38
GO REGULATION OF MITOTIC CELL CYCLE	391	-4.00	0.00	95	-3.09	0.02	210
GO REGULATION OF NITRIC OXIDE SYNTHASE ACTIVITY	37	3.09	0.02	262	3.73	0.00	46
GO KERATINIZATION	35	4.92	0.00	31	2.89	0.02	289
GO REGULATION OF WATER LOSS VIA SKIN	13	3.09	0.02	262	3.60	0.00	60
GO CORNIFIED ENVELOPE	32	4.95	0.00	29	2.88	0.02	294
GO MEMBRANE LIPID CATABOLIC PROCESS	21	3.09	0.02	262	3.59	0.00	61
GO REGULATION OF SYNAPSE STRUCTURE OR ACTIVITY	157	3.87	0.00	116	3.09	0.02	210
GO POSITIVE REGULATION OF TRIGLYCERIDE METABOLIC PROCESS	14	3.09	0.02	262	3.58	0.00	64
GO POSITIVE REGULATION OF MESONEPHROS DEVELOPMENT	18	3.19	0.00	205	3.24	0.00	122
GO MRNA METABOLIC PROCESS	478	-6.52	0.00	4	-2.88	0.03	331.5
GO REGULATION OF FIBROBLAST APOPTOTIC PROCESS	14	-3.09	0.02	262	-3.51	0.00	76
GO REGULATION OF HORMONE SECRETION	192	4.22	0.00	73	3.05	0.02	267
GO STEROID HYDROXYLASE ACTIVITY	15	3.01	0.02	320	4.04	0.00	22
GO CELL ACTIVATION INVOLVED IN IMMUNE RESPONSE	96	-3.72	0.00	133	-3.09	0.02	210
GO PHOSPHATIDYLINOSITOL PHOSPHATE BINDING	95	-3.09	0.02	262	-3.43	0.00	85
GO EPIDERMAL CELL	108	4.22	0.00	72	2.95	0.02	276

DIFFERENTIATION							
GO NEUROPEPTIDE HORMONE ACTIVITY	21	4.26	0.00	69	2.94	0.02	280
GO FEEDING BEHAVIOR	61	4.09	0.00	82	3.04	0.02	268
GO GLUCOSE BINDING	10	3.09	0.02	262	3.41	0.00	89
GO REGULATION OF MONONUCLEAR CELL MIGRATION	14	-3.21	0.00	200	-3.12	0.00	152
GO KERATINOCYTE DIFFERENTIATION	74	4.30	0.00	68	2.90	0.02	286
GO MICROTUBULE ORGANIZING CENTER	488	-5.06	0.00	24	-2.88	0.03	331.5
GO NEUROPEPTIDE SIGNALING PATHWAY	55	5.00	0.00	28	2.88	0.03	331.5
GO DIGESTION	67	3.59	0.00	157	3.09	0.02	210
GO IONOTROPIC GLUTAMATE RECEPTOR COMPLEX	29	3.09	0.02	262	3.35	0.00	106
GO PROTEIN TRANSPORTER ACTIVITY	86	-3.56	0.00	162	-3.09	0.02	210
GO RESPIRATORY BURST	10	-3.09	0.02	262	-3.31	0.00	113
GO POSITIVE REGULATION OF MRNA 3 END PROCESSING	16	-2.88	0.04	364	-4.18	0.00	11
GO REGULATION OF NEUROTRANSMITTER RECEPTOR ACTIVITY	23	3.09	0.02	262	3.30	0.00	114
GO PRODUCTION OF MOLECULAR MEDIATOR INVOLVED IN INFLAMMATORY RESPONSE	11	-2.88	0.04	364	-4.18	0.00	12
GO POSITIVE REGULATION OF INNATE IMMUNE RESPONSE	194	-4.55	0.00	48	-2.88	0.03	331.5
GO REGULATION OF RESPONSE TO BIOTIC STIMULUS	173	-3.09	0.02	262	-3.23	0.00	123
GO INTERMEDIATE FILAMENT CYTOSKELETON	147	6.08	0.00	8	2.83	0.03	379
GO SIGNAL TRANSDUCTION INVOLVED IN REGULATION OF GENE EXPRESSION	13	3.09	0.02	262	3.22	0.00	125
GO CELL ADHESION MEDIATED BY INTEGRIN	11	3.09	0.02	262	3.21	0.00	127
GO DOUBLE STRANDED RNA BINDING	54	-3.40	0.00	180	-3.09	0.02	210
GO ACROSOMAL VESICLE	49	3.09	0.02	262	3.21	0.00	128
GO REGULATION OF SYNAPSE ASSEMBLY	50	3.09	0.02	262	3.20	0.00	129
GO REGULATION OF PEPTIDE SECRETION	151	3.82	0.00	123	2.99	0.02	271
GO L ASCORBIC ACID BINDING	16	2.88	0.04	364	3.88	0.00	32
GO POSTSYNAPTIC MEMBRANE	129	3.33	0.00	187	3.09	0.02	210
GO DIGESTIVE SYSTEM PROCESS	39	3.08	0.02	314	3.45	0.00	84
GO INTERSPECIES INTERACTION BETWEEN ORGANISMS	541	-4.32	0.00	67	-2.88	0.03	331.5
GO ACTIN CYTOSKELETON REORGANIZATION	48	-3.73	0.00	131	-2.98	0.02	273
GO REGULATION OF PEPTIDE TRANSPORT	182	3.26	0.00	194	3.09	0.02	210
GO TOXIN TRANSPORT	32	-3.20	0.00	203	-3.09	0.02	210
GO REGULATION OF PLATELET ACTIVATION	24	-3.09	0.02	262	-3.13	0.00	151
GO TRIGLYCERIDE CATABOLIC PROCESS	12	2.88	0.04	364	3.71	0.00	50
GO REGULATION OF PROTEIN ACTIVATION CASCADE	20	-2.88	0.04	364	-3.69	0.00	52
GO CORE PROMOTER PROXIMAL REGION DNA BINDING	295	4.87	0.00	33	2.81	0.03	384
GO GLUTAMATE RECEPTOR ACTIVITY	12	3.12	0.00	210	3.09	0.02	210
GO ACTIVATION OF IMMUNE RESPONSE	308	-5.80	0.00	12	-2.75	0.04	411.5
GO ORGAN INDUCTION	10	-2.75	0.05	418.5	-4.55	0.00	6
GO SKIN DEVELOPMENT	165	3.98	0.00	98	2.88	0.03	331.5
GO ENDOLYSOSOME MEMBRANE	11	-2.75	0.05	418.5	-4.03	0.00	23
GO STEROL HOMEOSTASIS	40	2.91	0.02	328	3.29	0.00	116
GO T CELL HOMEOSTASIS	30	-2.75	0.05	418.5	-3.93	0.00	27
GO SINGLE ORGANISM CELLULAR LOCALIZATION	699	-4.66	0.00	41	-2.75	0.04	411.5

GO ANTIGEN PROCESSING AND PRESENTATION OF PEPTIDE ANTIGEN	131	-3.83	0.00	122	-2.88	0.03	331.5
GO RELAXATION OF CARDIAC MUSCLE	10	-2.75	0.05	418.5	-3.77	0.00	42
GO CEREBRAL CORTEX GABAERGIC INTERNEURON DIFFERENTIATION	10	3.23	0.00	198	3.05	0.02	265
GO EATING BEHAVIOR	21	2.88	0.04	364	3.38	0.00	99
GO TRANSCRIPTION FACTOR ACTIVITY RNA POLYMERASE II CORE PROMOTER PROXIMAL REGION SEQUENCE SPECIFIC BINDING	278	5.13	0.00	23	2.75	0.04	447
GO INTERMEDIATE FILAMENT	107	6.85	0.00	2	2.73	0.04	470
GO PHOSPHATIDYLINOSITOL BIOSYNTHETIC PROCESS	104	-3.09	0.02	262	-3.09	0.02	210
GO NEURON PROJECTION EXTENSION INVOLVED IN NEURON PROJECTION GUIDANCE	11	-3.09	0.02	262	-3.09	0.02	210
GO ANTIGEN RECEPTOR MEDIATED SIGNALING PATHWAY	142	-3.09	0.02	262	-3.09	0.02	210
GO T CELL RECEPTOR SIGNALING PATHWAY	115	-3.09	0.02	262	-3.09	0.02	210
GO REGULATION OF GLIOGENESIS	69	3.09	0.02	262	3.09	0.02	210
GO CYTOSOLIC TRANSPORT	160	-3.09	0.02	262	-3.09	0.02	210
GO PERICENTRIOLAR MATERIAL	17	-3.09	0.02	262	-3.09	0.02	210
GO SITE OF DOUBLE STRAND BREAK	27	-3.09	0.02	262	-3.09	0.02	210
GO ESTABLISHMENT OF MITOTIC SPINDLE ORIENTATION	15	-2.75	0.05	418.5	-3.64	0.00	57
GO POSITIVE REGULATION OF SMOOTH MUSCLE CELL MIGRATION	29	-2.75	0.05	418.5	-3.61	0.00	59
GO ATPASE ACTIVITY COUPLED	241	-4.20	0.00	74	-2.75	0.04	411.5
GO REGULATION OF MONOOXYGENASE ACTIVITY	46	2.75	0.05	445.5	3.78	0.00	41
GO TOLL LIKE RECEPTOR SIGNALING PATHWAY	72	-3.53	0.00	164	-2.88	0.03	331.5
GO FC RECEPTOR SIGNALING PATHWAY	158	-3.49	0.00	171	-2.88	0.03	331.5
GO VACUOLAR TRANSPORT	208	-4.01	0.00	92	-2.75	0.04	411.5
GO CILIARY TRANSITION ZONE	19	-2.88	0.04	364	-3.16	0.00	142
GO CYTOKINE ACTIVITY	112	3.41	0.00	178	2.88	0.03	331.5
GO MRNA PROCESSING	348	-6.12	0.00	7	-2.65	0.04	507
GO REGULATION OF CELL CYCLE PHASE TRANSITION	277	-3.91	0.00	112	-2.75	0.04	411.5
GO CARBOHYDRATE BINDING	166	3.26	0.00	193	2.88	0.03	331.5
GO TRANSCRIPTIONAL ACTIVATOR ACTIVITY RNA POLYMERASE II CORE PROMOTER PROXIMAL REGION SEQUENCE SPECIFIC BINDING	190	4.13	0.00	79	2.75	0.04	447
GO ORGANELLE MEMBRANE FUSION	74	-3.09	0.02	262	-3.05	0.02	264
GO REGULATION OF HORMONE LEVELS	324	3.69	0.00	139	2.78	0.03	388
GO REGULATION OF INTERFERON BETA PRODUCTION	42	-2.75	0.05	418.5	-3.34	0.00	109
GO REGULATION OF SYNAPSE ORGANIZATION	75	3.09	0.02	262	2.96	0.02	275
GO REGULATION OF NOREPINEPHRINE SECRETION	11	2.75	0.05	445.5	3.37	0.00	101
GO NEUROPEPTIDE RECEPTOR ACTIVITY	22	4.11	0.00	81	2.72	0.04	471
GO STEROID CATABOLIC PROCESS	13	2.75	0.05	445.5	3.33	0.00	110
GO NUCLEAR LOCALIZATION SEQUENCE BINDING	20	-2.75	0.05	418.5	-3.14	0.00	147
GO GUANYL NUCLEOTIDE BINDING	290	-3.59	0.00	155	-2.75	0.04	411.5
GO CELLULAR COMPONENT ASSEMBLY INVOLVED IN MORPHOGENESIS	158	-2.88	0.04	364	-3.09	0.02	210
GO MEIOTIC CELL CYCLE	104	-2.88	0.04	364	-3.09	0.02	210
GO NEUROMUSCULAR SYNAPTIC TRANSMISSION	16	2.88	0.04	364	3.09	0.02	210
GO DORSAL SPINAL CORD DEVELOPMENT	16	2.88	0.04	364	3.09	0.02	210
GO POSTTRANSCRIPTIONAL	368	-4.16	0.00	77	-2.65	0.04	507

REGULATION OF GENE EXPRESSION							
GO PHOSPHOLIPID EFFLUX	12	2.96	0.02	323	3.01	0.02	270
GO REGULATION OF DNA DEPENDENT DNA REPLICATION	38	-3.09	0.02	262	-2.88	0.03	331.5
GO PEPTIDE CROSS LINKING	42	3.09	0.02	262	2.88	0.03	331.5
GO CILIUM ORGANIZATION	120	-3.09	0.02	262	-2.88	0.03	331.5
GO ORGANELLE FUSION	100	-3.09	0.02	262	-2.88	0.03	331.5
GO CLUSTER OF ACTIN BASED CELL PROJECTIONS	100	3.09	0.02	262	2.88	0.03	331.5
GO DNA DEPENDENT ATPASE ACTIVITY	64	-4.03	0.00	88	-2.65	0.04	507
GO REGULATION OF MESONEPHROS DEVELOPMENT	21	2.92	0.02	325	2.92	0.02	282
GO VOLTAGE GATED POTASSIUM CHANNEL ACTIVITY	45	3.52	0.00	165	2.75	0.04	447
GO NUCLEOBASE CONTAINING COMPOUND TRANSPORT	157	-4.39	0.00	59	-2.58	0.05	562.5
GO POSITIVE REGULATION OF DEFENSE RESPONSE	275	-3.87	0.00	117	-2.65	0.04	507
GO IMMUNE RESPONSE REGULATING CELL SURFACE RECEPTOR SIGNALING PATHWAY	231	-3.85	0.00	120	-2.65	0.04	507
GO CYTOKINE PRODUCTION	91	-2.75	0.05	418.5	-3.09	0.02	210
GO PROTEIN LOCALIZATION TO VACUOLE	40	-2.75	0.05	418.5	-3.09	0.02	210
GO ESTABLISHMENT OF PROTEIN LOCALIZATION TO VACUOLE	28	-2.75	0.05	418.5	-3.09	0.02	210
GO POSITIVE REGULATION OF DNA TEMPLATED TRANSCRIPTION ELONGATION	19	-2.75	0.05	418.5	-3.09	0.02	210
GO OXIDOREDUCTASE ACTIVITY ACTING ON PAIRED DONORS WITH INCORPORATION OR REDUCTION OF MOLECULAR OXYGEN	92	3.09	0.02	262	2.86	0.03	371
GO REGULATION OF DEFENSE RESPONSE	552	-4.11	0.00	80	-2.58	0.05	562.5
GO RIBONUCLEOPROTEIN COMPLEX DISASSEMBLY	11	-3.08	0.02	315	-2.88	0.03	331.5
GO BRUSH BORDER	75	2.99	0.02	321	2.88	0.03	331.5
GO MEMBRANE FUSION	116	-2.94	0.02	324	-2.88	0.03	331.5
GO ANCHORED COMPONENT OF MEMBRANE	96	3.37	0.00	183	2.71	0.04	473
GO NEGATIVE REGULATION OF OSSIFICATION	60	3.11	0.00	211	2.75	0.04	447
GO NEPHRON TUBULE FORMATION	15	3.28	0.00	191	2.67	0.04	475
GO REGULATION OF INNATE IMMUNE RESPONSE	272	-3.94	0.00	104	-2.58	0.05	562.5
GO NUCLEAR TRANSPORT	287	-3.92	0.00	109	-2.58	0.05	562.5
GO ANTIGEN PROCESSING AND PRESENTATION	153	-3.91	0.00	111	-2.58	0.05	562.5
GO ANTIGEN PROCESSING AND PRESENTATION OF PEPTIDE ANTIGEN VIA MHC CLASS I	69	-3.09	0.02	262	-2.75	0.04	411.5
GO SERINE HYDROLASE ACTIVITY	142	3.52	0.00	168	2.65	0.04	507
GO SYNAPTIC MEMBRANE	164	3.41	0.00	179	2.65	0.04	507
GO MESENCHYMAL TO EPITHELIAL TRANSITION	14	2.88	0.04	364	2.88	0.03	331.5
GO EMBRYONIC SKELETAL SYSTEM DEVELOPMENT	95	2.88	0.04	364	2.88	0.03	331.5
GO TRANSCRIPTION ELONGATION FACTOR COMPLEX	36	-2.88	0.04	364	-2.88	0.03	331.5
GO EXCITATORY EXTRACELLULAR LIGAND GATED ION CHANNEL ACTIVITY	23	3.09	0.02	262	2.75	0.04	447
GO TRANSCRIPTIONAL REPRESSOR ACTIVITY RNA POLYMERASE II TRANSCRIPTION REGULATORY REGION SEQUENCE SPECIFIC BINDING	137	3.63	0.00	147	2.58	0.05	562.5
GO NEGATIVE REGULATION OF BEHAVIOR	10	2.75	0.05	445.5	3.05	0.02	266

GO CYSTEINE TYPE PEPTIDASE ACTIVITY	129	-3.61	0.00	151	-2.58	0.05	562.5
GO NEGATIVE REGULATION OF SECRETION	138	2.88	0.04	364	2.84	0.03	377
GO REGULATION OF PROTEIN COMPLEX ASSEMBLY	302	-2.88	0.04	364	-2.83	0.03	378
GO GLOBAL GENOME NUCLEOTIDE EXCISION REPAIR	28	-2.88	0.04	364	-2.82	0.03	380
GO RETROGRADE TRANSPORT ENDOSOME TO GOLGI	57	-2.88	0.04	364	-2.82	0.03	381
GO NEGATIVE REGULATION OF INTERLEUKIN 12 PRODUCTION	11	-2.75	0.05	418.5	-2.88	0.03	331.5
GO ELECTRON CARRIER ACTIVITY	96	-3.09	0.02	262	-2.65	0.04	507
GO NEUROTRANSMITTER RECEPTOR ACTIVITY	31	2.98	0.02	322	2.75	0.04	447
GO PHOSPHOLIPID BINDING	272	-3.12	0.00	209	-2.58	0.05	562.5
GO BIOTIN METABOLIC PROCESS	14	-2.88	0.04	364	-2.75	0.04	411.5
GO RIBOSOME BINDING	39	-2.88	0.04	364	-2.75	0.04	411.5
GO POSITIVE REGULATION OF MACROPHAGE CHEMOTAXIS	10	-2.75	0.05	418.5	-2.86	0.03	370
GO POSITIVE REGULATION OF MITOTIC CELL CYCLE	99	-2.75	0.05	418.5	-2.85	0.03	373
GO SECRETORY VESICLE	315	2.88	0.04	364	2.75	0.04	447
GO REGULATION OF RNA STABILITY	119	-3.09	0.02	262	-2.58	0.05	562.5
GO NEGATIVE REGULATION OF IMMUNE EFFECTOR PROCESS	73	-2.75	0.05	418.5	-2.75	0.04	411.5
GO NEGATIVE REGULATION OF OSTEOBLAST DIFFERENTIATION	37	2.90	0.02	329	2.65	0.04	507
GO PERIKARYON	60	2.75	0.05	445.5	2.75	0.04	447
GO MRNA BINDING	120	-2.75	0.05	418.5	-2.65	0.04	507
GO PROTEIN DEPHOSPHORYLATION	148	-2.88	0.04	364	-2.58	0.05	562.5
GO INTRACILIARY TRANSPORT PARTICLE	17	-2.75	0.05	418.5	-2.58	0.05	562.5
GO REGULATION OF PHOSPHOLIPID METABOLIC PROCESS	50	2.75	0.05	445.5	2.58	0.05	562.5

Supplementary Table 3. Significant (q<0.05) GO pathways for the cluster 3 normotensive SGA samples compared to the cluster 1 controls.

Pathway	Set Size	NTk Stat	NTk q-value	NTk Rank	NEk Stat	NEk q-value	NEk Rank
GO IMMUNE EFFECTOR PROCESS	340	11.85	0.00	2	4.64	0.00	12
GO RESPONSE TO TYPE I INTERFERON	44	9.41	0.00	5	4.74	0.00	9
GO INNATE IMMUNE RESPONSE	376	14.51	0.00	1	4.61	0.00	14
GO RESPONSE TO VIRUS	186	9.16	0.00	8	4.70	0.00	11
GO DEFENSE RESPONSE TO VIRUS	119	8.07	0.00	16	4.60	0.00	15
GO RESPONSE TO INTERFERON GAMMA	91	8.56	0.00	11	4.39	0.00	26
GO INTERFERON GAMMA MEDIATED SIGNALING PATHWAY	46	7.70	0.00	19	4.38	0.00	27
GO ADAPTIVE IMMUNE RESPONSE BASED ON SOMATIC RECOMBINATION OF IMMUNE RECEPTORS BUILT FROM IMMUNOGLOBULIN SUPERFAMILY DOMAINS	89	7.04	0.00	23	4.47	0.00	23
GO CELLULAR RESPONSE TO INTERFERON GAMMA	73	8.15	0.00	14	4.25	0.00	35
GO POSITIVE REGULATION OF IMMUNE RESPONSE	397	8.33	0.00	13	4.13	0.00	42
GO LEUKOCYTE MEDIATED IMMUNITY	113	6.65	0.00	28	4.35	0.00	31
GO REGULATION OF IMMUNE RESPONSE	601	11.21	0.00	3	4.01	0.00	58
GO NEGATIVE REGULATION OF MULTI ORGANISM PROCESS	113	6.90	0.00	24	4.23	0.00	37
GO ADAPTIVE IMMUNE RESPONSE	159	9.14	0.00	9	4.06	0.00	55

GO REGULATION OF B CELL ACTIVATION	81	5.73	0.00	52	4.61	0.00	13
GO NEGATIVE REGULATION OF B CELL ACTIVATION	24	5.53	0.00	63	5.79	0.00	2
GO DEFENSE RESPONSE TO OTHER ORGANISM	304	7.94	0.00	18	4.08	0.00	53
GO POSITIVE REGULATION OF IMMUNE SYSTEM PROCESS	637	10.46	0.00	4	3.96	0.00	69
GO NEGATIVE REGULATION OF VIRAL PROCESS	69	6.14	0.00	37	4.18	0.00	39
GO RESPONSE TO CYTOKINE	516	8.93	0.00	10	3.95	0.00	71
GO RESPONSE TO BIOTIC STIMULUS	602	9.39	0.00	6	3.82	0.00	81
GO NAD ADP RIBOSYLTRANSFERASE ACTIVITY	22	5.00	0.00	88	8.01	0.00	1
GO REGULATION OF INTERLEUKIN 1 BETA PRODUCTION	33	5.41	0.00	65	4.44	0.00	25
GO CELLULAR RESPONSE TO ZINC ION	12	5.73	0.00	51	4.14	0.00	41
GO INFLAMMATORY RESPONSE	294	9.33	0.00	7	3.76	0.00	92
GO CELLULAR RESPONSE TO CYTOKINE STIMULUS	426	8.11	0.00	15	3.80	0.00	85
GO CYTOKINE MEDIATED SIGNALING PATHWAY	306	7.29	0.00	22	3.89	0.00	78
GO POSITIVE REGULATION OF OXIDOREDUCTASE ACTIVITY	32	4.87	0.00	92	4.81	0.00	8
GO HUMORAL IMMUNE RESPONSE MEDIATED BY CIRCULATING IMMUNOGLOBULIN	23	5.25	0.00	73	4.38	0.00	28
GO PHAGOCYTIC CUP	15	4.77	0.00	101	5.39	0.00	4
GO NEGATIVE REGULATION OF IMMUNE RESPONSE	84	5.53	0.00	64	4.13	0.00	43
GO LIPOPOLYSACCHARIDE MEDIATED SIGNALING PATHWAY	28	5.70	0.00	54	4.07	0.00	54
GO ATP GENERATION FROM ADP	27	5.92	0.00	47	3.98	0.00	67
GO REGULATION OF OXIDOREDUCTASE ACTIVITY	66	4.80	0.00	98	4.59	0.00	16
GO B CELL MEDIATED IMMUNITY	47	4.83	0.00	96	4.49	0.00	22
GO ADP METABOLIC PROCESS	33	5.68	0.00	55	3.99	0.00	64
GO NEGATIVE REGULATION OF VIRAL GENOME REPLICATION	38	5.60	0.00	60	4.01	0.00	60
GO REGULATION OF INNATE IMMUNE RESPONSE	272	6.03	0.00	41	3.84	0.00	80
GO NUCLEOTIDE PHOSPHORYLATION	42	5.87	0.00	48	3.91	0.00	75
GO NEGATIVE REGULATION OF INNATE IMMUNE RESPONSE	25	4.88	0.00	91	4.23	0.00	36
GO REGULATION OF B CELL DIFFERENTIATION	20	4.64	0.00	117	4.73	0.00	10
GO LEUKOCYTE CHEMOTAXIS	76	5.96	0.00	45	3.78	0.00	86
GO POSITIVE REGULATION OF LEUKOCYTE CHEMOTAXIS	61	5.59	0.00	62	3.94	0.00	72
GO REGULATION OF INTERLEUKIN 1 PRODUCTION	40	4.89	0.00	90	4.12	0.00	45
GO POSITIVE REGULATION OF CYTOKINE PRODUCTION	271	6.74	0.00	27	3.63	0.00	112
GO REGULATION OF CYTOKINE PRODUCTION	420	8.05	0.00	17	3.51	0.00	128
GO GLUCOSE CATABOLIC PROCESS	21	5.64	0.00	58	3.77	0.00	90
GO REGULATION OF B CELL PROLIFERATION	41	4.51	0.00	135	4.51	0.00	21
GO POSITIVE REGULATION OF LEUKOCYTE MIGRATION	82	5.78	0.00	50	3.58	0.00	119
GO NAD METABOLIC PROCESS	42	5.36	0.00	66	3.66	0.00	103
GO COMPLEMENT ACTIVATION	31	4.62	0.00	122	4.08	0.00	51
GO IMMUNOGLOBULIN BINDING	12	4.61	0.00	123	4.09	0.00	50
GO T CELL MIGRATION	11	4.61	0.00	126	4.11	0.00	48
GO REGULATION OF TYPE I INTERFERON PRODUCTION	99	4.45	0.00	142	4.28	0.00	33
GO REGULATION OF LEUKOCYTE CHEMOTAXIS	70	5.19	0.00	75	3.64	0.00	111
GO PATTERN RECOGNITION RECEPTOR SIGNALING PATHWAY	89	5.30	0.00	70	3.57	0.00	122

GO REGULATION OF PHOSPHOLIPID METABOLIC PROCESS	50	5.09	0.00	80	3.62	0.00	115
GO RESPONSE TO INTERFERON ALPHA	18	4.62	0.00	121	3.92	0.00	74
GO REGULATION OF ADAPTIVE IMMUNE RESPONSE	88	4.70	0.00	110	3.77	0.00	88
GO NEGATIVE REGULATION OF IMMUNE SYSTEM PROCESS	277	6.26	0.00	34	3.31	0.00	169
GO LEUKOCYTE DIFFERENTIATION	222	6.52	0.00	30	3.29	0.00	174
GO MYELOID LEUKOCYTE MIGRATION	68	4.85	0.00	95	3.64	0.00	109
GO NEGATIVE REGULATION OF MULTICELLULAR ORGANISMAL METABOLIC PROCESS	11	4.19	0.00	168	4.17	0.00	40
GO PODOSOME	20	4.35	0.00	149	4.00	0.00	63
GO REGULATION OF INTERFERON GAMMA PRODUCTION	67	4.59	0.00	129	3.80	0.00	84
GO REGULATION OF MAST CELL ACTIVATION	31	4.20	0.00	167	4.12	0.00	46
GO CELLULAR RESPONSE TO CADMIUM ION	13	4.46	0.00	141	3.93	0.00	73
GO POSITIVE REGULATION OF ACUTE INFLAMMATORY RESPONSE	16	4.07	0.00	186	4.38	0.00	29
GO REGULATION OF LEUKOCYTE DIFFERENTIATION	172	6.35	0.00	31	3.24	0.00	186
GO REGULATION OF CYSTEINE TYPE ENDOPEPTIDASE ACTIVITY	179	4.61	0.00	125	3.71	0.00	96
GO ACUTE PHASE RESPONSE	19	3.99	0.00	203	4.51	0.00	20
GO REGULATION OF PEPTIDASE ACTIVITY	275	5.11	0.00	78	3.42	0.00	147
GO REGULATION OF LIPID STORAGE	34	3.84	0.00	220	5.03	0.00	5
GO POSITIVE REGULATION OF RESPONSE TO EXTERNAL STIMULUS	219	5.63	0.00	59	3.31	0.00	168
GO REGULATION OF HEMOPOIESIS	242	6.29	0.00	32	3.19	0.00	198
GO CAMERA TYPE EYE PHOTORECEPTOR CELL DIFFERENTIATION	11	-3.79	0.00	230	-5.43	0.00	3
GO LYMPHOCYTE MIGRATION	28	4.75	0.00	105	3.50	0.00	129
GO NADH METABOLIC PROCESS	28	5.13	0.00	77	3.38	0.00	158
GO REGULATION OF RESPONSE TO CYTOKINE STIMULUS	103	5.03	0.00	85	3.37	0.00	159
GO NEGATIVE REGULATION OF MYELOID LEUKOCYTE DIFFERENTIATION	33	4.51	0.00	134	3.62	0.00	113
GO NEGATIVE REGULATION OF CYTOKINE PRODUCTION	159	5.60	0.00	61	3.23	0.00	190
GO REGULATION OF MYELOID LEUKOCYTE DIFFERENTIATION	79	5.10	0.00	79	3.28	0.00	175
GO REGULATION OF LEUKOCYTE APOPTOTIC PROCESS	64	4.03	0.00	197	4.01	0.00	59
GO REGULATION OF PHOSPHATIDYLINOSITOL 3 KINASE ACTIVITY	36	4.65	0.00	115	3.43	0.00	142
GO REGULATION OF LIPID KINASE ACTIVITY	44	4.71	0.00	107	3.40	0.00	152
GO PHAGOCYTIC VESICLE MEMBRANE	44	4.49	0.00	138	3.54	0.00	126
GO CELLULAR RESPONSE TO BIOTIC STIMULUS	124	5.27	0.00	71	3.21	0.00	194
GO POSITIVE REGULATION OF INFLAMMATORY RESPONSE	73	4.63	0.00	119	3.41	0.00	149
GO CELL ACTIVATION INVOLVED IN IMMUNE RESPONSE	96	4.32	0.00	151	3.60	0.00	117
GO REGULATION OF ANTIGEN RECEPTOR MEDIATED SIGNALING PATHWAY	30	3.97	0.00	207	4.00	0.00	61
GO T CELL ACTIVATION INVOLVED IN IMMUNE RESPONSE	32	4.17	0.00	175	3.71	0.00	95
GO REGULATION OF INFLAMMATORY RESPONSE	199	5.25	0.00	72	3.19	0.00	199
GO GLUCOSE METABOLIC PROCESS	89	4.58	0.00	130	3.42	0.00	146
GO NEGATIVE REGULATION OF B CELL PROLIFERATION	12	3.47	0.00	274	4.85	0.00	6

GO LEUKOCYTE ACTIVATION	303	7.38	0.00	21	3.09	0.02	269.5
GO NEGATIVE REGULATION OF LEUKOCYTE DIFFERENTIATION	62	4.64	0.00	116	3.27	0.00	176
GO OVULATION	12	3.88	0.00	217	3.90	0.00	77
GO REGULATION OF DEFENSE RESPONSE	552	6.75	0.00	25	3.09	0.02	269.5
GO LEUKOCYTE CELL CELL ADHESION	186	6.61	0.00	29	3.09	0.02	269.5
GO POSITIVE REGULATION OF STRESS ACTIVATED PROTEIN KINASE SIGNALING CASCADE	113	4.46	0.00	139	3.34	0.00	163
GO NEGATIVE REGULATION OF TYPE I INTERFERON PRODUCTION	34	3.83	0.00	224	3.81	0.00	82
GO REGULATION OF PHAGOCYTOSIS	54	4.36	0.00	148	3.37	0.00	160
GO CELL CHEMOTAXIS	110	6.08	0.00	39	3.09	0.02	269.5
GO TRANSFERASE ACTIVITY TRANSFERRING PENTOSYL GROUPS	46	3.46	0.00	277	4.31	0.00	32
GO POSITIVE REGULATION OF CELL ACTIVATION	214	6.06	0.00	40	3.09	0.02	269.5
GO REGULATION OF INTERFERON ALPHA PRODUCTION	18	3.77	0.00	233	3.85	0.00	79
GO PROTEASOMAL PROTEIN CATABOLIC PROCESS	242	-4.37	0.00	146	-3.31	0.00	167
GO REGULATION OF LEUKOCYTE PROLIFERATION	153	5.96	0.00	44	3.09	0.02	269.5
GO LYMPHOCYTE MEDIATED IMMUNITY	81	5.94	0.00	46	3.09	0.02	269.5
GO REGULATION OF MYELOID CELL DIFFERENTIATION	143	4.63	0.00	120	3.20	0.00	196
GO CHEMOKINE MEDIATED SIGNALING PATHWAY	34	4.19	0.00	169	3.40	0.00	151
GO POSITIVE REGULATION OF TYPE I INTERFERON PRODUCTION	66	3.55	0.00	264	3.99	0.00	65
GO POSITIVE REGULATION OF DEFENSE RESPONSE	275	5.36	0.00	67	3.09	0.02	269.5
GO MYELOID LEUKOCYTE ACTIVATION	80	4.27	0.00	155	3.24	0.00	184
GO REGULATION OF LEUKOCYTE MIGRATION	111	5.23	0.00	74	3.09	0.02	269.5
GO MONOSACCHARIDE CATABOLIC PROCESS	45	4.53	0.00	133	3.11	0.00	214
GO POSITIVE REGULATION OF LEUKOCYTE PROLIFERATION	96	5.09	0.00	81	3.09	0.02	269.5
GO REGULATION OF MACROPHAGE DIFFERENTIATION	18	3.09	0.02	344	4.81	0.00	7
GO PYRUVATE METABOLIC PROCESS	46	4.30	0.00	152	3.19	0.00	200
GO CARBOHYDRATE KINASE ACTIVITY	15	3.54	0.00	266	3.77	0.00	89
GO POSITIVE REGULATION OF PHAGOCYTOSIS	38	3.72	0.00	238	3.59	0.00	118
GO CYTOSOLIC PROTEASOME COMPLEX	11	-4.18	0.00	172	-3.23	0.00	188
GO NEGATIVE REGULATION OF LIPID STORAGE	15	3.09	0.02	344	4.59	0.00	17
GO RESPONSE TO INTERFERON BETA	17	3.09	0.02	344	4.53	0.00	19
GO MATERNAL PLACENTA DEVELOPMENT	25	4.20	0.00	163	3.16	0.00	205
GO NEGATIVE REGULATION OF INTERLEUKIN 1 BETA PRODUCTION	10	3.09	0.02	344	4.45	0.00	24
GO POSITIVE REGULATION OF ADAPTIVE IMMUNE RESPONSE	53	3.71	0.00	240	3.44	0.00	138
GO CYTOKINE ACTIVITY	112	5.64	0.00	57	3.08	0.02	324
GO POSITIVE REGULATION OF LIPID STORAGE	15	3.09	0.02	344	4.21	0.00	38
GO NEGATIVE REGULATION OF MYELOID CELL DIFFERENTIATION	62	3.50	0.00	269	3.62	0.00	116
GO REGULATION OF MEMBRANE PROTEIN ECTODOMAIN PROTEOLYSIS	17	3.60	0.00	257	3.44	0.00	136
GO POSITIVE REGULATION OF INTERFERON ALPHA PRODUCTION	16	3.09	0.02	344	4.08	0.00	52
GO CELL ACTIVATION	423	8.49	0.00	12	2.88	0.03	385.5
GO REGULATION OF LYMPHOCYTE DIFFERENTIATION	96	4.57	0.00	131	3.09	0.02	269.5

GO PROTEIN ACTIVATION CASCADE	41	3.97	0.00	206	3.21	0.00	195
GO NEGATIVE REGULATION OF INTERLEUKIN 1 PRODUCTION	12	3.09	0.02	344	4.02	0.00	57
GO BLOOD MICROPARTICLE	62	4.56	0.00	132	3.09	0.02	269.5
GO SHORT CHAIN FATTY ACID METABOLIC PROCESS	11	-3.36	0.00	288	-3.62	0.00	114
GO GLUCOSE BINDING	10	3.60	0.00	258	3.42	0.00	145
GO REGULATION OF LYMPHOCYTE MIGRATION	28	3.83	0.00	222	3.25	0.00	182
GO ACTIVATION OF IMMUNE RESPONSE	308	7.52	0.00	20	2.88	0.03	385.5
GO REGULATION OF MONOOXYGENASE ACTIVITY	46	3.09	0.02	344	4.00	0.00	62
GO FIBRONECTIN BINDING	20	3.57	0.00	262	3.41	0.00	148
GO REGULATION OF ACUTE INFLAMMATORY RESPONSE	42	3.09	0.02	344	3.98	0.00	66
GO POSITIVE REGULATION OF T CELL PROLIFERATION	67	4.43	0.00	143	3.09	0.02	269.5
GO REGULATION OF B CELL APOPTOTIC PROCESS	13	3.09	0.02	344	3.95	0.00	70
GO VACUOLAR ACIDIFICATION	15	3.70	0.00	242	3.26	0.00	181
GO CARBOHYDRATE CATABOLIC PROCESS	80	4.76	0.00	103	3.07	0.02	328
GO PHAGOCYTIC VESICLE	69	3.78	0.00	231	3.15	0.00	208
GO RESPONSE TO OSMOTIC STRESS	54	4.19	0.00	171	3.09	0.02	269.5
GO LYMPHOCYTE DIFFERENTIATION	149	5.66	0.00	56	2.88	0.03	385.5
GO ACETYL COA BIOSYNTHETIC PROCESS	10	-3.09	0.02	344	-3.70	0.00	101
GO GRANULOCYTE MIGRATION	50	4.17	0.00	176	3.09	0.02	269.5
GO MYELOID CELL HOMEOSTASIS	75	4.17	0.00	177	3.09	0.02	269.5
GO REGULATION OF MULTI ORGANISM PROCESS	351	4.69	0.00	111	3.00	0.02	336
GO G PROTEIN COUPLED CHEMOATTRACTANT RECEPTOR ACTIVITY	11	3.09	0.02	344	3.65	0.00	106
GO PROTEASOME ACCESSORY COMPLEX	23	-4.13	0.00	181	-3.09	0.02	269.5
GO POSITIVE REGULATION OF B CELL ACTIVATION	53	3.09	0.02	344	3.64	0.00	108
GO NEGATIVE REGULATION OF PEPTIDASE ACTIVITY	151	4.05	0.00	192	3.09	0.02	269.5
GO VOLTAGE GATED SODIUM CHANNEL ACTIVITY	10	-3.09	0.02	344	-3.57	0.00	120
GO REGULATION OF INFLAMMATORY RESPONSE TO ANTIGENIC STIMULUS	11	2.88	0.03	430.5	4.26	0.00	34
GO LEUKOCYTE PROLIFERATION	52	4.01	0.00	199	3.09	0.02	269.5
GO LYMPHOCYTE CHEMOTAXIS	19	3.63	0.00	254	3.11	0.00	215
GO REGULATION OF IMMUNE EFFECTOR PROCESS	301	5.04	0.00	84	2.88	0.03	385.5
GO HYPEROSMOTIC RESPONSE	15	4.00	0.00	201	3.09	0.02	269.5
GO HEXOSE METABOLIC PROCESS	120	3.98	0.00	204	3.09	0.02	269.5
GO NEGATIVE REGULATION OF CANONICAL WNT SIGNALING PATHWAY	138	-3.09	0.02	344	-3.49	0.00	130
GO REGULATION OF STRESS ACTIVATED PROTEIN KINASE SIGNALING CASCADE	162	3.98	0.00	205	3.09	0.02	269.5
GO UBIQUITIN LIGASE COMPLEX	221	-3.15	0.00	298	-3.26	0.00	180
GO POSITIVE REGULATION OF IMMUNE EFFECTOR PROCESS	109	3.95	0.00	210	3.09	0.02	269.5
GO NUCLEOSIDE DIPHOSPHATE METABOLIC PROCESS	60	3.94	0.00	212	3.09	0.02	269.5
GO POSITIVE REGULATION OF LYMPHOCYTE MIGRATION	20	3.09	0.02	344	3.44	0.00	139
GO CYTOKINE RECEPTOR BINDING	163	3.92	0.00	214	3.09	0.02	269.5
GO RAN GTPASE BINDING	29	-3.09	0.02	344	-3.43	0.00	140
GO RIBONUCLEOSIDE DIPHOSPHATE METABOLIC PROCESS	48	3.91	0.00	215	3.09	0.02	269.5
GO CYTOPLASMIC PATTERN RECOGNITION RECEPTOR SIGNALING PATHWAY	28	2.88	0.03	430.5	4.02	0.00	56

GO REGULATION OF JUN KINASE ACTIVITY	64	4.19	0.00	170	3.08	0.02	321
GO LYMPHOCYTE ACTIVATION	245	6.74	0.00	26	2.75	0.04	471
GO REGULATION OF EXTRINSIC APOPTOTIC SIGNALING PATHWAY VIA DEATH DOMAIN RECEPTORS	44	2.88	0.03	430.5	3.98	0.00	68
GO CYTOKINE SECRETION	28	3.09	0.02	344	3.39	0.00	155
GO REGULATION OF LEUKOCYTE MEDIATED IMMUNITY	114	4.65	0.00	114	2.88	0.03	385.5
GO REGULATION OF VIRAL GENOME REPLICATION	60	3.77	0.00	234	3.09	0.02	269.5
GO LEUKOCYTE MIGRATION	200	6.26	0.00	33	2.75	0.04	471
GO CELLULAR RESPONSE TO DRUG	52	3.09	0.02	344	3.36	0.00	161
GO LYMPHOCYTE ACTIVATION INVOLVED IN IMMUNE RESPONSE	63	3.09	0.02	344	3.35	0.00	162
GO NODE OF RANVIER	10	-2.88	0.03	430.5	-3.91	0.00	76
GO NEGATIVE REGULATION OF HEMOPOIESIS	97	4.10	0.00	185	3.08	0.02	323
GO PROTEIN MODIFICATION BY SMALL PROTEIN REMOVAL	100	-3.72	0.00	239	-3.09	0.02	269.5
GO REGULATION OF CELL ACTIVATION	346	5.98	0.00	43	2.75	0.04	471
GO POSITIVE REGULATION OF MONOOXYGENASE ACTIVITY	18	2.88	0.03	430.5	3.76	0.00	91
GO T CELL DIFFERENTIATION	92	4.50	0.00	137	2.88	0.03	385.5
GO POSITIVE REGULATION OF INTERFERON GAMMA PRODUCTION	44	3.64	0.00	253	3.09	0.02	269.5
GO REGULATION OF NF KAPPAB IMPORT INTO NUCLEUS	33	2.88	0.03	430.5	3.71	0.00	97
GO POSITIVE REGULATION OF CHEMOTAXIS	95	4.77	0.00	100	2.79	0.03	428
GO REGULATION OF TYPE I INTERFERON MEDIATED SIGNALING PATHWAY	23	3.59	0.00	260	3.09	0.02	269.5
GO REGULATION OF SYMBIOSIS ENCOMPASSING MUTUALISM THROUGH PARASITISM	161	4.00	0.00	200	3.04	0.02	332
GO GLYCOSYLCERAMIDE METABOLIC PROCESS	10	2.88	0.03	430.5	3.70	0.00	102
GO TOLL LIKE RECEPTOR SIGNALING PATHWAY	72	4.33	0.00	150	2.88	0.03	385.5
GO POSITIVE REGULATION OF NF KAPPAB TRANSCRIPTION FACTOR ACTIVITY	98	3.49	0.00	272	3.09	0.02	269.5
GO FIBRINOLYSIS	10	2.75	0.04	502.5	4.13	0.00	44
GO LIPOXYGENASE PATHWAY	10	3.40	0.00	283	3.09	0.02	269.5
GO POSITIVE REGULATION OF MAP KINASE ACTIVITY	162	5.08	0.00	82	2.75	0.04	471
GO NEGATIVE REGULATION OF TUMOR NECROSIS FACTOR SUPERFAMILY CYTOKINE PRODUCTION	28	3.38	0.00	285	3.09	0.02	269.5
GO IRON ION TRANSPORT	45	2.88	0.03	430.5	3.53	0.00	127
GO LEUKOCYTE APOPTOTIC PROCESS	19	3.09	0.02	344	3.10	0.00	216
GO RESPONSE TO INTERLEUKIN 1	81	3.74	0.00	237	3.08	0.02	325
GO CELLULAR RESPONSE TO INTERLEUKIN 1	60	3.09	0.02	344	3.10	0.00	218
GO REGULATION OF INTERLEUKIN 1 SECRETION	18	2.88	0.03	430.5	3.47	0.00	132
GO REGULATION OF RESPONSE TO INTERFERON GAMMA	20	2.88	0.03	430.5	3.46	0.00	134
GO MYELOID CELL DIFFERENTIATION	164	4.86	0.00	94	2.75	0.04	471
GO LOW DENSITY LIPOPROTEIN PARTICLE	10	2.65	0.05	550.5	4.58	0.00	18
GO RESPONSE TO BACTERIUM	334	6.12	0.00	38	2.65	0.04	532
GO PROTEASOME COMPLEX	69	-4.07	0.00	187	-2.88	0.03	385.5
GO REGULATION OF CYTOKINE SECRETION	93	4.05	0.00	193	2.88	0.03	385.5
GO FC GAMMA RECEPTOR SIGNALING PATHWAY	67	4.70	0.00	109	2.75	0.04	471
GO CELL CORTEX REGION	11	-2.88	0.03	430.5	-3.39	0.00	153
GO I KAPPAB KINASE NF KAPPAB	57	2.88	0.03	430.5	3.39	0.00	154

SIGNALING							
GO NEGATIVE REGULATION OF OSTEOCLAST DIFFERENTIATION	19	3.03	0.02	388	3.19	0.00	197
GO CHEMOKINE BINDING	12	2.75	0.04	502.5	3.81	0.00	83
GO SH3 DOMAIN BINDING	95	3.99	0.00	202	2.88	0.03	385.5
GO POSITIVE REGULATION OF CELL CELL ADHESION	170	4.64	0.00	118	2.75	0.04	471
GO TRANSFERASE COMPLEX	602	-3.96	0.00	209	-2.88	0.03	385.5
GO POSITIVE REGULATION OF NEUTROPHIL MIGRATION	19	2.75	0.04	502.5	3.75	0.00	93
GO POSITIVE REGULATION OF VASCULAR ENDOTHELIAL GROWTH FACTOR PRODUCTION	20	2.88	0.03	430.5	3.31	0.00	166
GO REGULATION OF SYNAPTIC TRANSMISSION GABAERGIC	19	-2.65	0.05	550.5	-4.11	0.00	47
GO NEGATIVE REGULATION OF CYSTEINE TYPE ENDOPEPTIDASE ACTIVITY	74	3.47	0.00	273	3.07	0.02	326
GO RESPONSE TO MOLECULE OF BACTERIAL ORIGIN	245	5.35	0.00	68	2.65	0.04	532
GO RESPONSE TO DEXAMETHASONE	25	2.75	0.04	502.5	3.71	0.00	98
GO ENDOCYTIC VESICLE MEMBRANE	111	3.88	0.00	216	2.88	0.03	385.5
GO POSITIVE REGULATION OF MYELOID LEUKOCYTE MEDIATED IMMUNITY	14	2.75	0.04	502.5	3.70	0.00	100
GO REGULATION OF CYTOKINE PRODUCTION INVOLVED IN INFLAMMATORY RESPONSE	14	2.88	0.03	430.5	3.27	0.00	177
GO REGULATION OF INTERFERON BETA PRODUCTION	42	3.09	0.02	344	3.09	0.02	269.5
GO NEGATIVE REGULATION OF SMOOTH MUSCLE CELL PROLIFERATION	24	3.09	0.02	344	3.09	0.02	269.5
GO T CELL PROLIFERATION	28	3.09	0.02	344	3.09	0.02	269.5
GO RESPONSE TO MURAMYL DIPEPTIDE	11	3.09	0.02	344	3.09	0.02	269.5
GO PLASMA LIPOPROTEIN PARTICLE CLEARANCE	17	3.09	0.02	344	3.09	0.02	269.5
GO REGULATION OF LYMPHOCYTE MEDIATED IMMUNITY	77	3.09	0.02	344	3.09	0.02	269.5
GO POSITIVE REGULATION OF I KAPPAB KINASE NF KAPPAB SIGNALING	143	3.09	0.02	344	3.09	0.02	269.5
GO MHC PROTEIN COMPLEX	10	3.09	0.02	344	3.09	0.02	269.5
GO POSITIVE REGULATION OF INTERLEUKIN 1 BETA PRODUCTION	19	2.88	0.03	430.5	3.25	0.00	183
GO LYSOSOMAL LUMEN	67	5.01	0.00	87	2.65	0.04	532
GO POSITIVE REGULATION OF PHOSPHOLIPID METABOLIC PROCESS	32	2.88	0.03	430.5	3.21	0.00	192
GO RESPONSE TO PROTOZOAN	10	2.75	0.04	502.5	3.57	0.00	121
GO POSITIVE REGULATION OF LYMPHOCYTE DIFFERENTIATION	56	3.69	0.00	247	2.88	0.03	385.5
GO POSITIVE REGULATION OF HEMOPOIESIS	127	4.21	0.00	162	2.75	0.04	471
GO REGULATION OF LIPID METABOLIC PROCESS	216	4.20	0.00	164	2.75	0.04	471
GO REGULATION OF LYMPHOCYTE CHEMOTAXIS	14	2.75	0.04	502.5	3.46	0.00	133
GO HOMEOSTASIS OF NUMBER OF CELLS	144	4.20	0.00	165	2.75	0.04	471
GO NEGATIVE REGULATION OF VIRAL TRANSCRIPTION	20	2.65	0.05	550.5	3.77	0.00	87
GO LAMININ BINDING	26	3.61	0.00	255	2.88	0.03	385.5
GO POSITIVE REGULATION OF MONOCYTE CHEMOTAXIS	13	2.88	0.03	430.5	3.11	0.00	213
GO HUMORAL IMMUNE RESPONSE	84	4.36	0.00	147	2.73	0.04	499
GO REGULATION OF T CELL PROLIFERATION	110	4.13	0.00	182	2.75	0.04	471
GO POSITIVE REGULATION OF LEUKOCYTE MEDIATED IMMUNITY	61	3.51	0.00	268	2.88	0.03	385.5
GO BONE RESORPTION	17	2.65	0.05	550.5	3.66	0.00	104

GO REGULATION OF OSTEOCLAST DIFFERENTIATION	46	3.47	0.00	275	2.88	0.03	385.5
GO FEAR RESPONSE	20	-3.46	0.00	276	-2.88	0.03	385.5
GO POSITIVE REGULATION OF PROTEIN KINASE B SIGNALING	66	2.90	0.02	393	3.09	0.02	269.5
GO LYMPHOCYTE COSTIMULATION	48	3.44	0.00	280	2.88	0.03	385.5
GO REGULATION OF MONOCYTE CHEMOTAXIS	17	2.75	0.04	502.5	3.32	0.00	165
GO INTESTINAL ABSORPTION	14	3.09	0.02	344	3.05	0.02	330
GO NEGATIVE REGULATION OF PROTEOLYSIS	212	3.65	0.00	252	2.80	0.03	425
GO POSITIVE REGULATION OF LEUKOCYTE DIFFERENTIATION	96	3.96	0.00	208	2.75	0.04	471
GO POSITIVE REGULATION OF CANONICAL WNT SIGNALING PATHWAY	101	-2.85	0.03	467	-3.12	0.00	212
GO POSITIVE REGULATION OF CHEMOKINE PRODUCTION	36	2.75	0.04	502.5	3.27	0.00	178
GO IMMUNE RESPONSE REGULATING CELL SURFACE RECEPTOR SIGNALING PATHWAY	231	3.95	0.00	211	2.75	0.04	471
GO REGULATION OF B CELL MEDIATED IMMUNITY	27	2.65	0.05	550.5	3.45	0.00	135
GO DEFENSE RESPONSE TO BACTERIUM	109	4.30	0.00	154	2.65	0.04	532
GO EXTRINSIC COMPONENT OF CYTOPLASMIC SIDE OF PLASMA MEMBRANE	74	4.27	0.00	156	2.65	0.04	532
GO HEXOSE CATABOLIC PROCESS	37	4.27	0.00	157	2.65	0.04	532
GO GRANULOCYTE ACTIVATION	18	2.75	0.04	502.5	3.23	0.00	189
GO MAST CELL ACTIVATION	17	2.75	0.04	502.5	3.22	0.00	191
GO POSITIVE REGULATION OF LEUKOCYTE APOPTOTIC PROCESS	26	2.65	0.05	550.5	3.43	0.00	143
GO DIGESTIVE SYSTEM PROCESS	39	3.09	0.02	344	2.91	0.02	350
GO RESPONSE TO IMMOBILIZATION STRESS	19	2.88	0.03	430.5	3.09	0.02	269.5
GO REGULATION OF NITRIC OXIDE SYNTHASE ACTIVITY	37	2.88	0.03	430.5	3.09	0.02	269.5
GO CELLULAR DEFENSE RESPONSE	29	2.88	0.03	430.5	3.09	0.02	269.5
GO CCR CHEMOKINE RECEPTOR BINDING	16	2.88	0.03	430.5	3.09	0.02	269.5
GO UBIQUITIN LIKE PROTEIN SPECIFIC PROTEASE ACTIVITY	84	-2.88	0.03	430.5	-3.09	0.02	269.5
GO RESPONSE TO PURINE CONTAINING COMPOUND	122	4.17	0.00	174	2.65	0.04	532
GO REGULATION OF INTERLEUKIN 6 PRODUCTION	74	3.75	0.00	235	2.75	0.04	471
GO REGULATION OF CELL ADHESION MEDIATED BY INTEGRIN	35	3.66	0.00	251	2.75	0.04	471
GO POSITIVE REGULATION OF STAT CASCADE	45	3.05	0.02	386	2.99	0.02	339
GO OXIDOREDUCTION COENZYME METABOLIC PROCESS	81	4.04	0.00	195	2.65	0.04	532
GO REGULATION OF HISTONE DEACETYLATION	22	3.09	0.02	344	2.88	0.03	385.5
GO REGULATION OF RECEPTOR BINDING	13	3.09	0.02	344	2.88	0.03	385.5
GO POSITIVE REGULATION OF RESPONSE TO WOUNDING	107	3.09	0.02	344	2.88	0.03	385.5
GO ALPHA BETA T CELL ACTIVATION	37	3.09	0.02	344	2.88	0.03	385.5
GO CHEMOKINE RECEPTOR BINDING	29	3.09	0.02	344	2.88	0.03	385.5
GO CYTOKINE RECEPTOR ACTIVITY	57	3.09	0.02	344	2.88	0.03	385.5
GO POSITIVE REGULATION OF INTERLEUKIN 1 PRODUCTION	23	2.88	0.02	394	3.00	0.02	337
GO ORGANELLE LOCALIZATION	322	-2.75	0.04	474.5	-3.09	0.02	269.5
GO MYELOID LEUKOCYTE DIFFERENTIATION	84	3.42	0.00	281	2.75	0.04	471
GO PROTEIN CATABOLIC PROCESS	488	-2.88	0.03	430.5	-3.07	0.02	327
GO ERYTHROCYTE HOMEOSTASIS	62	3.82	0.00	226	2.65	0.04	532
GO POSITIVE REGULATION OF HISTONE DEACETYLATION	13	3.31	0.00	293	2.75	0.04	471

GO ACUTE INFLAMMATORY RESPONSE	43	2.88	0.03	430.5	3.03	0.02	334
GO POSITIVE REGULATION OF JUN KINASE ACTIVITY	53	3.09	0.02	344	2.81	0.03	424
GO REGULATION OF T CELL RECEPTOR SIGNALING PATHWAY	21	2.75	0.04	502.5	3.09	0.02	269.5
GO PINOCYTOSIS	10	2.75	0.04	502.5	3.09	0.02	269.5
GO REGULATION OF GRANULOCYTE CHEMOTAXIS	29	2.75	0.04	502.5	3.09	0.02	269.5
GO LEUKOCYTE HOMEOSTASIS	50	2.75	0.04	502.5	3.09	0.02	269.5
GO NEGATIVE REGULATION OF LYMPHOCYTE DIFFERENTIATION	31	2.75	0.04	502.5	3.09	0.02	269.5
GO REGULATION OF T CELL MIGRATION	20	2.75	0.04	502.5	3.09	0.02	269.5
GO PROTEIN O LINKED FUCOSYLATION	11	-2.88	0.03	430.5	-2.98	0.02	342
GO RESPONSE TO TRANSITION METAL NANOPARTICLE	114	3.09	0.02	344	2.76	0.03	431
GO REGULATION OF ESTABLISHMENT OF PLANAR POLARITY	100	-2.88	0.03	430.5	-2.92	0.02	349
GO RESPONSE TO ZINC ION	41	2.88	0.03	430.5	2.90	0.02	351
GO REGULATION OF TUMOR NECROSIS FACTOR SUPERFAMILY CYTOKINE PRODUCTION	75	3.60	0.00	256	2.65	0.04	532
GO HYDROLASE ACTIVITY HYDROLYZING O GLYCOSYL COMPOUNDS	65	3.49	0.00	270	2.65	0.04	532
GO POSITIVE REGULATION OF LIPID KINASE ACTIVITY	28	3.04	0.02	387	2.82	0.03	423
GO REGULATION OF WATER LOSS VIA SKIN	13	3.09	0.02	344	2.75	0.04	471
GO REGULATION OF STEROL TRANSPORT	30	3.09	0.02	344	2.75	0.04	471
GO TUMOR NECROSIS FACTOR RECEPTOR BINDING	22	3.09	0.02	344	2.75	0.04	471
GO CELLULAR RESPONSE TO VIRUS	17	2.88	0.03	430.5	2.88	0.03	385.5
GO NEGATIVE REGULATION OF LEUKOCYTE PROLIFERATION	58	2.88	0.03	430.5	2.88	0.03	385.5
GO DECIDUALIZATION	16	2.88	0.03	430.5	2.88	0.03	385.5
GO NEGATIVE REGULATION OF INTERLEUKIN 12 PRODUCTION	11	2.88	0.03	430.5	2.88	0.03	385.5
GO RESPONSE TO GONADOTROPIN	16	2.88	0.03	430.5	2.88	0.03	385.5
GO VESICLE LOCALIZATION	174	-2.65	0.05	550.5	-3.09	0.02	269.5
GO REGULATION OF RNA POLYMERASE II TRANSCRIPTIONAL PREINITIATION COMPLEX ASSEMBLY	13	-2.65	0.05	550.5	-3.09	0.02	269.5
GO REGULATION OF INTERLEUKIN 8 PRODUCTION	45	2.65	0.05	550.5	3.09	0.02	269.5
GO REGULATION OF NEUTROPHIL MIGRATION	22	2.75	0.04	502.5	3.05	0.02	331
GO SINGLE ORGANISM MEMBRANE BUDDING	61	-2.77	0.03	469	-2.88	0.03	385.5
GO GASTRULATION WITH MOUTH FORMING SECOND	25	-2.75	0.04	474.5	-2.88	0.03	385.5
GO REGULATION OF SODIUM ION TRANSMEMBRANE TRANSPORT	38	-2.75	0.04	474.5	-2.88	0.03	385.5
GO REGULATION OF CYTOKINE BIOSYNTHETIC PROCESS	68	3.09	0.02	344	2.65	0.04	532
GO MONOCYTE CHEMOTAXIS	22	3.09	0.02	344	2.65	0.04	532
GO REGULATION OF NEUTROPHIL CHEMOTAXIS	19	2.65	0.05	550.5	3.06	0.02	329
GO ALPHA BETA T CELL DIFFERENTIATION	33	2.75	0.04	502.5	2.88	0.03	385.5
GO REGULATION OF CHEMOKINE PRODUCTION	49	2.75	0.04	502.5	2.88	0.03	385.5
GO RESPIRATORY BURST	10	2.75	0.04	502.5	2.88	0.03	385.5
GO POSITIVE REGULATION OF NITRIC OXIDE SYNTHASE ACTIVITY	13	2.75	0.04	502.5	2.88	0.03	385.5
GO SIGNALING PATTERN RECOGNITION RECEPTOR ACTIVITY	14	2.65	0.05	550.5	2.95	0.02	346
GO HEMOGLOBIN METABOLIC PROCESS	10	2.88	0.03	430.5	2.75	0.04	471
GO DENDRITIC CELL DIFFERENTIATION	25	2.88	0.03	430.5	2.75	0.04	471

GO POSITIVE REGULATION OF ANTIGEN RECEPTOR MEDIATED SIGNALING PATHWAY	12	2.88	0.03	430.5	2.75	0.04	471
GO POSITIVE REGULATION OF PEPTIDASE ACTIVITY	130	2.88	0.03	430.5	2.75	0.04	471
GO REGULATION OF LIPID BIOSYNTHETIC PROCESS	94	2.94	0.02	390	2.65	0.04	532
GO DEFENSE RESPONSE TO GRAM POSITIVE BACTERIUM	41	2.75	0.04	502.5	2.79	0.03	427
GO TRANSITION METAL ION TRANSPORT	82	2.75	0.04	502.5	2.77	0.03	430
GO POSITIVE REGULATION OF B CELL PROLIFERATION	27	2.65	0.05	550.5	2.88	0.03	385.5
GO REGULATION OF CYSTEINE TYPE ENDOPEPTIDASE ACTIVITY INVOLVED IN APOPTOTIC SIGNALING PATHWAY	21	2.65	0.05	550.5	2.88	0.03	385.5
GO POSITIVE REGULATION OF EXTRINSIC APOPTOTIC SIGNALING PATHWAY	41	2.65	0.05	550.5	2.88	0.03	385.5
GO REGULATION OF POSTTRANSCRIPTIONAL GENE SILENCING	16	2.65	0.05	550.5	2.88	0.03	385.5
GO MYELOID CELL DEVELOPMENT	38	2.88	0.03	430.5	2.65	0.04	532
GO RESPONSE TO VITAMIN D	27	2.88	0.03	430.5	2.65	0.04	532
GO POSITIVE REGULATION OF LIPASE ACTIVITY	45	2.88	0.03	430.5	2.65	0.04	532
GO REGULATION OF ALPHA BETA T CELL ACTIVATION	47	2.75	0.04	502.5	2.75	0.04	471
GO POSITIVE REGULATION OF INTERLEUKIN 8 PRODUCTION	37	2.75	0.04	502.5	2.75	0.04	471
GO T CELL DIFFERENTIATION INVOLVED IN IMMUNE RESPONSE	20	2.75	0.04	502.5	2.75	0.04	471
GO REGULATION OF ALPHA BETA T CELL DIFFERENTIATION	33	2.75	0.04	502.5	2.75	0.04	471
GO ACTIVATION OF MAPKK ACTIVITY	43	2.88	0.03	430.5	2.59	0.05	565
GO ACTIVATION OF JUN KINASE ACTIVITY	28	2.65	0.05	550.5	2.75	0.04	471
GO NEGATIVE REGULATION OF INTERFERON GAMMA PRODUCTION	24	2.65	0.05	550.5	2.75	0.04	471
GO POSITIVE REGULATION OF LYMPHOCYTE MEDIATED IMMUNITY	47	2.65	0.05	550.5	2.75	0.04	471
GO RESPONSE TO SALT STRESS	16	2.65	0.05	550.5	2.75	0.04	471
GO T CELL MEDIATED IMMUNITY	22	2.65	0.05	550.5	2.75	0.04	471
GO REGULATION OF B CELL RECEPTOR SIGNALING PATHWAY	10	2.75	0.04	502.5	2.65	0.04	532
GO PROTEIN SECRETION	80	2.75	0.04	502.5	2.65	0.04	532
GO NEGATIVE REGULATION OF NF KAPPAB TRANSCRIPTION FACTOR ACTIVITY	55	2.75	0.04	502.5	2.65	0.04	532
GO CELL KILLING	32	2.75	0.04	502.5	2.65	0.04	532
GO PROTEIN UBIQUITINATION INVOLVED IN UBIQUITIN DEPENDENT PROTEIN CATABOLIC PROCESS	115	-2.65	0.05	550.5	-2.65	0.04	532
GO REGULATION OF CELLULAR PROTEIN CATABOLIC PROCESS	235	-2.65	0.05	550.5	-2.65	0.04	532
GO SODIUM ION TRANSPORT	85	-2.65	0.05	550.5	-2.62	0.04	563

9.4 Appendix D – Copyright permissions

WOLTERS KLUWER HEALTH, INC. LICENSE TERMS AND CONDITIONS

Mar 11, 2018

This Agreement between Katherine Leavey ("You") and Wolters Kluwer Health, Inc. ("Wolters Kluwer Health, Inc.") consists of your license details and the terms and conditions provided by Wolters Kluwer Health, Inc. and Copyright Clearance Center.

License Number	4306141298811
License date	Mar 11, 2018
Licensed Content Publisher	Wolters Kluwer Health, Inc.
Licensed Content Publication	Hypertension
Licensed Content Title	Circulating Angiogenic Factors in the Pathogenesis and Prediction of Preeclampsia
Licensed Content Author	Chun Lam,Kee-Hak Lim,S. Ananth Karumanchi
Licensed Content Date	Nov 1, 2005
Licensed Content Volume	46
Licensed Content Issue	5
Type of Use	Dissertation/Thesis
Requestor type	Individual
Portion	Figures/table/illustration
Number of figures/tables/illustrations	1
Figures/tables/illustrations used	Figure 1
Author of this Wolters Kluwer article	No
Title of your thesis / dissertation	Unsupervised Multi-Scale Analysis for the Identification of Placental Subtypes of Human Preeclampsia and Fetal Growth Restriction
Expected completion date	Jun 2018
Estimated size(pages)	250
Requestor Location	Katherine Leavey 1 King's College Circle Toronto, ON M5S1A8 Canada Attn: Katherine Leavey
Billing Type	Invoice
Billing Address	Katherine Leavey 1 King's College Circle Toronto, ON M5S1A8 Canada

Attn: Katherine Leavey

Total 0.00 CAD

Terms and Conditions

Wolters Kluwer Terms and Conditions

1. **Transfer of License:** Wolters Kluwer hereby grants you a non-exclusive license to reproduce this material for this purpose, and for no other use, subject to the conditions herein.
2. **Credit Line:** will be prominently placed and include: For books – the author(s), title of book, editor, copyright holder, year of publication; For journals – the author(s), title of article, title of journal, volume number, issue number, inclusive pages and website URL to the journal page.
3. **Warranties:** The requestor warrants that the material shall not be used in any manner which may be considered derogatory to the title, content, or authors of the material, or to Wolters Kluwer.
4. **Indemnity:** You hereby indemnify and hold harmless Wolters Kluwer and their respective officers, directors, employees and agents, from and against any and all claims, costs, proceeding or demands arising out of your unauthorized use of the Licensed Material.
5. **Geographical Scope:** Permission granted is non-exclusive, and is valid throughout the world in the English language and the languages specified in your original request.
6. Wolters Kluwer cannot supply the requestor with the original artwork, electronic files or a "clean copy."
7. Permission is valid if the borrowed material is original to a Wolters Kluwer imprint (Lippincott-Raven Publishers, Williams & Wilkins, Lea & Febiger, Harwal, Rapid Science, Little Brown & Company, Harper & Row Medical, American Journal of Nursing Co, and Urban & Schwarzenberg - English Language, Raven Press, Paul Hoeber, Springhouse, Ovid).
8. **Termination of contract:** If you opt not to use the material requested above please notify RightsLink or Wolters Kluwer within 90 days of the original invoice date.
9. This permission does not apply to images that are credited to publications other than Wolters Kluwer books/journals or its Societies. For images credited to non-Wolters Kluwer books or journals, you will need to obtain permission from the source referenced in the figure or table legend or credit line before making any use of the image(s) or table(s).
10. **Modifications:** With the exception of text size or color, no Wolters Kluwer material is permitted to be modified or adapted without publisher approval.
11. **Third party material:** Adaptations are protected by copyright, so if you would like to reuse material that we have adapted from another source, you will need not only our permission, but the permission of the rights holder of the original material. Similarly, if you want to reuse an adaptation of original LWW content that appears in another publishers work, you will need our permission and that of the next publisher. The adaptation should be credited as follows: Adapted with permission from Wolters Kluwer: Book author, title, year of publication or Journal name, article author, title, reference citation, year of publication. Modifications are permitted on an occasional basis only and permission must be sought by Wolters Kluwer.
12. **Duration of the license:** Permission is granted for a one-time use only within 12 months from the date of this invoice. Rights herein do not apply to future reproductions, editors, revisions, or other derivative works. Once the 12 - month term has expired, permission to renew must be submitted in writing.
    i. For content reused in another journal or book, in print or electronic format, the license is one-time use and lasts for the 1st edition of a book or for the life of the edition in case of journals.
    ii. If your Permission Request is for use on a website (which is not a journal or a book), internet, intranet, or any publicly accessible site, you agree to remove the material from such site after 12 months or else renew your permission request.
13. **Contingent on payment:** While you may exercise the rights licensed immediately upon issuance of the license at the end of the licensing process for the transaction, provided that you have disclosed complete and accurate details of your proposed use, no license is finally effective unless and until full payment is received from you (either by publisher or by CCC)

as provided in CCC's Billing and Payment terms and conditions. If full payment is not received on a timely basis, then any license preliminarily granted shall be deemed automatically revoked and shall be void as if never granted. Further, in the event that you breach any of these terms and conditions or any of CCC's Billing and Payment terms and conditions, the license is automatically revoked and shall be void as if never granted. Use of materials as described in a revoked license, as well as any use of the materials beyond the scope of an unrevoked license, may constitute copyright infringement and publisher reserves the right to take any and all action to protect its copyright in the materials.

14. **Waived permission fee:** If the permission fee for the requested use of our material has been waived in this instance, please be advised that your future requests for Wolters Kluwer materials may incur a fee.
15. **Service Description for Content Services:** Subject to these terms of use, any terms set forth on the particular order, and payment of the applicable fee, you may make the following uses of the ordered materials:
    i. **Content Rental:** You may access and view a single electronic copy of the materials ordered for the time period designated at the time the order is placed. Access to the materials will be provided through a dedicated content viewer or other portal, and access will be discontinued upon expiration of the designated time period. An order for Content Rental does not include any rights to print, download, save, create additional copies, to distribute or to reuse in any way the full text or parts of the materials.
    ii. **Content Purchase:** You may access and download a single electronic copy of the materials ordered. Copies will be provided by email or by such other means as publisher may make available from time to time. An order for Content Purchase does not include any rights to create additional copies or to distribute copies of the materials.

For Journals Only:

1. Please note that articles in the **ahead-of-print stage** of publication can be cited and the content may be re-used by including the date of access and the unique DOI number. Any final changes in manuscripts will be made at the time of print publication and will be reflected in the final electronic version of the issue. Disclaimer: Articles appearing in the Published Ahead-of-Print section have been peer-reviewed and accepted for publication in the relevant journal and posted online before print publication. Articles appearing as publish ahead-of-print may contain statements, opinions, and information that have errors in facts, figures, or interpretation. Accordingly, Wolters Kluwer, the editors and authors and their respective employees are not responsible or liable for the use of any such inaccurate or misleading data, opinion or information contained in the articles in this section.
2. Where a journal is being published by a learned society, the details of that society must be included in the credit line.
    i. **For Open Access journals:** The following statement needs to be added when reprinting the material in Open Access journals only: "promotional and commercial use of the material in print, digital or mobile device format is prohibited without the permission from the publisher Wolters Kluwer. Please contact permissions@lww.com for further information."
    ii. **Exceptions:** In case of reuse from **Diseases of the Colon & Rectum, Plastic Reconstructive Surgery, The Green Journal, Critical Care Medicine, Pediatric Critical Care Medicine, the American Heart Association Publications and the American Academy of Neurology** the following guideline applies: no drug/ trade name or logo can be included in the same page as the material re-used.
3. **Translations:** If granted permissions to republish a full text article in another language, Wolters Kluwer should be sent a copy of the translated PDF. Please include disclaimer below on all translated copies:
    i. ***Wolters Kluwer and its Societies take no responsibility for the accuracy of the translation from the published English original and are not liable for any errors which may occur.***
4. **Full Text Articles:** Reuse of full text articles in English is prohibited.

STM Signatories Only:

1. Any permission granted for a particular edition will apply also to subsequent editions and for editions in other languages, provided such editions are for the work as a whole in situ and does not involve the separate exploitation of the permitted illustrations or excerpts. Please click here to view the STM guidelines.

Other Terms and Conditions:

v1.17

Questions? customercare@copyright.com or +1-855-239-3415 (toll free in the US) or +1-978-646-2777.

ELSEVIER LICENSE
TERMS AND CONDITIONS

Mar 11, 2018

This Agreement between Katherine Leavey ("You") and Elsevier ("Elsevier") consists of your license details and the terms and conditions provided by Elsevier and Copyright Clearance Center.

License Number	4306190402839
License date	Mar 11, 2018
Licensed Content Publisher	Elsevier
Licensed Content Publication	American Journal of Obstetrics and Gynecology
Licensed Content Title	A placenta clinic approach to the diagnosis and management of fetal growth restriction
Licensed Content Author	John C. Kingdom,Melanie C. Audette,Sebastian R. Hobson,Rory C. Windrim,Eric Morgen
Licensed Content Date	Feb 1, 2018
Licensed Content Volume	218
Licensed Content Issue	2
Licensed Content Pages	15
Start Page	S803
End Page	S817
Type of Use	reuse in a thesis/dissertation
Intended publisher of new work	other
Portion	figures/tables/illustrations
Number of figures/tables/illustrations	1
Format	both print and electronic
Are you the author of this Elsevier article?	No
Will you be translating?	No
Original figure numbers	Figure 10
Title of your thesis/dissertation	Unsupervised Multi-Scale Analysis for the Identification of Placental Subtypes of Human Preeclampsia and Fetal Growth Restriction
Expected completion date	Jun 2018
Estimated size (number of pages)	250
Requestor Location	Katherine Leavey 1 King's College Circle Toronto, ON M5S1A8

	Canada Attn: Katherine Leavey
Publisher Tax ID	GB 494 6272 12
Total	0.00 CAD

Terms and Conditions

INTRODUCTION

1. The publisher for this copyrighted material is Elsevier. By clicking "accept" in connection with completing this licensing transaction, you agree that the following terms and conditions apply to this transaction (along with the Billing and Payment terms and conditions established by Copyright Clearance Center, Inc. ("CCC"), at the time that you opened your Rightslink account and that are available at any time at http://myaccount.copyright.com).

GENERAL TERMS

2. Elsevier hereby grants you permission to reproduce the aforementioned material subject to the terms and conditions indicated.
3. Acknowledgement: If any part of the material to be used (for example, figures) has appeared in our publication with credit or acknowledgement to another source, permission must also be sought from that source. If such permission is not obtained then that material may not be included in your publication/copies. Suitable acknowledgement to the source must be made, either as a footnote or in a reference list at the end of your publication, as follows:
"Reprinted from Publication title, Vol /edition number, Author(s), Title of article / title of chapter, Pages No., Copyright (Year), with permission from Elsevier [OR APPLICABLE SOCIETY COPYRIGHT OWNER]." Also Lancet special credit - "Reprinted from The Lancet, Vol. number, Author(s), Title of article, Pages No., Copyright (Year), with permission from Elsevier."
4. Reproduction of this material is confined to the purpose and/or media for which permission is hereby given.
5. Altering/Modifying Material: Not Permitted. However figures and illustrations may be altered/adapted minimally to serve your work. Any other abbreviations, additions, deletions and/or any other alterations shall be made only with prior written authorization of Elsevier Ltd. (Please contact Elsevier at permissions@elsevier.com). No modifications can be made to any Lancet figures/tables and they must be reproduced in full.
6. If the permission fee for the requested use of our material is waived in this instance, please be advised that your future requests for Elsevier materials may attract a fee.
7. Reservation of Rights: Publisher reserves all rights not specifically granted in the combination of (i) the license details provided by you and accepted in the course of this licensing transaction, (ii) these terms and conditions and (iii) CCC's Billing and Payment terms and conditions.
8. License Contingent Upon Payment: While you may exercise the rights licensed immediately upon issuance of the license at the end of the licensing process for the transaction, provided that you have disclosed complete and accurate details of your proposed use, no license is finally effective unless and until full payment is received from you (either by publisher or by CCC) as provided in CCC's Billing and Payment terms and conditions. If full payment is not received on a timely basis, then any license preliminarily granted shall be deemed automatically revoked and shall be void as if never granted. Further, in the event that you breach any of these terms and conditions or any of CCC's Billing and Payment terms and conditions, the license is automatically revoked and shall be void as if never granted. Use of materials as described in a revoked license, as well as any use of the materials beyond the scope of an unrevoked license, may constitute copyright infringement

and publisher reserves the right to take any and all action to protect its copyright in the materials.

9. Warranties: Publisher makes no representations or warranties with respect to the licensed material.

10. Indemnity: You hereby indemnify and agree to hold harmless publisher and CCC, and their respective officers, directors, employees and agents, from and against any and all claims arising out of your use of the licensed material other than as specifically authorized pursuant to this license.

11. No Transfer of License: This license is personal to you and may not be sublicensed, assigned, or transferred by you to any other person without publisher's written permission.

12. No Amendment Except in Writing: This license may not be amended except in a writing signed by both parties (or, in the case of publisher, by CCC on publisher's behalf).

13. Objection to Contrary Terms: Publisher hereby objects to any terms contained in any purchase order, acknowledgment, check endorsement or other writing prepared by you, which terms are inconsistent with these terms and conditions or CCC's Billing and Payment terms and conditions. These terms and conditions, together with CCC's Billing and Payment terms and conditions (which are incorporated herein), comprise the entire agreement between you and publisher (and CCC) concerning this licensing transaction. In the event of any conflict between your obligations established by these terms and conditions and those established by CCC's Billing and Payment terms and conditions, these terms and conditions shall control.

14. Revocation: Elsevier or Copyright Clearance Center may deny the permissions described in this License at their sole discretion, for any reason or no reason, with a full refund payable to you. Notice of such denial will be made using the contact information provided by you. Failure to receive such notice will not alter or invalidate the denial. In no event will Elsevier or Copyright Clearance Center be responsible or liable for any costs, expenses or damage incurred by you as a result of a denial of your permission request, other than a refund of the amount(s) paid by you to Elsevier and/or Copyright Clearance Center for denied permissions.

LIMITED LICENSE

The following terms and conditions apply only to specific license types:

15. **Translation**: This permission is granted for non-exclusive world **English** rights only unless your license was granted for translation rights. If you licensed translation rights you may only translate this content into the languages you requested. A professional translator must perform all translations and reproduce the content word for word preserving the integrity of the article.

16. **Posting licensed content on any Website**: The following terms and conditions apply as follows: Licensing material from an Elsevier journal: All content posted to the web site must maintain the copyright information line on the bottom of each image; A hyper-text must be included to the Homepage of the journal from which you are licensing at http://www.sciencedirect.com/science/journal/xxxxx or the Elsevier homepage for books at http://www.elsevier.com; Central Storage: This license does not include permission for a scanned version of the material to be stored in a central repository such as that provided by Heron/XanEdu.

Licensing material from an Elsevier book: A hyper-text link must be included to the Elsevier homepage at http://www.elsevier.com . All content posted to the web site must maintain the copyright information line on the bottom of each image.

Posting licensed content on Electronic reserve: In addition to the above the following clauses are applicable: The web site must be password-protected and made available only to bona fide students registered on a relevant course. This permission is granted for 1 year only.

You may obtain a new license for future website posting.

17. **For journal authors:** the following clauses are applicable in addition to the above:

Preprints:

A preprint is an author's own write-up of research results and analysis, it has not been peer-reviewed, nor has it had any other value added to it by a publisher (such as formatting, copyright, technical enhancement etc.).

Authors can share their preprints anywhere at any time. Preprints should not be added to or enhanced in any way in order to appear more like, or to substitute for, the final versions of articles however authors can update their preprints on arXiv or RePEc with their Accepted Author Manuscript (see below).

If accepted for publication, we encourage authors to link from the preprint to their formal publication via its DOI. Millions of researchers have access to the formal publications on ScienceDirect, and so links will help users to find, access, cite and use the best available version. Please note that Cell Press, The Lancet and some society-owned have different preprint policies. Information on these policies is available on the journal homepage.

Accepted Author Manuscripts: An accepted author manuscript is the manuscript of an article that has been accepted for publication and which typically includes author-incorporated changes suggested during submission, peer review and editor-author communications.

Authors can share their accepted author manuscript:

- immediately
  - via their non-commercial person homepage or blog
  - by updating a preprint in arXiv or RePEc with the accepted manuscript
  - via their research institute or institutional repository for internal institutional uses or as part of an invitation-only research collaboration work-group
  - directly by providing copies to their students or to research collaborators for their personal use
  - for private scholarly sharing as part of an invitation-only work group on commercial sites with which Elsevier has an agreement
- After the embargo period
  - via non-commercial hosting platforms such as their institutional repository
  - via commercial sites with which Elsevier has an agreement

In all cases accepted manuscripts should:

- link to the formal publication via its DOI
- bear a CC-BY-NC-ND license - this is easy to do
- if aggregated with other manuscripts, for example in a repository or other site, be shared in alignment with our hosting policy not be added to or enhanced in any way to appear more like, or to substitute for, the published journal article.

Published journal article (JPA): A published journal article (PJA) is the definitive final record of published research that appears or will appear in the journal and embodies all value-adding publishing activities including peer review co-ordination, copy-editing, formatting, (if relevant) pagination and online enrichment.

Policies for sharing publishing journal articles differ for subscription and gold open access articles:

Subscription Articles: If you are an author, please share a link to your article rather than the full-text. Millions of researchers have access to the formal publications on ScienceDirect, and so links will help your users to find, access, cite, and use the best available version.

Theses and dissertations which contain embedded PJAs as part of the formal submission can be posted publicly by the awarding institution with DOI links back to the formal publications on ScienceDirect.

If you are affiliated with a library that subscribes to ScienceDirect you have additional private sharing rights for others' research accessed under that agreement. This includes use for classroom teaching and internal training at the institution (including use in course packs and courseware programs), and inclusion of the article for grant funding purposes.

Gold Open Access Articles: May be shared according to the author-selected end-user license and should contain a CrossMark logo, the end user license, and a DOI link to the formal publication on ScienceDirect.

Please refer to Elsevier's posting policy for further information.

18. **For book authors** the following clauses are applicable in addition to the above: Authors are permitted to place a brief summary of their work online only. You are not allowed to download and post the published electronic version of your chapter, nor may you scan the printed edition to create an electronic version. **Posting to a repository:** Authors are permitted to post a summary of their chapter only in their institution's repository.

19. **Thesis/Dissertation**: If your license is for use in a thesis/dissertation your thesis may be submitted to your institution in either print or electronic form. Should your thesis be published commercially, please reapply for permission. These requirements include permission for the Library and Archives of Canada to supply single copies, on demand, of the complete thesis and include permission for Proquest/UMI to supply single copies, on demand, of the complete thesis. Should your thesis be published commercially, please reapply for permission. Theses and dissertations which contain embedded PJAs as part of the formal submission can be posted publicly by the awarding institution with DOI links back to the formal publications on ScienceDirect.

Elsevier Open Access Terms and Conditions

You can publish open access with Elsevier in hundreds of open access journals or in nearly 2000 established subscription journals that support open access publishing. Permitted third party re-use of these open access articles is defined by the author's choice of Creative Commons user license. See our open access license policy for more information.

Terms & Conditions applicable to all Open Access articles published with Elsevier:

Any reuse of the article must not represent the author as endorsing the adaptation of the article nor should the article be modified in such a way as to damage the author's honour or reputation. If any changes have been made, such changes must be clearly indicated.

The author(s) must be appropriately credited and we ask that you include the end user license and a DOI link to the formal publication on ScienceDirect.

If any part of the material to be used (for example, figures) has appeared in our publication with credit or acknowledgement to another source it is the responsibility of the user to ensure their reuse complies with the terms and conditions determined by the rights holder.

Additional Terms & Conditions applicable to each Creative Commons user license:

CC BY: The CC-BY license allows users to copy, to create extracts, abstracts and new works from the Article, to alter and revise the Article and to make commercial use of the Article (including reuse and/or resale of the Article by commercial entities), provided the user gives appropriate credit (with a link to the formal publication through the relevant DOI), provides a link to the license, indicates if changes were made and the licensor is not represented as endorsing the use made of the work. The full details of the license are available at http://creativecommons.org/licenses/by/4.0.

CC BY NC SA: The CC BY-NC-SA license allows users to copy, to create extracts, abstracts and new works from the Article, to alter and revise the Article, provided this is not done for commercial purposes, and that the user gives appropriate credit (with a link to the

formal publication through the relevant DOI), provides a link to the license, indicates if changes were made and the licensor is not represented as endorsing the use made of the work. Further, any new works must be made available on the same conditions. The full details of the license are available at http://creativecommons.org/licenses/by-nc-sa/4.0.
CC BY NC ND: The CC BY-NC-ND license allows users to copy and distribute the Article, provided this is not done for commercial purposes and further does not permit distribution of the Article if it is changed or edited in any way, and provided the user gives appropriate credit (with a link to the formal publication through the relevant DOI), provides a link to the license, and that the licensor is not represented as endorsing the use made of the work. The full details of the license are available at http://creativecommons.org/licenses/by-nc-nd/4.0.
Any commercial reuse of Open Access articles published with a CC BY NC SA or CC BY NC ND license requires permission from Elsevier and will be subject to a fee.
Commercial reuse includes:

- Associating advertising with the full text of the Article
- Charging fees for document delivery or access
- Article aggregation
- Systematic distribution via e-mail lists or share buttons

Posting or linking by commercial companies for use by customers of those companies.

20. **Other Conditions**:

v1.9

Questions? customercare@copyright.com or +1-855-239-3415 (toll free in the US) or +1-978-646-2777.

Title: Unsupervised Placental Gene Expression Profiling Identifies Clinically Relevant Subclasses of Human PreeclampsiaNovelty and Significance

Author: Katherine Leavey,Samantha J. Benton,David Grynspan,John C. Kingdom,Shannon A. Bainbridge,Brian J. Cox

Publication: Hypertension

Publisher: Wolters Kluwer Health, Inc.

Date: Jul 1, 2016

License Not Required

This request is granted gratis and no formal license is required from Wolters Kluwer. Please note that modifications are not permitted. Please use the following citation format: author(s), title of article, title of journal, volume number, issue number, inclusive pages and website URL to the journal page.

BACK CLOSE WINDOW